Deposition of sediment and associated heavy metals on floodplains

Nederlandse Geografische Studies / Netherlands Geographical Studies

ISSN 0169-4839

Netherlands Geographical Studies 337

Deposition of sediment and associated heavy metals on floodplains

Ivo Thonon

Utrecht 2006

Koninklijk Nederlands Aardrijkskundig Genootschap
Faculteit Geowetenschappen Universiteit Utrecht

This publication is identical to a dissertation submitted for the title of Doctor at the Universiteit Utrecht, The Netherlands. The public defence of this thesis took place on March 3, 2006.

Supervisors:

Prof. dr. Peter A. Burrough	Universiteit Utrecht/University of Oxford
Dr. Hans Middelkoop	Universiteit Utrecht
Dr. Marcel van der Perk	Universiteit Utrecht

Examination committee:

Prof. dr. ir. A. Jan Hendriks	Radboud Universiteit Nijmegen
Prof. dr. Salomon B. Kroonenberg	Technische Universiteit Delft
Prof. dr. Desmond E. Walling	University of Exeter
Prof. dr. Martin J. Wassen	Universiteit Utrecht
Dr. Nathalie E.M. Asselman	WL|Delft Hydraulics

The University Board (through the 'Networks in the Delta' programme) and the Coastal and River Systems Research group of the Universiteit Utrecht contributed financially to the research presented in this publication.

ISBN-10: 90-6809-377-0
ISBN-13: 978-90-6809-377-3

Graphic design, cartography and figures:
Rien Rabbers (GeoMedia, Faculty of Geosciences, Utrecht University)

Cover illustration: Dieneke Joosten

Printed in the Netherlands by Labor Grafimedia b.v. – Utrecht

Contents

Figures

Tables

To whom it concerns

Dankwoord

Warning: this preface is in Dutch, a strange Germanic language with unpronounceable combinations of consonants. A good example is the word *proefschrift* (thesis). Thanks to my professor Peter Burrough, the English of the next chapters is quite readable. Hence, there is no reason to run the risk of severe tongue damage by trying to make something out of this preface (or the Dutch summary) by reading it out loud. I hope you enjoy the book.

Volgens de traditie is dit het deel om mensen bedanken, voor zover ik dat niet in de *acknowledgements* aan het einde van de hoofdstukken doe. Als eerste valt die eer te beurt aan de coördinatoren van het onderzoeksprogramma *Networks in the Delta*: Paul Schot en Martin Dijst. Zonder hen zou de Facultaire Breedtestrategie en dus het geld voor mijn promotieonderzoek er niet eens zijn geweest...

Dan zijn er natuurlijk mijn dagelijks begeleiders, Hans Middelkoop en Marcel van der Perk. Zij schreven in 2000 het voorstel 'Het lot van sedimentgebonden verontreinigingen onder veranderingen in landgebruik en afvoercondities in de Rijn-Maas delta' waarop dit onderzoek is gebaseerd. Zij vulden elkaar prima aan en hielden elkaar in balans. Waar Hans en ik geen gat meer zagen in de vergelijkingen, hielp Marcel ons uit de brand met een fraaie afleiding. Als Marcel en ik geen geen inspiratie meer hadden voor een nette zin, wist Hans er wél eentje te bedenken. Waar Marcel op grote lijnen mijn artikelen een andere richting instuurde, gooide Hans op zinsniveau het roer om. Hans breidde mijn inleidingen uit tot mooie verhaaltjes, terwijl Marcel het dorre hout in mijn methoden en resultaten kapte (godzijdank waren de conclusies altijd wel in orde...). Hans en Marcel, mocht er ooit nog een NWO Yin & Yangprijs voor begeleiderkoppels komen, dan nomineer ik jullie.

Met mijn kamergenoten Anet – "jij hoeft je slibmatjes tenminste niet te interviewen" – Weterings en Michel – "maak je het niet te laat?" – Hagoort heb ik vier jaar Kamer 421A in het Van Unnik*gebouw* gedeeld. We hebben al eens tegen elkaar gezegd dat we het maar met elkaar troffen, maar dat bevestig ik hierbij nog maar eens. De paar maanden dat we niet bij elkaar op de kamer zaten vielen niet voor niets samen met mijn aio-dip. Immers, wie anders overtuigde me tijdens de traditionele 'vrijdagmiddaggesprekken' van het nut van mijn promotie-onderzoek, vroeg me uit over de uitkomst van dat afspraakje of maakte een SWAT-analyse van mijn karakter voor de loopbaanbegeleiding? Anet, na ongeveer twee maanden ging je transistor van 0 ('ik ken jou niet dus praat ik ook niet tegen je') op 1 ('ik ken je dus ik praat de hele tijd tegen je'). Je hebt mijn belangstelling voor alternatieve popmuziek gevoed met tips en bent meegeweest naar concerten en festivals (Lowlands, The Superheroes, Moloko, De Beschaving). Ik hoop dat je bij het Ruimtelijk Planbureau ook snel op stand 1 terecht komt. Michel, via nu.nl hield je ons op de hoogte van het reilen en zeilen van de wereld buiten onze kamer en met foksuk.nl relativeerde je

ons werk. Ook al was hij fout, ik moest toch altijd wel erg lachen om je kantoorhumor. Ik hoop dat je collega's van de gemeente Alphen aan den Rijn je humor ook weten te waarderen.

Het fenomeen 'collega' was bij mij erg breed(testrategisch) gedefinieerd. Je had die van 'Sociale' op de zesde, en die van 'Fysische' in de Zonneveld*vleugel*. En daartussen een flinke kloof die waarschijnlijk met nog geen tien Breedtestrategieën overbrugd kan worden. Gelukkig mocht ik altijd van twee walletjes eten. Soms zelfs letterlijk, want ik werd bij beide groepen met verjaardagen altijd wel uitgenodigd om een stuk taart te komen eten. Met de aio's van Sociale Geografie & Planologie ging ik kanoën, naar de kerstdiners, de film en uit eten, met de promovendi van Fysische Geografie naar lunchlezingen, op Ardennenexcursie, vergaderen en pizza eten. Ik vind het fantastisch dat ik die dingen heb kunnen doen met andere jonge mensen die in hetzelfde schuitje zaten als ik. Jullie van 'Sociale' bedank ik voor uitspraken als "Maar jij hoort toch gewoon bij óns?", jullie van 'Fysische' bedank ik voor opmerkingen als "Was er hier geen plek meer voor je dan?". De enige collega die ik bij name zal noemen is Menno Straatsma, degene met wie ik letterlijk in één schuitje heb gezeten. Menno, ik wens iedereen een veldwerkpartner toe die net zo mentaal en fysiek ontwikkeld is als jij!

Het lemma 'familie & vrienden' is zo mogelijk nog breder dan het lemma 'collega'. Papa en mama, bedankt dat jullie er altijd voor me zijn en gewoon mijn kamer voor me schilderden toen ik op veldwerk was. Cyrille, als kledingadviseur heb je ervoor gezorgd dat ik altijd netjes voor de dag kwam. Bedankt voor het maken van het maatpak voor mijn verdediging! Evian, al doe ik voor jou nog steeds "iets met bodem", toch lief dat je altijd weer bezorgd bent als ik naar een ver eng buitenland ga voor congres of werk. Harmony, *me niego escribirlo en inglés pero me gusta Canadá y me gustas tú (y ¡viva Skype!)*. De Haventjes: jullie zijn altijd al een tweede thuishaven geweest waar jullie 'drukdrukdruk'-neef even kon aanmeren. Mijn medebestuursleden en de fractie van D66 Utrecht: inderdaad, nu het proefschrift af is komt er een vacature voor algemeen secretaris. Met jullie kon ik altijd heerlijk ouwehoeren in Café Van Wegen. Net als overigens met de Jonge Democraten verderop in The Florin, bij jullie heb ik misschien nog wel meer geleerd dan bij het schrijven van dat hele proefschrift. Renate & Esther, jullie zijn wat mij betreft het beste wat SB Helios heeft voortgebracht, net zoals Valkstraat 2bis Karen & Eefje en Warande 92 Kitty aan mijn vriendenkring heeft toegevoegd. Jullie waren altijd zo blij voor me als ik weer eens zei dat ik "bijna klaar" was, je zou er bijna je promotie voor uitstellen om die blijdschap nog eens te voelen. Mirjam & Femke, bij jullie kon ik altijd terecht met mijn 'later als ik gepromoveerd ben'-dromen. Anne-Marie & Erik, jullie hielpen mij het Educatorium links te laten liggen met jullie kookkunsten. Koos Jan, ooit win jij nog eens het WK slibmatjesspuiten in de categorie 'fijne fractie'. Sendy, uiteraard sta je bij het lemma vrienden. Ik vond het tof de eindfase, de pizza's en Lowlands 2005 te mogen delen met zo'n toegewijde aio als jij.

Vení, vi y escribí.

Ivo Thonon

Utrecht, november 2005

1 Introduction

1.1 Background

Floodplains are important for both society and nature. For centuries, people have used floodplain areas to build their settlements in the vicinity of the river, which provides freshwater for irrigation and domestic use, and serves as a shipping route. The fertile floodplain soils are widely used for agriculture. Floodplains are also vital ecotones (Brunet *et al.* 1994; Benke *et al.* 2000; Tockner *et al.* 2000; Thoms 2003), which link natural areas along the river with other natural areas in its hinterland. However, many rivers have become contaminated, which may affect the many functions of the rivers and their floodplains. To assess the consequences of this contamination, we need knowledge on the transport and fate of contaminants within the river basin.

Suspended sediment provides excellent binding sites for many contaminants (Gibbs 1977; Horowitz 2000). Consequently, large amounts of contaminants are transported in particulate form to lower river reaches and their floodplains (Owens *et al.* 2001; Gordeev *et al.* 2004). Overbank deposition may therefore not only fertilize floodplain soils (Ogden & Thoms 2002), but may also cause contamination with substances such as nutrients (Walling *et al.* 2003; Van der Lee 2004), organic micropollutants (Japenga & Salomons 1993; Van Metre *et al.* 2000; Walling *et al.* 2003) or heavy metals (Leenaers 1991; Marron 1992; Foster & Charlesworth 1996; Wolterbeek *et al.* 1996; Middelkoop 2000; Dennis *et al.* 2003). On the timescale of years to centuries, most floodplains act as sinks for sediment (e.g., Walling 1999; Malmon *et al.* 2003). Especially storage of heavy metals represents a problem, since they are persistent, i.e., they are not degraded in nature and accumulate in organic tissue. For instance, floodplain vegetation (Vink 2000) and soil-dwelling organisms (Van Griethuysen *et al.* 2004; Van Vliet *et al.* 2005; Vijver 2005) tend to accumulate these potentially toxic heavy metals. Via the food chain, the heavy metals subsequently reach plant feeders (Notten *et al.* 2005) and predators (Kooistra *et al.* 2001; Van den Brink *et al.* 2003). This may threaten the viability of vulnerable species in the floodplain ecosystem (Hendriks *et al.* 1997). Because of their adverse physiological effects, heavy metals also lead to losses in agricultural production (Noppert *et al.* 1993). Heavy metals may also reach groundwater after dissolution (Römkens *et al.* 2003; Dijkstra *et al.* 2004), where they can be transported to a wider area. Thus, deposition of sediments and associated heavy metals merits study, particularly in such important parts of landscape and society as river floodplains.

1.2 Previous research

Despite the important role of sediments in the construction of floodplains and as a substrate, natural resource or contaminant source, floodplain deposition for a long time received less

attention from geomorphologists than upstream soil erosion, in-stream sediment transport and other channel processes:

"*The final element of the process triumvirate [erosion, transport, deposition] has received comparatively less attention from geomorphologists and yet alluvial rivers build a wide range of depositional forms.*" (Knighton 1984).

"*Allen (1978) observed that overbank processes were largely ignored relative to channel processes and this situation persists today.*" (Marriott 1998).

Literature surveys by Adams & Perrow (1999) and Kondolf & Piégay (2003) have shown that Marriott's remark remains valid: river channels and bed processes receive more attention than floodplains. Still, despite this persisting focus on river channels and bed processes, research on floodplain deposition has rapidly expanded over the past two decades.

The first studies on contemporary floodplain deposition were empirical. Kesel *et al*. (1974), Mansikkaniemi (1985), Gretener & Strömquist (1986), Walling *et al*. (1986) and Lambert & Walling (1987) studied overbank deposition with reconnaissance surveys and sediment traps. James (1985) and Pizutto (1987), by contrast, followed a modelling approach to unravel the deposition process. At the same time, Förstner & Wittmann (1983), Salomons & Förstner (1984) and Horowitz (1985) pointed out that the sediments that constitute the floodplain soils may carry abundant amounts of heavy metals. Bradley & Cox (1986, 1990), Leenaers (1991) and Marron (1992) showed that floodplains may indeed store considerable amounts of sediment-bound heavy metals.

After this pioneering period, research diversified. First of all, studies aimed at quantifying contemporary floodplain deposition rates (Walling *et al*. 1992; Mertes 1994; Middelkoop & Asselman 1998; Thoms *et al*. 2000b; Steiger *et al*. 2001; Terry *et al*. 2002) and found these to vary from a few millimetres to some centimetres per year. Although these rates seem to be low, deposition of sediments (Walling *et al*. 1998, 1999; Thoms *et al*. 2000a) and contaminants (Middelkoop 2000; Walling *et al*. 2003; Walling & Owens 2003) on floodplains may have a considerable impact on sediment and contaminant budgets of river systems. Thanks to these research efforts, "*The role of floodplains in sediment and particulate-bound contaminant storage is now well established*" (Nanson & Croke 2002).

Other studies have shown sedimentation amounts and patterns to vary widely within and between floodplains and have attempted to explain these variations at the floodplain scale (Marriott 1992; Asselman & Middelkoop 1995; Middelkoop & Asselman 1998; Simm & Walling 1998; Steiger & Gurnell 2002). Researchers also investigated factors operating on larger spatial scales that could explain this variability, such as variations in upstream sediment delivery (Asselman 1997; Van Dijk 2001), temporal variability in suspended sediment concentrations (Asselman & Middelkoop 1998; Benedetti 2003) and along-stream variability in flow characteristics (Lecce 1997; Wyżga 1999). These last two groups of studies made clear that there are two primary factors that determine where and how much sediment is deposited on floodplains: their topography and the hydrodynamics of the overbank flow. Still, floodplain deposition remains a complex process

with a lot of factors involved (Brown 1996). Studies that integrate these factors in large river basins are therefore scarce (Asselman *et al*. 2003).

In an attempt to integrate the factors affecting floodplain deposition, research efforts also focused at the modelling of floodplain deposition. Several authors built floodplain sedimentation models for application on different spatial scales and in different floodplain environments (Nicholas & Walling 1997; Middelkoop & Van der Perk 1998; Asselman & Van Wijngaarden 2002; Sweet *et al*. 2003). However, most of these models were only directed at *sedimentation*; only few model studies concerned floodplain *contamination* (Stewart *et al*. 1998). Van der Perk *et al*. (1992) described a distributed model for one floodplain and Stewart *et al*. (1998) gave a detailed model for a small reach, but no similar spatially distributed model exists yet for the whole reach of a larger river. In addition, most floodplain deposition models need information on the characteristics of the suspended matter, such as the *effective* particle size and settling velocity (Droppo *et al*. 1998, 2000). Since these differ highly from the *absolute* particle size of floodplain deposits (Nicholas & Walling 1996; Walling & Woodward 2000), characteristics of settling sediment have to be measured *in situ* (Asselman & Middelkoop 1995). This, unfortunately, has hardly been done (Asselman 1999b), which makes it difficult to calibrate floodplain deposition models in an adequate way (Droppo *et al*. 2000).

The spatial variation in particle size and composition of floodplain deposits has attracted increasing attention in recent years (He & Walling 1998; Middelkoop & Asselman 1998; Simm & Walling 1998; Walling *et al*. 1998a). This is not surprising, since the heavy metal concentration increases with decreasing grain size and increasing organic matter content (Salomons & Förstner 1984; Horowitz 1985; Horowitz & Elrick 1987). This correlation necessitates measurements of grain size and organic matter content to determine the fate of preferentially bound contaminants such as heavy metals (Lecce & Pavlowsky 2004). Data on characteristics of overbank deposits are nevertheless scarce, especially in the case of deposits originating from high-magnitude overbank floods (Walling *et al*. 1998a) on floodplains along larger rivers (Middelkoop & Asselman 1998).

In the near future, a number of factors and processes that influence sediment and heavy metal deposition on floodplains may change:

- Climate change may alter the discharge regime of rivers (Knox 1993; Pfister *et al*. 2004), thereby changing the conditions for sediment deposition such as floodplain inundation durations and frequencies (Middelkoop 1995).
- Land-use change due to re- or deforestation, land abandonment or changing agricultural policy in upstream areas may increase or decrease sediment supply to rivers (Longfield & Macklin 1999; Stam 2002; Asselman *et al*. 2003).
- Despite increasingly strict legislation concerning emission of heavy metals on surface waters (e.g., EEC 1991 versus EC 1998), heavy metal emissions have not declined in the past 15 years and may even rise in the near future (CIW 2004). Legislation such as the European Water Framework Directive (EC 2000) demands a 'good ecological potential' of regulated rivers, yet their floodplains are often considerably polluted due to past heavy-metal emissions (e.g., Foster & Charlesworth 1996). This may have serious consequences for the way in which floodplains are managed and the amount of emissions tolerated.

- Integrative river basin management demands that floodplain rehabilitation is integrated in river rehabilitation plans (Jungwirth *et al.* 2005). Floodplain rehabilitation often envisages the creation of secondary channels, the restoration of nature (such as the characteristic floodplain forests) and the removal of artificial levees (Silva *et al.* 2001). These measures may all change the floodplain topography and the patterns of overbank flows, hence affect deposition patterns and amounts (Asselman 1999a; Baptist *et al.* 2004).

Changes in these factors are sometimes interrelated (e.g., climate change may also affect the vegetation density and hence the amount of soil erosion and subsequent sediment supply to rivers) and may either enhance or weaken each other's effects. This makes it difficult to assess their aggregated effect on the basis of individual studies concerned with one factor at a time. Until now, however, the combined impact of these factors on deposition of sediments and heavy metals on large lowland river floodplains has not been quantified. Furthermore, in spite of the numerous research efforts over the last decades, some issues have remained unsolved. These issues have been translated in a number of interrelated research questions:

1. What are the *current spatial patterns* in amounts and characteristics of sediment and associated heavy metal deposition on floodplains of large lowland river branches?
2. What is the *relative importance of the key factors* controlling the deposition of sediments and heavy metals on floodplains along large lowland rivers and how do these factors interact?
3. How do *future changes* in climate, land use, heavy-metal emissions and floodplain topography interact and affect patterns and amounts of sediment and metal deposition on lowland river floodplains?

1.3 Research goals

The general aim of the research is to predict changes in patterns and quantities of overbank deposition when environmental variables such as climate, upstream land use and floodplain topography change. In addition, the research also aims to (Fig. 1.5):

1. Determine the *current* patterns and amounts of sediment and associated heavy-metal deposition on floodplains.
2. Quantify the key processes that determine the deposition of sediment and heavy metals on floodplains.
3. Assess the sensitivity of the key processes to changes in variables such as climate, upstream land use and local topography.

1.4 Study area

The research in this thesis focuses on deposition of sediment and associated heavy metals on the lower River Rhine floodplains in The Netherlands. The choice for this study area has several reasons:

- The River Rhine basin is one of the most densely-populated and heavily-industrialized areas in Northwest Europe. For instance, besides major agglomerations like Frankfurt am Main, Stuttgart, Mannheim and Nürnberg, one of the largest urban agglomerations of Europe, the *Ruhrstadt* ('Ruhr City'), is located in the River Rhine basin (McClave 1996). Consequently, land-use change and new environmental legislation directly affect sediment loads and heavy-metal emissions.
- According to scenario studies, climate change may have a drastic impact on the discharge of the River Rhine. Shabalova *et al*. (2003) suggest higher probabilities of flooding in winter. More inundations of floodplains would also affect sediment and heavy-metal deposition. Because of the increased flooding risk, the Dutch government envisages major river rehabilitation plans in the Dutch lower River Rhine to accommodate peak discharges. The most presumable scenario of plans costs € 2.2 billion and involves the excavation of 25 million m^3 of sediments (V&W 2005). This will drastically influence the floodplain topography and flow patterns during flooding.
- The present study can benefit from previous work on the (lower) River Rhine by Kwadijk (1993), Asselman (1997, 2000), Middelkoop (1997), Vink (2002), Asselman *et al*. (2003) and Maas *et al*. (2003). In addition, the studies by Zorn (2005), Wijnhoven *et al*. (*subm*.) and Schipper (*in prep*.) could directly benefit from the results of this study because they were based in the same study area.
- Both the individual *and* combined impact of the future changes affects the overbank deposition on the lower Rhine River floodplains.

The River Rhine basin (Fig. 2.2) measures about 185,000 km^2, of which 20,000 km^2 are located in The Netherlands (Wolters *et al*. 2001). The River Rhine is about 1320 km long and flows through three distinct landscapes: mountains in its far upstream reach, hills in its middle reach and lowland in its lower reach. The Rive Rhine springs from the Rheinwaldhorn Glacier in the Swiss Alps (3,350 m a.s.l.). In Germany, the river flows through the 50-km wide Upper Rhine River Valley with middle mountains in the east and west: the Vosges (source area of the Mosel River) and the Black Forest, after which it cuts through a middle mountain area, the *Rheinisches Schiefergebirge*. The eastern and northeastern part of the middle basin mainly consists of an undulating landscape. The Swabian and Franconian Alb, source areas of the Neckar and Main tributaries of the River Rhine, separate these parts from the Danube basin. Downstream of this area, the Ruhr tributary joins the river while it flows in the northwestern part of its basin: The North German Lowland and The Netherlands. Here, the river mainly flows through Quaternary deposits (fluvial clays, loess and cover sands), with ice-pushed ridges as the only relief, and ends in the North Sea.

In the River Rhine basin land use is mainly agricultural, with in the German part 37 % arable land, 17 % pastures, 30 % woodland and 16 % built-up and other (McClave 1996). The basin's climate is in general temperate, with an average temperature of 9 °C. The only exceptions are the Alpine area, with a mountain climate, and the basin's far eastern part, having a more continental character (McClave 1996). The annual precipitation amounts follow the elevation, declining from sometimes more than 2000 mm in the Alpine region and around 1400 mm in its valleys (mostly in the form of snow in the winter), via 1000–1400 mm in the middle mountains to about 600–800 mm in North German Lowlands and The Netherlands (Hendl 1994).

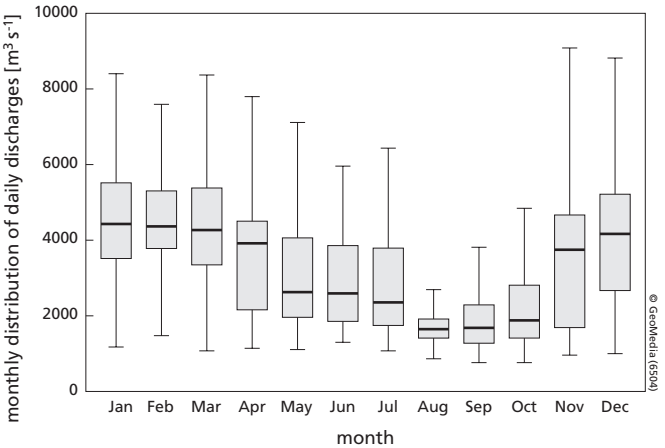

Figure 1.1 The distribution of daily River Rhine discharges per month at the Dutch-German border for 1901–2004.

The River Rhine's average discharge is approximately 2250 $m^3 s^{-1}$ at the Dutch-German border. Peak discharges may reach values above 9,000 $m^3 s^{-1}$ at the Dutch-German border and mainly occur during the winter season (due to rain) or early spring (due to snowmelt or rain) (Fig. 1.1). Shortly downstream from the Dutch-German border, the River Rhine splits in several distributaries: The Waal, IJssel and Nederrijn/Lek Rivers (Fig. 1.2). The Waal River discharges two-third of the River Rhine discharge that enters The Netherlands, whereas the IJssel River takes account of one-ninth and the Nederrijn/Lek two-ninth.

The lower River Rhine transports on average 3 10^9 kg of suspended sediment per year (Asselman *et al.* 2003), most of which is carried during low to moderate discharges (Fig. 1.3). Attached to the suspended sediment, the river carries approximately 1.2 10^6 kg Zn, 2.3 10^5 kg Pb, 1.9 10^5 kg Cu and 4 10^3 kg Cd per year (this study) to The Netherlands, where these heavy metals may subsequently be deposited on floodplains during floods. Because of past industrial activities in the Rhine basin, most Dutch floodplain soils are severely polluted with heavy metals (Middelkoop 2000).

The lower Rhine River floodplains are 'embanked floodplains'. These stretches of land are located between the river channel and a major embankment and are periodically flooded by the river (Fig. 1.4). The Dutch have constructed these major embankments between the 11th and the 14th century to protect the hinterland from flooding during peak discharges (Hesselink *et al.* 2003). Along the Waal River, at many places minor embankments directly along the river channel protect the floodplains from inundations by low-magnitude floods (Fig. 1.4). The IJssel River is mostly only bordered by natural levees, which are in general lower and discontinuous. At discharges exceeding 5000 to 7000 $m^3 s^{-1}$ at the Dutch-German border, the river inundates the floodplains with minor embankments. This occurs on average once every 6 to 7 years (Middelkoop 1997). Floodplains without minor embankments, however, may already be inundated at about 3500 $m^3 s^{-1}$, which occurs 4 to 5 times per year (Middelkoop 1997).

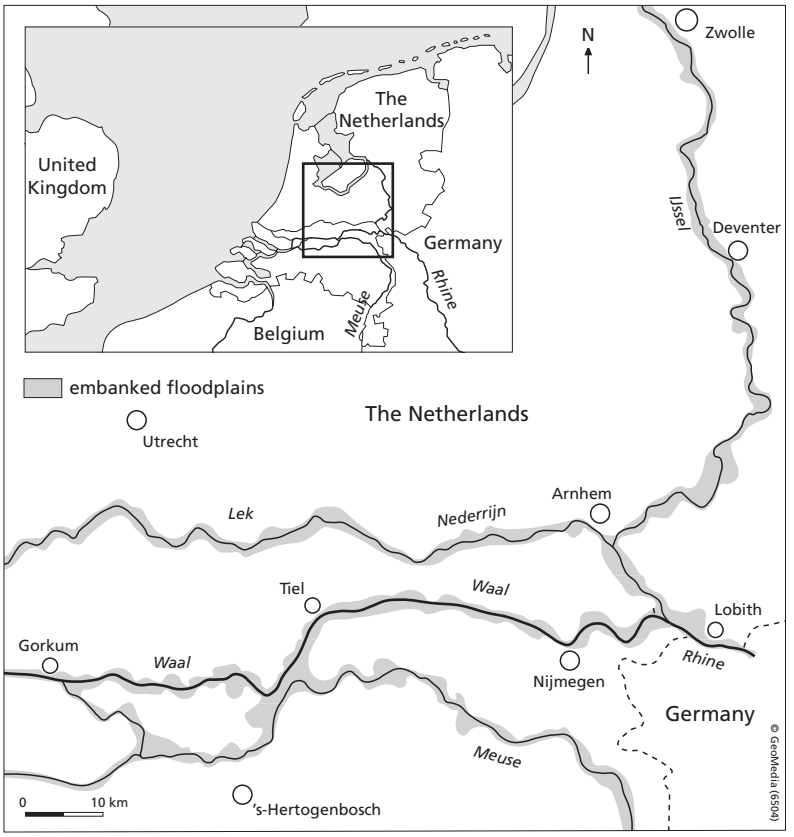

Figure 1.2 The lower Rhine River distributaries within The Netherlands.

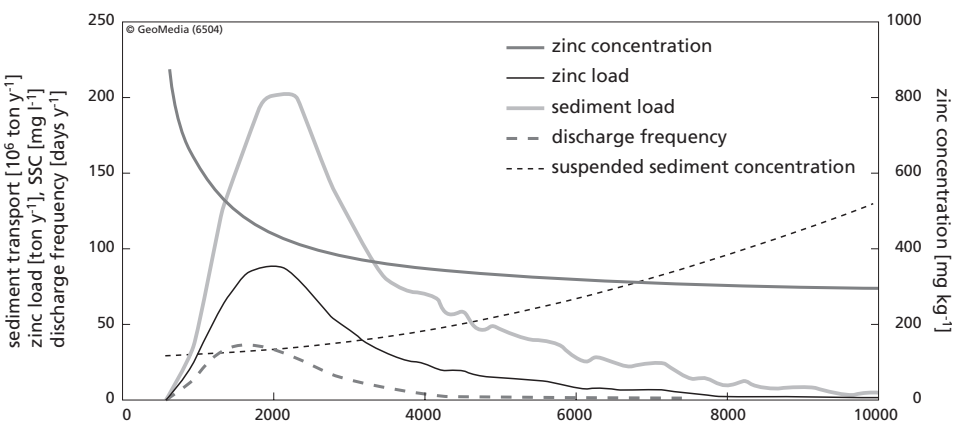

Figure 1.3 The transport of zinc and sediment and their concentrations in the river water at the Dutch-German border.

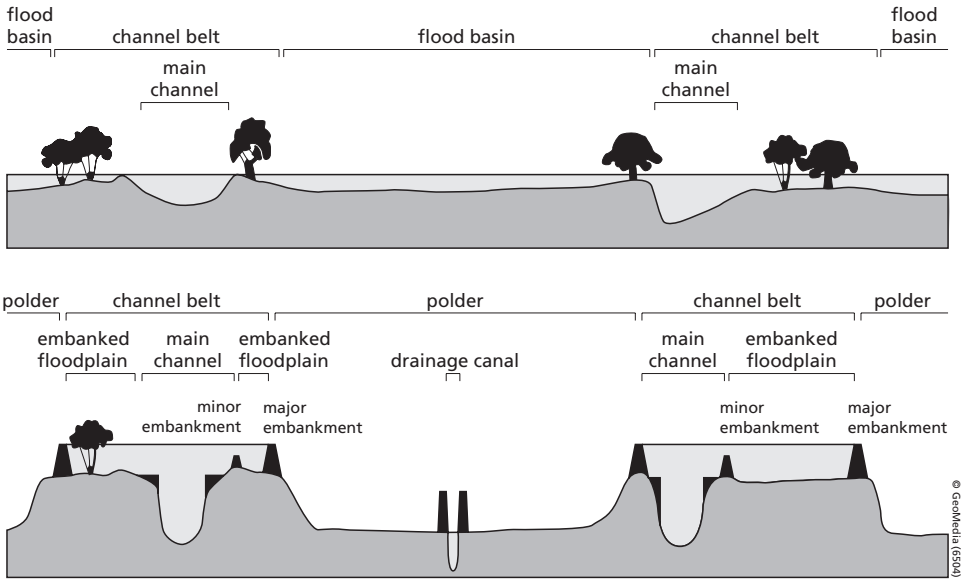

Figure 1.4 The Dutch lowland river area with its main characteristics. Adapted from: Hesselink (2002).

Land use in the Dutch lower River Rhine floodplains is mainly agricultural: of the 280 km^2 of floodplain area, 180 km^2 are agricultural area (Silva *et al.* 2001). Pasture (production grass land) covers about 60 %. Floodplain lakes (9 %), natural grass land (6 %), arable land and woodland (both 5 %) are only of minor importance (Silva *et al.* 2001). These figures are however about to change. The Dutch floodplains are a vital part of the Dutch Ecological Main Structure (*Ecologische Hoofdstructuur*, EHS) (LNV 2000) and its European counterpart Natura 2000 (EEC 1992; EC 1997). This means that in 2015 at least 100 to 110 km^2 of new nature should be realized in the Dutch River Rhine and Meuse floodplains (LNV 2000). Most recent government plans add 18 km^2 of extra nature in the Dutch lower River Rhine floodplains to these existing plans (V&W 2005). Because these plans concentrate on the Waal River (TK 2005), in some areas of this distributary the plans could lead to 50 % more natural areas in the period 1985–2025 (Lenders *et al.* 1998). Together with the other plans in V&W (2005) including the removal of minor embankments, excavation of secondary channels and the lowering of floodplains, these plans lead to more divers vegetation, which increases the hydrodynamics in the river area.

1.5 Research methods and thesis outline

To answer the research questions and meet the research goals, I carried out the following steps (Fig. 1.5):

- Literature review: I reviewed literature on factors and processes that may influence sediment and associated heavy metal deposition on floodplains to obtain an overview on this matter. This review is given in Chapter 2.
- Field measurements of floodplain deposition: I applied sediment traps in different floodplain sections along two river branches to assess the characteristics, amounts and patterns of contemporary deposition. Furthermore, I correlated these patterns and amounts with topographical and hydrodynamic factors. I also used these empirical data to check the floodplain deposition model (see below).
- Field measurements of suspended matter: I deployed a LISST-ST (*L*aser i*n* s*itu* *S*cattering *T*ransmissometry-*S*ettling *T*ube; Agrawal & Pottsmith 2001) during inundations of two floodplains to measure *in situ* settling velocities and floc sizes of suspended matter. Chapter 4 gives the results of these measurements. These results were also input to the floodplain deposition model.
- Modelling floodplain deposition: I developed a new floodplain deposition model (MoCSED) that minimizes numerical dispersion in a raster-GIS environment. For this purpose we implemented the Method of Characteristics (Konikow & Bredehoeft 1978) in the *PCRaster Dynamic Modelling Language* (Wesseling *et al.* 1996). Chapter 5 describes the model, and compares it to field data.
- Scenario analysis: I applied the MoCSED model to different scenarios of climate, upstream land-use and local topographical change for two floodplains that are to be rehabilitated in the near future. In these two floodplains I assessed both the present and future sediment and heavy-metal load and deposition pattern. Chapter 6 describes the outcomes of the scenario analysis.

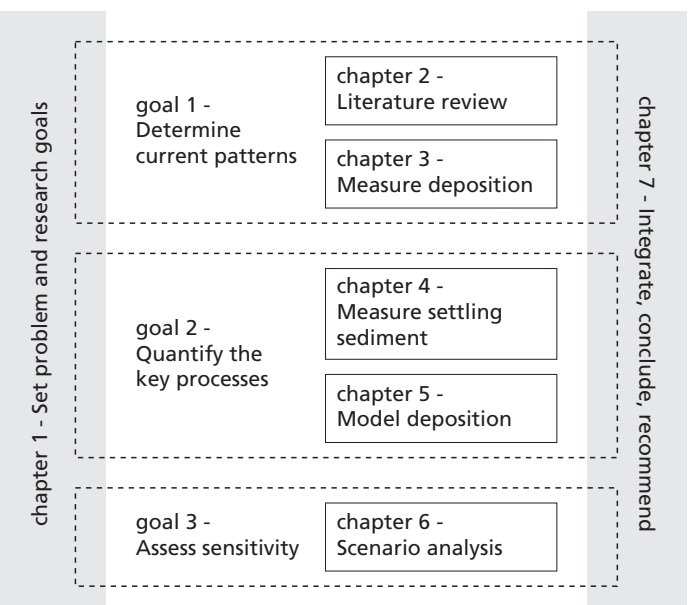

Figure 1.5 Outline of the thesis.

References

Adams, W.M. & M.R. Perrow (1999), Scientific and institutional constraints on the restoration of European floodplains. Geological Society Special Publication 163, pp. 89–97.

Agrawal, Y.C. & H.C. Pottsmith (2000), Instruments for particle size and settling velocity observations in sediment transport. Marine Geology 168, pp. 89–114.

Asselman, N.E.M. (1997), Suspended sediment in the river Rhine – The impact of climate change on erosion, transport and deposition. Utrecht: Koninklijk Nederlands Aardrijkskundig Genootschap/Faculteit Geowetenschappen, Universiteit Utrecht (Netherlands Geographical Studies 234).

Asselman, N.E.M. (1999a), The use of floodplain sedimentation measurements to evaluate the effects of river restoration works. Geological Society Special Publication 163, pp. 111–122.

Asselman, N.E.M. (1999b), Slibmodellering in RvR – fase 1. Delft: WL|Delft Hydraulics (WL Report R3337).

Asselman, N.E.M. (2000), Fitting and interpretation of sediment rating curves. Journal of Hydrology 234/3-4, pp. 228–248.

Asselman, N.E.M. & H. Middelkoop (1995), Floodplain sedimentation: quantities, patterns and processes. Earth Surface Processes and Landforms 20, pp. 481–499.

Asselman, N.E.M. & H. Middelkoop (1998), Temporal variability of contemporary floodplain sedimentation in the Rhine-Meuse delta, The Netherlands. Earth Surface Processes and Landforms 23/7, pp. 595–609.

Asselman, N.E.M., H. Middelkoop& P.M. Van Dijk (2003), The impact of changes in climate and land use on soil erosion, transport and deposition of suspended sediment in the River Rhine. Hydrological Processes 17/16, pp. 3225–3244.

Asselman, N.E.M. & M. van Wijngaarden (2002), Development and application of a 1D floodplain sedimentation model for the River Rhine in The Netherlands. Journal of Hydrology 268, pp. 127–142.

Allen, J.R.L. (1978), Keynote address: achievements and prospects in fluvial sedimentology. In: A.G. Miall, ed., Fluvial sedimentology. Canadian Society of Petroleum Geologists (Memoir 5).

Benedetti, M.M. (2003), Controls on overbank deposition in the Upper Mississippi River. Geomorphology 56, pp. 271–290.

Benke, A.C., I. Chaubey, G.M. Ward & E.L. Dunn (2000), Flood pulse dynamics in an unregulated river floodplain in the southeast U.S. coastal plain. Ecology 81/10, pp. 2730–2741.

Baptist, M.J., W. Ellis Penning, H. Duel, A.J.M. Smits, G.W. Geerling, G.E.M. van der Lee & J.S.L. van Alphen (2004), Assessment of Cyclic Floodplain Rejuvenation on flood levels and biodiversity along the Rhine River. River Research and Applications 20/3, pp. 285–297.

Bradley, S.B. & J.J. Cox (1986), Heavy metals in the Hamps and Manifold valleys, North Staffordshire, U.K.: Distribution in floodplain soils. The Science of the Total Environment 50, pp. 103–128.

Bradley, S.B. & J.J. Cox (1990), The significance of the floodplain to the cycling of metals in the River Derwent catchment, U.K.. The Science of the Total Environment 97-98, pp. 441–454.

Brown, A.G. (1996), Floodplain palaeoenvironments. In: M.G. Anderson, D.E. Walling & P.D. Bates, eds., Floodplain processes. Chichester, U.K.: John Wiley, pp. 95–138.

Brunet, R.C., G. Pinay, F. Gazelle & L. Roques (1994), Role of the floodplain and riparian zone in suspended matter and nitrogen retention in the Adour River, South-West France. Regulated Rivers: Research & Management 9, pp. 55–63.

CIW (2004), Water in focus 2004 – Annual report on water management in the Netherlands; http://www.waterinbeeld.nl/WIB2004E/index.html. The Hague: Commissie Integraal Waterbeheer, Ministerie van Verkeer & Waterstaat.

Dennis, I.A., M.G. Macklin, T.J. Coulthard & P.A. Brewer (2003), The impact of the October-November 2000 floods on contaminant metal dispersal in the River Swale catchment, North Yorkshire, U.K. Hydrological Processes 17/8, pp. 1641–1657.

Dijkstra, J.J., J.C.L. Meeussen & R.N.J. Comans (2004), Leaching of heavy metals from contaminated soils: an experimental and modeling study. Environmental Science & Technology 38/16, pp. 4390–4395.

Droppo, I.G., D.E. Walling & E.D. Ongley (1998), Suspended sediment structure: implications for sediment and contaminant transport modeling. IAHS Publication 249, pp. 437–444.

Droppo, I.G., D.E. Walling & E.D. Ongley (2000), The influence of floc size, density and porosity on sediment and contaminant transport. IAHS Publication 263, pp. 141–147.

EC (1997), Council Directive 97/62/EC of 27 October 1997 adapting to technical and scientific progress Directive 92/43/EEC on the conservation of natural habitats and of wild fauna and flora. Official Journal L 305, pp. 42–65.

EC (1998), Commission Directive 98/15/EC of 27 February 1998 amending Council Directive 91/271/EEC with respect to certain requirements established in Annex I thereof (Text with EEA relevance). Official Journal L 067, pp. 29–30.

EC (2000), Directive 2000/60/EC of the European Parliament and of the Council of 23 October 2000, establishing a framework for Community action in the field of water policy. Official Journal L 327, pp. 1–72.

EEC (1991), Council Directive 91/271/EEC of 21 May 1991 concerning urban waste-water treatment. Official Journal L 135, pp. 40–52.

EEC (1992), Council Directive 92/43/EEC of 21 May 1992 on the conservation of natural habitats and of wild fauna and flora. Official Journal L 206, pp. 7–50.

Förstner, U. & G.T.W. Wittmann (1983), Metal pollution in the aquatic environment. Berlin: Springer.

Foster, I.D.L. & S.M. Charlesworth (1996), Heavy metals in the hydrological cycle: trends and explanation. Hydrological Processes 10, pp. 227–261.

Gibbs, R.J. (1977), Transport phases of transition metals in the Amazon and Yukon Rivers. Geological Society of America Bulletin 88, pp. 829–843.

Gordeev, V.V., V. Rachold & I.E. Vlasova (2004), Geochemical behaviour of major and trace elements in suspended particulate material of the Irtysh river, the main tributary of the Ob river, Siberia. Applied Geochemistry 19, pp. 593–610.

Gretener, B. & L. Strömquist (1987), Overbank sedimentation rates of fine grained sediments. A study of the recent deposition in the lower River Fyrisån. Geografiska Annaler 69A/1, pp. 139–146.

He, Q. & D.E. Walling (1998), An investigation of the spatial variability of the grain size composition of floodplain sediments. Hydrological Processes 12/7, pp. 1079–1094.

Hendl, M. (1994), Klima. In: H. Liedtke & J. Marcinek, eds., Physische Geographie Deutschlands. Gotha, Germany: Justus Perthes, pp. 23–119.

Hendriks, J., J. de Jonge, P. den Besten & J. Faber (1997), Gifstoffen in het rivierengebied – Een belemmering voor natuurontwikkeling? Landschap 14/3, pp. 219–233.

Hesselink, A.W. (2002), History makes a river – Morphological changes and human interference in the river Rhine, The Netherlands. Utrecht: Koninklijk Nederlands Aardrijkskundig Genootschap/Faculteit Geowetenschappen, Universiteit Utrecht (Netherlands Geographical Studies 292).

Hesselink, A.W., H.J.T. Weerts & H.J.A. Berendsen (2003), Alluvial architecture of the human-influenced river Rhine, The Netherlands. Sedimentary Geology 161/3-4, pp. 229–248.

Horowitz, A.J. (1985), A primer on trace metal-sediment chemistry. Washington, DC: United States Geological Survey (USGS Water Supply Paper 2277).

Horowitz, A.J. (2000), NASQAN*: the design and implementation of a large-river suspended sediment and trace element flux programme. IAHS Publication 263, pp. 3–18.

Horowitz, A.J. & K. Elrick (1987), The relation of stream sediment surface area, grain size, and composition to trace element chemistry. Applied Geochemistry 2, pp. 437–451.

James, C.S. (1985), Sediment transfer to overbank sections. Journal of Hydraulic Research 23/5, pp. 435–452.

Japenga, J. & W. Salomons (1993), Dyke-protected floodplains: a possible chemical time bomb? Land Degradation & Rehabilitation 4/4, pp. 373–380.

Jungwirth, M., G. Haidvogl, S. Hoensinner, S. Muhar, S. Schmutz & H. Waidbacher (2005), Leitbild-specific measures for the rehabilitation of the heavily modified Austrian Danube River. Archiv für Hydrobiologie 155/1-4, pp. 7–36 (Large Rivers 15).

Knighton, D. (1984), Fluvial forms and processes. London: Edward Arnold.

Knox, J.C. (1993), Large increases in flood magnitude in response to modest changes in climate. Nature 361, pp. 430–432.

Kondolf, G.M. & H. Piégay (2003), Tools in fluvial geomorphology: problem statement and recent practice. In: G.M. Kondolf & H. Piégay, eds., Tools in fluvial geomorphology. Chichester, U.K.: John Wiley, pp. 3–22.

Konikow, L.F. & J.D. Bredehoeft (1978), Computer model of two-dimensional solute transport and dispersion in ground water. Techniques of Water-resources investigations of the United States Geological Survey. Reston, Virginia, USA: United Stated Geological Survey (Automated data processing and computations book 7).

Kooistra, L., R.S.E.W. Leuven, R. Wehrens, L.M.C. Buydens & P.N. Nienhuis (2001), A procedure for incorporating spatial variability in ecological risk assessment of Dutch river floodplains. Environmental Management 28, pp. 359–373.

Kesel, R.H., K.C. Dunne, R.C. McDonald, K.R. Allison & B.E. Spicer (1974), Lateral erosion and overbank deposition on the Mississippi River in Louisiana caused by 1973 flooding. Geology 2, pp. 461–464.

Kwadijk, J. (1993), The impact of climate change on the discharge of the River Rhine. Utrecht: Koninklijk Nederlands Aardrijkskundig Genootschap/Faculteit Geowetenschappen, Universiteit Utrecht (Netherlands Geographical Studies 171).

Lambert, C.P. & D.E. Walling (1987), Floodplain sedimentation: a preliminary investigation of contemporary deposition within the lower reaches of the River Culm, Devon, U.K. Geografiska Annaler 69A/3-4, pp. 393–404.

Lecce, S.A. (1997), Spatial patterns of historical overbank sedimentation and floodplain evolution, Blue River, Wisconsin. Geomorphology 18, pp. 265–277.

Lecce, S.A. & R.T. Pavlowsky (2004), Spatial and temporal variations in the grain-size characteristics of historical flood plain deposits, Blue River, Wisconsin, USA. Geomorphology 61, pp. 361–371.

Leenaers, H. (1991), Deposition and storage of solid-bound heavy metals in the floodplains of the River Geul (The Netherlands). Environmental Monitoring and Assessment 18/3, pp. 79–103.

Lenders, H.J.R., R.S.E.W. Leuven, P.H. Nienhuis, K.D. Oostinga & P.J.M. van den Heuvel (1998), Ecological rehabilitation of floodplains along the middle reach of the river Waal: a prosperous future for fauna target species? In: P.H. Nienhuis, R.S.E.W. Leuven & A.J.M. Ragas, eds., New concepts for sustainable management of river basins. Leiden, The Netherlands: Backhuys, pp. 115–130.

LNV (2000), Natuur voor mensen, mensen voor natuur – Nota natuur, bos en landschap in de 21e eeuw. The Hague: Ministerie van Landbouw, Natuur & Voedselkwaliteit.

Longfield, S.A. & M.G. Macklin (1999), The influence of recent environmental change on flooding and sediment fluxes in the Yorkshire Ouse basin. Hydrological Processes 13/7, pp. 1051–1066.

Maas, G.J., B. Makaske, P.W.F.M. Hommel, B.S.J. Nijhof & H.P. Wolfert (2003), Verstoring en successie: Rivierdynamiek en stroomdalvegetaties in de uiterwaarden van de Rijntakken. Wageningen, The Netherlands: Wageningen University and Research Centre (Alterra-rapport 759).

Malmon, D.V., T. Dunne & S.L. Reneau (2003), Stochastic theory of particle trajectories through alluvial valley floors. Journal of Geology 111, pp. 525–542.

Mansikkaniemi, H. (1985), Sedimentation and water quality in the flood basin of the River Kyrönjoki in Finland. Fennia 163/1, pp. 155–194.

Marriott, S. (1992), Textural analysis and modelling of a flood deposit: River Severn, U.K. Earth Surface Processes and Landforms 17, pp. 687–697.

Marriott, S.B. (1998), Channel-floodplain interactions and sediment deposition on floodplains. In: R.G. Bailey, P.B. José & B.R. Sherwood, eds., United Kingdom Floodplains. Otley, U.K.: Westbury Academic & Scientific.

Marron, D.C. (1992), Floodplain storage of mine tailings in the Belle Fourche River system: a sediment budget approach. Earth Surface Processes and Landforms 17, pp. 675–685.

McClave, D.E. (1996), The society and its environment. In: E. Solsten, ed., Germany: A country study. Washington, DC: Federal Research Division, Library of Congress, pp. 131–192.

Mertes, L.A. (1994), Rates of flood-plain sedimentation on the central Amazon River. Geology 22, pp. 171–174.

Middelkoop, H. (1995), The impact of climate change on the sedimentation rates on the embanked floodplains in the Netherlands. Studies in Environmental Science 65B, pp. 931–936.

Middelkoop, H. (1997), Embanked floodplains in the Netherlands: Geomorphological evolution over various time scales. Utrecht: Koninklijk Nederlands Aardrijkskundig Genootschap/Faculteit Geowetenschappen, Universiteit Utrecht (Netherlands Geographical Studies 224).

Middelkoop, H. (2000), Heavy-metal pollution of the Rhine and Meuse floodplains in the Netherlands. Netherlands Journal of Geosciences 79/4, pp. 411–428.

Middelkoop, H. & Asselman, N.E.M. (1998), Spatial variability of floodplain sedimentation at the event scale in the Rhine-Meuse delta, The Netherlands. Earth Surface Processes and Landforms 23, pp. 561–573.

Middelkoop, H. & Van der Perk, M. (1998), Modelling spatial patterns of overbank sedimentation on embanked floodplains. Geografiska Annaler 80A/2, pp. 95–109.

Nanson, G.C. & Croke, J.C. (2002), Emerging issues in flood plain research. IAHS Publication 276, pp. 271–278.

Nicholas, A.P. & D.E. Walling (1996), The significance of particle aggregation in the overbank deposition of suspended sediment on river floodplains. Journal of Hydrology 186, pp. 275–293.

Nicholas, A.P. & D.E. Walling (1997), Modelling flood hydraulics and overbank deposition on river floodplains. Earth Surface Processes and Landforms 22/1, pp. 59–77.

Noppert, F., J.W. Dogger, F. Balk & A.J.M. Smits (1993), Secondary poisoning in a terrestrial food chain: a probabilistic approach. In: H.J.P. Eijsackers & T. Hamers, eds., Integrated soil and sediment approach: a basis for proper protection. Dordrecht, The Netherlands: Kluwer Academic, pp. 303–307.

Notten, M.J.M., A.J.P. Oosthoek, J. Rozema & R. Aerts (2005), Heavy metal concentrations in a soil-plant-snail food chain along a terrestrial soil pollution gradient. Environmental Pollution 138, pp. 178–190.

Ogden, R. & M.C. Thoms (2002), The importance of inundation to floodplain soil fertility in a large semi-arid river. Internationale Vereinigung für Theoretische und Angewandte Limnologie 28, pp. 744– 749.

Owens, P.N., D.E. Walling, J. Carton, A.A. Meharg, J. Wright & G.J.L. Leeks (2001), Downstream changes in the transport and storage of sediment-associated contaminants (P, Cr and PCBs) in agricultural and industrialized drainage basins. The Science of the Total Environment 266, pp. 177–186.

Pfister, L., J. Kwadijk, A. Musy, A. Bronstert, & L. Hoffmann (2004), Climate change, land use change and runoff prediction in the Rhine-Meuse basins. River Research and Applications 20/3, pp. 229–241.

Pizzuto, J.E. (1987), Sediment diffusion during overbank flows. Sedimentology 34/2, pp. 301–317.

Römkens, P.F.A.M., L.T.C. Bonten, R.P.J.J. Rietra, J.E. Groenenberg, A.C.C. Plette & J. Bril (2003), Uitspoeling van zware metalen uit landbouwgronden; Schatting van de bijdrage van uitspoeling uit landbouwgronden aan de belasting van het oppervlaktewater: modelaanpak en resultaten. Wageningen, The Netherlands: Wageningen University and Research Centre (Alterra-rapport 791/RIZA-rapport 2003.018).

Salomons, W. & Förstner, U. (1984), Metals in the hydrocycle. Berlin: Springer.

Schipper, A. (*in preparation*), Ecological risks of heavy metal pollution in river floodplains. PhD Thesis, Nijmegen, The Netherlands: Radboud Universiteit Nijmegen.

Silva, W., F. Klijn, & J.P.M. Dijkman (2001), Room for the Rhine branches in The Netherlands – what the research has taught us. Arnhem/Delft, The Netherlands: RIZA/WL|Delft Hydraulics (RIZA-report 2001.031).

Simm, D.J. & D.E. Walling (1998), Lateral variability of overbank sedimentation on a Devon flood plain. Hydrological Sciences Journal 43/5, pp. 715–732.

Stam, M.H. (2002), Effects of land-use and precipitation changes on floodplain sedimentation in the nineteenth and twentieth centuries (Geul River, The Netherlands). Special Publication of the International Association of Sedimentologists 32, pp. 251–267.

Steiger, J., A.M. Gurnell (2002), Spatial hydrogeomorphological influences on sediment and nutrient deposition in riparian zones: observations from the Garonne River, France. Geomorphology 49, pp. 1–23.

Steiger, J., A.M. Gurnell, P. Ergenzinger & D. Snelder (2001), Sedimentation in the riparian zone of an incising river. Earth Surface Processes and Landforms 26/1, pp. 91–108.

Stewart, M.D., P.D. Bates, D.A. Price & T.P. Burt (1998), Modelling the spatial variability in floodplain soil contamination during flood events to improve chemical mass balance estimates. Hydrological Processes 12/8, pp. 1233–1255.

Sweet, R.J, A.P. Nicholas, D.E. Walling & X. Fang, (2003), Morphological controls on medium-term sedimentation rates on British lowland river floodplains. Hydrobiologia 494, pp. 177–183.

Terry, J.P., S. Garimella & R.A. Kostaschuk (2002), Rates of floodplain accretion in a tropical island river system impacted by cyclones and large floods. Geomorphology 42, pp. 171–182.

Thoms, M.C. (2003), Floodplain–river ecosystems: lateral connections and the implications of human interference. Geomorphology 56/3-4, pp. 335–349.

Thoms, M., J.M. Foster, & B. Gawne (2000a), Flood-plain sedimentation in a dryland river: the River Murray, Australia. IAHS Publication 263, pp. 227–235.

Thoms, M.C., C.R. Parker & M. Simons (2000b), The dispersal and storage of trace metals in the Hawkesbury River valley. In: S. Brizga, & B. Finlayson, eds., River management: The Australasian experience. Chichester, U.K.: John Wiley, pp. 197–219.

TK (2005), Nota ruimte – Deel 3A: Aangepast kabinetsstandpunt naar aanleiding van behandeling in de Tweede Kamer. The Hague: Tweede Kamer der Staten Generaal (brief Tweede Kamer, Vergaderjaar 2004–2005, 29435, nummer 154).

Tockner, K., F. Malard & F.J. Ward (2000), An extension of the flood pulse concept. Hydrological Processes 14/16-17, pp. 2861–2883.

Van den Brink, N.W., N.M. Groen, J. De Jonge & A.T.C. Bosveld (2003), Ecotoxicological suitability of floodplain habitats in The Netherlands for the little owl (*Athene noctua vidalli*). Environmental Pollution 122/1, pp. 127–134.

Van der Lee, G.E.M., H. Olde Venterink, & N.E.M. Asselman, (2004), Nutrient retention in floodplains of the Rhine distributaries in The Netherlands. River Research and Applications 20, pp. 315–325.

Van der Perk, M., A.C.D. Ertsen & W. Bleuten (1992), Modellering van slibsedimentatie van zware-metalenbelasting in een uiterwaard langs de Waal. H_2O 25/9, 233–237.

Van Dijk, P.M. (2001), Soil erosion and associated sediment supply to rivers – Seasonal dynamics, soil conservation measures and impacts of climate change. PhD Thesis, Amsterdam: Universiteit van Amsterdam.

Van Griethuysen, C., J. van Baren, E.T.H.M. Peeters & A.A. Koelmans (2004), Trace metal availability and effects on benthic community structure in floodplain lakes. Environmental Toxicology and Chemistry 23/3, pp. 668–681.

Van Metre, P.C., B.J. Mahler & E.T. Furlong (2000), Urban sprawl leaves its PAH signature. Environmental Science & Technology 34/19, pp. 4064–4070.

Van Vliet, P.C.J., S.E.A.T.M. van der Zee & W.C. Ma (2005), Heavy metal concentrations in soil and earthworms in a floodplain grassland. Environmental Pollution 138/3, pp. 506–517.

Vijver, M.G. (2005), The ins and outs of bioaccumulation; Metal bioaccumulation kinetics in soil invertebrates in relation to availability and physiology. PhD Thesis, Amsterdam: Vrije Universiteit (Thesis VU-IES 2005-1).

Vink, J., ed. (2000), Mechanismen van opname, accumulatie en toxiciteit van zware metalen bij uiterwaardenvegetatie. Lelystad, The Netherlands: RIZA (RIZA rapport 2000.016).

Vink, R.J. (2002), Heavy metal fluxes in the Elbe and Rhine river basins: Analysis and modelling. PhD Thesis, Amsterdam: Vrije Universiteit.

V&W (2005), PKB Ruimte voor de Rivier: Deel 1 – Deel B: Nota van toelichting. The Hague: Ministerie van Verkeer & Waterstaat.

Walling, D.E. (1999), Linking land use, erosion and sediment yields in river basins. Hydrobiologia 410, pp. 223–240.

Walling, D.E., S.B Bradley & C.P. Lambert (1986), Conveyance losses of suspended sediment within a floodplain system. IAHS Publication 159, pp. 119–131.

Walling, D.E. & Q. He (1998), The spatial variability of overbank sedimentation on river floodplains. Geomorphology 24, pp. 209–223.

Walling, D.E. & P.N. Owens (2003), The role of overbank floodplain sedimentation in catchment contaminant budgets. Hydrobiologia 494, pp. 83–91.

Walling, D.E., P.N. Owens & G.J.L. Leeks (1998a), Erratum to "The characteristics of overbank deposits associated with a major flood event in the catchment of the River Ouse, Yorkshire, U.K.". Catena 32/3-4, pp. 309–331.

Walling, D.E., P.N. Owens & G.J.L. Leeks (1998b), The role of channel and floodplain storage in the suspended sediment budget of the River Ouse, Yorkshire, U.K. Geomorphology 22, pp. 225–242.

Walling, D.E., P.N. Owens & G.J.L. Leeks (1999). Rates of contemporary overbank sedimentation and sediment storage on the floodplains of the main channel systems of the Yorkshire Ouse and River Tweed, U.K.. Hydrological Processes 13/7, pp. 993–1009.

Walling, D.E., P.N. Owens, J. Carter, G.J.L. Leeks, S. Lewis, A.A. Meharg, & J. Wright (2003), Storage of sediment-associated nutrients and contaminants in river channel and floodplain systems. Applied Geochemistry 18, pp. 195–220.

Walling, D.E. & J.C. Woodward (2000), Effective particle size characteristics of fluvial suspended sediment transported by lowland British rivers. IAHS Publication 263, pp. 129–139.

Wesseling, C.G., D. Karssenberg, W.P.A. Van Deursen & P.A. Burrough (1996), Integrating dynamic environmental models in GIS: the development of a Dynamic Modelling language. Transactions in GIS 1/1, pp. 40–48.

Wijnhoven, S., I. Thonon, G. Van der Velde, R.S.E.W. Leuven, M.I. Zorn, H.J.P. Eijsackers & A.J.M. Smits (*submitted*), The impact of bioturbation by small mammals on heavy metal redistribution in floodplains. Water, Air and Soil Pollution.

Wolterbeek, H.T., T.G. Verburg & T.G. van Meerten (1996), On the 1995 flooding of the rivers Meuse, Rhine and Waal in The Netherlands: metal concentrations in deposited river sediments. Geoderma 71/1-2, pp. 143–156.

Wolters, H.A., M. Platteeuw & M.M. Schoor, eds. (2001), Richtlijnen voor inrichting en beheer van uiterwaarden – ecologie en veiligheid gecombineerd. Lelystad, The Netherlands: RIZA (RIZA rapport 2001.059).

Wyżga, B. (1999), Estimating mean flow velocity in channel and floodplain areas and its use for explaining the pattern of overbank deposition and floodplain retention. Geomorphology 28, pp. 218–297.

Zorn, M.I. (2005), The floodplain upside down – Interactions between earthworm bioturbation, flooding and pollution. PhD Thesis, Amsterdam: Vrije Universiteit.

2 The chain of factors and processes affecting deposition of sediment and associated heavy metals on floodplains

"*Of all the political, economic and technical constraints on floodplain restoration, perhaps the most significant is the lack of scientific knowledge.*" (Brookes 1996).

"*Effective ecotone management requires an integrated approach in which land and water issues and sediment aspects are all considered. This requires a better understanding of the fate of sediment (…) and the influences controlling them.*" (Thoms *et al.* 2000a).

2.1 Introduction

In recent years, deposition of sediment (e.g., Benedetti 2003; Steiger *et al.* 2001; Van der Lee *et al.* 2004; Walling 1999a) and associated heavy metals (e.g., Middelkoop 2000; Thoms *et al.* 2000b; Vink & Behrendt 2002; Walling *et al.* 2003) on lowland river floodplains has received a lot of attention from researchers. Their studies have shown that a wide range of processes and factors influences the pattern and amount of the sediment and associated metal deposition (Fig. 2.1). First, the amount of heavy metals emitted by industries and households in the upstream part of the catchment determines the degree of contamination of the water and sediments (left part of Fig. 2.1). Then, during transport within the river, suspended sediment concentrations and water pH determine the partitioning of heavy metals over the dissolved and sediment-associated fractions (Horowitz 1985). In the lower reaches, the river may deposit these sediment-associated metals on floodplains. Discharge, flow velocity, grain size and settling velocity determine the amount and pattern of this deposition (Simm 1995) (grey area of Fig. 2.1). Eventually, physical and chemical soil characteristics like pH, redox potential and clay content determine the amount of metals that plants and animals may take up and the groundwater may receive (Salomons & Förstner 1984).

Especially for contaminated rivers like those in densely populated and industrialized countries, it is important to understanding why, where and how contamination of floodplains with heavy metals takes place. Environmental regulation has curtailed metal emissions (e.g., EEC 1991; EC 1998), but metal concentrations remain in most cases above background level (CIW 2004). As such, the River Rhine continues to deposit sediment-associated metals on its floodplains. Yet, new environmental regulations (e.g., EC 2000), climate change (Middelkoop *et al.* 2001), upstream land-use change (Asselman *et al.* 2003) and floodplain rehabilitation (Silva *et al.* 2001) may affect the chain of processes governing this metal deposition (Fig. 2.1). Understanding this

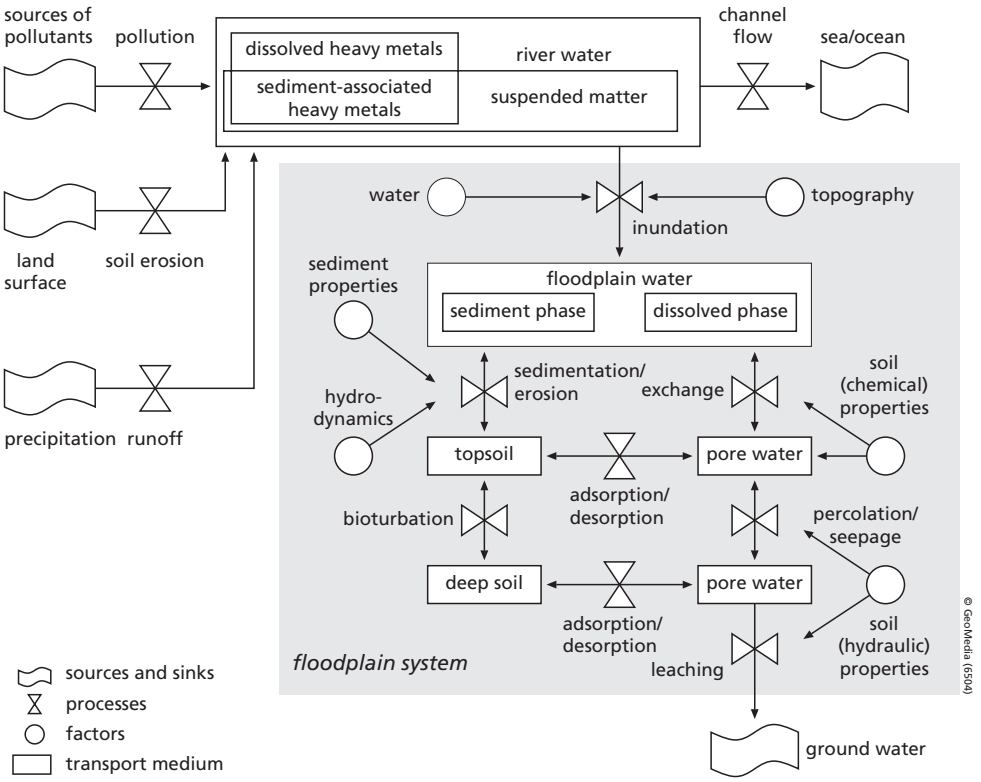

Figure 2.1 Processes and factors governing the fate of heavy metals in the course from the uplands to the sea.

process chain helps to assess the effect these changes could have on the heavy-metal deposition on lowland river floodplains. Yet, an understanding of the total sequence of factors and processes affecting floodplain deposition is still lacking (Walling 1999b; Asselman *et al*. 2003).

The purpose of this chapter is to review this chain of processes affecting heavy-metal deposition. It gives special attention to the River Rhine and its floodplains, since the River Rhine is an excellent example of a lowland river with a densely populated and industrialized basin (Förstner 1989). The review will follow the outline given in Fig. 2.1.

2.2 Sources and transport of sediment and heavy metals

2.2.1 Sediment yield

In large rivers such as the River Rhine, suspended sediment yield is supply-limited. Three aspects affecting sediment yield are important for heavy-metal deposition. Firstly, the amount of soil erosion is important because it determines the *potential* sediment load in rivers. Secondly,

sediment delivery determines the *actual* sediment load in rivers. Thirdly, the grain size of the material affects the heavy metal concentrations on the sediment (see Section 2.2.4).

Asselman (1997) reviewed soil erosion studies in the River Rhine basin. In addition, she developed the Rhine Soil Loss Model, based on the Universal Soil Loss Equation. Her calculations show that soil erosion may vary from 23 ton km^{-2} y^{-1} in the Lahn Catchment (Hessen, Central Germany, Fig. 2.2) to more than 10,000 ton km^{-2} y^{-1} in the Alps. Van Dijk (2001) developed the somewhat more expanded RECODES model ('The Rhine model for evaluating effects of Environmental Change On Delivery of Eroded soil to Streams') based on the GAMES model by Dickinson *et al.* (1986). He gives values for soil erosion ranging from 52.2 ton km^{-2} y^{-1} in the Saar catchment (Saarland, Western Germany, Fig. 2.2) to more than 312 ton km^{-2} y^{-1} in the Rhine stretch between Basel and Maxau (Fig. 2.2). He concluded that soil erosion in the Rhine River catchment mainly occurs in the Swiss *Mittelland*, on vineyard slopes along the central reach of the river and on the hills in the loess regions in Central Germany. Yet, mainly because of deposition in Swiss lakes, only about half of the eroded soil is delivered to the River Rhine channel (Van Dijk 2001), leading to a total average sediment delivery of only 73 ton km^{-2} y^{-1}.

Far less studies exist on sediment delivery than on soil erosion (Walling 1990; Slattery & Burt 1997; Asselman *et al.* 2003). Foster *et al.* (1990) and Naden & Cooper (1998) argue that *"the links between the hillslope and river channel remain less well understood"* and are *"ill defined"*. Fryirs & Brierley (2001) noted that *"off-site implications of sediment transfer have seldom been assessed in terms of catchment-wide sediment budgets"*. Yet, Foster *et al.* (1990) argue that *"in evaluating the 'off-farm' impacts of soil erosion, (…), an understanding of sediment delivery and transfer mechanisms is of vital significance"*.

The efficiency of a catchment in delivering the eroded soil to the river network is often denoted with the sediment delivery ratio (SDR). This is the ratio between transported and eroded soil, being defined at the outlet of the catchment. Walling & Webb (1992) and Walling (1990) point out that SDRs mostly are low because much of the sediment is stored within the catchment and may never reach the outlet or only with a time lag. This is often the case in larger catchments, since these exhibit longer distances to the river and hence more possibilities for (temporal) storage of eroded sediment (Steegen *et al.* 2000). This storage of sediment especially occurs in summer when crops cover the fields and provide ample locations for sedimentation. Hence, in summer SDRs tend to be low because of retention of sediment within the fields (Steegen *et al.* 1998). In winter, this retention possibility is absent due to low soil cover. However, during winter low transport capacity of the overland flow limits sediment transfer to the river (Slattery & Burt 1997). Therefore, although the absolute amount of eroded sediment is higher during winter than summer, SDRs in cultivated catchments tend to be low in winter, too. Dedkov (2004) shows that in cultivated catchment increasing catchment size leads to a decreasing SDR, probably because of these increasing possibilities for sediment retention. The Rhine catchment, being large in size and intensively cultivated at the same time, also has a low SDR. Of the sediment that has reached the river channel, only 27 % reaches the Dutch-German border, being $3.1\ 10^6$ ton y^{-1} (Asselman *et al.* 2003). In addition, Asselman (1997) indicates that the SDRs for the Rhine subcatchments decrease with increasing subcatchment size, amount of soil erosion and discharge.

Figure 2.2 The Rhine basin.

In the headwaters, two counteracting processes determine how median grain size is related to discharge. On the one hand, selective erosion by overland flow mainly provides fine-grained sediment: more runoff leads to finer material (Walling 1990; Slattery & Burt 1997; Erskine *et al*. 2002). On the other hand, overland flow increases the discharge of small headwater streams. This increases the flow's competence to carry coarser sediment (Walling 1990; Steegen *et al*. 1998, 2000), more runoff leads to more coarse sediment. Unfortunately, few investigations have been made to clarify which of the two processes prevails. Slattery & Burt (1997) argue that more runoff leads to a larger amount of fine particles. They attribute this to the direct delivery of fines by overland flow through rills and wheel tracks to the river, while they observed coarser sediment being deposited before reaching the river network. They also expect break up of aggregates at higher discharges because of increased shear. A third factor they mention is the depletion of coarse grains by selective deposition on riverbanks, causing downstream fining (Simm & Walling 1998). Walling *et al*. (1998a) indeed indicated that floodplain deposits are coarser than the suspended load in the stream water for some British streams. However, He & Walling (1998) could not find clear evidence for this. For the River Rhine at the Dutch-German border, Asselman & Middelkoop (1998) report that the median grain size (d_{50}) decreases with increasing discharge, being approximately 35 μm at 1500 $m^3 s^{-1}$ at the Dutch-German border and decreasing to about 10 μm for discharges above 4000 $m^3 s^{-1}$.

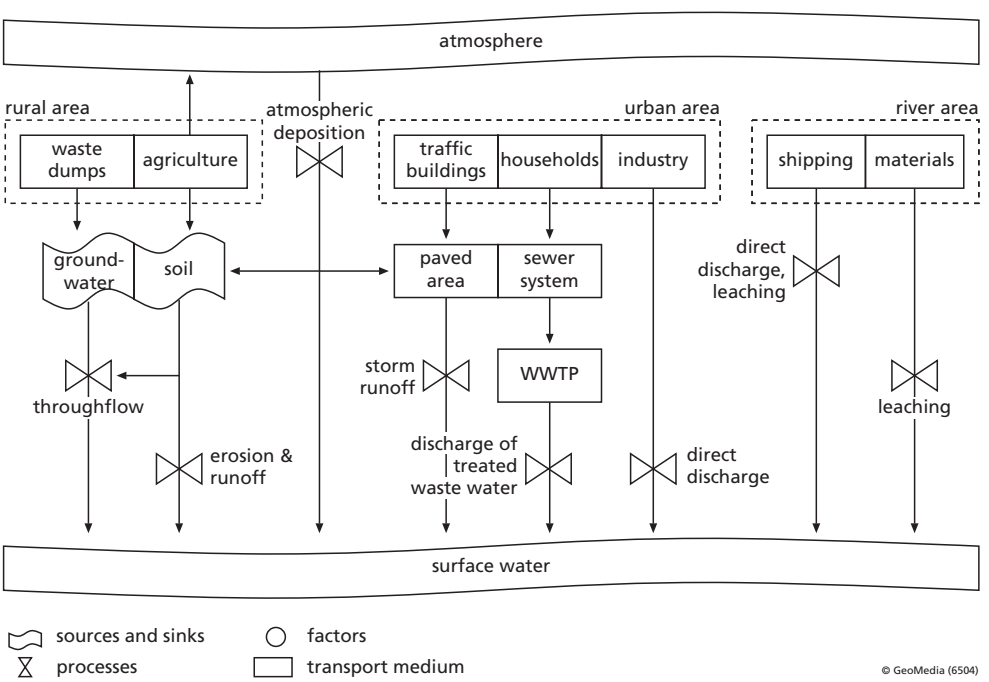

Figure 2.3 Processes, compartments and sources of heavy metals on their way to surface water. Adapted from: Vink & Peters (2003).

2.2.2 Sources and input of heavy metals

In general, sources of contamination are divided in point and diffuse sources. Vink *et al.* (1999) and Vink & Behrendt (2002) subdivided these sources as follows (Fig. 2.3):

- Point sources:
  - direct industrial effluents;
  - wastewater treatment plants (WWTPs).
- Diffuse sources:
  - surface runoff (including load from atmospheric deposition);
  - groundwater flow;
  - soil erosion;
  - agriculture (application of manure, fertilizers and pesticides);
  - diffuse loads of paved urban areas (atmospheric deposition, traffic, corrosion);
  - combined sewer overflows.

According to Vink & Behrendt (2002), in the Rhine catchment 70 (Cu) to 76 % (Cd) of the heavy metals come from diffuse sources (including soil erosion). Heavy metals enter the river system in three phases: dissolved, as aerosols or attached to soil particles (Förstner & Wittmann 1983). Although most metals enter the river in dissolved form, in neutral to alkaline conditions they soon adhere to suspended matter in the river (Blanc *et al.* 1999; Audrey *et al.* 2004; see Section 2.2.3).

Another classification can be made according to natural or anthropogenic sources. 'Semi-natural' sources such as surface runoff, soil erosion and groundwater flow are nowadays responsible for about half the load of heavy metals in the Rhine River (Vink & Behrendt 2002; Fig. 2.4). Weathering and subsequent erosion of sediment causes a large part of input, especially for lead (Fig. 2.4). Soil erosion of natural soils provides a major part of the background concentration of heavy metals in sediments. Table 2.1 gives an indication of the level of these background concentrations. Despite the abundance of literature on erosion of mine tailings in some areas (e.g., Miller 1997; Allen & Salomons 1995, 1997), this appears to be of minor importance in the Rhine catchment.

Table 2.1 Background values [mg kg^{-1}] for the most important heavy metals in contemporaneous contamination.

River	Zn	Pb	Cu	Cd
Earth's crust [a]	16–130	1–20	4–87	0.035–0.3
Agricultural topsoil [b]	60	27	20	0.3
Loess [c]	45	32	14	
Lower Rhine [d]	95	30	25	
Holocene Meuse [e]	101	28	18	
Meuse [f]	82	26	16	2.1

Sources: a. Range for igneous and sedimentary rocks in Turekian & Wedepohl (1961); b. Vink (2002); c. Hindel et al. (1996); d. Middelkoop (2002); e. values for Holocene non-calcareous sediments in Tebbens *et al.* (2000); f. average values for Meuse tributaries in southern Belgium (Swennen & Van der Sluys 1998).

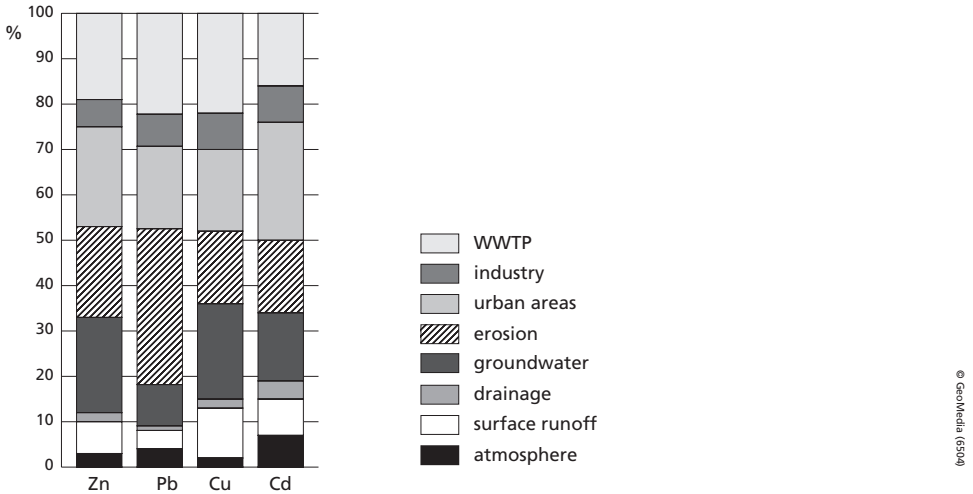

Figure 2.4 Contribution of different sources to heavy metal loads in the River Rhine. Adapted from: Vink & Behrendt (2002).

Of the anthropogenic sources, urban areas are the main contributors of heavy metals (Thoms & Tiel 1995; Foster & Charlesworth 1996; Fig. 2.4). Urban areas, industry and WWTPs taken together contribute about 50 % (Vink & Behrendt 2002; Fig. 2.4). Despite an enormous decline in the past decades (Vink & Peters 2003; Rautengarten 1993), a number of industries still emits heavy metals to surface waters. Obviously the electroplating and steel industry figure among them (Förstner & Wittmann 1983; Vink *et al*. 1999), but also book printers, paint producers and textile factories emit heavy metals (Sin *et al*. 2001). Gordeev *et al*. (2004) attributed a threefold increase in cadmium concentration of suspended matter in the Ob River to industrial and municipal sewage in the city of Omsk. Schouten *et al*. (2000) reported that the cadmium content in freshly deposited sediment along the Meuse River downstream from the industrial area of Liege (Belgium) is more than tenfold the upstream content.

Förstner & Wittmann (1983) already indicated that urban storm-water runoff, sewage overflows and residential water contribute most heavy metals to surface water. Vink & Behrendt (2002) point out that nowadays wastewater treatment plants are the main contributing point sources of heavy metals (Fig. 2.4). Yet, the concentration of pollutants in urban storm-water runoff may attain 100 to 1000 times the concentrations for treated wastewater (Bradley 1977, *in* Förstner & Wittmann 1983), making this the most polluting of the urban sources (Foster & Charlesworth 1996). In either case, elevated levels of copper, zinc, lead and to a lesser extent cadmium result from corrosion of roofs and the water supply and traffic exhausts (Förstner & Wittmann 1983; Rautengarten 1993).

Major anthropogenic atmospheric sources of heavy metals are the combustion of fossil fuels, incinerators, smelting and cement production (Förstner & Wittmann 1983; Rautengarten 1993). Via deposition of aerosols these heavy metals either enter the surface water directly via channel precipitation or indirectly via the catchment (Fig. 2.3).

A third anthropogenic source of heavy-metal contamination is agriculture (Fig. 2.3; Table 2.1). Soil fertilizers, manure, fungicides and herbicides may all contain heavy metals (Wong *et al.* 2002), of which 0.4 to 3 % directly flows into the surface water (Vink *et al.* 1999). Fertilizers based on phosphate often contain fairly large amounts of trace metals such as cadmium (Förstner & Wittmann 1983). Also manure may contain elevated amounts of heavy metals (mainly copper). Winegrowers use for example fungicides such as copper sulphate (Van der Perk *et al.* 2004). Because of the presence of vineyards in the central part of the Rhine basin, this is locally an important source of heavy metals in the surface water. Martin (1997) found lead and zinc concentrations twice as high as background values in the floodplains of a small Rhine tributary without any industrial history. These elevated levels may thus be attributed to the combination of atmospheric and agricultural sources.

2.2.3 Partitioning of heavy metals

Table 2.2 gives an overview of the partitioning between sediment and dissolved phase for a number of streams, including the River Rhine. The sediment-water distribution coefficient (K_d value), pH of the river water, provenance (i.e., catchment geology) of the suspended load and contamination degree determine this partitioning.

A general way of describing the sediment-water partitioning of heavy metals is the partition/distribution coefficient or K_d value. A lower distribution coefficient means a higher solubility and more heavy metals in the water phase. This distribution coefficient is defined as

$$K_d = [M]_{sed}/[M]_{dis} \tag{2.1}$$

in which K_d = distribution coefficient [l kg^{-1}], $[M]_{sed}$ = heavy-metal concentration in sediment phase [mg kg^{-1}] and $[M]_{dis}$ = heavy-metal concentration in water phase [mg l^{-1}].

Distribution coefficients are not only metal-dependent but also depend on sediment characteristics and total concentration of dissolved elements. The most important sediment characteristic in this respect is the cation exchange capacity (CEC), depending on clay, organic matter content and pH. The element concentrations encompass both cation and anion concentrations. Cation concentrations determine the competition for binding sites between ions with different valences (e.g., between Na^+ and Zn^{2+}). Anions may provide possibilities for complexation (e.g., $CdCl^+$), although this is only important in brackish and salt water (Appelo & Postma 1994).

Because notably sediment properties vary widely, values for the K_d coefficient typically vary over several orders of magnitude for one metal in one river (Veselý *et al.* 2001; Vink 2002; Carlon *et al.* 2004). Yet, no universal equation is available to derive K_d from water chemistry, nor is the K_d coefficient for one river applicable to another river (Lofts & Tipping 1998, 2000). Still, it can be used to calculate the values in Table 2.2:

$$F_{sed} = 1 - \frac{1}{(SSC \cdot K_d) + 1} \tag{2.2}$$

with F_{sed} = Fraction of heavy metal attached to sediment [–], SSC = suspended sediment concentration [kg l^{-1}].

Leaving all other factors equal, the influence of pH on metal solubility is straightforward: a decrease in pH leads to an increase in heavy metals in the dissolved phase. At higher pH levels, sediments attain a negative charge, thus attracting heavy metals from the dissolved phase (Mouvet & Bourg 1983). In addition, at lower pH levels more H^+ ions compete with heavy metals for binding places at the suspended matter (see also Section 2.4.3).

Organic matter can disturb this straightforward influence of pH. Yin *et al.* (2002) attribute this to the high affinity of heavy metals for organic molecules. If these molecules are part of suspended organic matter, high levels of total organic carbon (TOC) hamper the increase in metal solubility with decreasing pH level (Gundersen & Steinnes 2003). However, if the organic molecules are dissolved, metal solubility increases with increasing dissolved organic matter content and the influence of pH decreases (Yin *et al.* 2002).

Table 2.2 Percentage of total heavy-metal load bound to suspended matter in different rivers.

Reference	River	Zn	Pb	Cu	Cd
Martin & Meybeck (1979)	(1 – DTI) [a]	50–90	90–99	50–90	
Audry *et al.* (2004)	Lot, France	95	99	91	94
Blanc *et al.* (1999)	Lot, France				92
Gibbs (1977)	Yukon, Alaska			96	
Gibbs (1977)	Amazon, Brasil			93	
Tarras-Wahlberg *et al.* (2001)	Puyango, Ecuador	87	97	59	63
Shafer *et al.* (1997)	Milwaukee, USA	85	90	49	74
ICWS (1994) [b]	Rhine (1984–1992), Netherlands	76	93	51	70
Salomons & Förstner (1984)	Rhine (1970s), Germany	70	78	64	75
Mouvet & Bourg (1983)	Meuse, Netherlands	64	94	65	
Vink (2002)	Rhine (1993–1997), Netherlands	56	86	41	62
Shafer *et al.* (1999) [c]	Wisconsin, USA	66	75	24	39
Shafer *et al.* (1997)	Wolf, USA	43	38	24	27
Gundersen & Steinnes (2003)	Glåma, Norway	8		28	10

a. Dissolved Transport Index; b. *in:* Vink (2002); c. Average of 14 streams.

Table 2.3 Log K_d values [log l kg^{-1}] for four heavy metals in several rivers.

Reference	River	Zn	Pb	Cu	Cd
Lofts & Tipping (1998)	East-English rivers	4.63	5.41	4.52	4.75 [a]
Veselý *et al.* (2001)	54 Czech rivers [b]	4.87	5.44	4.67	
Vink (2002)	Elbe River	4.95	5.65	4.43	4.82

a. Source: Tipping *et al.* (1998); b. Variation was in general two orders of magnitude.

Table 2.2 illustrates the effect of geology. Organic soils lead to high loads in the dissolved and colloidal phase (i.e., attached to particles that are smaller than 0.45 μm) because of high TOC contents (Förstner & Wittmann 1983; Gundersen & Steinnes 2003). The Wolf and the Røa soils – the latter being a tributary of the Glåma River – both illustrate this. All other rivers in Table 2.2 have catchments of clastic origin, hence carry the majority of the heavy-metal load in the sediment phase.

The influence of the contamination degree on the partitioning seems not very clear. On the one hand, Salomons & Förstner (1984) stated that the high pollution level of the River Rhine in the seventies led to little heavy metals in the sediment phase (Table 2.2). Foster & Charlesworth (1996) showed that the total Pb concentration is negatively correlated with the part that is sediment-associated. On the other hand, Vink (2002) found a lower percentage of sediment-bound heavy metals in the Rhine River during the 1990s than Salomons & Förstner (1984) for the 1970s (Table 2.2). In the 1990s, the river was less polluted. In addition, Blanc *et al.* (1999) found a higher affinity for the sediment phase in a polluted tributary of the Lot River than in the less polluted main stretch. Still, the Rhine River seems to follow the general trend that Martin & Meybeck (1979) outlined as the Dissolved Transport Index or DTI (Table 2.2), with more than half of the Cu and Zn and almost all Pb transported in the sediment-associated phase (Table 2.2).

2.2.4 Sediment characteristics and heavy metal concentrations

The River Rhine apparently mainly transports heavy metals in the sediment phase. Sediment characteristics such as specific surface area, grain size, clay and organic matter content determine the amount of binding places available for heavy metals, hence determine the *potential* heavy-metal concentrations. Grain size is the most important characteristic with respect to metal contamination (Förstner & Wittmann 1983; Horowitz 1985), a decreasing particle size and increasing clay content means increasing heavy-metal concentrations (e.g., Salomons & Förstner 1984; Koelmans 1998; Tebbens *et al.* 2000; Middelkoop 2000).

In addition to clay minerals, fulvic and humic acids also provide many binding sites for heavy metals (Förstner & Wittmann 1983). In freshly deposited sediments, heavy-metal concentrations increase with organic-matter content (Koelmans 1998; Middelkoop 2000; El Bilali *et al.* 2002). In older floodplain deposits, however, virtually no or only very weak relationships have been found (e.g., Martin 1997, 2000, 2004; Taylor 1996). One explanation for this is that heavy metals can also be transported in coatings on quartz grains (sand) (Macklin & Dowsett 1989) or in the form of ore grains (Leenaers & Rang 1989; Lecce & Pavlowsky 1997). This mode of transport disturbs the negative grain size-heavy metal relationship (Moore *et al.* 1989). Another explanation is migration of heavy metals in the soil profile (Hudson-Edwards *et al.* 1998; Ciszewski & Malik 2004), thereby disturbing relationships that existed in fresh deposits.

2.3 Temporal variation in sediment-associated metal concentrations

2.3.1 Long-term variation

Since floodplains are major sinks for contaminated sediments (e.g., Walling *et al.* 2003), historic floodplain deposits show the long-term fluctuations in sediment-associated metal concentrations in rivers (Hudson-Edwards *et al.* 1999). Since most of the sources associated with urban and industrial development only became active after the Industrial Revolution, this is also the starting point for a sharp rise in heavy-metal concentrations in suspended sediments. The Industrial Revolution started in the 18th century in the UK and the 19th century in the rest of Europe and the USA. Since Germany was among the last European countries to industrialize, the River Rhine has a much shorter history of pollution than the English rivers. For instance, Bradley & Cox (1986) mention that metal mining in North Staffordshire started in 1622, with its heydays around 1760 and 1790. Hudson-Edwards *et al.* (1998, 1999) indicate that mining in northern England even started in Roman times. This contrasts with the chronology that Middelkoop (2000, 2002) reported for the historic floodplain deposits along the lower River Rhine.

Before 1860, industrial activity is negligible and heavy-metal concentrations in the River Rhine are on pre-industrial level (See Table 2.2 for natural background values). Pre-industrial levels amounted maximally 150 mg kg^{-1} for zinc, 75 mg kg^{-1} for lead and 20 mg kg^{-1} for copper. From 1860 onwards, metal concentrations increased, notably in the beginning of the 20th century, and reach a peak during the early 1930s. This resulted in maximum concentrations of about 1450 mg kg^{-1} for zinc, 490 mg kg^{-1} for lead and 130 mg kg^{-1} for copper. During and shortly after the Second World War, the industrial production temporarily decreased, as do the metal concentrations. After the war, rebuilding of the German industry led to a second increase of contamination, culminating in the 1960s in a second peak in concentrations: 850 mg kg^{-1} Zn,

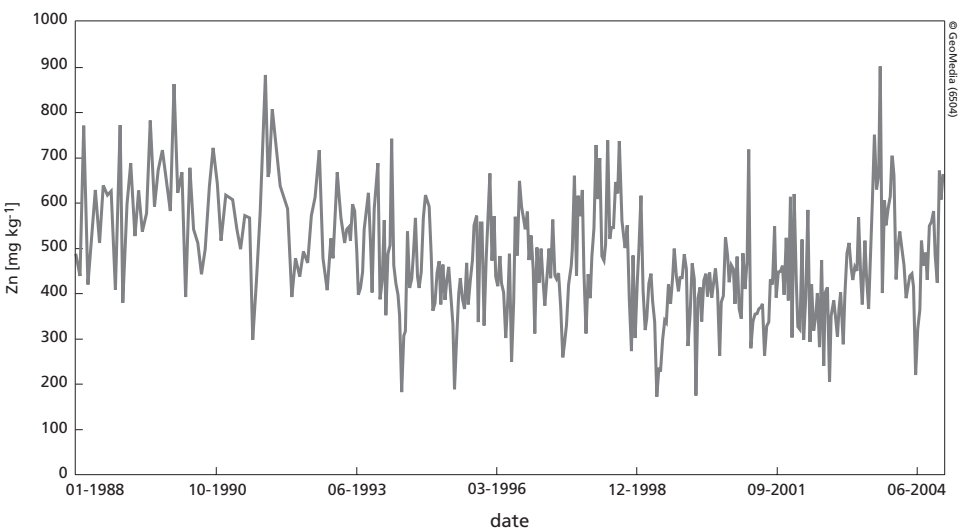

Figure 2.5 Zinc concentrations in suspended matter sampled in the River Rhine at the Dutch-German border for 1988–2004. Source: V&W (2005).

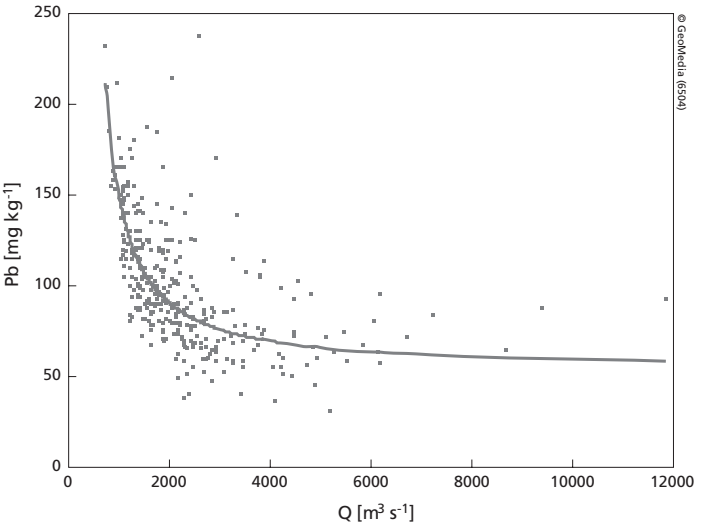

Figure 2.6 Relation between discharge and sediment-bound Pb concentration in the River Rhine for 1995–2003.

200 mg kg^{-1} Pb and 150 mg kg^{-1} Cu. In the 1970s to 1990s, national (e.g., V&W 1999) and international (e.g., EEC 1991; EC 1998) environmental laws curtailed metal emissions, resulting in lower metal concentrations. Nowadays, concentrations in the River Rhine at the Dutch-German border fluctuate around 500 mg kg^{-1} Zn (Fig. 2.5), 90 mg kg^{-1} Pb, 80 mg kg^{-1} Cu and 1.5 mg kg^{-1} Cd (V&W 2005).

2.3.2 Intra-event and seasonal variation

On a seasonal basis, not upstream sources but the storage of heavy metals in the riverbed governs heavy-metal transport and concentrations. During low flow conditions in summer, fine sediments accumulate in the main river channel (Walling *et al.* 1998b). Since these sediments are often rich in organic matter, they contain large amounts of heavy metals and may even scavenge them from the water phase (Gao *et al.* 2003). When a peak flow occurs, the river stage rises and the increased shear stress remobilizes these fine contaminated bed sediments. This leads to a flush of sediment with increased heavy-metal concentrations (Ciszewski 2001; Nagano *et al.* 2003). This increase is most marked during the first flood of the season (Carton *et al.* 2000). For the River Rhine Asselman (1999c) noted this 'flush effect', which contributed to increased SSCs. Its contribution to increased heavy-metal concentrations has not yet been established for the Rhine River.

Salomons & Förstner (1984) and Middelkoop *et al.* (2002) reported that heavy-metal concentrations decrease with an increase in discharge (Fig. 2.6). At high discharges due to rainfall events, soil erosion provides less contaminated sediments (Ciszewski 2001; Table 2.1). These less contaminated sediments dilute the influx of heavy metals from sewage overflows, urban runoff and remobilisation of contaminated bed sediments (Salomons & Förstner 1984), thereby leading to lower concentrations at higher discharges. During low flow conditions, when little discharge

events due to rainfall occur, soil erosion is only a minor source of sediments. Instead, industrial and municipal emissions exhibiting higher contamination degrees contribute most of the heavy metals. This results in higher metal concentrations during lower discharges.

2.3.3 Inter-event variations

During a discharge event, heavy metal emissions and soil erosion do not take place at the same pace and time. Having an equal input of heavy metals in the river, increasing soil erosion may lead to lower heavy-metal concentrations in the sediments due to dilution with cleaner eroded sediment (Ciszewski 2001; Dennis *et al.* 2003). Urban areas, which are the main contributors of heavy metals, drain their overland flow faster to the river channel than rural areas, which are the main contributors of less contaminated sediments. This time lag between heavy metal and sediment delivery to the river often results in a peak in heavy-metal concentrations before the suspended sediment concentration (SSC) and discharge peak (Foster & Charlesworth 1996). The time lag between the SSC and discharge peaks is normally one to three days in the Rhine River, leading to a clockwise hysteresis between SSC and discharge (Asselman & Middelkoop 1998). Because heavy-metal concentrations in the River Rhine are only sampled biweekly (Middelkoop 2000), the magnitude of the time lag between the peak in heavy-metal concentrations and the discharge peak has not yet been determined for the River Rhine.

2.4 Deposition of sediment-associated heavy metals on floodplains

2.4.1 Spatial trends in sediment and associated metal deposition

The first work by Mansikkaniemi (1985), Gretener & Strömquist (1987) and Lambert & Walling (1987) on floodplain deposition along small streams was only directed at sediment deposition. Leenaers & Rang (1989) and Macklin & Dowsett (1989) later showed this floodplain deposition to be often associated with heavy-metal contamination, despite the cease of large-scale metal mining in upstream areas (Section 2.3.1).

After research on spatial patterns and amounts of contemporary floodplain deposition (e.g., Asselman & Middelkoop 1995; Middelkoop & Asselman 1998; Walling & He 1997, 1998b) and characteristics of this deposition (e.g., Marriott 1992; He & Walling 1997, 1998; Simm & Walling 1998; Walling *et al.* 1996, 1998a), recent research has also focused on deposition of sediment-associated heavy metals on floodplains (e.g., Carton *et al.* 2000; Middelkoop 2000; Schouten *et al.* 2000; Dennis *et al.* 2003; Walling *et al.* 2003). From this wealth of research on sediment and associated metal deposition on floodplain, we can derive some general trends:

1. The amount of sediment deposition [kg m^{-2}] increases with:
   a. decreasing distance to the river (Marriott 1992; Walling & He 1997; Middelkoop & Asselman 1998; Walling 1999; Thoms *et al.* 2000a);
   b. increasing valley width (Lecce 1997; Lecce & Pavlowsky 2001; Thoms *et al.* 2000b);
   c. decreasing stream power, flow velocity or shear stress (Lecce 1997; Asselman 1999a, 1999d);

d. decreasing floodplain elevation (Lecce & Pavlowsky 2001), increasing water depth (Walling 1999) or increasing inundation frequency (Moody & Troutman 2000; Hren *et al.* 2001);
e. increasing SSC (Asselman *et al.* 2003).

2. The median grain size decreases and the organic matter and clay content increase with:
   a. increasing distance to the river (Marriott 1992; Walling *et al.* 1996, 1998; Middelkoop 2000; Thoms *et al.* 2000b);
   b. decreasing floodplain elevation (Schouten *et al.* 2000) or increasing water depth (Walling *et al.* 1996).

3. The heavy-metal concentration in floodplain deposition increases with:
   a. more frequent flooding at lower discharges (Schouten *et al.* 2000; Middelkoop 2000; Middelkoop *et al.* 2002);
   b. increasing organic matter content (Middelkoop 2000; El Bilali *et al.* 2002; Gao *et al.* 2003);
   c. increasing clay content and decreasing median grain size (Förstner & Wittmann 1983; Middelkoop 2000; Ciszewski 2001);
   d. increasing distance to the river (Middelkoop 2000; Thoms *et al.* 2000b).

These trends are interrelated. For instance, an equal amount of water that flows through a narrower valley has a larger flow velocity than when the same amount of water were to flow through a wider valley (1b). This causes the flow shear stress to exceed the critical shear stress for deposition for more particle sizes, hence less sedimentation (1c). Larger particles have higher settling velocities and have thus soon settled from water flowing over the floodplain, leading to trend 1a. The remaining finer particles only settle when the transfer of momentum of the river channel to the floodplain decreases and flow shear stresses decrease, which occurs at larger distances from the river (2a). Since heavy metals are predominantly associated with these finer particles (Section 2.3.2, trend 3b/c), this also leads to higher metal concentrations with increasing distance from the river (3d). However, the decrease in the amount of deposition with increasing distance to the river (1a) outweighs the parallel increase in clay and organic matter content (2a), leading to less heavy-metal deposition per unit area with increasing distance to the river (Middelkoop 2000).

Apparently, physical variables such as settling velocity, flow velocity and flow shear stress influence patterns and amount of heavy-metal deposition. Yet, large topographical differences, which also exist within and between Rhine River floodplains, may complicate these patterns (Nicholas & Walling 1997; Middelkoop & Asselman 1998; Sweet *et al.* 2003). Moreover, the above trends have been established for floodplains that are not bordered by minor embankments or marked natural levees. They may not be valid for the floodplains with protection against minor floods (Wyżga 1999) that typically occurs along the lower River Rhine. Until now, researchers have hardly explicitly addressed the influence of these large topographical differences and flood protection on the trends and characteristics of floodplain deposition.

2.4.2 Floodplain deposition models

To enable the prediction of complex overbank deposition patterns and to enhance understanding of the deposition process, a number of researchers developed floodplain deposition models. James (1985) and Pizzuto (1987) both developed 1D floodplain sedimentation models to model trend 1a (Section 2.4.1). James (1985) modelled turbulent diffusion of sediment from the channel to the floodplain. However, not diffusion but transverse convection is one of the main mechanisms of sediment transfer in natural, meandering rivers such as the River Rhine (Marriott 1998; Middelkoop & Asselman 1998; Asselman & Van Wijngaarden 2002). Pizzuto's model does neither include the transfer of sediment by secondary currents on the channel-floodplain interface, nor spatial variability of diffusivity and is consequently also of limited value (Marriott 1998).

Howard (1992) proposed a 1D model for long-term evolution of floodplain elevation, based on similar principles as used by James (1985) and Pizzuto (1987). His model not only reflects trend 1a but also 1d (Section 2.4.1).

$$DR = (h_{max} - h_{act}) \cdot (DR_f + DR_c \, e^{-D/\lambda}) \tag{2.3}$$

with DR = deposition rate, h_{max} = maximum floodplain elevation, h_{act} = local floodplain elevation, DR_f = the position-independent deposition rate of fine sediment, DR_c = the position-dependent deposition rate of coarse sediment by overbank diffusion, λ = a characteristic diffusion length scale, D = distance to nearest channel. However, distance to the river does not influence the settling of fine fractions. In addition, the model parameters do not have a physical meaning, thereby limiting its applicability.

Asselman & Van Wijngaarden (2002) developed a 1D deposition model for floodplain sections using more physically-based parameters. They used the concept of settling tanks as proposed by Chen (1975) and later used by Asselman (1999a, 1999b) and Narinesingh *et al.* (2000). Chen (1975) defined deposition as

$$DR = \alpha \cdot w_s \cdot C \cdot (1 - e^{-(\alpha \cdot w_s / h)t}) \tag{2.4}$$

with DR = deposition rate, w_s = settling velocity, C = suspended sediment concentration, t = inundation time and α = the 'Krone factor'. The 'Krone factor' is defined as (Krone 1962),

$$\alpha = 1 - (\tau / \tau_{cr}) \qquad \text{for } \tau < \tau_{cr}, \tag{2.5}$$

$$\alpha = 0 \qquad \text{for } \tau \geq \tau_{cr} \tag{2.6}$$

with τ = shear stress and τ_{cr} = critical shear stress for sediment deposition. Eqs. 2.5 & 2.6 state that sedimentation only takes place for shear stresses lower than the critical shear stress for sediment deposition. Otherwise the sediment will remain in suspension. The term between brackets in Eq. 2.4 is called the 'trapping efficiency'. A larger settling velocity leads to a larger efficiency, whereas a higher flow velocity leads to a lower efficiency due to a higher τ and hence a

lower α (Eq. 2.5). The approach is simple and is useful for calculation of deposition along major river branches such as the Rhine River. Yet, it does not take account of topography nor flow patterns, two crucial factors controlling the spatial pattern of floodplain deposition (Walling *et al.* 1999).

Nicholas & Walling (1997) developed a spatially-distributed (2D) deposition model. It derives the flow pattern from a hydraulic module and the topography from a digital elevation model. Nicholas & Walling (1997) computed the deposition rate using

$$DR = k \cdot w_s \cdot C \cdot h_w \tag{2.7}$$

where h_w = water depth and k is an empirical factor that needs to be calibrated with data on sediment deposition. Middelkoop & Van der Perk (1998) adopted α instead of k to derive sediment deposition in their raster-based model:

$$DR = w_s \cdot C \cdot \alpha \cdot T \tag{2.8}$$

with T = residence time of the suspended sediment in a cell.

This approach has the advantage that it is simple and applicable in a raster-GIS environment while preserving the physical basis of Eq. 2.7. Still, the approach also suffers from two disadvantages. First, data on settling velocities and critical shear stresses are hardly available for floodplain environments (Asselman 1999b; Asselman & Middelkoop 1995; Van Wijngaarden 1999; Walling & Woodward 2000), which makes it difficult to optimize the model. Second, raster-based models suffer from numerical dispersion, which is an unwanted artefact of the numerical modelling technique and should be avoided.

2.5 Post-depositional redistribution

After sediment and heavy metals have been deposited on a floodplain, processes start to redistribute them. Bioturbating animals such as earthworms, moles and voles redistribute the soil over the soil profile and may take up some of the heavy metals attached to it. Other metals dissolve and may percolate to the groundwater, thereby leaving the floodplain soil system.

2.5.1 Bioturbation

Bioturbation is the transfer from soil by digging, feeding, excreting and locomotion (movement) of soil organisms (Wang & Matisoff 1997). By changing the physical and chemical properties of the soil, this may also result in a change in pore water flux, which can subsequently influence the dissolution of heavy metals (see also Section 2.5.3). Reible *et al.* (1996) pointed out that, in the absence of erosion, bioturbation is the most important soil moving process. The 'turnover rate' characterizes the importance of this process. The most active and important group of soil organisms with respect to bioturbation are probably the earthworms (Müller-Lemans & Van Dorp 1996; Bunzl 2002). Tyler *et al.* (2001) found that earthworms could homogenise the topsoil in well-drained soils within a few decades at most. Müller-Lemans & Van Dorp (1996) report a

turnover rate of 5–20 years for the top 10 to 20 cm under grassland soil in Western Europe. Zorn *et al*. (2005a) reported that the amount of soil that earthworms bring to the surface each year (1.4 mm) may be more than the yearly deposition amount in lower River Rhine floodplains.

Flooding severely affects earthworms such as *Lumbricus rubellus* in both growth and survival rate (Zorn *et al.* 2005b). Since floodplain rehabilitation may lead to more and prolonged flooding of floodplains, this may limit their contribution to the transfer of metals to the soil surface via bioturbation (Wijnhoven *et al.*, *subm.*). At the same time the contribution to metal deposition during flooding may increase. Until now, research has only addressed this probable shift in contributing sources of metal deposition on floodplains in a preliminary way (Klok *et al.* 2005).

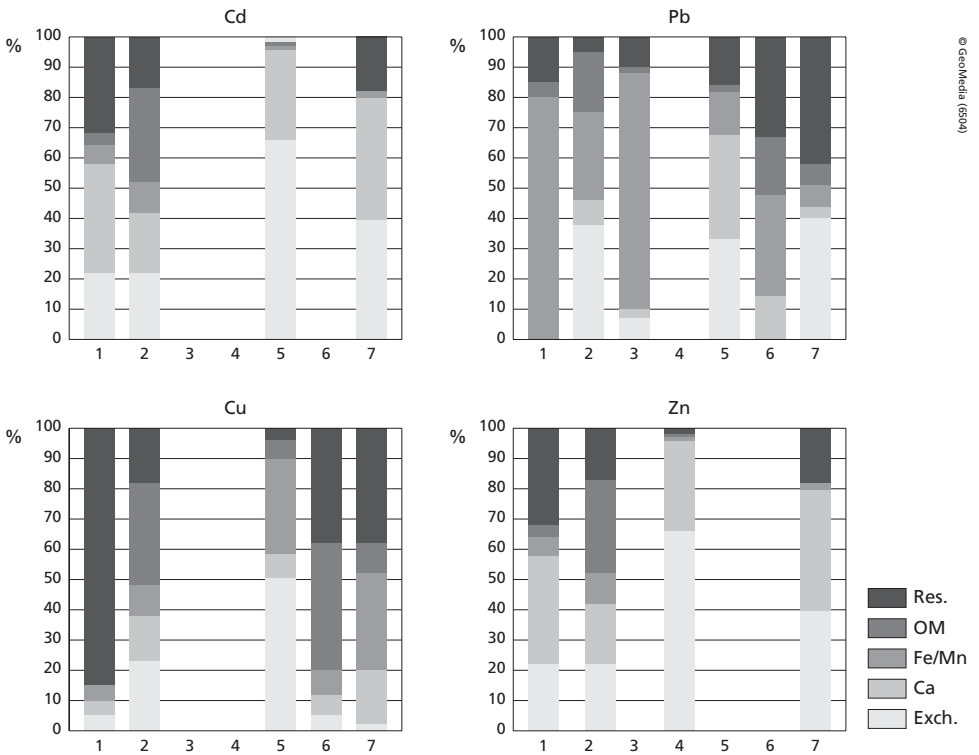

Figure 2.7 Distribution of heavy metals over the five fractions according to different sources. Sources: 1 Macklin & Dowsett (1989) for medium sand overbank deposits; 2 Bradley & Cox (1990) and Bradley (1995) for overbank deposits; 3 Macklin (1996) for medium sand overbank deposits; 4 Leenaers & Rang (1989) for >63 µm of flood deposits, om & Res. merged; 5 El Bilali *et al*. (2002) for lake sediments; 6 Wong *et al*. (2002) for paddy rice soils; 7 Jain (2004) for bed sediments. Res. = residual fraction, Exch. = exchangeable fraction (see text).

2.5.2 Bioavailability of heavy metals

Tessier *et al.* (1979) developed a classification scheme for heavy metals to characterize their potential mobility in soils. The classes decrease in solubility and bioavailability from 1 to 5 and are called fractions. They defined them as follows (Fig. 2.7):

1. Exchangeable: subjected to sorption-desorption processes, extracted with $MgCl_2$.
2. Bound to carbonates: subjected to pH changes, extracted with NaOAc–HOAc.
3. Bound to Fe/Mn oxides: subjected to Eh (redox) changes, extracted with NH_2OH–HCl + HOAc.
4. Bound to organic matter: subjected to breakdown by oxidation, extracted with H_2O_2.
5. Residual: metals incorporated in primary and secondary minerals, extracted with HF + $HClO_4$.

Tarras-Wahlberg *et al.* (2001) criticised this classification because lack of knowledge of the sediments and lack of sensitivity of the extractions can make interpretation of the results difficult. Instead, ecotoxicologists (e.g., Hobbelen *et al.* 2004) often use an extraction with 0.01 M $CaCl_2$ to derive the 'bioavailable fraction'. This is the fraction of heavy metals that is readily available for uptake by organisms. Meyer (2002) criticizes the use of the 'bioavailable fraction', since it is subjected to change and can only be determined for one point in time. We therefore use the more general term 'bioavailability'.

The bioavailability of heavy metals increases when redox potential and pH decrease and the amount of dissolved organic matter increases. A lower redox potential leads to dissolution of heavy metals by dissolving the metal-binding Fe/Mn oxides (fraction 3) (Hesterberg 1998). For example, Hudson-Edwards *et al.* (1998) found a shift towards more reactive and soluble phases of heavy metals in an overbank soil profile due to a fluctuating water table and corresponding changes in redox potential. However, a lower redox potential can also lead to less mobile heavy metals. They may then bind to very insoluble sulphides (Van Griethuysen *et al.* 2004).

When pH decreases, heavy metals are exchanged for H^+ on clay and organic matter binding sites. This leads to dissolution of these heavy metals. In addition, Hudson-Edwards *et al.* (1998) found more exchangeable heavy metals at a low pH caused by breakdown of organic matter. Because organic matter provides an excellent binding agent for heavy metals in general (Hesterberg 1998) and copper in particular (Bradley & Cox 1987; Yin *et al.* 2002), its dissolution also leads to more bioavailable heavy metals.

2.5.3 Uptake of heavy metals by plants and animals

After having been dissolved, heavy metals can enter plants via the root system. The amount of uptake depends on the same soil factors that govern solubility of heavy metals, including pH, CEC, moisture content, and texture. Normally one or two of these factors explain most of the variation in bioavailability of heavy metals. For instance, Álvarez *et al.* (2003) report that the bioavailability of Cu and Zn is mainly controlled by pH and organic carbon content. The lower River Rhine floodplains are all carbonate buffered and have a high pH. Consequently, bioavailability and hence uptake by soil fauna is low (Hobbelen *et al.* 2004). This explains why health problems with meat or milk from cattle in floodplains are not to be expected, although

cows ingest large amounts of soil when grazing (Japenga *et al*. 1990). In addition, Vijver *et al*. (2003) found that earthworms take up less than 30 % via ingestion of soil. The predominant route of heavy-metal accumulation is out of the pore water via the skin. Since pore water concentrations are very low in floodplain soils with high pH, effects again are low (Hobbelen *et al*. 2004).

2.6 Future changes

In recent years we have seen a major advance in our understanding of present factors and processes that control the fate of sediment-associated heavy metals in the fluvial environment (Fig. 2.1). Yet, changes such as climate change, upstream land-use change, environmental policy, floodplain rehabilitation and nature restoration are about to change these factors and processes. The prediction of these changes and their impact on the floodplain deposition has not made considerable progress yet. Studies often only focus on parts of the system (Fig. 2.1):

- Due to climate change, magnitude and frequency of peak discharges may increase in the near future. The International Panel on Climate Change (IPCC, Houghton *et al*. 2001) predicted a global increase in temperature of +1.4 to +5.8 °C in 2100. For North-Western Europe, regional climate models predict an increase in autumn/winter precipitation of 6 to 15 % and a decrease in summer precipitation of 12 % (Shabalova *et al.* 2003). Together with enhanced snowmelt in spring because of a rise in temperature, the increase in winter precipitation may lead to an increase in average winter discharges of about 50 % (Shabalova *et al.* 2003) and increased frequency of peak flows in the River Rhine (Kwadijk & Middelkoop 1994). These flows may also remobilise contaminated upstream bank sediments (Longfield & Macklin 1999; Dennis *et al.* 2003), which may subsequently be deposited on lower River Rhine floodplains during one of the more frequent and longer inundations (Middelkoop *et al*. 2001). As such, climate change is due to increase sediment and heavy-metal deposition on floodplains.
- Because of upstream land abandonment, Asselman *et al.* (2003) predicted a decline in soil erodibility of the agricultural soils in the River Rhine basin. Since they found the increase in erosivity of the rainfall due to climate change to be smaller than the decrease in erodibility, sediment loads in the River Rhine will probably decrease.
- Because of environmental policy, in the near future total metal loads may decline and diffuse sources may even become more important. For instance, the contribution from industrial point sources to the copper pollution in the Elbe River will probably decline from almost 70 % in 1985–1990 to only a few percent in 2020 (Vink & Peters 2003). In addition, European environmental laws such as the European Urban Wastewater Treatment Directive (EEC 1991; EC 1998) target WWTPs. Vink (2002) indicated that the implementation of this directive might lead to around 7 % lower metal loads in 2015. The Water Framework Directive (EC 2000) nevertheless aims to control quasi-diffuse sources such as the application of sewage sludge as well (Apitz & White 2003). Although the directive neglects floodplain deposits as secondary sources of metal contamination (Förstner 2002), it may still result in further decline of heavy-metal loads.
- Floodplain rehabilitation comprises projects such as removal of minor embankments, excavation of secondary channels and lowering of floodplain levels (Silva *et al*. 2001). They

may result in more floodplain deposition because of increased inundation frequencies (Asselman 1999a). In addition, due to these projects floodplains will probably be inundated at lower discharges. Therefore, metal concentrations in deposited sediments could also rise (Middelkoop *et al.* 2002; Fig. 2.5). It is therefore probable that floodplain rehabilitation gives rise to enhanced sediment and metal deposition on floodplains.

- Because reforestation leads to lower soil pH and less soil organic matter (Hesterberg 1998), nature restoration in floodplains can lead to remobilization of stored heavy metals if the acid-neutralizing capacity (i.e., the soil carbonate buffer) is not maintained (Gäbler 1997). Lower River Rhine floodplains could therefore be called 'chemical time bombs' (Stigliani *et al.* 1991), because changes in environmental factors could potentially release large amounts of toxic elements. For instance, Vink & Peters (2003) calculated that a decline in soil pH of 0.5 due to reforestation in combination with ceased liming might cause a rise of 40 % in total heavy metal emissions in the Elbe River basin because of increased metal solubility.

Until now, no integral assessment has been made of the impact of these changes on heavy-metal deposition in floodplains. Due to the on-going contamination of surface waters and sediments with heavy metals, their potential toxic effects and huge costs involved in sanitation, it is important to understand how, where and when the deposition of heavy metals is going to change. Especially in areas such as the lower River Rhine, where a lot of changes interact, their relative and combined impact merits study. Taken into account its possible future changes, the suite of factors and processes that determine the fate of heavy metals in lowland river floodplains clearly remains a challenging subject for further research.

References

Allen, R.J. & W. Salomons, eds. (1995), Heavy metal aspects of mining pollution and its remediation. Journal of Geochemical Exploration 52/1-2, pp. 1–380.

Allen, R.J. & W. Salomons, eds. (1997), Mining and metals in the environment. Journal of Geochemical Exploration 58/2-3, pp. 93–330.

Álvarez, E., M.L. Fernández Marcos, C. Vaamonde & M.J. Fernández-Sanjurjo (2003), Heavy metals in the dump of an abandoned mine in Galicia (NW Spain) and in the spontaneously occurring vegetation. The Science of the Total Environment 313, pp. 185–197.

Apitz, S. & S. White (2003), A Conceptual Framework for River-Basin-Scale Sediment Management. Journal of Soils and Sediments 3/3, pp. 132–138.

Appelo, C.A.J. & D. Postma (1994), Geochemistry, groundwater and pollution. Rotterdam: Balkema.

Asselman, N.E.M. & H. Middelkoop (1995), Floodplain sedimentation: quantities, patterns and processes. Earth Surface Processes and Landforms 20, pp. 481–499.

Asselman, N.E.M. (1997), Suspended sediment in the River Rhine – The impact of climate change on erosion, transport and deposition. Utrecht: Koninklijk Nederlands Aardrijkskundig Genootschap/Faculteit Geowetenschappen, Universiteit Utrecht (Netherlands Geographical Studies 234).

Asselman, N.E.M. & H. Middelkoop (1998), Temporal variability of contemporary floodplain sedimentation in the Rhine-Meuse delta, The Netherlands. Earth Surface Processes and Landforms 23/7, pp. 595–609.

Asselman, N.E.M. (1999a), The use of floodplain sedimentation measurements to evaluate the effects of river restoration works. Geological Society Special Publication 163, pp. 111–122.

Asselman, N.E.M. (1999b), Slibmodellering in RvR– fase 2. Delft, The Netherlands: WL|Delft Hydraulics (WL Report R3337).

Asselman, N.E.M. (1999c), Suspended sediment dynamics in a large drainage basin: the River Rhine. Hydrological Processes 13/10, pp. 1437–1450.

Asselman, N.E.M. (1999d), Effective discharge for overbank sedimentation on an embanked floodplain along the River Waal, The Netherlands. Special Publication of the International Association of Sedimentologists 28, pp. 61–69.

Asselman, N.E.M., H. Middelkoop & P.M. Van Dijk (2003), The impact of changes in climate and land use on soil erosion, transport and deposition of suspended sediment in the River Rhine. Hydrological Processes 17/16, pp. 3225–3244.

Asselman, N.E.M. & M. van Wijngaarden (2002), Development and application of a 1D floodplain sedimentation model for the River Rhine in The Netherlands. Journal of Hydrology 268, pp. 127–142.

Audry, S., J. Schäfer, G. Blanc, C. Bossy & G. Lavaux (2004), Anthropogenic components of heavy metal (Cd, Zn, Cu, Pb) budgets in the Lot-Garonne fluvial system (France). Applied Geochemistry 19/5, pp. 769–786.

Baptist, M.J., W. Ellis Penning, H. Duel, A.J.M. Smits, G.W. Geerling, G.E.M. van der Lee & J.S.L. van Alphen (2004), Assessment of Cyclic Floodplain Rejuvenation on flood levels and biodiversity along the Rhine River. River Research and Applications 20/3, pp. 285–297.

Benedetti, M.M. (2003), Controls on overbank deposition in the Upper Mississippi River. Geomorphology 56, pp. 271–290.

Blanc, G., Y. Lapaquellerie, N. Maillet & P. Anschutz (1999), A cadmium budget for the Lot-Garonne fluvial system (France). Hydrobiologia 410, pp. 331–341.

Bradford, W.L. (1977), Urban stormwater pollutant loadings: a statistical summary through 1972. Journal of Water Pollution Control Federation 49, pp. 613–622.

Bradley, S.B. (1995), Long-term dispersal of metals in mineralised catchments by fluvial processes. In: I.D.L. Foster, A.M. Gurnell & B.W. Webb, eds., Sediment and water quality in river catchments. Chichester, U.K.: John Wiley, pp. 161–177.

Bradley, S.B. & J.J. Cox (1987), Heavy metals in the Hamps and Manifold valleys, North Staffordshire, U.K.: Partitioning of metals in floodplain soils. The Science of the Total Environment 65, pp. 135–153.

Bradley, S.B. & J.J. Cox (1990), The significance of the floodplain to the cycling of metals in the River Derwent catchment, U.K.. The Science of the Total Environment 97-98, pp. 441–454.

Brookes, A. (1996), Floodplain restoration and rehabilitation. In: M.G. Anderson, D.E. Walling & P.D. Bates, eds., Floodplain processes. Chichester, U.K.: John Wiley, pp. 553–576.

Bunzl, K. (2002), Transport of fallout radiocesium in the soil by bioturbation: a random walk model and application to a forest soil with a high abundance of earthworms. The Science of the Total Environment 293, pp. 191–200.

Carlon, C., M. Dalla Valle & A. Marcomini (2004), Regression models to predict water–soil heavy metals partition coefficients in risk assessment studies. Environmental Pollution 127/1, pp. 109–115.

Carton, J., D.E. Walling, P.N. Owens & G.J.L. Leeks (2000), Spatial and temporal variability of the chromium content of suspended and flood-plain sediment in the River Aire, Yorkshire, U.K. IAHS Publication 263, pp. 219–226.

Ciszewski, D. (2001), Flood-related changes in heavy metal concentrations within sediments of the Biała Przemsza River. Geomorphology 40/3-4, pp. 205–218.

Ciszewski, D. & I. Malik (2004), The use of heavy metal concentrations and dendrochronology in the reconstruction of sediment accumulation, Mała Panew River Valley, southern Poland. Geomorphology 58/1-4, pp. 161–174.

CIW (2004), Water in focus 2004 – Annual report on water management in the Netherlands. http://www.waterinbeeld.nl/WIB2004E/index.html. The Hague: Commissie Integraal Waterbeheer, Ministerie van Verkeer & Waterstaat.

Chen, C.-N. (1975), Design of sediment retention basins. Proceedings of the National Symposium on Urban Hydrology and Sediment Control, Lexington, USA, pp. 285–298.

Dedkov, A. (2004), The relationship between sediment yield and drainage basin area. IAHS Publication 288, pp. 197–204.

Dennis, I.A., M.G. Macklin, T.J. Coulthard & P.A. Brewer (2003), The impact of the October-November 2000 floods on contaminant metal dispersal in the River Swale catchment, North Yorkshire, U.K. Hydrological Processes 17/8, pp. 1641–1657.

Dickinson, W.T., R.P. Rudra & D.J. Clark (1986), A delivery ratio approach for seasonal transport of sediment. IAHS Publication 159, pp. 237–251.

EC (1998), Commission Directive 98/15/EC of 27 February 1998 amending Council Directive 91/271/EEC with respect to certain requirements established in Annex I thereof (Text with EEA relevance). Official Journal L 067, pp. 29–30.

EC (2000), Directive 2000/60/EC of the European Parliament and of the Council of 23 October 2000, establishing a framework for Community action in the field of water policy. Official Journal L 327, pp. 1–72.

EEC (1991), Council Directive 91/271/EEC of 21 May 1991 concerning urban waste-water treatment. Official Journal L 135, pp. 40–52.

El Bilali, L., P.E. Rasmussen, G.E.M. Hall & D. Fortin (2002), Role of sediment composition in trace metal distribution in lake sediments. Applied Geochemistry 17/9, pp. 1171–1181.

Erskine, W.D., A. Mahmoudzadeh & C. Myers (2002), Land use effects on sediment yields and soil loss rates in small basins of Triassic sandstone near Sydney, Nsw, Australia. Catena 49/4, pp. 271–287.

Förstner, U. (1989), Contaminated sediments. Berlin: Springer (Lecture notes in Earth Sciences 21).

Förstner, U. (2002), Sediments and the European Water Framework Directive. Journal of Soils & Sediments 2/2, p. 54.

Förstner, U. & G.T.W. Wittmann (1983), Metal pollution in the aquatic environment. Berlin: Springer.

Foster, I.D.L. & S.M. Charlesworth (1996), Heavy metals in the hydrological cycle: trends and explanations. Hydrological Processes 16, pp. 227–261.

Foster, I., R. Grew & J. Dearing (1990), Magnitude and frequency of sediment transport in agricultural catchments: a pared lake-catchment study in Midland England. In: J. Boardman, I.D.L. Foster & J.A. Dearing, eds., Soil erosion on agricultural land. Chichester, U.K.: John Wiley.

Fryirs, K. & Brierley, G.J. (2001), Variability in sediment delivery and storage along river courses in Bega catchment, NSW, Australia: implications for geomorphic river recovery. Geomorphology 38/3-4, pp. 237–265.

Gäbler, H.-E. (1997), Mobility of heavy metals as a function of pH of samples from an overbank sediment profile contaminated by mining activities. Journal of Geochemical Exploration 58, pp. 185–194.

Gao, Q., Z. Tao, M. Xie, K. Cui & F. Zeng (2003), Effects of hydrological processes on the chemical composition of riverine suspended sediment in the Zhujiang River, China. Hydrological Processes 17/12, pp. 2365–2373.

Gibbs, R.J. (1977), Transport phases of transition metals in the Amazon and Yukon Rivers. Geological Society of America Bulletin 88, pp. 829–843.

Gretener, B. & L. Strömquist (1987), Overbank sedimentation rates of fine grained sediments. A study of the recent deposition in the lower River Fyrisån. Geografiska Annaler 69A/1, pp. 139–146.

Gordeev, V.V., V. Rachold, & I.E. Vlasova (2004), Geochemical behaviour of major and trace elements in suspended particulate material of the Irtysh river, the main tributary of the Ob river, Siberia. Applied Geochemistry 19/4, pp. 593–610.

Gundersen, P. & E. Steinnes (2003), Influence of pH and TOC concentration on Cu, Zn, Cd and Al speciation in rivers. Water Research 37/2, pp. 307–318.

Hardy, R.J., P.D. Bates & M.G. Anderson (2000), Modelling suspended sediment deposition on a fluvial floodplain using a two-dimensional dynamic finite element model. Journal of Hydrology 229, pp. 202–218.

He, Q. & D.E. Walling (1997), Spatial variability of the particle size composition of overbank floodplain deposits. Water, Air and Soil Pollution 99, pp. 71–80.

He, Q. & D.E. Walling, (1998), An investigation of the spatial variability of the grain size composition of floodplain sediments. Hydrological Processes 12/7, pp. 1079–1094.

Hesterberg, D. (1998), Biogeochemical cycles and processes leading to changes in mobility of chemicals in soils. Agriculture, Ecosystems and Environment 67, pp. 121–133.

Hindel, R., J. Schalich, W. de Vos, J. Ebbing, R. Swennen & I. van Keer (1996), Vertical distribution of elements in overbank sediment profiles from Belgium, Germany and The Netherlands. Journal of Geochemical Exploration 56/2, pp. 105–122.

Hobbelen, P.H.F., J.E. Koolhaas & C.A.M. van Gestel (2004), Risk assessment of heavy metal pollution for detritivores in floodplain soils in the Biesbosch, the Netherlands, taking bioavailability into account. Environmental Pollution 129, pp. 409–419.

Horowitz, A.J. (1985), A primer on trace metal-sediment chemistry. Washington, DC: United States Geological Survey (USGS Water Supply Paper 2277).

Houghton, J.T., Y. Ding, D.J. Griggs, M. Noguer, P.J. van der Linden, X. Dai, K. Maskell, & C.A. Johnson, eds. (2001), Climate change 2001: the scientific basis – Contribution of Working Group I to the Third assessment report of the Intergovernmental Panel on Climate Change. Cambridge, U.K.: Cambridge University Press.

Hren, M.T, C.P. Chamberlain & F.J. Magilligan (2001), A combined flood surface and geochemical analysis of metal fluxes in a historically mined region: a case study from the New World Mining District, Montana. Environmental Geology 40, pp. 1334–1346.

Hudson-Edwards, K.A., M.G. Macklin, C.D. Curtis & D.J. Vaughan, (1998), Chemical remobilization of contaminant metals within floodplain sediments in an incising river system: implications for dating and chemostratigraphy. Earth Surface Processes and Landforms 23/8, pp. 671–684.

Hudson-Edwards, K.A., M.G. Macklin & M.P. Taylor (1999), 2000 years of sediment-borne heavy metal storage in the Yorkshire Ouse basin, NE England, U.K. Hydrological Processes 13/7, pp. 1087–1102.

Howard, A.D. (1992), Modeling channel migration and floodplain sedimentation in meandering streams. In: P.A. Carling & G.E. Petts, eds., Lowland floodplain rivers – Geomorphological perspectives. Chichester, U.K.: John Wiley, pp. 1–41.

ICWS (1994), Project Onderzoek Rijn Fase IV: Stofbalansen Oostelijk Havengebied Rotterdam 1989–1992 (ICWS-rapport 94.03).

James, C.S. (1985), Sediment transfer to overbank sections. Journal of Hydraulic Research 23/5, pp. 435–453.

Japenga, J., K.H. Zschuppe, A.J. de Groot & W. Salomons (1990), Heavy metals and organic micropollutants in floodplains of the river Waal, a distributary of the river Rhine, 1958–1981. Netherlands Journal of Agricultural Science 38, pp. 381–397.

Klok, C., M. Zorn, J.E. Koolhaas, H. Eijsackers & C.A.M. van Gestel (2005), Does reproductive plasticity in *Lumbricus rubellus* improve the recovery of populations in frequently inundated river floodplains? Soil Biology & Biochemistry (in press).

Koelmans, A.A. (1998), Geochemistry of suspended and settling solids in two freshwater lakes. Hydrobiologia 364/1, pp. 15–29.

Krone, R.B. (1962), Flume studies of the transport of sediments in estuarial shoaling – Final report. University of California, Berkeley (USA).

Kwadijk, J. & H. Middelkoop (1994), Estimation of impact of climate change on the peak discharge probability of the River Rhine. Climatic Change 27, pp. 199–224.

Lambert, C.P. & D.E. Walling (1987), Floodplain sedimentation: a preliminary investigation of contemporary deposition within the lower reaches of the River Culm, Devon, U.K. Geografiska Annaler 69A/3-4, pp. 393–404.

Lecce, S.A. (1997), Spatial patterns of historical overbank sedimentation and floodplain evolution, Blue River, Wisconsin. Geomorphology 18, pp. 265–277.

Lecce, S.A. & R.T. Pavlowsky (1997), Storage of mining-related zinc in floodplain sediments, Blue River, Wisconsin. Physical Geography 18/5, pp. 424–439.

Lecce, S.A. & R.T. Pavlowsky (2001), Use of mining-contaminated sediment tracers to investigate the timing and rates of historical flood plain sedimentation. Geomorphology 38, pp. 85–108.

Leenaers, H. & M.C. Rang (1989), Metal dispersal in the fluvial system of the River Geul: The role of discharge, distance to the source, and floodplain geometry. IAHS Publication 184, pp. 47–55.

Lofts, S. & E. Tipping (1998), An assemblage model for cation binding by natural particulate matter. Geochimica et Cosmochimica Acta 62/15, pp. 2609–2625.

Lofts, S. & E. Tipping (2000), Solid-solution metal partitioning in the Humber rivers: application of WHAM and SCAMP. The Science of the Total Environment 251-252, pp. 381–399.

Longfield, S.A. & M.G. Macklin (1999), The influence of recent environmental change on flooding and sediment fluxes in the Yorkshire Ouse basin. Hydrological Processes 13, pp. 1051–1066.

Macklin, M.G. & R.B. Dowsett (1989), The chemical and physical speciation of trace metals in fine grained overbank flood sediments in the Tyne basin, North-east England. Catena 16, pp. 135–151.

Mansikkaniemi, H. (1985), Sedimentation and water quality in the flood basin of the River Kyrönjoki in Finland. Fennia 163/1, pp. 155–194.

Marriott, S. (1992), Textural analysis and modelling of a flood deposit: River Severn, U.K. Earth Surface Processes and Landforms 17, pp. 687–697.

Marriott, S.B. (1998), Channel-floodplain interactions and sediment deposition on floodplains. In: Bailey, R.G., P.V. José & B.R. Sherwood, eds., United Kingdom floodplains. Otley, U.K.: Westbury Academic & Scientific.

Martin, C.W. (1997), Heavy metal concentrations in floodplain surface soils, Lahn River, Germany. Environmental Geology 30/1-2, pp. 119–125.

Martin, C.W. (2000), Heavy metal trends in floodplain sediments and valley fill, River Lahn, Germany. Catena 39/1, pp. 53–68.

Martin, C.W. (2004), Heavy metal storage in near channel sediments of the Lahn River, Germany. Geomorphology 61/3-4, pp. 275–285.

Martin, J.M. & M. Meybeck (1979), Elemental mass balance of material carried by major world rivers. Marine Chemistry 7/3, pp. 173–206.

Meyer, J.S. (2002), The utility of the terms "bioavailability" and "bioavailable fraction" for metals. Marine Environmental Research 53/5, pp. 417–423.

Middelkoop, H. (2000), Heavy-metal pollution of the river Rhine and Meuse floodplains in the Netherlands. Netherlands Journal of Geosciences 79/4, pp. 411–428.

Middelkoop, H. (2002), Reconstructing floodplain sedimentation rates from heavy metal profiles by inverse modelling. Hydrological Processes 16/1, pp. 47–64.

Middelkoop, H. & N.E.M. Asselman (1998), Spatial variability of floodplain sedimentation at the event scale in the Rhine-Meuse delta, The Netherlands. Earth Surface Processes and Landforms 23, pp. 561–573.

Middelkoop, H., K. Daamen, D. Gellens, W. Grabs, J.C.J. Kwadijk, H. Lang, B.W.A.H. Parmet, B. Schädler, J. Schulla & K. Wilke (2001), Impact of climate change on hydrological regimes and water resources management in the Rhine basin. Climatic Change 49/1-2, pp. 105–128.

Middelkoop, H., I. Thonon & M. van der Perk (2002), Effective discharge for heavy metal deposition on the lower River Rhine flood plains. IAHS Publication 276, pp. 151–159.

Middelkoop, H. & M. van der Perk (1998), Modelling spatial patterns of overbank sedimentation on embanked floodplains. Geografiska Annaler 80A/2, pp. 95–109.

Miller, J.R. (1997), The role of fluvial geomorphic processes in the dispersal of heavy metals from mine sites. Journal of Geochemical Exploration 58/2-3, pp. 101–118.

Moody, J.A. & B.M. Troutman (2000), Quantitative model of the growth of floodplains by vertical accretion. Earth Surface Processes and Landforms 25, pp. 115–133.

Moore, J.M., E.J. Brook & C. Jones (1989), Grain size partitioning of metals in contaminated, coarse-grained river floodplain sediment: Clark Fork River, Montana, U.S.A. Environmental Geology & Water Sciences 14/2, pp. 107–115.

Mouvet, C. & A.C.M. Bourg (1983), Speciation (including adsorbed species) of copper, lead, nickel and zinc in the Meuse River. Observed results compared to values calculated with a chemical equilibrium computer program. Water Research 17/6, pp. 641–649.

Müller-Lemans, H. & F. van Dorp (1996), Bioturbation as a mechanism for radionuclide transport in soil: relevance of earthworms. Journal of Environmental Radioactivity 31/1, pp. 7–20.

Naden, P.S. & D.M. Cooper (1999), Development of a sediment delivery model for application in large river basins. Hydrological Processes 13/7, pp. 1011–1034.

Nagano, T., N. Yanase, K. Tsuduki & S. Nagao (2003), Particulate and dissolved elemental loads in the Kuji River related to discharge rate. Environment International 28/7, pp. 649–658.

Narinesingh, P., G.J. Klaassen & D. Ludikhuize (2000), Floodplain sedimentation along extended river reaches. Journal of Hydraulic Research 37, pp. 827–845.

Nicholas, A.P. & D.E. Walling (1997), Modelling flood hydraulics and overbank deposition on river floodplains. Earth Surface Processes and Landforms 22/1, pp. 59–77.

Pizzuto, J.E. (1987), Sediment diffusion during overbank flows. Sedimentology 34/2, pp. 301–317.

Rautengarten, A. (1993), Sources of heavy metal pollution in the Rhine basin. Land Degradation & Rehabilitation 4/4, pp. 339–349.

Reible, D.D., V. Popow, K.T. Valsaraj, U.J. Thibodeaux, F. Lin, M. Dikshit, M.A. Todaro & J.W. Fleeger (1996), Contaminant fluxes from sediment due to Tubificid Oligochaete bioturbation. Water Research 30/3, pp. 704–714.

Salomons, W. & Förstner, U. (1984), Metals in the hydrocycle. Berlin: Springer.

Schouten, C.J.J., M.C. Rang, B.A. de Hamer & H.R.A. van Hout (2000), Strongly polluted deposits in the Meuse river floodplain and their effects on river management. In: A.J.M. Smits, P.H. Nienhuis, & R.S.E.W. Leuven, eds., New approaches to river management. Leiden, The Netherlands: Backhuys, pp. 33–50.

Shabalova, M.V., W.P.A. van Deursen & T.A. Buishand (2003), Assessing future discharge of the river Rhine using regional climate model integrations and a hydrological model. Climate Research 23/3, 233–246.

Shafer, M.M., J.T. Overdier, J.P. Hurley, D. Armstrong & D. Webb (1997), The influence of dissolved organic carbon, suspended particulates, and hydrology on the concentration, partitioning and variability of trace metals in two contrasting Wisconsin watersheds (U.S.A.). Chemical Geology 136/1-2, pp. 71–97.

Shafer, M.M., J.T. Overdier, H. Phillips, D. Webb, J.R. Sullivan, & D.E. Armstrong (1999), Trace metal levels and partitioning in Wisconsin rivers. Water, Air, and Soil Pollution 110/3-4, 273–311.

Silva, W., F. Klijn & J.P.M. Dijkman, eds. (2001), Room for the Rhine branches in The Netherlands – What the research has taught us. Arnhem, The Netherlands: RIZA (RIZA rapport 2001.031).

Simm, D.J. (1995), The rates and patterns of overbank deposition on a lowland floodplain. In: I. Foster, A. Gurnell & B. Webb, eds., Sediment and water quality in river catchments. Chichester, U.K.: John Wiley, pp. 247–264.

Simm, D.J. & D.E. Walling (1998), Lateral variability of overbank sedimentation on a Devon flood plain. Hydrological Sciences Journal 43/5, pp. 715–732.

Sin, S.N., H. Chua, W. Lo & L.M. Ng (2001), Assessment of heavy metal cations in sediments of Shing Mun River, Hong Kong. Environment International 26/5-6, pp. 297–301.

Slattery, M.C. & T.P. Burt (1997), Particle size characteristics of suspended sediments in hillslope runoff and stream flow. Earth Surface Processes and Landforms 22/8, pp. 705–719.

Steegen, A., G. Govers, L. Beuselinck, J. Nachtergaele, I. Takken & J. Poesen (1998), Variations in sediment yield from an agricultural drainage basin in central Belgium. IAHS Publication 249, pp. 177–185.

Steegen, A., G. Govers, J. Nachtergaele, I. Takken, L. Beuselinck & J. Poesen (2000), Sediment export by water from an agricultural catchment in the Loam Belt of central Belgium. Geomorphology 33/1-2, pp. 25–36.

Steiger, J., A.M. Gurnell, P. Ergenzinger & D. Snelder (2001), Sedimentation in the riparian zone of an incising river. Earth Surface Processes and Landforms 26/1, pp. 91–108.

Stigliani, W.M., P. Doelman, W. Salomons, R. Schulin, G.R.B. Smidt, S.E.A.T.M. van der Zee (1991), Chemical time bombs: predicting the unpredictable. Environment 33/4, pp. 26–30.

Sweet, R.J, A.P. Nicholas, D.E. Walling & X. Fang (2003), Morphological controls on medium-term sedimentation rates on British lowland river floodplains. Hydrobiologia 494, pp. 177–183.

Swennen, R. & J. van der Sluys (1998), Zn, Pb, Cu and As distribution patterns in overbank and medium-order stream sediment samples: their use in exploration and environmental geochemistry. Journal of Geochemical Exploration 65/1, pp. 27–45.

Tarras-Wahlberg, N.H., A. Flachier, S.N. Lane & O. Sangfors (2001), Environmental impacts and metal exposure of aquatic ecosystems in rivers contaminated by small scale gold mining: the Puyango River basin, southern Ecuador. The Science of the Total Environment 278/1-3, pp. 239–261.

Taylor, M.P. (1996), The variability of heavy metals in floodplain sediments: a case study from mid Wales. Catena 28, pp. 71–87.

Tebbens, L.A., A. Veldkamp & S.B. Kroonenberg (2000), Natural compositional variation of the river Meuse (Maas) suspended load: a 13 ka bulk geochemical record from the upper Kreftenheye and Betuwe Formations in northern Limburg. Netherlands Journal of Geosciences 79/4, pp. 391–409.

Tessier, A., P.G.C. Campbell & M. Bisson (1979), Sequential extraction procedure for the speciation of particulate trace metals. Analytical Chemistry 51/7, pp. 844–851.

Thoms, M. & P. Thiel (1995), The impact of urbanisation on the bed sediments of South Creek, New South Wales. Australian Geographical Studies 33/1, pp. 31–43.

Thoms, M., J.M. Foster & B. Gawne (2000a), Flood-plain sedimentation in a dryland river: the River Murray, Australia. IAHS Publication 263, pp. 227–235.

Thoms, M.C., C.R. Parker & M. Simons (2000b), The dispersal and storage of trace metals in the Hawkesbury River valley. In: S. Brizga, & B. Finlayson, eds., River management: The Australasian experience. Chichester, U.K.: John Wiley, pp. 197–219.

Tipping, E., S. Lofts, & A.J. Lawlor (1998), Modelling the chemical speciation of trace metals in the surface waters of the Humber system. The Science of the Total Environment 210-211, pp. 63–77.

Turekian, K.K. & K.H. Wedepohl (1961), Distribution of the elements in some major units of the earth's crust. Geological Society of America Bulletin 72, pp. 175–192.

Tyler, A.N., S. Carter, D.A. Davidson, D.J. Long & R. Tipping (2001), The extent and significance of bioturbation on 137Cs in upland soils. Catena 43, pp. 81–99.

Van der Lee, G.E.M., H. Olde Venterink & N.E.M. Asselman (2004), Nutrient retention in floodplains of the Rhine distributaries in The Netherlands. River Research and Applications 20/3, pp. 315–325.

Van der Perk, M., V. Jetten, E. Heskes, M. Segers & I. Wijntjes (2004), Transport and retention of copper fungicides in vineyards. IAHS Publication 288, pp. 437–443.

Van Dijk, P.M. (2001), Soil erosion and associated sediment supply to rivers – Seasonal dynamics, soil conservation measures and impacts of climate change. PhD Thesis, Amsterdam: Universiteit van Amsterdam.

Van Griethuijsen, C., J. van Baren, E.T.H.M. Peeters & A.A. Koelmans (2004), Trace metal availability and effects on benthic community structure in floodplain lakes. Environmental Toxicology and Chemistry 23/3, pp. 668–681.

Veselý, J., V. Majer, J. Kučera & V. Havránek (2001), Solid–water partitioning of elements in Czech freshwaters. Applied Geochemistry 16/4, pp. 347–350.

Vink, R.J. (2002), Heavy metal fluxes in the Elbe and Rhine basins: analysis and modelling. PhD Thesis, Amsterdam: Vrije Universiteit.

Vink, R. & H. Behrendt (2002), Heavy metal transport in large river systems: heavy metal emissions and loads in the Rhine and Elbe river basins. Hydrological Processes 16/16, pp. 3227–3244.

Vink, R.J., H. Behrendt & W. Salomons (1999), Point and diffuse source analysis of heavy metals in the Elbe drainage area: Comparing heavy metal emissions with transported river loads. Hydrobiologia 410, pp. 307–314.

Vink, R. & S. Peters (2003), Modelling point and diffuse heavy metal emissions and loads in the Elbe basin. Hydrological Processes 17/7, pp. 1307–1328.

Vijver, M.G., J.P.M. Vink, C.J.H. Moermans, C.A.M. van Gestel (2003), Oral sealing using glue: a new method to distinguish between intestinal and dermal uptake of metals in earthworms. Soil Biology and Biochemistry 35/1, pp. 125–132.

V&W (1999), Fourth national policy document on water management. http://www.waterland.net/nw4/English/index.html. The Hague: Ministerie van Verkeer & Waterstaat.

V&W (2005), Waterbase. http://www.waterbase.nl. The Hague: Ministerie van Verkeer & Waterstaat.

Walling, D.E. (1990), Linking the field to the river: sediment delivery from agricultural land. In: J. Boardman, I.D.L. Foster & J.A. Dearing, eds., Soil erosion on agricultural land. Chichester, U.K.: John Wiley, pp. 129–152.

Walling, D.E. (1999a), Invited lecture: River floodplains as sediment sinks. In: A.W. Jayawardena, J.H.W. Lee & Z.Y. Wang, eds., River sedimentation – Theory and application. Rotterdam: Balkema, pp. 465–474.

Walling, D.E. (1999b), Linking land use, erosion and sediment yields in river basins. Hydrobiologia 410, pp. 223–240.

Walling, D.E. & Q. He (1997), Investigating spatial patterns of overbank sedimentation on river floodplains. Water, Air and Soil Pollution 99, pp. 9–20.

Walling, D.E. & Q. He (1998), The spatial variability of overbank sedimentation on river floodplains. Geomorphology 24, pp. 209–223.

Walling, D.E., Q. He & A.P. Nicholas (1996), Floodplains as suspended sediment sinks. In: M.G. Anderson, D.E. Walling & P.D. Bates, eds., Floodplain processes. Chichester, U.K.: John Wiley, pp. 399–439.

Walling, D.E., P.N. Owens & G.J.L. Leeks (1998a), Erratum to "The characteristics of overbank deposits associated with a major flood event in the catchment of the River Ouse, Yorkshire, U.K.". Catena 32/3-4, pp. 309–331.

Walling, D.E., P.N. Owens & G.J.L. Leeks (1998b), The role of channel and floodplain storage in the suspended sediment budget of the River Ouse, Yorkshire, U.K. Geomorphology 22, pp. 225–242.

Walling, D.E., P.N. Owens & G.J.L. Leeks (1999). Rates of contemporary overbank sedimentation and sediment storage on the floodplains of the main channel systems of the Yorkshire Ouse and River Tweed, U.K. Hydrological Processes 13/7, pp. 993–1009.

Walling, D.E., P.N. Owens, J. Carter, G.J.L. Leeks, S. Lewis, A.A. Meharg & J. Wright (2003), Storage of sediment-associated nutrients and contaminants in river channel and floodplain systems. Applied Geochemistry 18/2, pp. 195–220.

Walling, D.E. & B.W. Webb (1992), Water quality – I. Physical characteristics. In: P. Calow & G.E. Petts, eds., The rivers handbook – Hydrological and ecological principles, Volume I. Oxford, U.K.: Blackwell, pp. 49–72.

Walling, D.E. & J.C. Woodward (2000), Effective particle size characteristics of fluvial suspended sediment transported by lowland British rivers. IAHS Publication 263, pp. 129–139.

Wang, X. & G. Matisoff (1997), Solute transport in sediments by a large freshwater oligochaete, *Branchiura sowerbyi*. Environmental Science & Technology 31/7, pp. 1926–1933.

Wijnhoven, S., I. Thonon, G. van der Velde, R.S.E.W. Leuven, M.I. Zorn, H.J.P. Eijsackers & A.J.M. Smits (*submitted*), The impact of bioturbation by small mammals on heavy metal redistribution in floodplains. Water, Air and Soil Pollution.

Wong, S.C., X.D. Li, G. Zhang, S.H. Qi & Y.S. Min (2002), Heavy metals in agricultural soils of the Pearl River Delta, South China. Environmental Pollution 119, pp. 33–44.

Wyżga, B. (1999), Estimating mean flow velocity in channel and floodplain areas and its use for explaining the pattern of overbank deposition and floodplain retention. Geomorphology 28, pp. 218–297.

Yin, Y., C.A. Impellitteri, S.-J. You & H.E. Allen (2002), The importance of organic matter distribution and extract soil:solution ratio on the desorption of heavy metals from soils. The Science of the Total Environment 287, pp. 107–119.

Zorn, M.I., C.A.M. van Gestel & H. Eijsackers (2005a), Contribution of different earthworm species to top soil mixing in a sandy and a clayey soil after 80 days incubation. In: M.I. Zorn, The floodplain upside down – Interactions between earthworm bioturbation, flooding and pollution. PhD Thesis, Amsterdam: Vrije Universiteit, pp. 121–132.

Zorn, M.I., C.A.M. van Gestel & H. Eijsackers (2005b), Species-specific earthworm population responses in relation to flooding dynamics in a Dutch floodplain soil. Pedobiologia 49/3, pp. 189–198.

3 The influence of floodplain morphology and river works on spatial patterns of overbank sediment and heavy-metal deposition

Submitted as: Thonon, I., H. Middelkoop & M. van der Perk, The influence of floodplain morphology and river works on spatial patterns of overbank deposition. Netherlands Journal of Geosciences.

"*The lack of baseline-data for large river-floodplain systems in the temperate climates of developed countries presents an enormous problem to those attempting to restore such systems.*" (Brookes 1996).

"*There is, (…), clearly a need for more information of overbank sediment deposits, particularly those related to high-magnitude, low-frequency events, which, by definition, are the most difficult to document.*" (Walling *et al*. 1998).

"*There is still a need for more information on the grain-size characteristics of overbank deposits.*" (Lecce & Pavlowsky 2004).

"*Further work is required to identify the key controls on this [spatial] variability.*" (Walling *et al*. 2004).

Abstract

Floodplain deposition constitutes an important part of the sediment and contaminant budget of many large rivers throughout the world. The amount, patterns and characteristics of floodplain deposition are determined at the scale of the river branch by the channel sinuosity, floodplain and valley width, whereas factors such as morphology and flow patterns are of importance at the floodplain scale. Human influence may change these factors at both scales, but little is known about the subsequent impact of these changes on overbank deposition at the scale of the floodplain and the river branch.

We studied the differences in sediment and heavy-metal deposition along two river branches of the lower Rhine River: the Waal and IJssel River. The floodplains along the Waal River branch (average discharge: 1500 m^3 s^{-1}) have strongly been influenced by man. Artificial levees protect

them from low-magnitude floods and they have often been levelled. The wide floodplains along the meandering IJssel River (average discharge: 250 $m^3 s^{-1}$), in contrast, still exhibit their characteristic ridge-and-swale topography and natural levees.

Floodplains along both river branches exhibit a number of spatial trends: with increasing distance to the sediment source, amounts of sediment deposition decrease. Clay, organic matter and heavy metal content increase with decreasing floodplain elevation and metal concentrations increase with increasing clay and organic matter content. These trends are, however, far less pronounced in the Waal River floodplains. In addition, exceptions to the general trends show the importance of local hydrodynamic conditions during an inundation, which stresses the need for a model-based approach. Furthermore, the individual Waal River floodplains receive more and finer sediment per inundation because of their higher trapping efficiencies than the IJssel River floodplains. At the scale of the river branch the situation reverses for conveyance losses. The large extent of the floodplains along the IJssel River relative to its sediment discharge during peak events results in a considerable conveyance loss and a downstream exhaustion of suspended matter, which is not noted in the Waal River. This shows that both the individual floodplain sections and the total river branch should be taken into account when explaining the role of overbank deposition as part of a river's sediment and metal budget.

Keywords

Rhine River, floodplain topography, sediment, heavy metal, sedimentation, spatial variability.

3.1 Introduction

Floodplain deposition is an important process in the storage and cycling of sediments, nutrients and contaminants in river basins (e.g., Mertes 1994; Gomez *et al.* 1997; Middelkoop & Asselman 1998; Walling 1999; Thoms *et al.* 2000; Nanson & Croke 2002; Walling & Owens 2003). The patterns, amounts and characteristics of floodplain sedimentation have been studied extensively (e.g., Marriott 1992; Guccione 1993; He & Walling 1997; Simm & Walling 1998; Walling & He 1998; Walling *et al.* 1998; Lecce & Pavlowsky 2004; Walling *et al.* 2004). With respect to the sediment-associated contaminants, especially deposition of heavy metals received attention of numerous authors (e.g., Leenaers & Rang 1989; Lecce & Pavlowsky 1997; Hudson-Edwards *et al.* 1999; Middelkoop 2000; Hren *et al.* 2001). Most studies on variability in overbank deposition focused at small streams (e.g., Lambert & Walling 1987; Simm & Walling 1998; Walling *et al.* 2003), concerned historical floodplain deposits (e.g., Taylor 1996; Lecce & Pavlowsky 1997, 2004) or used modelling (e.g., Nicholas & Walling 1997; Sweet *et al.* 2003; Van der Lee *et al.* 2004). Studies of contemporary overbank deposition of sediment and heavy metals on large river floodplains (Kesel *et al.* 1974; Mertes 1994; Middelkoop & Asselman 1998; Middelkoop 2000) related to high-magnitude/low-frequency events (Walling *et al.* 1998) are however relatively scarce. Yet, empirical studies on contemporary sediment and heavy-metal deposition are still needed to gain insight in the key variables that determine spatial variability of floodplain

deposition (Walling *et al.* 2004) and for calibration and validation of floodplain deposition models (Gomez *et al.* 1997; Lecce & Pavlowsky 2004).

In general, variability in overbank deposition of sediment and heavy metals is determined by factors that operate at two scales: at the scale of the river branch and the individual floodplain section. Channel morphology, floodplain width, sediment load and discharge regime determine most of the variability in floodplain deposition between river branches (Lecce 1997; Foster *et al.* 2002; Sweet *et al.* 2003; Lecce & Pavlowsky 2004). Variation in hydraulic patterns of overbank flow and local topography form the main source of variability in deposition within and between floodplains (Lambert & Walling 1987; Nicholas & Walling 1997; Lecce & Pavlowsky 2004). Although these two groups of factors differ considerably, only some authors have directly compared the variation in floodplain deposition at these two spatial scales (e.g., Foster *et al.* 2002; Sweet *et al.* 2003).

Human influence through, for example, the construction of river training works and artificial levees, may considerably alter the factors that determine overbank deposition along rivers (Hesselink *et al.* 2003; Kesel 2003). Studying the differences between modified and pristine rivers gives information about the direction river rehabilitation should take and its effects on floodplain deposition (Brookes 1996). Yet, often it is not possible nor desirable to fully restore modified rivers to their pristine condition (Stanford *et al.* 1996). In those cases it is more appropriate to study *less* modified floodplains (Ward *et al.* 2002).

The aim of this study is therefore

- to assess the variation in characteristics and amounts of overbank deposition within and between individual floodplain sections and between a modified and less modified river branch of a large river;
- to relate this spatial variation to the topographical and hydrological factors that govern overbank deposition at the two spatial scales.

We compared embanked floodplains along two distributaries of the lower River Rhine: the heavily influenced floodplains along Waal River, exhibiting artificial levees and levelled floodplains, and the less disturbed IJssel River floodplains, with natural levees and a classical ridge-and-swale floodplain topography. We obtained sediment trap data for seven floodplains and five inundations. From the sediment samples we determined amounts of sediment deposition, grain-size characteristics, organic matter content and heavy-metal concentrations. For each trap location we determined the duration of sediment conveyance, distance to the river channel and elevation. We combined these data to hypothesize the possible sources of variation and subsequently used statistics to test these hypotheses at the scale of both the distributary and individual floodplain section.

3.2 Study area

The River Rhine basin is located in North-western Europe and measures approximately 185,000 km^2. The river is about 1320 km in length and has a mean discharge of about 2250 $m^3 s^{-1}$ at the Dutch-German border. Currently the River Rhine transports about 3 10^9 kg of suspended sediment per year (Asselman *et al*. 2003; Thonon *et al*., *subm*.). Associated with this sediment, the river transports about 1.2 10^6 kg Zn, 2.3 10^5 kg Pb, 1.9 10^5 kg Cu and 4 10^3 kg Cd per year. Downstream of the Dutch-German border, the River Rhine divides in the Waal River and the Pannerdens Canal (Fig. 3.1). The Pannerdens Canal subsequently splits in the Nederrijn River and the IJssel River. The Waal River discharges two-third of the River Rhine discharge (1500 $m^3 s^{-1}$ on average), the Nederrijn River two-ninth (500 $m^3 s^{-1}$) and the IJssel River the remaining one-ninth (250 $m^3 s^{-1}$).

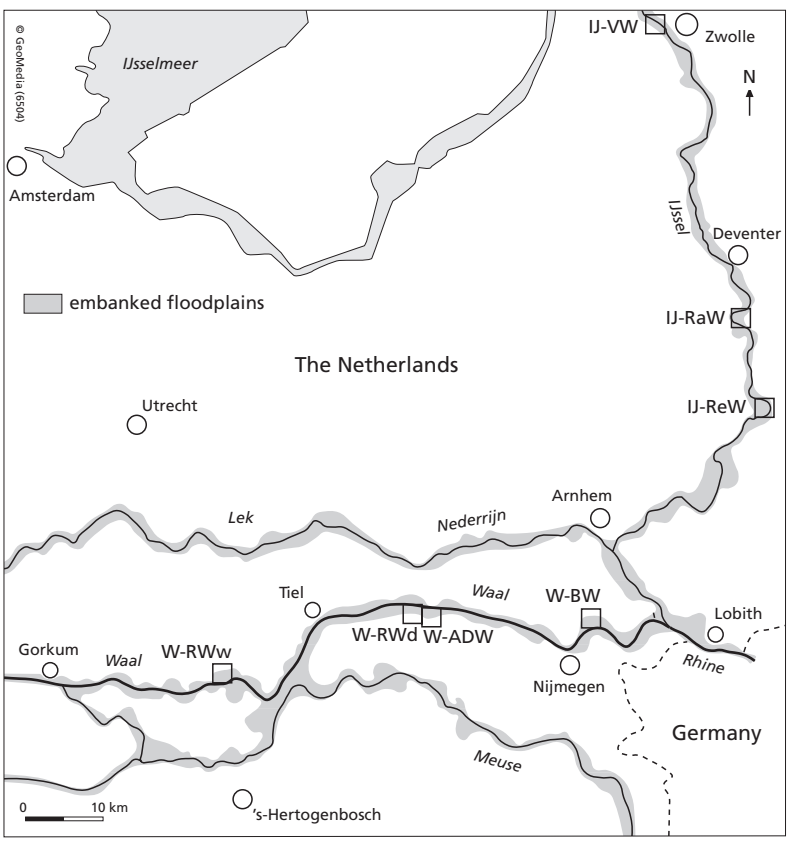

Figure 3.1 Locations of the studied river branches and floodplains. See Table 3.1 for explanation of codes for floodplains.

Both the Waal and IJssel River branches have been embanked and harnessed by groynes. The major embankments serve as flood defence for low-lying areas close to the river. The groynes ensure that no meandering takes place and that the river channel remains deep enough for shipping. Still, the two river branches exhibit some differences that influence overbank deposition (Table 3.1, Fig. 3.2). The Waal River's floodplains are three to four times as wide as the river channel (Table 3.1). The floodplains are often bordered at the side of the river channel by high minor embankments (Bemmelsche Waard or W-BW floodplain and Afferdensche & Deestsche Waarden or W-ADW floodplain) or pronounced natural levees (Rijswaard at Waardenburg or W-RWw floodplain). These protect the floodplains from being inundated by low-magnitude peak discharges. The Rijswaard at Druten or W-RWd floodplain is an exception for the Waal River: it is not protected from low-magnitude flooding (Fig. 3.2). The IJssel River, by contrast, is often only (partly) bordered by natural levees. Two distinct features from IJssel floodplains are their relatively large widths (floodplain/channel width ratios around 10, Table 3.1) and the characteristic ridge-and-swale morphology. The Ravenswaarden (IJ-RaW) and Reuversweerd

Table 3.1 General information on the floodplains in the study area.

River branch	Code	Floodplain name (in Dutch)	Protection	Q_{inund} [a] [$m^3 s^{-1}$]	Size [km^2]	F/C ratio [b]
Waal River	W-BW	Bemmelsche Waard	High minor embankment	6500	4	4
	W-ADW	Afferdensche & Deestsche Waarden	High minor embankment	6300	3	3
	W-RWd	Rijswaard at Druten	None	> 3500	0.5	1
	W-RWw	Rijswaard at Waardenburg	High natural levee	> 5000	3.5	3
IJssel River	IJ-ReW	Reuverswaard	Natural levee (partly)	> 3000	3	9
	IJ-RaW	Ravenswaarden	Natural levee (partly)	> 3000	2.5	14
	IJ-VW	Vreugderijker Waard	Natural levee (partly)	> 5000	1.5	3.5

a. The discharge at which the river inundates the floodplain (Q_{inund}) is given for the Dutch-German border. A > ('larger than') sign indicates that the river only partly inundate the floodplain at that discharge. b. The maximum floodplain width/channel width ratio.

Table 3.2 General information on inundation events (see also Fig. 3.2).

Flood-plain	n of traps	Inundation period	Q_{peak} [a] [$m^3 s^{-1}$]	SSC_{peak} [a,b] [$mg\ l^{-1}$]	Inundation duration [c]	Sed. supply duration [c]
W-BW	46	Jan. 2003	9372	107	11.3	6.0
W-ADW	41	Feb. 2002	7958	57	10.0	5.2
W-RWd	21	Jan. 2002	5250	130	6.5	6.5
W-RWw	17	Mar. 2001	8664	79	10.2	4.4
IJ-ReW	25	Mar. 2001	8664	79	29.6	17.7
IJ-RaW	56	Jan. 2004	6632	90	21.9	18.9
IJ-VW	20	Mar. 2001	8664	79	25.4	25.4
Total	226	2001–2004			15.5	11.3

a. Source: V&W (2005). b. SSC_{peak} = suspended sediment concentration at peak of discharge event. c. Average values in days for sediment traps. Sediment supply duration is the average time during which sediment could settle on a trap.

Figure 3.2 The studied floodplains. All the maps have the same scale as the map of the W-RWd and W-ADW floodplain sections and the same legend as depicted in the map of the W-BW floodplain.

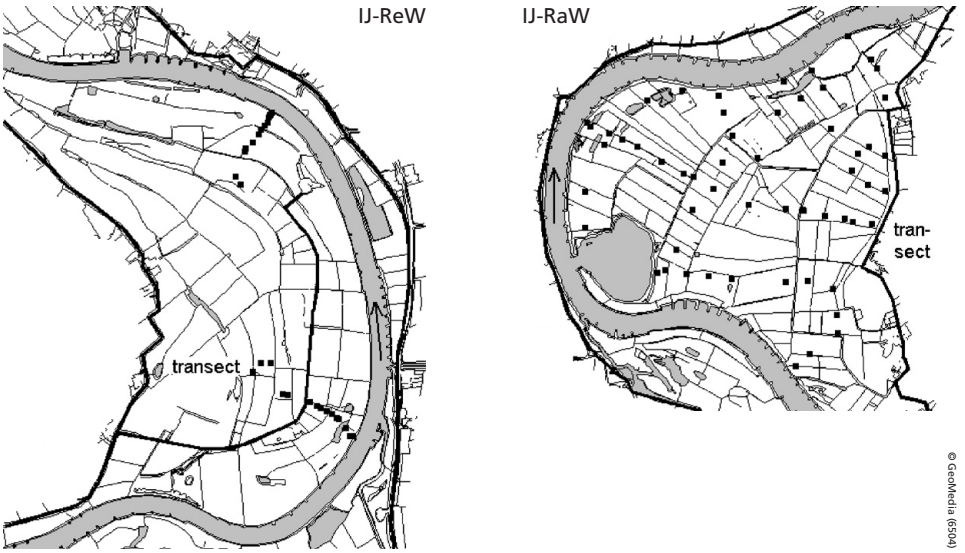

(Figure 3.2 continued)

(IJ-ReW) and to a lesser extent the Vreugderijker Waard (IJ-VW) floodplains are examples of these features (Table 3.1, Fig. 3.2). Land use in all floodplains is mainly pasture with some floodplain forest, shrub-, reed- and marshland. Arable land is only present in the W-BW and W-ADW floodplains.

3.3 Materials and methods

3.3.1 Sampling and analytical techniques

Fig. 3.3 shows the hydrographs and sedigraphs and Table 3.2 shows the characteristics of the inundations for which we deployed sediment traps. We gathered the data for the W-ADW and W-RWd in cooperation with Wijnhoven *et al.* (*subm.*) and for the W-RWw, IJ-ReW and IJ-VW floodplains with Maas *et al.* (2003). This cooperation explains the somewhat different sampling designs for the different floodplains (Fig. 2), with a stratified random sampling in the W-ADW and W-RWd floodplains, few transects in the W-RWw, IJ-ReW and IJ-VW and transects covering the whole floodplain in the W-BW and IJ-RaW floodplains. All studies nevertheless applied the same traps as used by Asselman & Middelkoop (1998). These traps have a pliable base of 50 × 50 cm with artificial grass tufts of 2 cm. We placed them in the floodplains in advance of an inundation, using five steel pins to attach them to the floodplain soil. After recession of the floodwater, we gathered all sediment traps and transported them to the laboratory in plastic bags. We retrieved the sediment from the traps using a high-pressure cleaner. After drying at 105 °C, we weighed each sample and calculated the deposition amounts [g m^{-2}].

After homogenizing the soil samples we took subsamples of 2.5 g to determine Al, Zn, Pb, Cu and Cd concentrations. After extracting the metals using 25 ml 2 M HNO_3 and 40 minutes

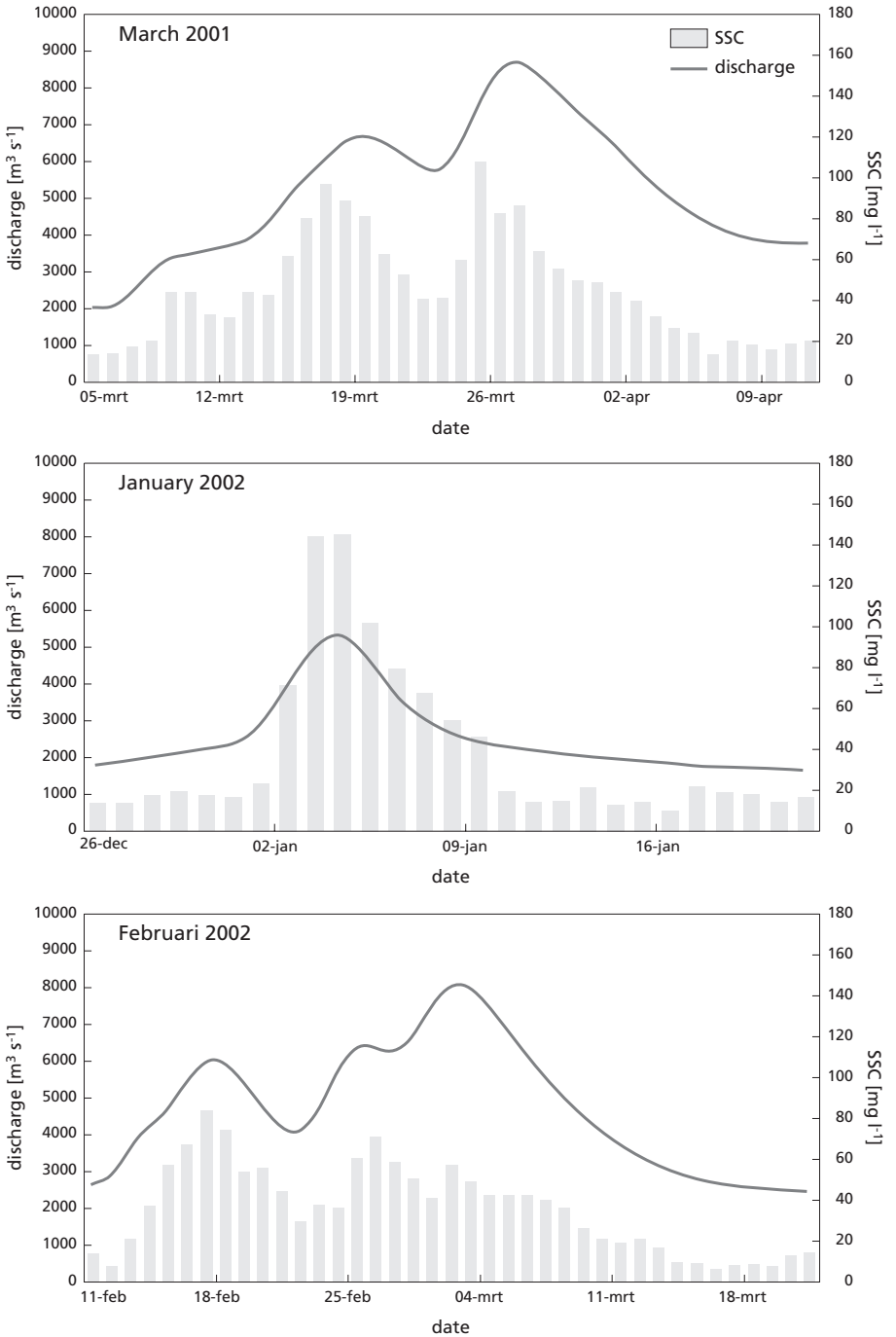

Figure 3.3 Discharge curves for the five sampled peak discharges. Data source: V&W (2005).

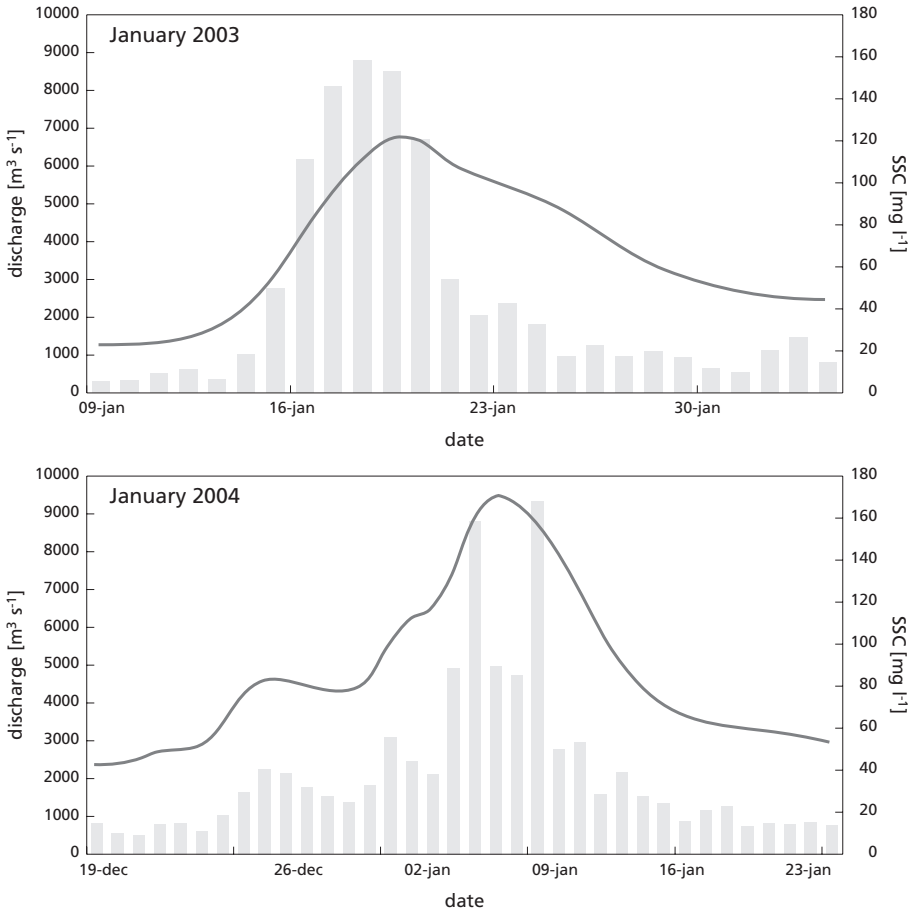

' GeoMedia (659A)

(Figure 3.3 continued)

heating in a microwave oven we measured the dissolved concentration of heavy metals using Inductively Coupled Plasma-Atomic Emission Spectrometry (ICP-AES). We determined organic matter (OM) content by loss on ignition. Dispersed grain size was analyzed with the Coulter LS 230 after removal of carbonate and organic matter. We considered median grain size (d_{50}), clay (0–2 μm), fine silt (2–16 μm), coarse silt (16–63 μm) and sand (63–2000 μm) percentage. Following Brown (1985), we discriminated between sandy levee deposits with $d_{50} > 63$ μm and overbank deposits with $d_{50} < 63$ μm and only studied the latter.

3.3.2 Hydrological and topographical data

Elevation above sea level for every sediment trap was derived from the Actual Height model of The Netherlands (AHN, *Adviesdienst Geo-informatie & ICT*, *Rijkswaterstaat*, Delft, The Netherlands), which is a digital elevation model with a resolution of 5 × 5 meter based on laser

altimetry data. Relative floodplain elevation was calculated by subtracting the absolute elevation by the mean summer water level in the river channel.

We calculated the inundation period for every trap by analyzing the location and elevation of the trap and water levels measured at the nearest measurement station (V&W 2005). In case the trap was behind a natural levees, minor embankments or other obstacle, we assumed these first had to be overtopped before inundation of the trap could occur. Then we counted for each trap the time it was under water. We assumed that drainage of the flood water directly followed the falling stage in the river channel. In floodplains with a minor embankment drainage proceeded via a sluice. To obtain the (potential) duration of sediment conveyance, we counted the time during which the water level in the river channel was higher than the height of the minor embankment or natural levee. Only in this situation transfer of sediment from the channel to the floodplain may take place.

For statistical tests we always used a Students' t test (for two samples) or ANOVA (for more than two samples), a one-sided significance level (α) of .05 and all available samples for the floodplain or river branch under consideration.

3.4 Results

3.4.1 Variation between river branches and floodplain sections

Table 3.3 gives the grain size data for the studied floodplains. During the five events from March 2001 to January 2004 an average of 1.1 kg m^{-2} of sediment was deposited on the studied floodplains. The Waal River floodplains receive significantly more sediment per unit area than the IJssel River floodplains ($p = .001$). Furthermore, the amounts of sediment deposition in the IJssel River floodplains are significantly different from each other ($p = .000$), indicating a downstream trend, with less sedimentation occurring farther downstream (Table 3.3). The Waal River does not exhibit these significant differences ($p = .070$) or a downstream trend.

A typical floodplain deposit contained 22 % clay, 47 % fine silt, 21 % coarse silt, 10 % sand and 14 % organic matter. These values are similar to values for Waal and Meuse River floodplains reported by Asselman & Middelkoop (1998) for major floods in 1995 and 1993. The Waal River floodplain deposits, however, only contain a few percent sand and have a d_{50} of around 7 μm. Although the W-RWw clearly is an exception with 19 % sand and a d_{50} of 17 μm, the Waal River floodplain deposits are significantly finer than those along the IJssel River ($p = .000$). The IJ-RaW floodplain deposits are significantly richer ($p = .001$) in organic matter (20 %) than other floodplains (14 %). Data from V&W (2005) nevertheless indicate that the percentage of organic matter in the suspended matter during the inundation of January 2004 (Fig. 3.3) was only at an average level of 5 to 6 %. This may indicate that most organic matter in the IJ-RaW floodplain developed in the floodwater, for example as algae growth.

Average heavy metal concentrations in the deposited sediments (for Zn 295 mg kg^{-1}, Pb 89 mg kg^{-1}, Cu 50 mg kg^{-1} and Cd 2.8 mg kg^{-1}, Table 3.4) are all above the background values (Middelkoop 2002). Cd concentrations in sediments deposited on the floodplains that inundated

during March 2001 (IJ-ReW, IJ-VW and W-RWw; Table 3.4) are however significantly higher (p =.001). Data sampled at the Dutch-German border by V&W (2005) confirmed that during the beginning of 2001 Cd concentrations were incidentally elevated in suspended matter. Overall, no trends or clear differences between floodplain sections or river branches seem to exist for the heavy metal concentrations.

3.4.2 Variation within floodplain sections

Fig. 3.4 gives the cross-sections for the most characteristic transect of every studied floodplain (see Fig. 3.2 for the location of the transects) for the floodplain topography, sedimentation amount, and the clay, organic matter and zinc content of the deposited sediments. We only depicted zinc concentrations since this is the most abundant heavy metal (Table 3.4). In addition, Horowitz & Elrick (1987) and Middelkoop (2000) showed that the other heavy metal concentrations exhibit the same trend as zinc. Note that we included the sandy levee deposits in these cross-sections only for visual purposes.

Fig. 3.4 shows there are a number of spatial trends in the characteristics of the overbank deposits. Firstly, it appears that sediment deposition decreases with increasing distance to the river. Walling & He (1998) and Middelkoop & Asselman (1998) found this trend as well. The two clear exceptions to this trend are a) the W-RWd floodplain, where the opposite trend is visible (Fig. 3.4) because the secondary channel in its south acts as a major sediment source (Fig. 3.2), and b) the W-ADW floodplain, which does not seem to exhibit a decrease in sedimentation amount with distanc to the river. The trend seems to be stronger in the IJssel than in the Waal River floodplains. For instance, in the W-BW floodplain the amount of sediment deposition declines by one third over a distance of approximately 600 meter, whereas in the IJ-ReW and IJ-RaW this decline already takes place within 200 meter.

A second trend is the increase of the sedimentation and the clay content with decreasing floodplain elevation. This trend was also noted by for example Walling & He (1998) and Lecce & Pavlowsky (2001). The only exception is the W-RWw floodplain, featured by an increasing sedimentation with increasing elevation, although this trend is probably influenced by the decreasing distance to the river (Fig. 3.4). Because of the larger topographical differences, again the trend seems to be more pronounced in the IJssel River floodplains than in the Waal River floodplains.

A third trend is the increasing zinc concentration with increasing clay and organic matter content, which is notably clear in the W-RWw, IJ-ReW and IJ-RaW floodplains (Fig. 3.4). Horowitz & Elrick (1987) and Middelkoop (2000) found a similar trend in suspended matter and floodplain deposits. With distance to the river, however, zinc concentration hardly shows a consistent trend. When leaving out the sandy deposits with low zinc content close to river channel in the IJssel River floodplains, zinc concentration fluctuates with clay and organic matter content in the IJ-ReW, IJ-RaW and W-ADW floodplains, but no trend is discernible (Fig. 3.4). In the W-BW the zinc concentration remains more or less constant while the clay and organic matter content slightly increase when moving away from the river channel. In the IJ-VW floodplain this is even more pronounced, with clearly increasing organic matter content but rather constant zinc concentrations. In the W-RWd floodplain, even the opposite trend is

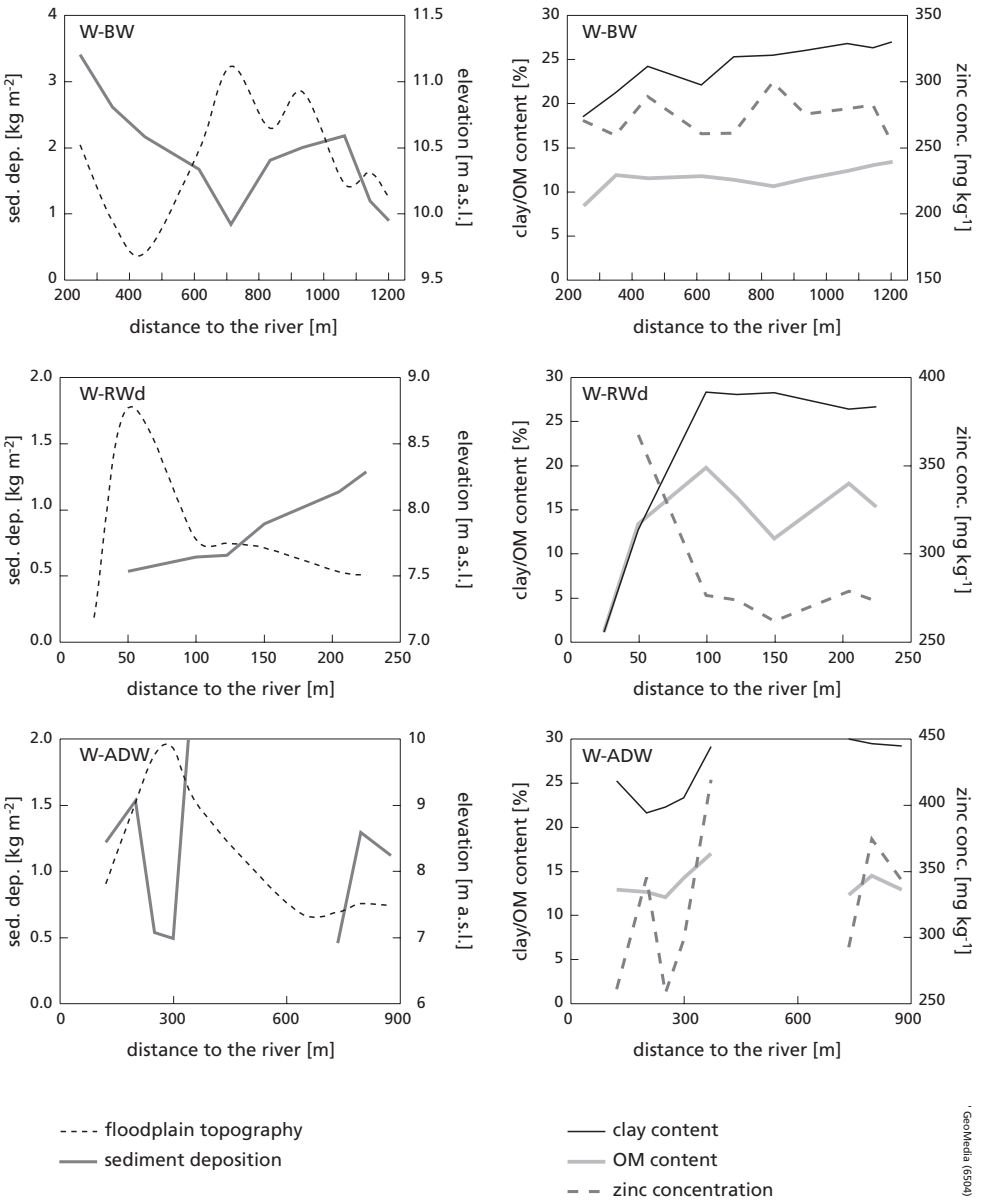

Figure 3.4 Cross-sections for the seven floodplains along the indicated transects in Fig. 3.2, with floodplain elevation and amount of sediment deposition on the left and clay, organic matter and zinc content on the right. Note the sandy levee deposit on the W-RWd transect was 32 kg m^{-2} and on the W-RaW transect 35 kg m^{-2}. Both sedimentation amounts were therefore not depicted.

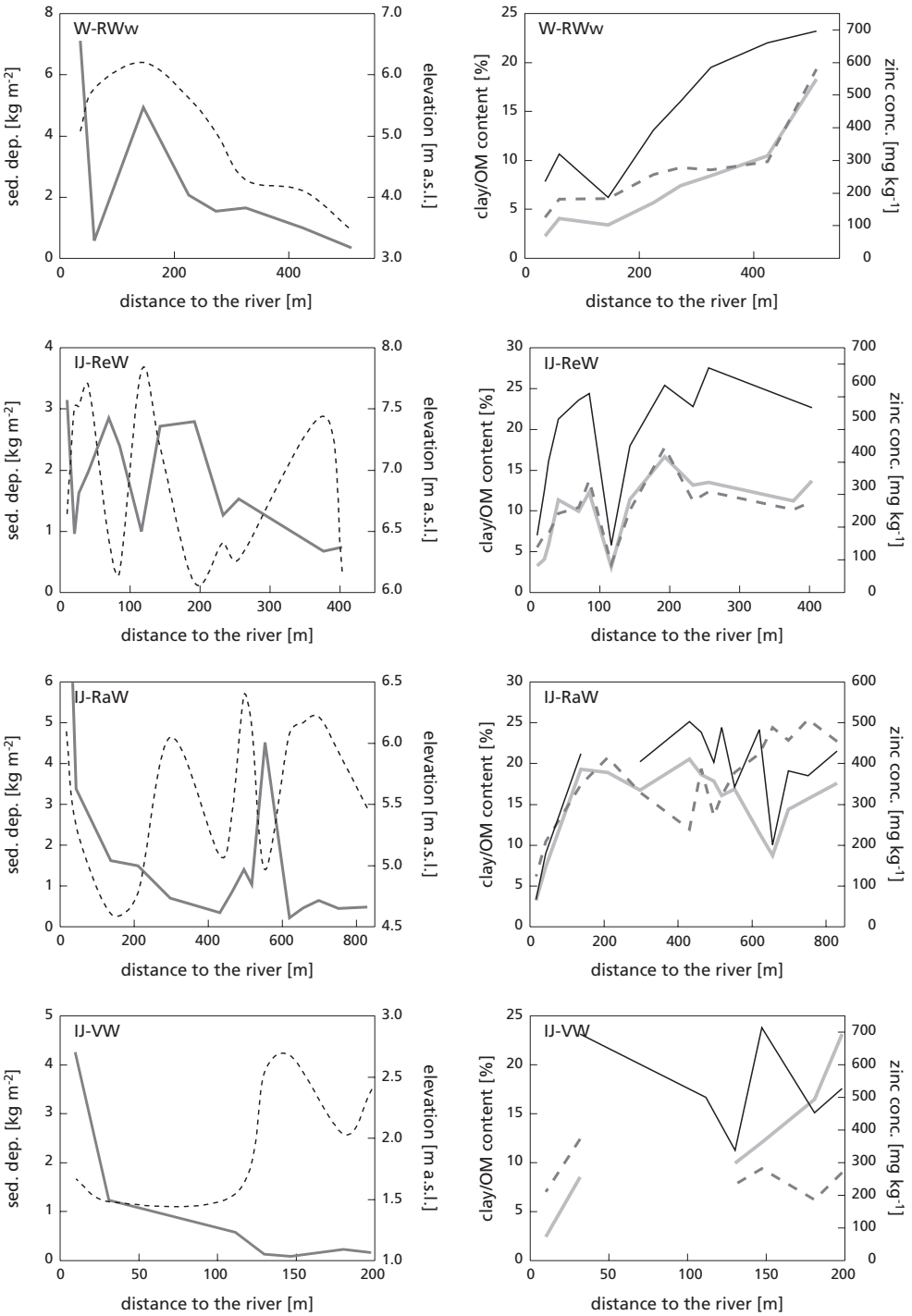
W-RWw
sed. dep. [kg m-2]
elevation [m a.s.l.]
clay/OM content [%]
zinc conc. [mg kg-1]
distance to the river [m]
IJ-ReW
IJ-RaW
IJ-VW

Table 3.3 Sediment variables for the deposited sediments in the studied floodplains (Fig. 3.2).

Variable	Sed. dep. [g m^{-2}]			Clay content [%]			Sand content [%]			om content [%]			d_{50} [µm]		
Statistic	**Range**	$\bar{X}$	*s*	**Range**	$\bar{X}$	*s*	**Range**	$\bar{X}$	*s*	**Range**	$\bar{X}$	*s*	**Range**	$\bar{X}$	*s*
W-BW	430–3730	1538	946	16–36	24	3.4	0–16	2	4.0	8–19	12	1.9	3–14	6	2.1
W-ADW	297–3461	1661	840	12–30	25	4.0	0–36	4	7.6	8–21	14	2.8	4–48	8	8.4
W-RWd	336–3286	1037	715	13–31	26	4.1	0–29	2	6.3	10–20	15	2.7	5–29	7	5.2
W-RWw	217–3812	1439	972	11–27	18	4.3	1–48	19	13	4–18	10	3.7	5–62	17	15
IJ-ReW	376–2849	1503	804	8–28	21	5.0	1–53	14	14	4–17	11	2.9	5–63	13	14
IJ-RaW	173–1989	762	438	10–26	20	4.1	3–45	15	11	7–29	20	4.7	5–45	11	7.5
IJ-VW	67–1401	438	377	11–26	19	4.9	5–49	22	14	5–23	12	4.5	6–61	17	17
Total	67–3812	1144	847	8–36	22	5.0	0–49	10	13	4–29	14	5.0	3–63	10	10

Table 3.4 Heavy metal concentrations in the deposited sediment (Table 3.3) on the studied floodplains (Fig. 3.2).

Variable	[Zn] [mg kg^{-1}]			[Pb] [mg kg^{-1}]			[Cu] [mg kg^{-1}]			[Cd] [mg kg^{-1}]		
Statistic	**Range**	$\bar{X}$	*s*	**Range**	$\bar{X}$	*s*	**Range**	$\bar{X}$	*s*	**Range**	$\bar{X}$	*s*
W-BW	194–343	273	27	64–147	88	16	37–72	50	6	2.1–3.2	2.8	.3
W-ADW	176–656	342	93	59–181	97	24	30–101	58	14	1.9–5.6	3.1	.7
W-RWd	233–395	288	44	54–119	79	18	35–61	50	5	2.2–3.5	2.7	.3
W-RWw	181–580	285	86	42–168	80	26	23–76	44	12	1.7–6.6	(4.1)	1.0
IJ-ReW	144–444	255	62	38–112	70	17	20–68	40	11	2.7–6.4	(4.3)	.9
IJ-RaW	131–432	303	69	57–131	91	14	34–70	56	9	1.2–4.0	2.6	.7
IJ-VW	108–379	277	74	47–141	92	22	24–48	39	8	3.0–5.3	(4.3)	.7
Total	108–656	295	72	38–181	89	21	23–101	50	12	1.2–6.6	2.8 [a]	1.0

a. Values in parentheses are left out of calculation of mean value for Cd.

present: the zinc concentrations decrease with increasing distance to the river and increasing clay and organic matter content (Fig. 3.4). As in the case with the increasing sedimentation with distance to the river, this probably also relates to the secondary channel acting as a source of less contaminated sediment.

3.5 Discussion

3.5.1 Variation in deposition between river branches and floodplain sections

Variation in amount of sediment deposition. The Waal River floodplains receive significantly more sediment per unit area than the IJssel River floodplains. However, although we measured sedimentation within the same lowland river system, we still measured during different peak discharges, which differed in suspended matter concentrations and duration (Fig. 3.3). Calculating the apparent settling velocity ($w_{s,a}$) corrects for these flood-dependent variables and reflects the general deposition rate for a floodplain:

$$w_{s,a} = S / (SSC \cdot T) \tag{3.1}$$

with $w_{s,a}$ = apparent settling velocity [m s^{-1}], S = sedimentation amount [g m^{-2}] (Table 3.3), SSC = average suspended sediment concentration during the period of sediment conveyance over the floodplain (Fig. 3.3) [mg l^{-1}] and T = duration of sediment conveyance [s] (Table 3.2).

The median values for the apparent settling velocity for the floodplains vary between 2.1 10^{-6} (IJ-VW) and 6.8 10^{-5} m s^{-1} (W-ADW) (Fig. 3.5). These values are rather small compared to values for real flocs reported by Droppo *et al.* (1997, 2000). Droppo (2003) states that flocs normally settle with velocities ranging from 1 to 2.5 10^{-3} m s^{-1}. Those values are however valid for individual flocs, whereas our values indicate how much sediment is deposited given the amount and time available for deposition. In other words, the $w_{s,a}$ found here indicates the average trapping efficiency for a floodplain.

The Waal River floodplains have a significantly higher $w_{s,a}$ (4.2 10^{-5} m s^{-1} on average) than the IJssel River (7.9 10^{-6} m s^{-1} on average) (p =.000). This may be attributed to the minor embankments of the Waal River floodplains, which favours quiescent flow conditions and hence settling of suspended matter, and the lack of minor embankments along the IJssel River floodplains, where larger flow velocities keep the flocs in suspension.

Another reason for the higher $w_{s,a}$ for the Waal River floodplains may be the general characteristics of the Waal River. The broad Waal River routes two-third of the River Rhine discharge, the narrow IJssel River only one-ninth. Besides, major embankments confine the Waal River 'valley', which is consequently narrower than the largely unconfined IJssel River valley (Fig. 3.2). This yields generally low F/C ratios in the Waal River and clearly higher ratios in the IJssel River (Table 3.1). This combination results in more confined flow, considerably larger water depths and hence more sediment conveyance over the Waal River floodplains than over the IJssel River floodplains. Consequently, in the Waal River, more water and sediment is available per unit distance of floodplain. This subsequently results in more deposition, provided confinement of flow does not lead to shear stresses that exceed the critical shear stress for sediment deposition. Such flow velocities, however, do not occur, because the minor embankments drastically decrease the transfer of momentum from the river channel to the floodplain. Because the higher discharge of sediment over the Waal River floodplains takes place at larger but still sufficiently low flow velocities for deposition, this results in higher sedimentation quantities on the Waal River floodplains than on the IJssel River floodplains. This contrasts with both Lecce (1997) and Wyżga (1999), who found that when valley width decreases, flow becomes more confined and flow velocities increase, thereby decreasing sediment deposition.

Variation in grain size. The deposits on the Waal River floodplains are significantly finer than on the IJssel River floodplains. There seem to be two topographical and morphological reasons for this phenomenon. Firstly, the minor embankments along the Waal River not only reduce the transfer of momentum in the river water, they also hamper the inflow of sandy material in the

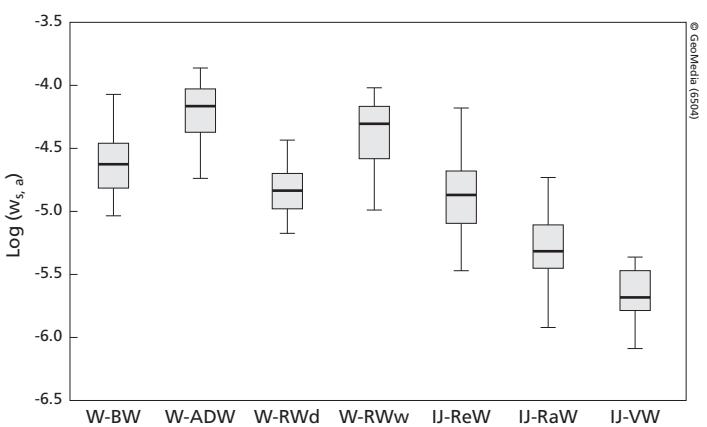

Figure 3.5 Apparent settling velocity ($w_{s,a}$) for all floodplains.

lower part of the water column (Middelkoop & Asselman 1998). Because the natural levees of the IJssel River are lower, more sand can enter the floodplains along this river branch.

Secondly, the Waal River has a lower sinuosity than the strongly meandering IJssel River (Figs. 3.1 and 3.2). Bathurst *et al.* (2002) found that transfer of sandy sediment (in their experiment having a d_{50} of 100 μm) only takes place in a confined strip along a straight channel, whereas it was deposited further away on the floodplain in the case of a meandering channel because of stronger convective flow over the floodplain. Hudson & Heitmuller (2003) found that the distance of sediment transfer onto the floodplain was larger for more pronounced meanders because of increased flow competence. Furthermore, the IJssel River floodplains are in general located on inner bends. These inner bends may receive more sandy sediment than outer bends due to the helical flow (Ten Brinke *et al.* 1998; Bathurst *et al.* 2002). In addition, direct transport of sand may take place when river water flows over the inner bends during peak discharges (Ten Brinke 2004). In short, because of the more pronounced meandering of the IJssel River and the absence of minor embankments, sand apparently may be transferred further into the floodplain, resulting in sandier floodplain deposits than on the Waal River floodplains.

Variation in downstream trend in sediment deposition. The IJssel River manifests significant different apparent settling velocities (Fig. 3.5) for its floodplains, whereas the Waal River does not. In addition, the IJssel River exhibits a downstream trend in sediment deposition. Both features seem to have the same background. Conveyance losses of the IJssel River floodplains are clearly higher than those of the Waal River floodplains (Asselman & Van Wijngaarden 2002). Retention of the suspended matter entering the river branch during a high-magnitude flood (7000–9000 $m^3 s^{-1}$) may reach 93 % on the floodplains of the IJssel River, whereas this is only 8 % for the Waal River (Van der Lee *et al.* 2004). Although the individual Waal River floodplains trap more of the entering sediment (Fig. 3.5) because of the quiescent conditions behind their minor embankments, the river branch also transports approximately six times more suspended sediment than the IJssel River. Hence, the relative loss of sediment for the total river branch is small and downstream exhaustion is hardly noticeable. The IJssel River, on the contrary, conveys little sediment and water over its wide floodplains (F/C ratio in Table 3.1). Although the individual floodplains may trap little conveyed sediment, their total surface along the river branch relative to the amount of transported sediment is considerable. This results in high trapping efficiencies (Van der Lee *et al.* 2004), which subsequently lead to a downstream exhaustion of suspended matter.

3.5.2 Variation within floodplain sections

Relation between sedimentation and distance to the river. For floodplains without flood protection, sedimentation amounts tend to decrease exponentially with increasing distance to the river (see relations for the IJssel River floodplains in Fig. 3.6). This is because at locations further away from the sediment source (usually the river channel), less sediment is available for deposition because of exhaustion of suspended matter. In addition, sediment conveyance to locations farther away from the river channels is limited due to lower flow velocities. However, a floodplain with a secondary source of sediment, such as the W-RWd floodplain, does not feature this significant trend. Apparently, the secondary channel is a more important source of sediment than the river channel (see also Fig. 3.4). Moreover, in the W-ADW floodplain the sedimentation amount

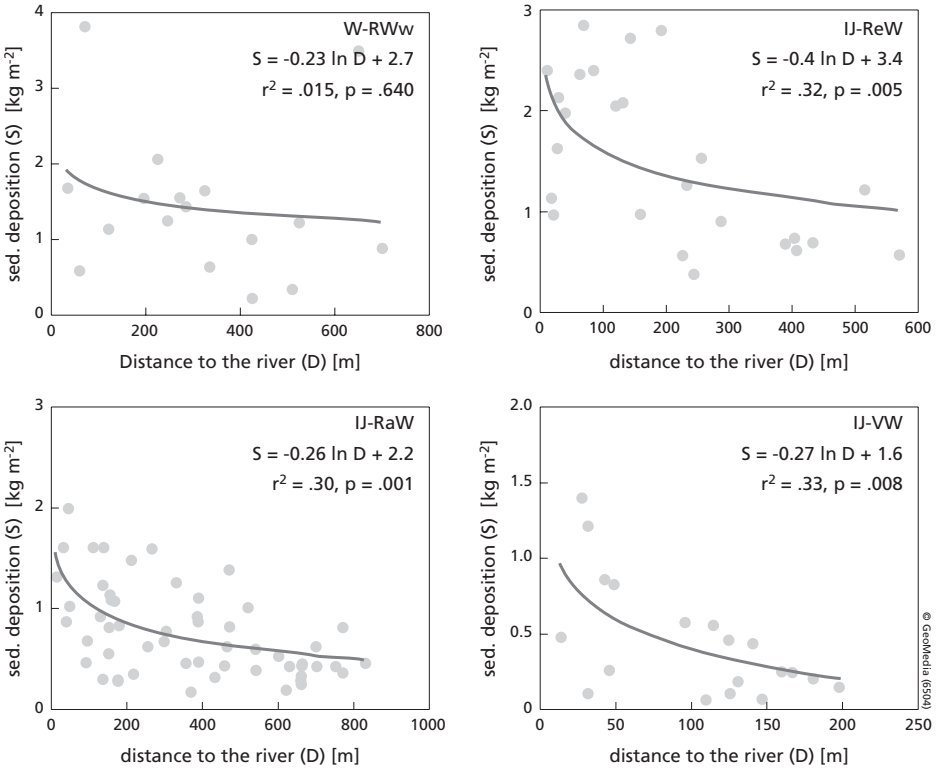

Figure 3.6 Relation between distance to the river and sediment deposition for the W-RWw floodplain and the three IJssel River floodplains.

increases with increasing distance to the river (r^2 = .27, p = .017). This may be explained by the inundation pattern: the river water first enters the floodplain in the northeast through a sluice, thereby inundating the lower distal parts of the floodplain in the southeast (Fig. 3.2). Only when the minor embankment is overtopped, the river water also inundates the higher parts closer to the minor embankment. The cases of the W-RWd and W-ADW floodplains show that it may be better to speak of 'distance to the sediment source' than of 'distance to the river'.

The other floodplains with minor embankments do not exhibit a significant (W-RWw floodplain, Fig. 3.6) or only a weak (W-BW floodplain, r^2 = .12, p = .016) decrease in sedimentation amount with increasing distance to the river. The minor embankment and natural levee inhibit the entrance of sediment (predominantly sand) in the lower part of the water column (Middelkoop & Asselman 1998). This means that the important sandy sedimentation close to the river hardly takes place within the confinement of the floodplains. Consequently, differences between closer and distal parts of the floodplain are smaller, leading to low or even insignificant relations between sedimentation amount and distance to the river. Furthermore, because minor embankments also control hydrodynamics during flooding, little variation in flow velocity and

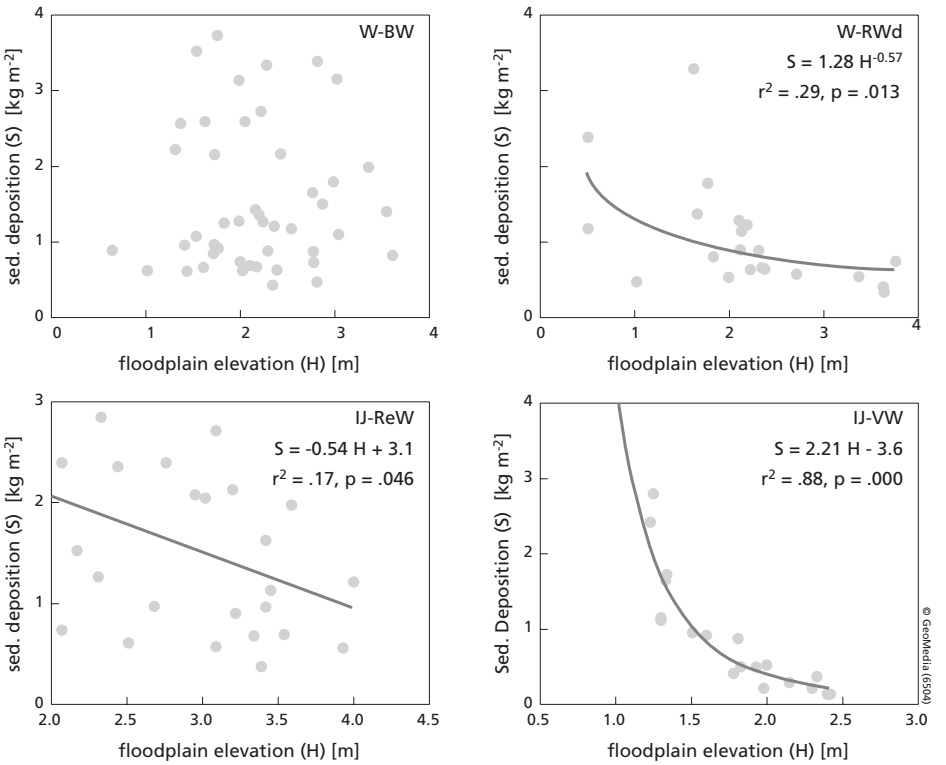

Figure 3.7 Relation between floodplain elevation and sedimentation amount for one floodplains with minor embankments (W-BW) and three floodplains without protection against low-magnitude floods (W-RWd, IJ-VW and IJ-ReW).

inundation duration takes place, leading to relatively homogeneous sediment deposits behind flood protection works (Wyżga 1999).

Relation between sedimentation and floodplain elevation. All three IJssel River floodplains and the W-ADW (r^2 = .20, p = .003) and W-RWd floodplain show a significant decrease in sedimentation amount with increasing floodplain elevation (Fig. 3.7), but the W-BW (Fig. 3.7) and W-RWw (r^2 = .01, p = .65) floodplain do not. The significant relation for the W-ADW, however, has the same reason as the trend with distance to the river mentioned above: the lower parts in the southeast are inundated first. The higher parts are only inundated when the river water overtops the minor embankment. Hence, once more there appears to be a division between floodplains with and without protection against low-magnitude floods. The latter has a significant decrease of sedimentation with increasing floodplain elevation and the former not. Yet, there may also be a morphological reason for this difference. The topographical variation in the natural and unlevelled IJssel River floodplains is considerably higher than in the levelled Waal River floodplains. For instance, about 70 % of the sample points in the W-BW and W-RWd floodplain lie within a vertical range of one meter (Fig. 3.7). The combination of a narrow

elevation range with strong local variation in sediment deposition (Asselman & Middelkoop 1995) leads to insignificant correlations. In the IJ-RaW and IJ-ReW floodplain, on the contrary, the elevation range is about 2 m (Fig. 3.7), with weak but significant correlations between floodplain elevation and sedimentation amounts. This shows that not only the general trend in topography but also the magnitude of topographical variation relative to the short-range spatial variation in sediment deposition amounts influences its spatial trend.

OM-metal and clay-metal relations. Fig. 3.8 gives the relations between the clay and organic matter content with the zinc concentration for the floodplains that inundated in March 2001 (W-RWw, IJ-ReW and IJ-VW floodplains):

$$[Zn] = 8.0\ C + 115.3\ (r^2 = .27, p = .000, n = 55) \quad (3.2)$$

$$[Zn] = 7.8\ OM + 185.6\ (r^2 = .16, p = .001, n = 58) \quad (3.3)$$

with $[Zn]$ = zinc concentration [mg kg^{-1}], C = clay percentage and OM = organic matter percentage.

The relation between zinc concentration and om content (r^2 = .16) is considerably weaker than with clay content (r^2 = .27). This may indicate that the organic matter consists of different components (e.g., humic and fulvic acids, autochthonous organic matter). Each component has a different binding capacity and varies in relative abundance with each event or with discharge. For the clay composition of the River Rhine suspended sediment, Van Eck (1982) gives a 6 : 3 : 1 ratio for illite : smectites : kaolinite. Van der Weijden & Middelburg (1992) compared this ratio with Hellmann & Bruns' (1968) data for Koblenz (Germany) and concluded that the two mineralogical compositions were similar. This indicates that the clay composition is more constant, which results in a more constant binding capacity at high pH and less variation in zinc concentration.

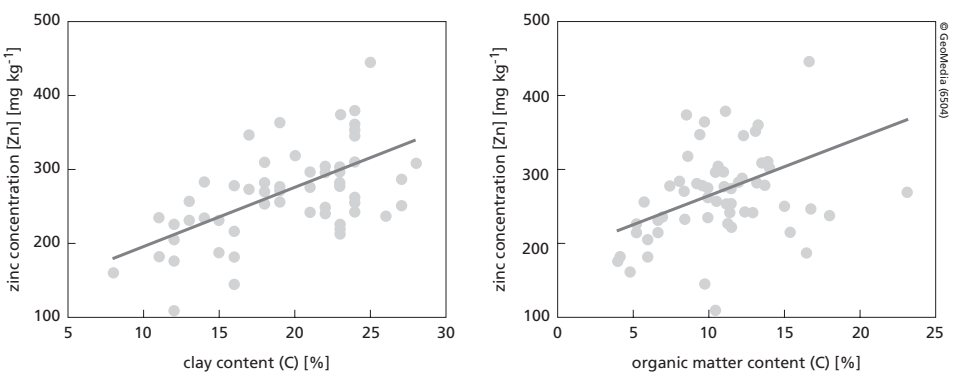

Figure 3.8 Relation between zinc concentration and clay (n = 55) and organic matter (n = 58) content for the lower River Rhine.

At individual floodplain level, the relations between metal concentrations and clay/organic matter content generally resemble those given by Eqs. 2 and 3 (Table 3.5). The only exceptions are the clay–[Zn] relation for the W-RWd floodplain (probably because of mixture of sediment coming from the river and the secondary channel), the OM–[Zn] relation for the IJ-RaW (probably due to addition of local organic matter) and IJ-VW floodplain and both relations for the W-BW floodplain (Table 3.5). For the floodplains with flood protection, the explained variance of the relations seems to decrease with increasing flood-protection height (Table 3.5). The reason

Table 3.5 OM–[Zn] and clay–[Zn] relations for the three floodplains with protection against low-magnitude flooding, with the floodplains with flood protection sorted in ascending height of protection. Non-significant relations are denoted with 'n.s.'.

	Floodplains without flood protection				**Floodplains with flood protection**		
Floodplain	W-RWd	IJ-ReW	IJ-RaW	IJ-VW	W-RWw	W-ADW	W-BW
OM–[Zn]	$Y = 8.5\,x + 154$ $r^2 = 0.32$	$y = 16.4\,x + 81.1$ $r^2 = 0.59$	$y = -5.2\,x + 407$ $r^2 = 0.13$	$y = -2.9\,x + 312$ n.s.	$y = 19.9\,x + 92.7$ $r^2 = 0.79$	$y = 18.3\,x + 84.9$ $r^2 = 0.32$	$y = 0.1\,x + 270$ n.s.
Clay–[Zn]	$Y = -6.3\,x + 451$ $r^2 = 0.34$	$y = 9.1\,x + 68.1$ $r^2 = 0.52$	$y = 9.8\,x + 109$ $r^2 = 0.36$	$y = 8.4\,x + 117$ $r^2 = 0.31$	$y = 12.4\,x + 56.3$ $r^2 = 0.59$	$y = 10.2\,x + 82.9$ $r^2 = 0.33$	$y = 0.2\,x + 267$ n.s.

for this is the decreasing variation in OM content of the overbank deposition with increasing flood protection height. For instance, the coefficient of variation (CV = s / $\bar{X}$) for organic matter content declines from 37 % for the W-RWw floodplain with only a natural levee to 16 % for the W-BW floodplain with a high minor embankment. This may indicate that a higher flood protection or floodplain elevation leads to a more homogeneous sediment character. We may explain this by the decreasing variation in suspended sediment characteristics with increasing discharge. Both median grain size (Asselman & Middelkoop 1998) and metal concentrations (Middelkoop *et al.* 2002) of the suspended matter show little variation at moderate to high discharges (> 6000 m^3 s^{-1}). Floodplains that are only inundated at these higher discharges thus receive rather homogeneous sediment, not only with respect to grain size, but also with respect to organic matter content and heavy metal concentrations.

3.6 Conclusions and implications

There are clear spatial differences in deposition and sediment characteristics between the floodplains along the human influenced Waal and less influenced IJssel River. These differences become manifest at two spatial scales: at the scale of the river branches and at the scale of their individual floodplain sections.

At the scale of the river branch, we could relate differences in sedimentation amount, grain size and downstream exhaustion of suspended matter to geomorphological and hydrological variables such as the ratio of the floodplain width ('valley width') to the channel width, sinuosity, and water depths and flow velocities during peak discharges. The narrower floodplains of the Waal River transport large amounts of sediment and water to the sea during floods. This combination leads to major conveyance of sediment over the floodplains, where low flow velocities lead to considerable deposition of predominantly finer particles. The IJssel River floodplains, by contrast, experience less sediment conveyance during peak flows because its smaller discharge of sediment and water being distributed over much wider floodplains. Yet, this combination results in high trapping efficiencies of the floodplains, resulting in a downstream exhaustion of the relatively little sediment that is available for deposition. Because the high degree of meandering leads to convective transport of sand to the floodplains, IJssel River floodplains trap significantly coarser sediments.

At the scale of the individual floodplain sections, we have confirmed a number of trends for the IJssel River that have been reported in literature for smaller rivers and the Waal River. In general, sedimentation amount decreases with increasing distance to the river and increasing floodplain elevation. Heavy metal concentrations increase with increasing clay and organic matter content. Yet, exceptions to these trends show that topographical variables, such as distance to the river and floodplain elevation often do not suffice to describe the pattern in more complex situations. For instance, there may be secondary sources of sediment besides the river channel itself or complex hydrodynamic patterns at the onset of inundation. Furthermore, the presence of protection against low-magnitude flooding such as minor embankments and natural levees may drastically reduce the amount of spatial variation in floodplain deposits. It appears that this reduction increases with increasing height of the flood protection.

The comparison of the findings at the two scales shows that situation for sediment trapping capabilities for individual floodplains reverses at the scale of the river branch. The flood-protected Waal River floodplains trap a large part of the sediment influx, but only a small part of the total sediment transport through the river branch during peak discharges. Individual IJssel River floodplains without minor embankments experience less sediment trapping. Yet, because the total surface of the floodplains is large relative to the sediment and water discharge of the river branch, conveyance losses are considerable and even lead to downstream exhaustion of suspended matter. This shows that both the individual floodplain and the river branch scale have to be taken into account when explaining sediment and metal budgets for lowland rivers.

We summarize the implications of these findings as follows:

- At the scale of the river branch, morphological and hydrological parameters may explain a major part of the variation in floodplain deposition. This means that measuring these parameters at this scale already gives considerable insight in the process, amounts and spatial patterns of floodplain deposition. Measuring these relatively straightforward parameters could also help to give a first approximation of a sediment and contaminant budget for a river branch.
- At the scale of the floodplain, simple one-dimensional/bivariate relations may not adequately describe the spatial pattern of contemporary floodplain deposition. Larger floodplains and/or floodplains with more complex topography and hydrodynamics during inundations may exhibit different relations than those generally reported in literature. In those cases floodplain deposition models could be of help, provided that their spatial resolution and the hydrodynamic input data are detailed enough. Yet, it is paradoxical that we still have to rely on empirical data on contemporary floodplain deposition to calibrate these models and to point out model flaws.

Acknowledgements

We kindly thank Bart Makaske and Gilbert Maas (Alterra, Wageningen University and Research Centre) for collecting and providing the sediment traps from the W-ReW, W-RWw and IJ-VW floodplains. We also thank Diane Heemsbergen, Petra van Vliet, Sander Wijnhoven, Leo Thonon, Dick Middelkoop, Peter Burrough, Boris Nolte, Karen Winkelman, Menno Straatsma and Koos Jan Niesink for their valuable help in placing and collecting the sediment traps in the other floodplains. Koos Jan Niesink and Saskia Keesstra subsequently collected the sediment from the traps. Roel van Elsas (Mineral Separation Laboratory, Vrije Universiteit Amsterdam) helped to homogenize the retrieved sediment. Ton Warmenhoven, Marieke van Duin and Kees Klawer carried out the laboratory (grain size and heavy metal) analyses.

References

Asselman, N.E.M. (1999), The use of floodplain sedimentation measurements to evaluate the effects of river restoration works. Geological Society Special Publication 163, pp. 111–122.

Asselman, N.E.M. & H. Middelkoop (1995), Floodplain sedimentation: quantities, patterns and processes. Earth Surface Processes and Landforms 20, pp. 481–499.

Asselman, N.E.M. & H. Middelkoop (1998), Temporal variability of contemporary floodplain sedimentation in the Rhine-Meuse delta, The Netherlands. Earth Surface Processes and Landforms 23/7, pp. 595–609.

Asselman, N.E.M., H. Middelkoop & P.M. van Dijk (2003), The impact of changes in climate and land use on soil erosion, transport and deposition of suspended sediment in the River Rhine. Hydrological Processes 17/16, pp. 3225–3244.

Asselman, N.E.M. & M. van Wijngaarden (2002), Development and application of a 1D floodplain sedimentation model for the River Rhine in The Netherlands. Journal of Hydrology 268/1-4, pp. 127–142.

Bathurst, J.C., I.A. Benson, E.M. Valentine & C. Nalluri (2002), Overbank sediment deposition patterns for straight and meandering flume channels. Earth Surface Processes and Landforms 27, pp. 659–665.

Brookes, A. (1996),. Floodplain restoration and rehabilitation. In: M.G. Anderson, D.E. Walling & P.D. Bates, eds., Floodplain processes. Chichester, U.K.: John Wiley, pp. 553–576.

Brown, A.G., (1985), Traditional and multivariate techniques in the interpretation of floodplain sediment grain size variations. Earth Surface Processes and Landforms 10/3, pp. 281–291.

Droppo, I.G. (2003), A new definition of suspended sediment: implications for the measurement and prediction of sediment transport. IAHS Publication 283, pp. 3–12.

Droppo, I.G., G.G. Leppard, D.T. Flannigan & S.N. Liss (1997), The freshwater floc: a functional relationship of water and organic and inorganic floc constituents affecting suspended sediment properties. Water, Air and Soil Pollution 99, pp. 43–54.

Droppo, I.G., D.E. Walling & E.D. Ongley (2000), The influence of floc size, density and porosity on sediment and contaminant transport. IAHS Publication 263, pp. 141–147.

Guccione, M.J. (1993), Grain-size distribution of overbank sediment and its use to locate channel positions. Special Publication of the International Association of Sedimentologists 17, pp. 185–194.

Gomez, B., D. Phillips, F.J. Magilligan & L.A. James (1997), Floodplain sedimentation and sensitivity: summer 1993 flood, Upper Mississippi Valley. Earth Surface Processes and Landforms 22/10, pp. 923–936.

Horowitz, A.J. & K.A. Elrick (1987), The relation of stream sediment surface area, grain size and composition to trace element chemistry. Applied Geochemistry 2, pp. 437–451.

Foster, J.M., M.C. Thoms & M. Parsons (2002), Using multivariate statistical techniques to interpret patterns of flood plain sedimentation. IAHS Publication 276, pp. 451–461.

He, Q. & D.E. Walling (1997), Spatial variability of the particle size composition of overbank floodplain deposits. Water, Air and Soil Pollution 99, pp. 71–80.

He, Q. & D.E. Walling (1998), An investigation of the spatial variability of the grain size composition of floodplain sediments. Hydrological Processes 12/7, pp. 1079–1084.

Hellmann, H. & F.-J. Bruns (1968), Die chemische Zusammensetzung der ungelösten Stoffe des Rheins. Deutsche Gewässerkundliche Mitteilungen 12, pp. 162–166.

Hesselink, A.W., H.J.T. Weerts & H.J.A. Berendsen (2003), Alluvial architecture of the human-influenced river Rhine, The Netherlands. Sedimentary Geology 161/3-4, pp. 229–248.

Hren, M.T, C.P. Chamberlain & F.J. Magilligan (2001), A combined flood surface and geochemical analysis of metal fluxes in a historically mined region: a case study from the New World Mining District, Montana. Environmental Geology 40, pp. 1334–1346.

Hudson-Edwards, K.A., M.G. Macklin & M.P. Taylor (1999), 2000 years of sediment-borne heavy metal storage in the Yorkshire Ouse basin, NE England, U.K. Hydrological Processes 13/7, pp. 1087–1102.

Hudson, P.F. & F.T. Heitmuller (2003), Local- and watershed-scale controls on the spatial variability of natural levee deposits in a large fine-grained floodplain: Lower Pánuco Basin, Mexico. Geomorphology 56, pp. 255–269.

Kesel, R.H., 2003. Human modifications to the sediment regime of the Lower Mississippi River flood plain. Geomorphology 56/3-4, pp. 325–334.

Kesel, R.H, K.C. Dunne, R.C. McDonald, K.R. Allison & B.E. Spicer (1974), Lateral erosion of overbank deposition on the Mississippi River in Louisiana, caused by 1973 flooding. Geology 2, pp. 461–464.

Lambert, C.P. & D.E. Walling (1987), Floodplain sedimentation: a preliminary investigation of contemporary deposition within the lower reaches of the River Culm, Devon, U.K. Geografiska Annaler 69A/3-4, pp. 393–404.

Lecce, S.A. (1997), Spatial patterns of historical overbank sedimentation and floodplain evolution, Blue River, Wisconsin. Geomorphology 18/3-4, pp. 265–277.

Lecce, S.A. & R.T. Pavlowsky (1997), Storage of mining-related zinc in floodplain sediments, Blue River, Wisconsin. Physical Geography 18/5, pp. 424–439.

Lecce, S.A. & R.T. Pavlowsky (2001), Use of mining-contaminated sediment tracers to investigate the timing and rates of historical flood plain sedimentation. Geomorphology 38, pp. 85–108.

Lecce, S.A. & R.T. Pavlowsky (2004), Spatial and temporal variations in the grain-size characteristics of historical flood plain deposits, Blue River, Wisconsin, USA. Geomorphology 61/3-4, pp. 361–371.

Leenaers, H. & Rang, M.C. (1989), Metal dispersal in the fluvial system of the River Geul: The role of discharge, distance to the source, and floodplain geometry. IAHS Publication 184, pp. 47–55.

Maas, G.J., B. Makaske, P.W.F.M. Hommel, B.S.J. Nijhof & H.P. Wolfert (2003), Verstoring en successie: Rivierdynamiek en stroomdalvegetaties in de uiterwaarden van de Rijntakken. Wageningen, The Netherlands: Wageningen University & Research Centre (Alterra-rapport 759).

Marriott, S., 1992. Textural analysis and modelling of a flood deposit: River Severn, U.K. Earth Surface Processes and Landforms 17, pp. 687–697.

Mertes, L.A., (1994), Rates of flood-plain sedimentation on the central Amazon River: Geology 22, pp. 171–174.

Middelkoop, H. (2000), Heavy-metal pollution of the river Rhine and Meuse floodplains in the Netherlands. Netherlands Journal of Geosciences 79/4, pp. 411–428.

Middelkoop, H. (2002), Reconstructing floodplain sedimentation rates from heavy metal profiles by inverse modelling. Hydrological Processes 16/1, pp. 47–64.

Middelkoop, H. & N.E.M. Asselman (1998), Spatial variability of floodplain sedimentation at the event scale in the Rhine-Meuse delta, The Netherlands. Earth Surface Processes and Landforms 23/6, pp. 561–573.

Middelkoop, H., I. Thonon & M. van der Perk (2002), Effective discharge for heavy metal deposition on the lower River Rhine flood plains. IAHS Publication 276, pp. 151–159.

Nanson, G.C. & J.C. Croke (2002), Emerging issues in flood plain research. IAHS Publication 276, pp. 271–278.

Nicholas, A.P. & D.E. Walling (1997), Modelling flood hydraulics and overbank deposition on river floodplains. Earth Surface Processes and Landforms 22/1, pp. 59–77.

Simm, D.J. & D.E. Walling (1998), Lateral variability of overbank sedimentation on a Devon flood plain. Hydrological Sciences Journal 43/5, pp. 715–732.

Stanford, J.A., J.V. Ward, W.J. Liss, C.A. Frissell, R.N. Williams, J.A.Lichatowich & C.C. Coutant (1996), A general protocol for restoration of regulated rivers. Regulated Rivers: Research & Management 12, pp. 391–413.

Sweet, R.J., A.P. Nicholas, D.E. Walling & X. Fang (2003), Morphological controls on medium-term sedimentation rates on British lowland river floodplains. Hydrobiologia 494/1, pp. 177–183.

Taylor, M.P. (1996), The variability of heavy metals in floodplain sediments: a case study from mid Wales. Catena 28, pp. 71–87.

Ten Brinke, W. (2004), De beteugelde rivier: Bovenrijn, Waal, Pannerdensch Kanaal, Nederrijn-Lek en IJssel in vorm. Diemen, The Netherlands: Veen Magazines.

Ten Brinke, W.B.M., M.M. Schoor, A.M. Sorber & H.J.A. Berendsen (1998), Overbank sand deposition in relation to transport volumes during large-magnitude floods in the Dutch sand-bed Rhine River system. Earth Surface Processes and Landforms 23/9, pp. 809–824.

Thoms, M.C., Foster, J.M. and Gawne, B. (2000), Flood-plain sedimentation in a dryland river: the River Murray, Australia. IAHS Publication 263, pp. 227–236.

Thonon, I., H. Middelkoop & M. van der Perk (*submitted*), The impact of river rehabilitation, climate and land-use change on the deposition of sediment and heavy metals on floodplains. River Research and Applications.

Van Eck, G.T.M. (1982), Geochemie van zwevend materiaal en water in het Hollands Diep/Haringvliet. PhD Thesis, Utrecht: Faculteit Geowetenschappen, Universiteit Utrecht.

Van der Lee, G.E.M, H. Olde Venterink & N.E.M. Asselman (2004), Nutrient retention in floodplains of the Rhine distributaries in The Netherlands. River Research and Applications 20, pp. 315–325.

Van der Weijden, C.H. & J.J. Middelburg (1989), Hydrogeochemistry of the River Rhine: long term and seasonal variability, elemental budgets, base levels and pollution. Water Research 23/10, pp. 1247–1266.

V&W (2005), Waterbase; http://www.waterbase.nl. The Hague: Ministerie van Verkeer & Waterstaat.

Walling, D.E. (1999), Invited lecture: river floodplains as sediment sinks. In: A.W. Jayawardena, J.H.W. Lee & Z.Y. Wang, eds., River sedimentation; Theory and applications. Rotterdam: Balkema.

Walling, D.E., Fang, D., Nicholas, A.P. and Sweet, R.J., 2004. The grain size characteristics of overbank deposits on the flood plains of British lowland rivers. IAHS Publication 288: 226–234.

Walling, D.E. & Q. He (1998), The spatial variability of overbank sedimentation on river floodplains. Geomorphology 24/2-3, pp. 209–223.

Walling, D.E. & P.N. Owens (2003), The role of overbank floodplain sedimentation in catchment contaminant budgets. Hydrobiologia 494/1, pp. 83–91.

Walling, D.E., P.N. Owens & G.J.L. Leeks (1998), Erratum to "The characteristics of overbank deposits associated with a major flood event in the catchment of the River Ouse, Yorkshire, U.K.". Catena 32/3-4, pp. 309–331.

Ward, J.V., F. Malard & K. Tockner (2002), Landscape ecology: a framework for integrating pattern and process in river corridors. Landscape Ecology 17/Supplement 1, pp. 35–45.

Wijnhoven, S., I. Thonon, G. van der Velde, R.S.E.W. Leuven, M.I. Zorn, H.J.P. Eijsackers & A.J.M. Smits (*submitted*), The impact of bioturbation by small mammals on heavy metal redistribution in floodplains. Water, Air and Soil Pollution.

Wyżga, B. (1999), Estimating mean flow velocity in channel and floodplain areas and its use for explaining the pattern of overbank deposition and floodplain retention. Geomorphology 28/3-4, pp. 218–297.

4 In situ measurements of sediment settling characteristics in floodplains using a LISST-ST

Published as: Thonon, I., J.R. Roberti, H. Middelkoop, M. van der Perk & P.A. Burrough (2005), *In situ* measurements of sediment settling characteristics in floodplains using a LISST-ST. Earth Surface Processes and Landforms 30/10, pp. 1327–1343.

"*Until now it is insufficiently known (…) how the composition of the sediment varies in space and what the effective settling velocity due to flocculation is.*" (translated from Dutch) (Asselman 1999a).

"*Attention should [also] be paid to an instrument with which* in situ*, undisturbed information regarding floc size and fall velocities can be measured.*" (Van Wijngaarden 1999).

"In situ *measurements of settling velocities are required.*" (Asselman & Middelkoop 1995).

"Models for the prediction of the transport of sediment and associated contaminants will produce erroneous estimates if [these] floc characteristics are not integrated into model computations." (Droppo *et al*. 2000).

Abstract

Due to a lack of data on settling velocities (w_s) and grain size distributions (GSDs) in floodplain environments, sedimentation models often use calibrated rather than measured parameters. Since the characteristics of suspended matter differ from those of deposited sediment, it is impossible to derive the w_s and GSD from the latter. Therefore, one needs to measure *in situ* suspended sediment concentrations (SSCs), settling velocities, effective grain sizes and sedimentation fluxes. For this purpose we used the LISST-ST, a laser particle sizer combined with a settling tube.

In 2002 (twice) and 2004, we located the LISST-ST with an Optical Backscatter Sensor and sediment traps in two floodplains in The Netherlands: one along the unembanked IJssel River, another along the embanked Waal River. Measurements revealed that the SSC in the floodplains varied in relation to the SSC in the river channel. Smaller flocs dominated the SSC, while larger flocs dominated the *potential* sedimentation fluxes. The *in situ* GSD in the IJssel floodplain was significantly coarser than in the Waal floodplain, while the dispersed median grain sizes were

equal for both floodplains. Therefore, the dispersed median grain size was two to five times smaller than the effective one.

The *in situ* grain size exhibited a significant positive relationship with w_s, although the w_s for the largest flocs showed high variability. Consequently, the variability in sedimentation fluxes was also large. In the actual sedimentation fluxes, and hence in sedimentation models, *in situ* grain sizes up to about 20 μm can be neglected. In floodplain sedimentation models the relation between settling velocity and *in situ* grain size can be used instead of Stokes' law, which is only valid for dispersed grain sizes. These models should also use adequate data on flow conditions as input, since these strongly influence the suspended sediment characteristics.

Keywords

Floodplain sedimentation, grain size distribution, settling velocity, flocculation, Rhine River.

4.1 Introduction

Floodplain sedimentation models need input data on sediment characteristics such as suspended sediment concentrations (SSCs), settling velocities and grain sizes (e.g., Hardy *et al*. 2000; James 1985; Nicholas & Walling 1997). Unfortunately, these sediment characteristics cannot be derived from deposited sediments, for example from sediment traps. Nicholas & Walling (1996, 1997) and Walling & Woodward (1993, 2000) showed large differences in the size distributions of primary particles derived from sediment traps and the coagulated particles (flocs) in the river water. To distinguish between these two populations of particles, they introduced the terms *ultimate* (dispersed) and *effective* (flocculated) grain sizes. Since no systematic relationship exists between the ultimate and effective grain sizes (Eisma *et al*. 1996), ultimate grain sizes cannot be used in modelling (Droppo *et al*. 1998; Nicholas & Walling 1996; Slattery & Burt 1995, 1997) and effective grain sizes have to be measured *in situ*.

In previous studies, several approaches have been adopted to measure settling characteristics *in situ*. In one of the earliest approaches, the Owen tube (Owen 1971) and similar settling tubes were operated from a ship to measure settling velocities. These kind of tubes were lowered in a horizontal position into the water for sampling and subsequently turned vertical. They were then lifted to the deck of the research vessel for the measurement of the settling characteristics. The turning of the tube however causes water circulation and subsequent break-up of flocs (Dyer *et al*. 1996; Dearnaley 1996).

A second approach uses optical systems such as *in situ* video system (e.g., RWS-VIS by Van Leussen & Cornelisse 1993) or still cameras like the NIOZ-Camera (Eisma *et al*. 1990). However, their main disadvantage is the "*complicated and labour-intensive post processing*" (Van der Lee 2000) needed to extract the sizes and settling velocities of the recorded flocs.

A third approach is based on laser diffraction principles (Agrawal *et al.* 1991). Examples of laboratory devices using this technique are the Coulter LS and the Malvern Mastersizer. Bale & Morris (1991), Bale (1996) and Dyer *et al.* (1996) adapted the Mastersizer for *in situ* deployment. The LISST-ST (Agrawal & Pottsmith 2000), however, is especially designed for *in situ* deployment and functions autonomously. Furthermore, its settling tube makes it possible to measure *in situ* floc settling velocities without having to take the device out of the water or putting the settling tube in a vertical position.

All these approaches have resulted in a large amount of data on settling velocities and floc sizes in marine and estuarine environments. However, despite frequent calls for *in situ* measurements of sediment characteristics in floodplains (Asselman 1997, 1999a, 2003; Asselman & Middelkoop 1995; Van Wijngaarden 1997, 1999; Walling & Woodward 2000), data on sediment characteristics in riverine environments have remained scarce. Therefore, in floodplain sedimentation models, calibrated rather than measured settling velocities prevail, such as in Asselman & Van Wijngaarden (2002) and Middelkoop & Van der Perk (1998). Using Stokes' law to calculate settling velocities is not possible. That law is only valid for primary particles and not for flocs. Since calibration can lead to suboptimal results and does not permit the quality of the input parameters to be assessed, it is advisable to use measured suspended sediment characteristics instead.

In this study, we aimed to:

- Determine suspended sediment concentrations, settling velocities, effective grain sizes and sedimentation fluxes on floodplains during overbank flow and relate these to the flow characteristics;
- Establish the relation between the effective grain size and the settling velocity;
- Relate the effective to the ultimate grain size distributions.

We report on three series of measurements of *in situ* suspended matter characteristics, deploying the LISST-ST in two different floodplains along distributaries of the Rhine River in The Netherlands. We compare the measurement results of the LISST-ST with other sensors and manual samples. Next, we present results on floc sizes, SSCs, settling velocities and sedimentation fluxes and discuss their relations with discharge and river characteristics. We end with a discussion of the implications of these findings for the modelling of floodplain sedimentation.

4.2 Materials and methods

4.2.1 Study area and data collection

We performed measurements in two floodplain sections along distributaries of the River Rhine the Afferdensche & Deestsche Waarden (abbreviated as ADW floodplain) along the Waal River and the Spankerensche Waard (SW floodplain) along the IJssel River (Fig. 4.1). The ADW floodplain is protected by a minor embankment and hence experiences low flow velocities during inundation (up to a few cm s^{-1}). The SW floodplain is only protected by a low natural levee, leading to higher flow velocities during flooding (up to 20 cm s^{-1}). The Rhine River drains large

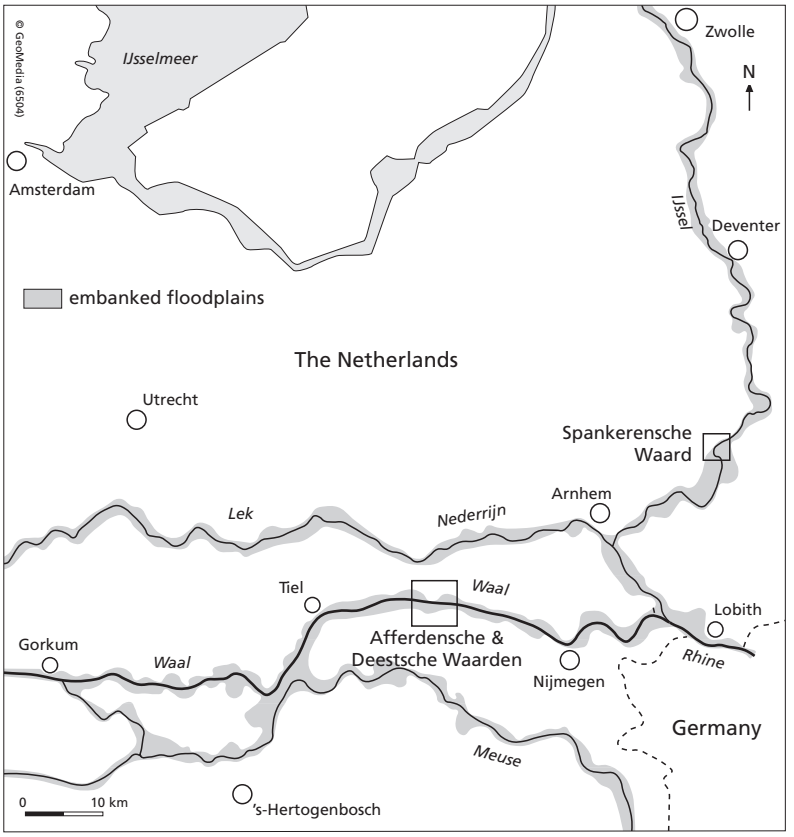

Figure 4.1 Locations of the study areas and the distributaries of the Rhine River.

parts of Central and Western Europe and discharges 2300 $m^3 s^{-1}$ on average, of which the Waal River drains two-third and the IJssel River one-ninth.

In 2002, we measured twice in the ADW floodplain: the first time from 27 February to 21 March ('ADW 1' dataset), the second time from 24 March to 3 April ('ADW 2' dataset). Both times we installed the equipment at the same location in the same measuring frame (Fig. 4.3). The frame was located 100 m away from the minor embankment in the lee side of a non-inundated area and about 2 km from the inflow point (Fig. 4.2a). The first time we could only install the LISST-ST with the aid of a diver because the floodplain was already flooded. The second time pre-flood conditions also allowed the installation of a turbidity meter and sediment traps.

In 2004, we installed the full equipment set (LISST-ST, turbidity meter and sediment traps) in the SW floodplain. Again, the measuring frame stood about 2 km from the point of inflow. This time it was located 300 m away from the river channel and about 100 m away from an abandoned side-channel (Fig. 4.2b). The flooding occurred from 17 to 28 January and yielded the 'SW' data set.

4.2.2 LISST-ST: principles, functioning and data analysis

Both LISST-ST devices employed were Type C, marketed by Sequoia Scientific, Inc. (Redmond, WA, USA) and described in Agrawal & Pottsmith (2000). This type can measure particle sizes between 2.5 and 500 μm. However, particles smaller than 2.5 μm and small particles that are aggregated into flocs also give a signal in the class with the smallest size fraction. The LISST-ST (Fig. 4.4) consists of a vertically placed cylindrical settling tube with mechanical doors and of a horizontal steel casing holding the optical measuring system and a battery pack. The LISST-ST in fact is a suspended sediment trap that monitors the settling of the enclosed suspended sediment by laser diffraction in a cylindrical settling tube of 50 mm diameter and approximately 33 cm in height. The measurement volume is located 30 cm from the top of the settling tube

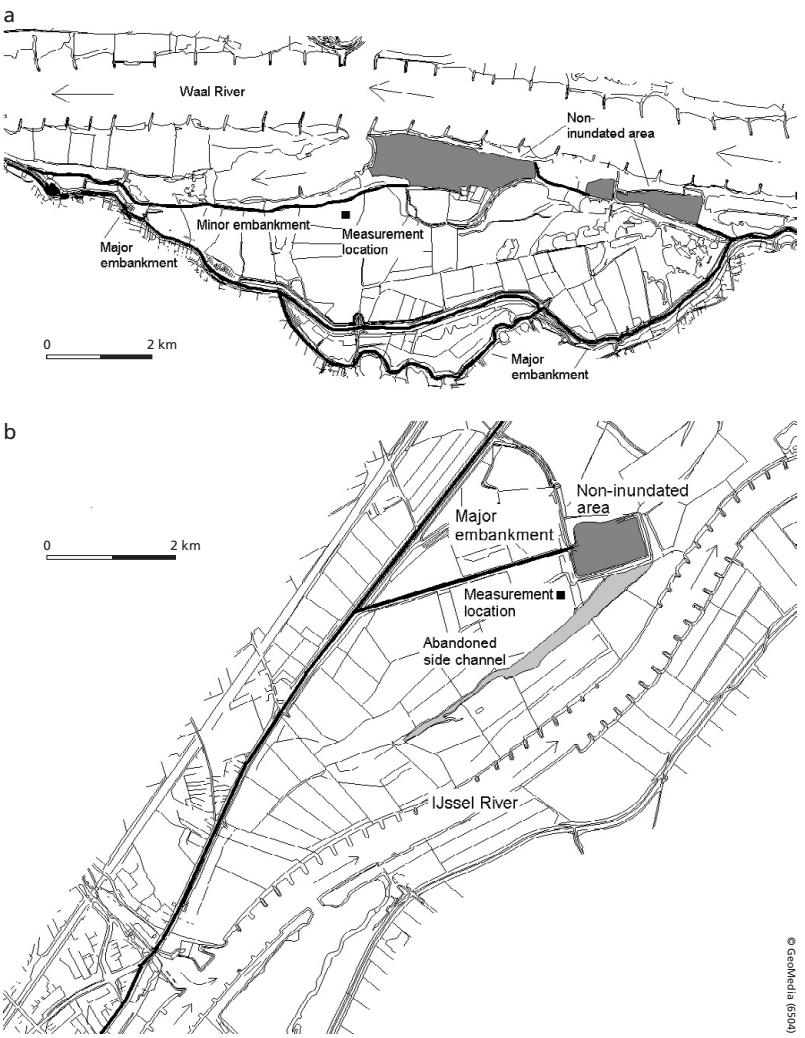

Figure 4.2 The ADW floodplain (a) and the SW floodplain (b).

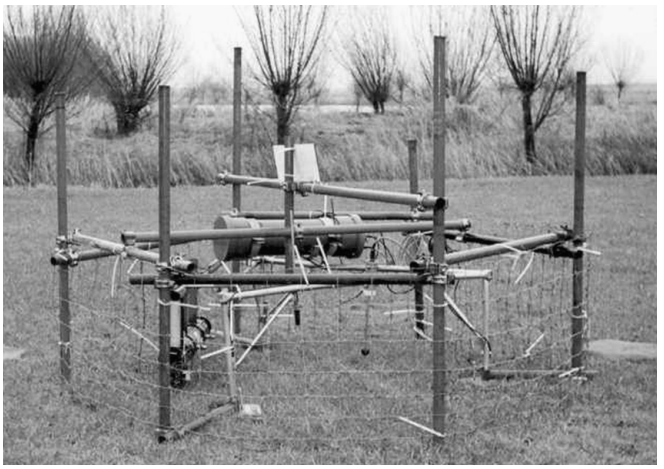

Figure 4.3 The measuring frame as installed in the SW floodplain photographed in downstream direction. The size of the toolbox on the left is about 50 cm for scale. We used the same set up in the ADW floodplain.

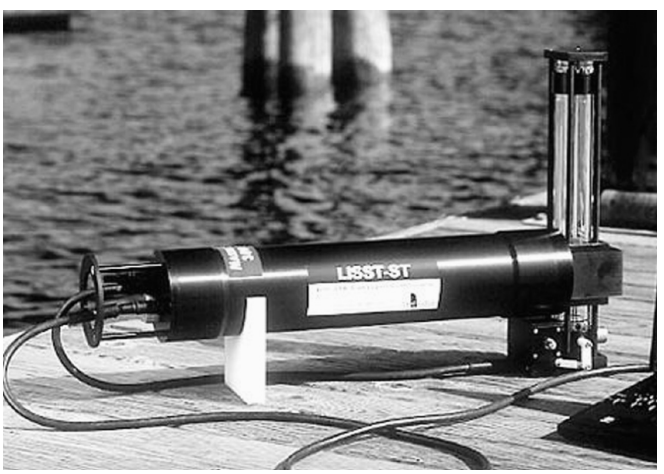

Figure 4.4 The LISST-ST combined particle sizer and settling tube measures 86.36 × 48.90 cm. The horizontal tubing holds the laser. The settling tube (32.4 cm long) can be seen on the right. Photograph: Sequoia Scientific, Inc.

where a laser beam intersects settling particles. A lens projects the diffracted laser light on concentric ring detectors that are positioned in the focal plane of the laser (at the right of the horizontal tubing in Fig. 4.4). The remaining light of the beam is focused through a pinhole on to a photodiode for measurement of the laser transmission (clarity).

Suspended sediment can enter the settling tube through eight openings of 20 mm diameter at the top of the tube. A similar set of openings is located at the bottom of the tube as exit. The

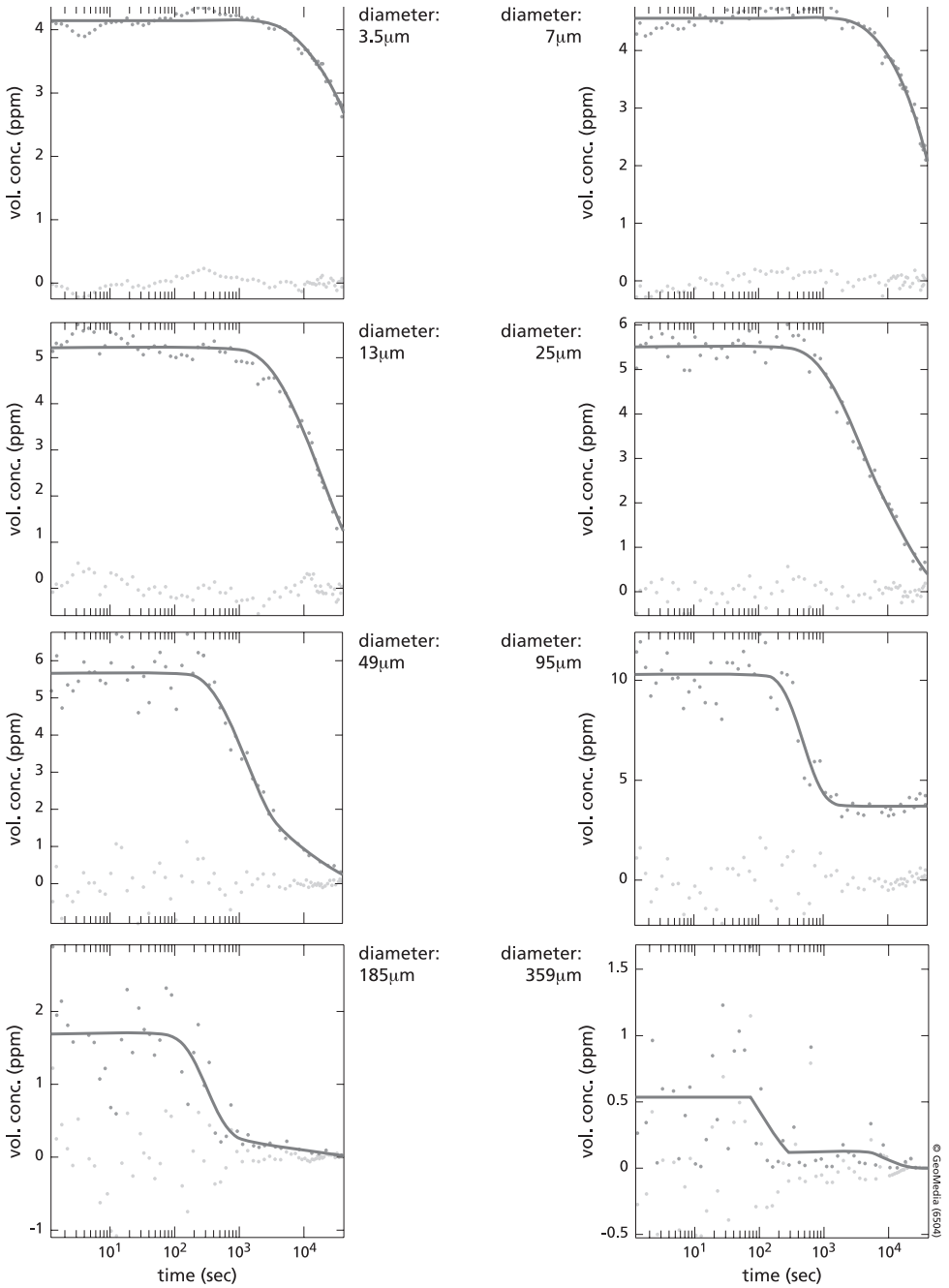

Figure 4.5 Results of the fitting procedure of the Matlab model by Van Wijngaarden & Roberti (2002). The lower dots around zero show the difference between the model fit and the data cloud of a sample from the SW data set.

interior of the tube can be sealed by a mechanism that places two cylindrical slides over the holes.

Every settling experiment begins with the opening of these doors. After this, a propeller at the bottom of the tube flushes the old water sample while at the same time a new sample is drawn in. Since the water does not flow in isokinetically and the flow generates turbulence and subsequent floc break-up, the sampled sediment can be less coarse than the real sediment distribution (Van Kessel 2003; Van Wijngaarden & Roberti 2002). When the doors are closed again, the water sample stays in the settling tube for 12 hours. The initially homogeneously distributed flocs settle to the bottom of the tube, passing the laser beam and causing diffraction of the laser light on the 32 rings of the detector. However, biofouling of the laser lens and gradual running out-of-focus of the laser during the measurements could change this diffraction. This may cause an error that cannot be quantified. Using the full Mie scattering theory (Mie 1908), which relates the size of the particle to the amount of laser light received by each of the 32 rings, the volume concentration of each size fraction of particles can be calculated. During the twelve hours of settling, a total of 71 scans were made on logarithmically spaced time intervals.

We used the model by Van Wijngaarden & Roberti (2002) for the estimation of the settling velocities. To have enough data in each size class, the 32 ring data were resampled to eight size classes. These eight size classes have their midpoints logarithmically spaced at 3.5, 6.8, 13.1, 25.4, 49.2, 95.5, 185 and 359 μm (see Table 4.1 for the size ranges). The model fits the data with a bimodal settling velocity distribution. The model's initial fit passes through the point midrange of the declining volume concentrations for each of the eight size classes (Fig. 4.5). Then the model determines the difference between the fit and the data. Next, it minimizes this difference using the non-linear least squares technique in Matlab (the 'nonlsqlin' function). This function incorporates several minimization algorithms such as Gauss-Newton and Levenberg-Marquardt. We used it with default settings with some constraints on the fitting variables.

Using the fitted bimodal settling velocity distribution, the model calculates the corresponding floc density distribution using Stokes' law. For each particle size class, two floc densities are fitted: a higher and a lower one. For the size classes with the smallest particles often only the lower fitted densities were physically plausible. This is explained by the following: when laser light falls on larger flocs, it is also partially diffracted by their smaller constituent particles (Van Wijngaarden & Roberti 2002), thereby creating aliases ('ghost particles') in the smaller size fractions. These ghost particles settle at the same rate as the larger flocs. Therefore it seems as if a part of the smaller size fractions is falling with a higher settling velocity. This higher settling velocity resulted in anomalously high densities for the smaller size classes. Therefore, for these size classes we selected the lower floc densities and settling velocities.

Table 4.1 The class names for the eight resampled size classes of the LISST-ST data with their corresponding size ranges (all in μm).

Class	**3.5**	**6.8**	**13.1**	**25.4**	**49.2**	**95.5**	**185**	**359**
Size range	2.5–4.8	4.8–9.4	9.4–18.2	18.2–35.4	35.4–68.6	68.6–133	133–258	258–500

For the size classes with the larger particles, the fitted higher densities approached published floc densities for freshwater environments (Droppo *et al*. 1997, 1998, 2000) closer than the fitted lower densities. Therefore, we chose these higher densities and settling velocities for the larger particles. Still, floc densities followed the same trend as mentioned in the literature (Dyer & Manning 1999; Droppo *et al*. 1997, 1998, 2000), i.e., decreasing floc density with increasing floc size. The floc densities and their corresponding settling velocities were finally used to calculate dry mass concentrations and mass-weighted mean grain sizes.

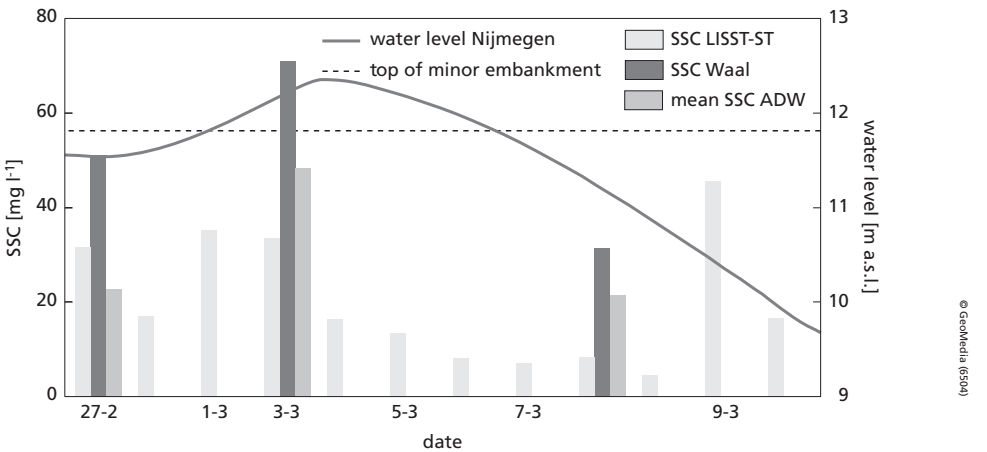

Figure 4.6 Water level at Nijmegen (nearest station), the SSC of the 0.5-l measurements for the ADW floodplain (n = 16) and Waal River (n = 1) and the SSC as measured by the LISST-ST during the inundation of early March 2002 (ADW 1 data set).

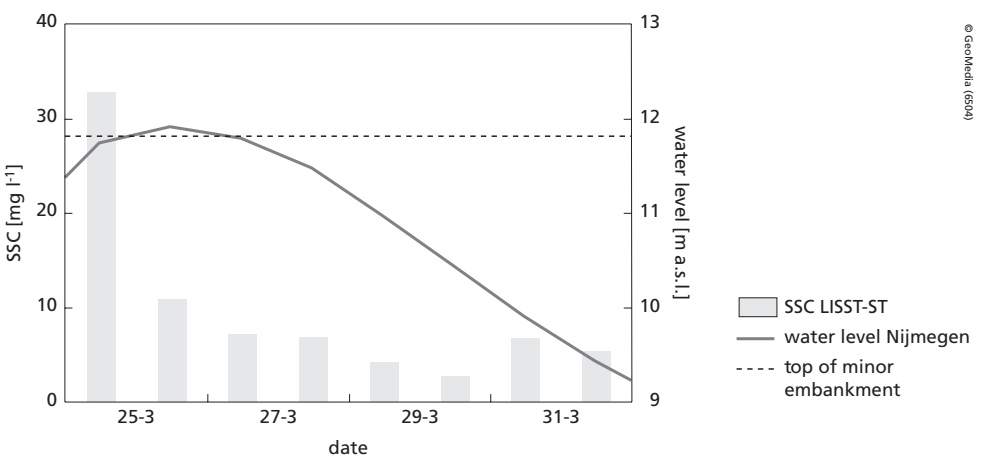

Figure 4.7 Water level at Nijmegen (nearest station) and the LISST-ST SSC for the ADW floodplain near the River Waal during the inundation of late March 2002 (ADW 2 data set).

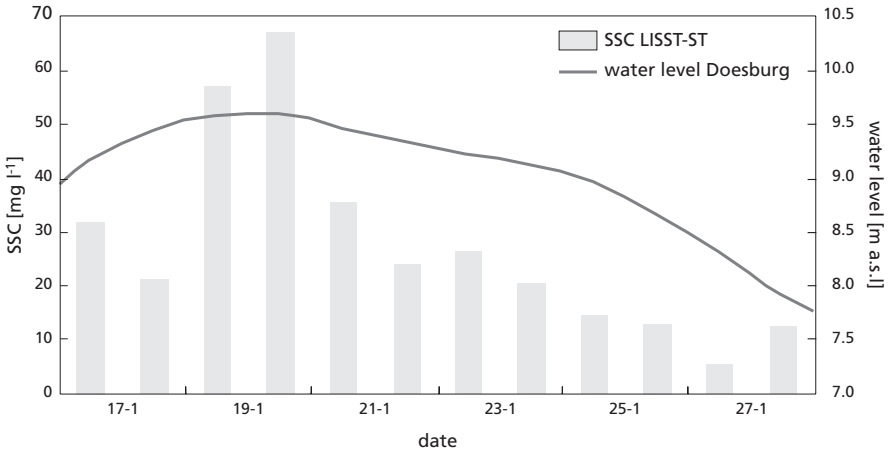

Figure 4.8 Water level at Doesburg (nearest gauging station) and the SSC as measured by the LISST-ST for the measurements of January 2004 in the sw floodplain along the IJssel River (SW data set).

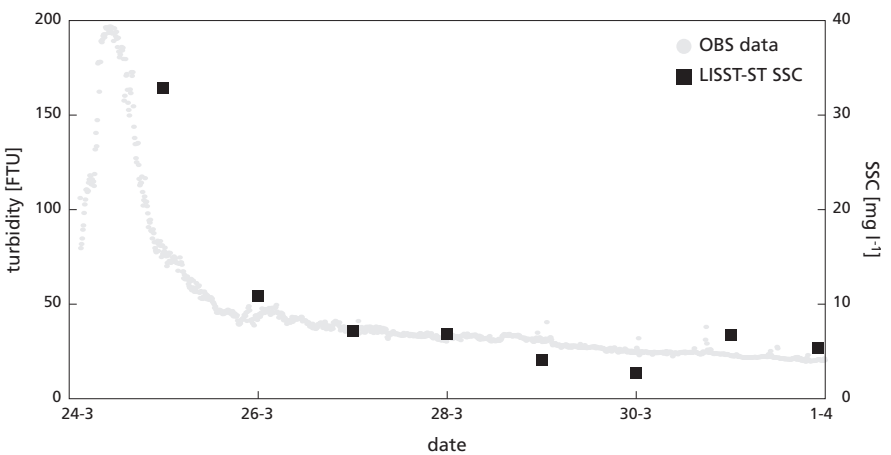

Figure 4.9 OBS and LISST-ST measurement results from ADW 2 data set.

4.2.3 Other measurements: OBS, manual samples and sediment traps

To check the LISST-ST SSC measurements independently, we deployed an Optical Backscatter Sensor (OBS), in this case a Seapoint Turbidity Meter (Seapoint Sensors, Inc., Exeter, NH, usa). An OBS measures the turbidity of the water in Formazin Turbidity Units (FTU), which varies under ideal conditions linearly with SSC. A disadvantage of the OBS technique is its size-dependency: the smaller the particles, the stronger the signal at a constant concentration. This makes field calibration often necessary. However, as previous research indicated a fairly constant mean grain size at larger discharges in the Rhine River (Asselman & Middelkoop 1998), and

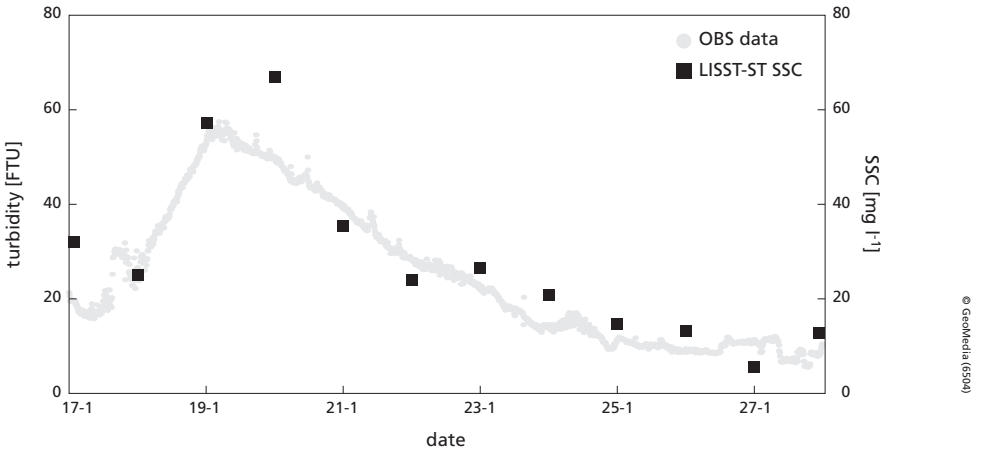

Figure 4.10 OBS and LISST-ST measurement results from the SW data set.

we mainly used the OBS as a qualitative check for the LISST-ST, there was no need for field calibration.

As a second check of the LISST-ST SSC measurements, in the ADW 1 and SW field campaigns, we sampled three and five 20 l buckets of water close to the measuring frame at the top of the discharge peak. In 2004, we gathered enough sediment to enable analysis of the ultimate grain size using a Coulter LS 230 laser diffraction device (Beckman-Coulter, Inc., Fullerton CA, USA). In addition, we sampled three sets of sixteen 0.5-l water samples on the floodplain and one in the river channel to establish the spatial pattern of the SSC for the ADW 1 data set.

Finally, in late March 2002 (ADW 2 data set) and January 2004 (SW data set) we put sediment traps close to the measuring frame. These traps are made of artificial grass (50 × 50 cm in size with 2 cm long grass tufts) and similar to those used by Lambert & Walling (1987) and Asselman & Middelkoop (1995, 1998). The ultimate grain sizes from the collected sediment was analysed using the Coulter LS 230.

4.3 Results of the field measurements

4.3.1 Suspended sediment concentrations (SSCs)

All three data sets showed the same pattern in SSC evolution in the course of the flood: an initial rise followed by a decline, although the ADW 1 & 2 data (Figs. 4.6 & 4.7) showed a stronger decline in SSC than the SW data (Fig. 4.8). The OBS measurements confirmed this pattern (Figs. 4.9 & 4.10).

The three 20-l samples of the ADW 2 data set gave SSCs of 62 to 71 mg l^{-1}, which is higher than the results of the average of the 0.5-l samples (48 mg l^{-1}) and much higher than the LISST-ST

value (33 mg l^{-1}) (Fig. 4.6). However, the five 20-l samples in the IJssel data set gave a SSC of 55 mg l^{-1} on average, which is similar to the value obtained by the LISST-ST at the same day (i.e., 57 mg l^{-1}, Fig. 4.8).

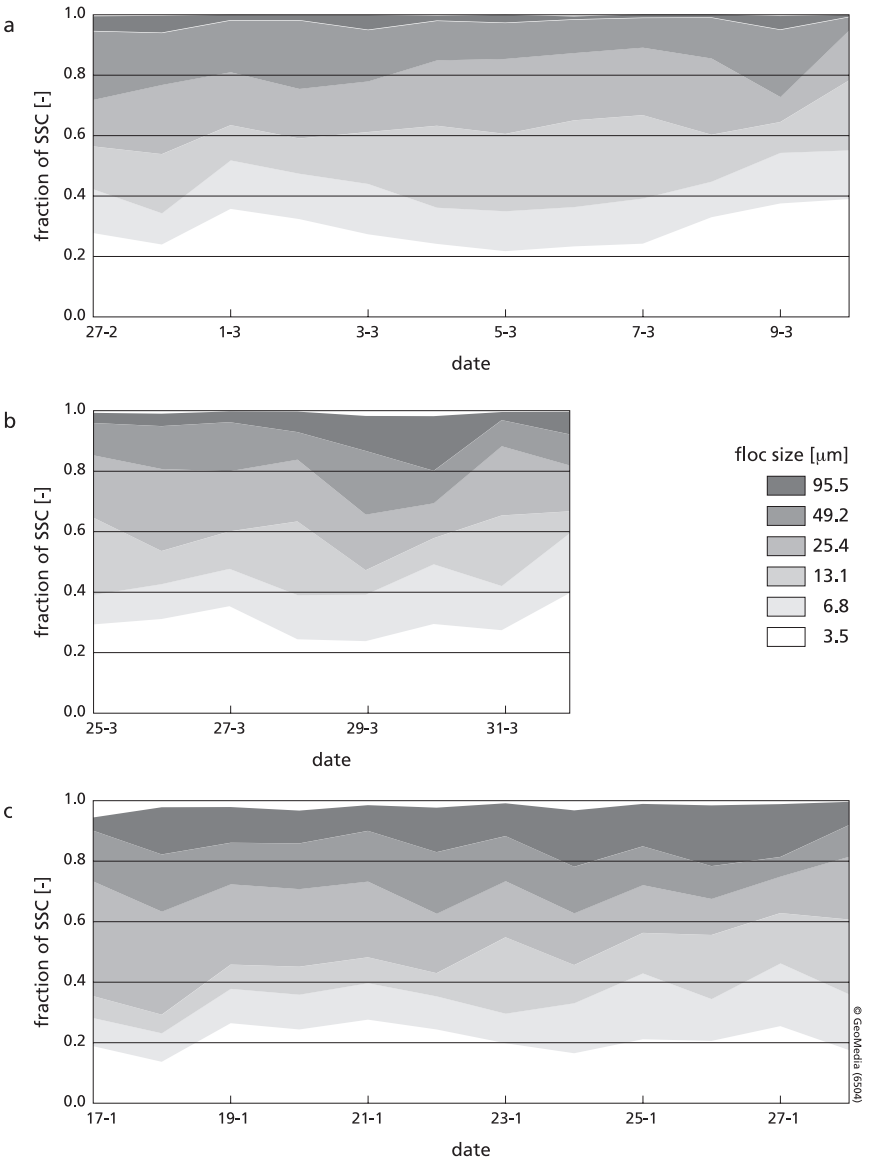

Figure 4.11 Grain size distributions for ADW 1 (a), ADW 2 (b) and SW data sets (c). Note that grain size classes are in μm are depicted as fraction of total mass concentration of particles and the two size fractions that include the largest particles are not depicted.

4.3.2 Grain size distributions (GSD)

In all three time series, the two largest size fractions hardly contributed to the SSC (Figs. 4.11 & 4.12). In the case of the SW data, the contribution of the 25.4 µm class declined during the course of the flood event (Fig. 4.11c). In the ADW data sets, however, the 3.5 µm class contributed most to the mass concentration, with the 95.5 µm class contributing only little (Figs. 4.11a & b). The interpolated median grain size (MGS) for the ADW 1 & 2 data was only 9 µm on average, while this was 25 µm for the SW data.

The variability in the GSDs is modest. The highest coefficient of variation (CV, standard deviation divided by mean) of the three data sets is 23.6 % for the ADW 2 data set. Its mean grain sizes range from 18.6 to 32.8 µm. This variability in GSDs, together with the variability in

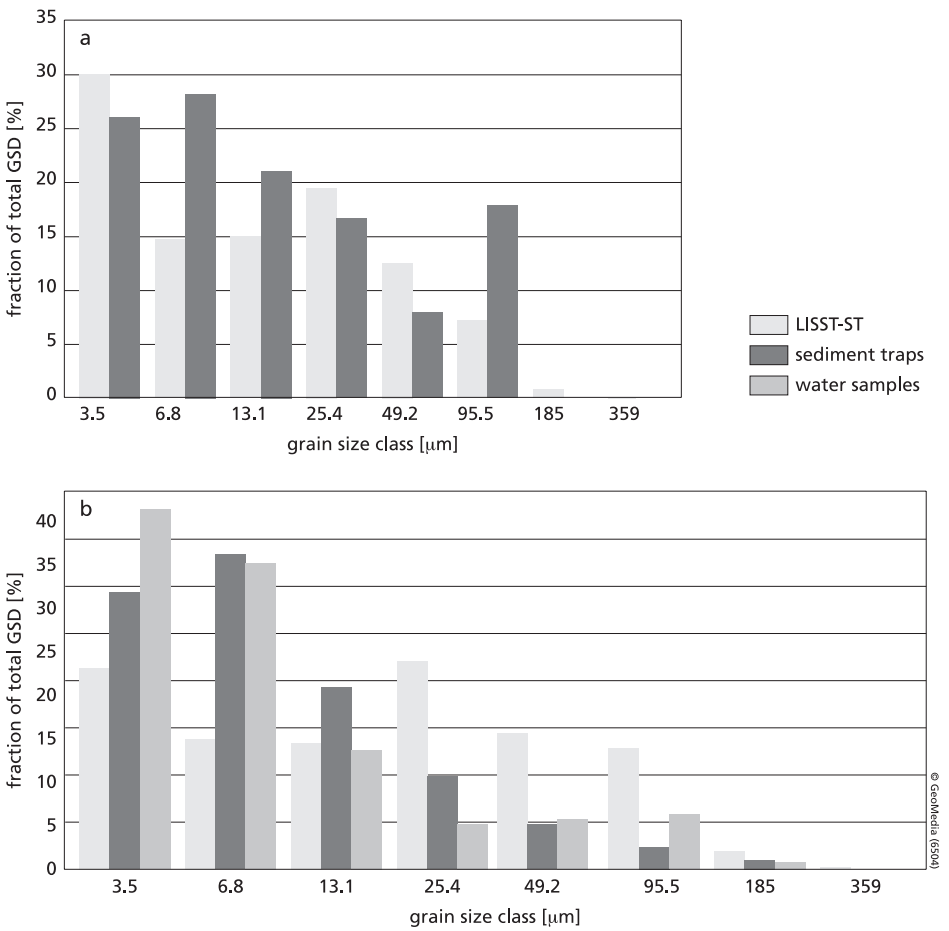

Figure 4.12 Effective (LISST-ST) and ultimate (sediment traps and water samples) GSDs for ADW 2 (a) and SW data set (b). $n = 5$ For the sediment traps (both times) and $n = 1$ for the bulked 20-l water samples.

settling velocities, affects the variability in sedimentation fluxes (see Section on 'Sedimentation fluxes').

To compare the effective GSD of the LISST-ST with the ultimate GSDs of the sediment traps and the 20-l water samples, the average effective GSDs for the ADW 2 (n = 8) and SW (n = 12) data sets were calculated. Next, the GSDs of the sediment traps and water samples had to be rescaled to the size range measured by the LISST-ST. This size range begins at 2.5 μm (Table 4.1), while the Coulter can measure particles from 0.04 μm onwards. Therefore, Fig. 4.12 only represents that part of the ultimate GSDs larger than 2.5 μm. However, composite particles with an effective size larger than 2.5 μm could be composed of particles with an ultimate grain size smaller than 2.5 μm. If the ultimate grain sizes smaller than 2.5 μm would also be included, the contrast between effective and ultimate GSDs would even be more pronounced than shown in Fig. 4.12. Bearing this limitation in mind, it becomes clear from Fig. 4.12 that the effective and ultimate grain sizes were different for both the ADW 2 and SW data sets. For instance, in the ADW 2 data set the ultimate 6.8 μm class contributed twice as much to the total amount of sediment as its effective counterpart (Fig. 4.12a). Furthermore, the 95.5 μm class was absent in the ultimate GSD but represented some seven percent of the effective GSD. Therefore, the ultimate MGS was only 5 μm. In the SW data, having an ultimate MGS of 4.5 μm, these differences were even more pronounced (Fig. 4.12b).

4.3.3 Settling velocities

The r^2 for each fitted curve (Fig. 4.5) always exceeded 0.85 for the six classes encompassing the finest grains. However, the r^2 values for the 185 and 359 μm size classes fluctuated in the ADW 1 & 2 data between 0.60 and 0.40, while they were 0.88 and 0.61 for the SW data. These lower r^2 values were caused by smaller amounts of particles and larger amounts of variability, showing up as larger scatter in Fig. 4.13. Besides, their coefficients of variation (CVs) amount up to 128 and 139 %, whereas the average CVs were 44, 56 and 46 % for the ADW 1, ADW 2 and SW data. Because of this large variability, only the settling velocities in the size fractions of 3.5 μm and 13.1 μm did not differ significantly between the three datasets (Kruskal-Wallis H test, two-sided α = .05, p = .923 and .137, respectively). Despite this large variability, we could also establish a relationship (depicted as a grey line in Fig. 4.13) between the effective grain size and settling velocity:

$$w_s = a \cdot D^b \tag{4.1}$$

with w_s = floc settling velocity [mm s^{-1}], D = grain size (equivalent spherical diameter) [μm], a = 2.7 10^{-4} and b = 1.57. The regression coefficient was 0.99 (n = 32). It should be noted we binned our data in eight classes, which drastically reduced within-class variance (Hill *et al.* 1998).

4.3.4 Sedimentation fluxes

The sedimentation flux for a size class (Fig. 4.14) is the product of its momentary dry mass concentration (Figs. 4.6 to 4.8) and its settling velocity (Fig. 4.13). In the settling tube, the flow shear stress τ_w is close to zero and therefore below the critical threshold for sedimentation τ_{cr}. Therefore, all sediment with a w_s of > 7.5 10^{-3} mm s^{-1} (= length of the tube divided by duration of settling experiment) can potentially settle. However, since the ambient τ_w in the floodplain is

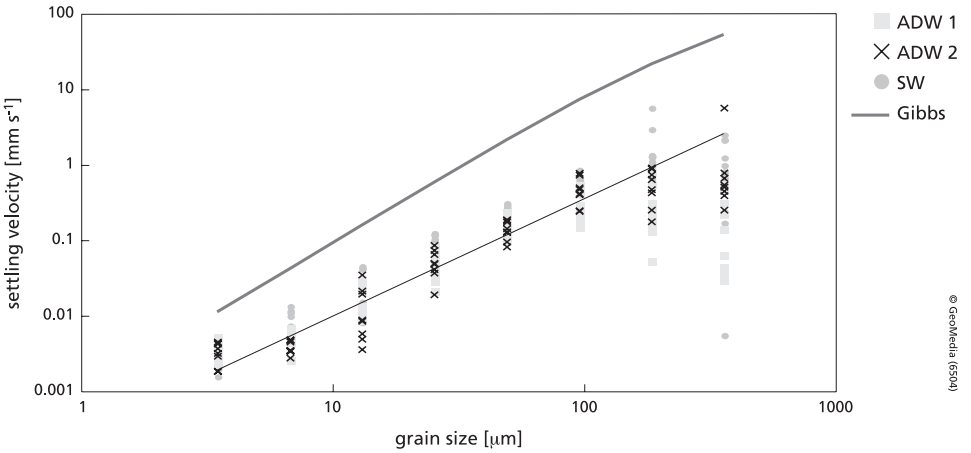

Figure 4.13 Floc settling velocities according to LISST-ST measurements versus theoretical settling velocity as described in Gibbs *et al.* (1971). The trend line is described by Equation 1, the 'Gibbs' curve is taken from Fig. 1 in Gibbs *et al.* (1971).

higher and particles are less prone to settlement, the reported fluxes have to be seen as *potential* sedimentation fluxes.

Because the sedimentation flux is a product of a moderately varying SSC and the highly varying settling velocity, it is highly variable itself as well. Therefore, the importance of classes fluctuates strongly and no consistent trend is visible in Fig. 4.14a & b. Only Fig. 4.14c shows a steadily increasing share for the 95.5 μm class, but this share again drops for the last experiment.

Comparing Fig. 4.11 with Fig. 4.14 it readily becomes clear that the larger size fraction contributes more to the sedimentation flux than could have been expected on the basis of SSC alone. For example, in the ADW 2 data set the 3.5 μm class always prevailed (Fig. 4.11b) while its contribution was negligible in the sedimentation mass flux (left out in Fig. 4.14b). Instead, the 95.5 μm class dominated the flux in the ADW 2 and SW data sets. In the ADW 1 data set, however, the 49.2 μm class made the largest contribution to the mass settling flux (Fig. 4.14a). As in the other cases, its largest contribution resulted from a high settling velocity (Fig. 4.13).

For comparison with the sediment-trap data we integrated the sedimentation fluxes for the ADW 2 and SW data. This gave a potential sedimentation amount of 468 and 5343 g m^{-2}, respectively, while the sediment traps had retained 267 (n = 4) and 527 (n = 5) g m^{-2}. So, at the ADW floodplain 57 % of the potential sedimentation flux was reached, whereas only 8 % was reached on the SW floodplain.

4.4 Discussion

4.4.1 Suspended sediment concentrations

The rise-and-fall pattern of the SSC during the passage of the discharge peak follows the suspended sediment dynamics in the lower Rhine River (Asselman 1999b): a relatively sharp rise in SSC that peaks before the water level reaches a maximum, followed by a more gradual decrease in SSC. In floodplain systems, however, the SSC also drops because of sedimentation during the transport to the sampling location. The SSC in the ADW floodplain declines more rapidly because of the minor embankment. This impedes inflow of new sediment at water levels lower than the embankment level (Figs. 4.6 & 4.7) and promotes sedimentation. Since the SW floodplain is not embanked, at similar water levels the flow still conveys sediment over the floodplain.

For the ADW 1 data, it is clear that the SSC as measured by the LISST-ST is much lower than the SSC in the manual water samples. In the SW data, however, the manually sampled and LISST-ST SSC show only little difference. Van Kessel (2003) mentioned that LISST-ST instruments generally give a SSC that is roughly 75 % of the real SSC. This is caused by insufficient suction of water into the tube at the intake of a sample (i.e., non-isokinetic sampling). This partly explains the lower LISST-ST values with respect to the manual samples (Fig. 4.6) but implies an overcompensation for the SW data set (Fig. 4.8).

4.4.2 Grain size distributions

During their 2 km long trajectory along the floodplain, the larger particles settle before reaching the sampling location. As such, the *in situ* (effective) GSD at the sampling locations is most probably less coarse than the effective GSD of the inflowing water. It would require another LISST-ST close to the river channel to see how large this effect due to sedimentation is and which grain size fractions settle first. The embankment of the ADW floodplain enhances the sedimentation effect by blocking transfer of momentum of the river water to the overbank flow (Wyżga 1999). This reduces the shear stress in the overbank flow, enabling finer fractions to settle (cf. Nicholas & Walling 1996). This in turn leads to a significantly finer effective GSD for the ADW floodplain than for the SW floodplain. Their ultimate GSDs hardly differ, however (Fig. 4.12): 75 % of the grains belong to the size range 2.5–18.2 μm for the ADW 2 data, whereas this percentage is 82 for the SW floodplain. This shows that a difference in the effective GSD because of flocculation does not have to lead to a difference in ultimate GSD.

The effective MGS (9 μm for the ADW floodplain and 25 μm for the SW floodplain) was two to five times larger than the ultimate MGS of approximately 5 μm. This ratio is larger than the one found by Nicholas & Walling (1996) (almost parity), but close to those found by Phillips & Walling (1999) and Walling & Woodward (2000). They found an effective GSD that was four to six times coarser than its ultimate counterpart. Asselman & Middelkoop (1995) found an ultimate MGS in the 2–8 μm class and an effective MGS of about 32 μm for Waal River floodplains, hence a ratio of four to sixteen. These authors, however, used resuspended sediment to measure the effective GSD. Since this could have aggregated in the time between sampling and analysing, their method is probably less reliable than the one used in this study.

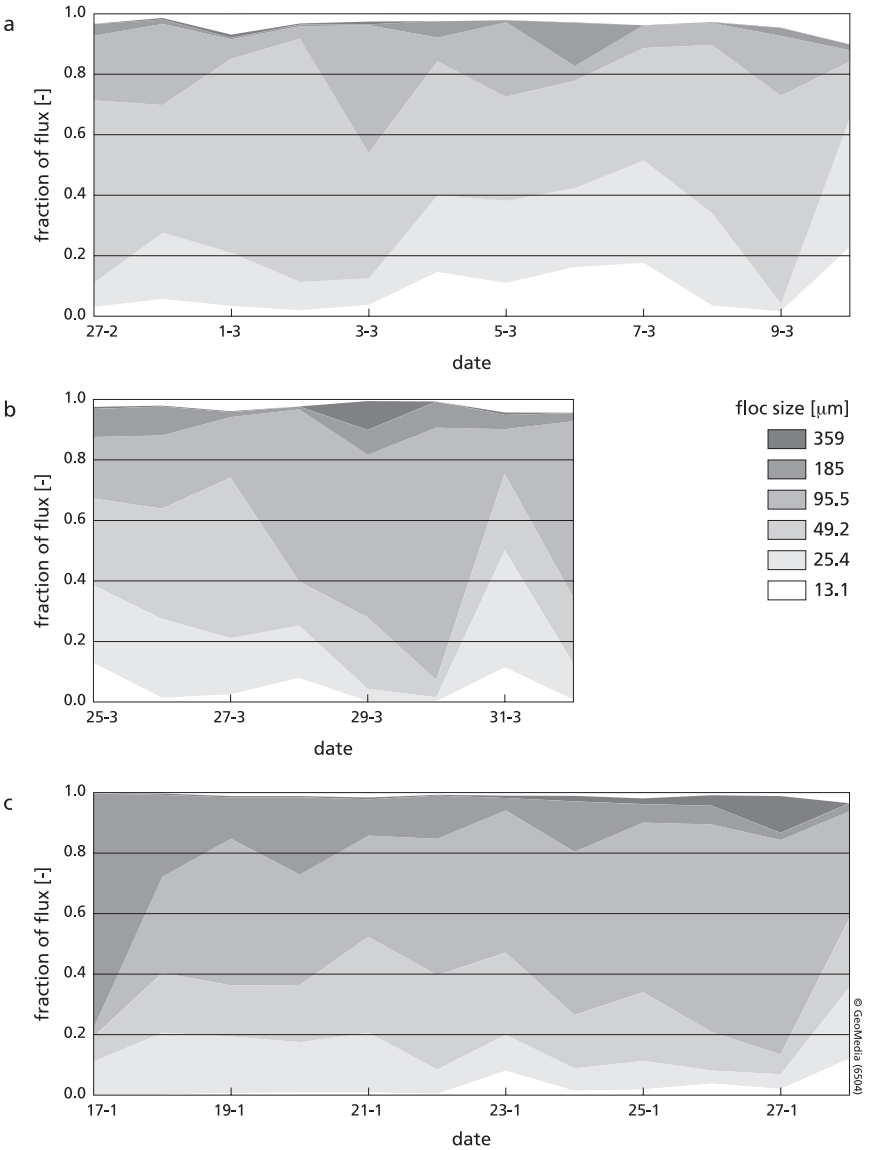

Figure 4.14 Sedimentation flux distributions for ADW 1 (a), ADW 2 (b) and SW (c) data sets. See also Fig. 4.11a, b & c. Grain size classes are in μm.

4.4.3 Settling velocities

The variability in settling velocities is large and increases with increasing floc size (see Fig. 4.13). This is not unusual. For instance, Dyer & Manning (1999) reported a variation in settling velocities measured in estuarine environments that often amounted one to two magnitudes. Mikkelsen (2002) reported ranges of variation in median w_s spanning one magnitude. In the

English Humber estuary, Millward *et al.* (1999) measured median w_s values varying from 1 10^{-3} to 2 10^{-1} mm/s for median floc sizes ranging from 44 to 166 μm.

The cause for this variability in the w_s–floc size relationship lies in the structure and composition of the flocs. Two flocs having the same equivalent spherical diameter can have a completely different structure and composition, resulting in different settling velocities. They can differ in

- orientation of their long axis: flocs with the long axis parallel to the direction of movement settle faster than those with their long axis perpendicular to it (Droppo *et al.* 1998);
- aspect ratio: elongated flocs settle slower than cylindrical or disk shaped ones (Li & Ganczarczyk 1987; Droppo *et al.* 1998);
- density: flocs mainly consisting of high-density clastic material settle faster than those predominantly made up of low-density organic material;
- porosity: a porous floc settles faster than a solid, compact floc because the flow of water through the floc lowers the hydrodynamic resistance (Li & Ganczarczyk 1987; Droppo *et al.* 2000).

Despite the inherent variability in flocs and their settling velocities, the relationship between settling velocity and floc size (Fig. 4.13; Eq. 4.1) is promising, taken into account the high r^2. Previous studies in marine environments found similar equations. The relationship in Eq. 4.1 (with a = 2.7 10^{-4} and b = 1.57) closely resembles the one reported by Mikkelsen & Pejrup (2001) for Danish coastal waters (with a = 2.6 10^{-4} and b = 1.53). Sternberg *et al.* (1999) found a = 2 10^{-4} and b = 1.54 for the Californian shelf, which is very similar,. Although for a given D Eq. 4.1 gives higher settling velocities than those by Mikkelsen & Peyrup (2001) and Sternberg *et al.* (1999), most settling velocities measured in marine and estuarine environments plot somewhat higher than our data (e.g., Dyer *et al.* 1996; Hill *et al.* 1998; Mikkelsen 2002; Van der Lee 2000). This is probably due to the increased ionic concentration in the sea water, which promotes flocculation (Eisma 1993).

Data on settling velocities in freshwater environments as found by other workers are mostly consistent with our results. Droppo *et al.* (1997, 2000) reported settling velocities for freshwater flocs larger than 100 μm that plot at the upper end of our data cloud. Data for lower river reaches in the Rhine-Meuse delta reported by Van Wijngaarden & Roberti (2002) are consistent with our results. Van Wijngaarden (1999) reported more scattered settling velocities. However, she analyzed individual particles instead of binned classes. This gives rise to higher variation as Hill *et al.* (1998) pointed out.

In a previous study (Thonon & Van der Perk 2003), we also determined settling velocities in floodplain systems. However, at that time we applied the default Sequoia software to calculate settling velocities and densities. Since the Sequoia software does not take account of the effect of ghost particles, it calculated anomalously high densities for the 3.5 and 6.8 μm classes. The Van Wijngaarden & Roberti (2002) model allows to choose the lower of the two fitted densities, which helps to reduce the effect of ghost particles.

4.4.4 Sedimentation fluxes

In contrast to the GSDs, which are dominated by smaller particles (Fig. 4.11), larger particle sizes dominate the mass sedimentation fluxes (Fig. 4.14). This is due to their higher settling velocities (Fig. 4.13). However, because of their inherent variability, these settling velocities also cause larger variation in the sedimentation fluxes than in the GSDs (e.g., compare constant pattern in Fig. 4.11b with fluctuating pattern in Fig. 4.14b). This shows the importance of variations in settling velocity, which are due to differences in floc structure and composition, for the sedimentation fluxes. Since sedimentation models also give sedimentation fluxes, these models will also be sensitive for variations in settling velocities.

The actual settling percentage of the ADW data (57 %) is far more than the one for the SW data set (8 %). Comparing these percentages with the sedimentation flux distributions in Figs. 4.14b & c gives some idea of the smallest particle size that could settle. 57 % Of the sedimentation flux includes part of the 35.4–68.6 μm size range and the total 68.6–500 μm size range. Eight percent of the distribution of the SW floodplain only includes the part of the 133–258 μm size range and the total 359 μm class. This large difference is due to the higher flow velocities in the SW floodplain than in the ADW floodplain. In case of higher flow velocities, less sediment settles: τ_{cr} will be exceeded by τ_w for more particle sizes. Middelkoop & Asselman (1998) and Middelkoop & Van der Perk (1998) also pointed at quiescent conditions and longer residence times that favour settling behind minor embankments.

The distribution of the different grain sizes in the potential sedimentation flux of Fig. 4.14b & c is strikingly different from the ultimate grain size distribution of Fig. 4.12a & b. The size range of 2.5–18.2 μm contributes 7 % to the *potential* sedimentation flux in the ADW 2 data set and 4 % to the flux in the SW floodplain. However, their contribution to the *actual* sedimentation flux will be close to zero since these particles will probably remain in suspension. This contrasts with their large contribution to the ultimate GSD: the 2.5–18.2 μm size range represent 75 (ADW 2 data) to 82 % (SW data) of all grains. Smaller primary particles do not settle on their own, but they still contribute four fifth of the sedimentation amount as they are included in flocs in the coarse-silt- and sand-sized ranges that actually settle. The difference between actual and potential sedimentation also explains why the different flow conditions did not lead to different ultimate grain size distributions: all effective particle sizes are composed of the finest ultimate particle sizes. This was also found by Nicholas & Walling (1996) for British streams. Finally, it shows that particles up to about 20 μm (the size of fine silt) can be neglected in modelling sedimentation. This confirms Slattery & Burt (1995) and Droppo *et al.* (1998), who indicated that using ultimate grain sizes – which are often smaller than 20 μm – can lead to serious errors in the calibration of sedimentation models.

4.4.5 Implications for floodplain sedimentation models

When the three size ranges representing the smaller particles are left out of the GSD of the suspended sediment for the ADW 1 & 2 data sets, a distribution with particles that can potentially settle remains. In these adapted distributions, the MGS both times is located in the 18.2–35.4 μm size range. In their floodplain sedimentation models, Asselman (1999a), Asselman & Van Wijngaarden (2002) and Middelkoop & Van der Perk (1998) used an overall settling velocity of 7.0 10^{-2} mm s^{-1}. This corresponds to an effective floc size of 34 μm when

recalculated with Eq. 4.1, which is also located in the 18.2–35.4 μm size range. This indicates that a value within this size range is a plausible overall settling velocity in floodplain sedimentation modelling. Moreover, it shows that probably only one effective grain size suffices for modelling purposes. This is because the smallest particles most probably do not settle whereas the largest flocs and sand particles already settle when they enter the floodplain. The settling velocity for the remainder of the floc population can be approached using one effective settling velocity.

Van Wijngaarden (1997, 1999) used a value for w_s of 5.8 10^{-3} mm s^{-1} for fine cohesive sediment and 1.2 10^{-1} mm s^{-1} for flocculated sediment. These settling velocities correspond with grain sizes of 7.0 μm and 49 μm according to Eq. 4.1. Hardy *et al.* (1999) used a w_s that is similar to the one Van Wijngaarden used for flocculated sediment (1.16 10^{-1} mm s^{-1}). However, they reported a MGS of 13 μm instead of a value close to 49 μm, meaning they used Stokes' law to derive their settling velocity. The curve by Gibbs *et al.* (1971) in Fig. 4.13 shows Stokes' law greatly overestimates the settling velocity. Because parameters in floodplain sedimentation models are usually calibrated, overestimating settling velocities has large consequences for other parameters. Therefore, we recommend the use of empirical relations or *in situ* measured settling velocities in floodplain sedimentation modelling and the use of Stokes' law only in the case of ultimate grain sizes.

4.5 Conclusions and recommendations

Measurements of *in situ* sediment settling characteristics using a LISST-ST laser diffraction device revealed that:

- The suspended sediment concentration in the overbank flow is lower but varies proportionally with the SSC in the river water and the turbidity of the floodplain water. However, we cannot fully explain the difference between the SSC in manual samples and those measured by the LISST-ST. Therefore we recommend more consistent sampling during LISST-ST deployment and, if possible, calibration of the LISST-ST with water samples.
- Because of higher flow velocities and greater transfer of momentum, the effective (flocculated, *in situ*) grain size distribution for the floodplain along the IJssel River is significantly coarser (median grain size = 25 μm) than for the Waal floodplain (MGS = 9 μm). However, the effective GSD for the water entering the floodplains is probably coarser. Further study is needed to verify this by using a second LISST-ST close to the river channel. That study could also investigate the influence the floodplain (shear) has on flocculation or break-up of flocs.
- Despite the difference in effective GSDs, the ultimate (deposited, dispersed) GSDs are similar, showing that a different effective GSD does not necessarily lead to a different ultimate GSD. The effective GSD is two to five times coarser than the ultimate GSD, showing the effect flocculation has on the GSD. This ratio is similar to ratios reported in previous studies, but resuspension of deposited particles is probably a less reliable means of determining the effective grain size.
- Settling velocities exhibit a large variability that increases with increasing grain size. Although the w_s-D relation for floodplains is similar to the one for marine and estuarine

environments, its w_s is often somewhat smaller. The correct determination of settling velocities should receive more attention in modelling, since their variation has important implications for model outcomes. Settling velocities are best measured *in situ*. In analysing them, we recommend using software that can cope with 'ghost particles' in the smaller size range. If it is not possible to measure the w_s *in situ*, empirical relationships such as the one presented in Eq. 4.1 can be used instead of Stokes' law. For modelling purposes, probably one effective grain size or settling velocity is sufficient.

- The larger effective particle sizes dominate the *potential* sedimentation flux, despite representing a low proportion of the suspended sediment. The smaller particles probably remain in suspension, since their τ_{cr} will always be lower than the shear stress of the overbank flow. Therefore, in floodplain sedimentation models the contribution of the smallest effective particle sizes to the sedimentation can often be neglected. However, because the smaller primary particles are included within the larger flocs, the former dominate in the *actual* sedimentation. The actual sedimentation fluxes are higher in the quiescent conditions behind the minor embankment of the Waal River than in the free flowing water of the unprotected IJssel floodplains. Since flow conditions also influence the median effective grain size, care should be taken to model these properly.

Acknowledgements

We are greatly indebted to Marjolein van Wijngaarden (RIZA Dordrecht, now at Directorate-General Water of the Ministry of Public Works, Waterways & Water Management) and Petra Jeurissen (RIKZ Den Haag) for providing the LISST-ST devices to us. Next, we thank Mr. Henny for giving us permission to install the frame and Mr. Kusters and Mr. Willems for keeping an eye on the devices. We also thank Sander Wijnhoven (Radboud Universiteit Nijmegen) for installing the LISST-ST during the inundation in early March 2002, Chris Roosendaal for constructing the measurement frames and Marcel van Maarseveen for programming the LISST-ST and downloading the data from it. Yogesh Agrawal (Sequoia Scientific) helped with the data analyses. Ton van Warmenhoven carried out the ultimate grain size analyses, Menno Straatsma took the 0.5-l samples and Ton Visser (RIZA Dordrecht) and Claus van den Brink (RIZA Arnhem) provided flow velocity calculations. The two anonymous reviewers are thanked for their remarks concerning language and discussion points.

References

Agrawal, Y.C., I.N. McCave & J.B. Riley (1991), Laser diffraction size analysis. In: J.P.M. Syvitski, ed., Principles, methods, and application of particle size analysis. Cambridge, U.K. : Cambridge University Press, pp. 119–128.

Agrawal, Y.C. & H.C. Pottsmith (2000), Instruments for particle size and settling velocity observations in sediment transport. Marine Geology 168/1-4, pp. 89–114.

Asselman, N.E.M. & H. Middelkoop (1995), Floodplain sedimentation: quantities, patterns and processes. Earth Surface Processes and Landforms 20, pp. 481–499.

Asselman, N.E.M. & H. Middelkoop (1998), Temporal variability of contemporary floodplain sedimentation in the Rhine-Meuse delta, The Netherlands. Earth Surface Processes and Landforms 23/7, pp. 595–609.

Asselman, N.E.M. (1997), Suspended sediment in the river Rhine: The impact of climate change on erosion, transport and deposition. Utrecht: Koninklijk Nederlands Aardrijkskundig Genootschap/Faculteit Geowetenschappen, Universiteit Utrecht (Netherlands Geographical Studies 234).

Asselman, N.E.M. (1999a), Slibmodellering in RvR – fase 1. Delft, The Netherlands: WL| Delft Hydraulics (WL report R3337).

Asselman, N.E.M. (1999b), Suspended sediment dynamics in a large drainage basin: the River Rhine. Hydrological Processes 13/10, pp. 1437–1450.

Asselman, N.E.M. (2003), Slibsedimentatie in noodoverloop- en retentiegebieden. Delft, The Netherlands: WL|Delft Hydraulics (WL report Q3249).

Asselman, N.E.M. & M. van Wijngaarden (2002), Development and application of a 1D floodplain sedimentation model for the River Rhine in The Netherlands. Journal of Hydrology 268/1-4, pp. 127–142.

Bale, A.J. (1996), In situ laser optical particle sizing. Journal of Sea Research 36/1-2, pp. 31–36.

Bale, A.J. & A.W. Morris (1991), In situ size measurements of suspended particles in estuarine and coastal waters using laser diffraction. In: J.P.M. Syvitski, ed., Principles, methods, and application of particle size analysis, Cambridge, U.K. Cambridge University Press, pp. 197–208.

Dearnaley, M.P. (1996), Direct measurements of settling velocities in the Owen tube: a comparison with gravimetric analysis. Journal of Sea Research 36/1-2, pp. 41–47.

Dyer, K.R., J. Cornelisse, M.P. Dearnaley, M.J. Fennessy, S.E. Jones, J. Kappenberg, I.N. McCave, M. Pejrup, W. Puls, W. van Leussen & K. Wolfstein (1996), A comparison of in situ techniques for estuarine floc settling velocity measurements. Journal of Sea Research 36/1-2, pp. 15–29.

Dyer, K.R. & A.J. Manning (1999), Observation of the size, settling velocity and effective density of flocs, and their fractal dimensions. Journal of Sea Research 41/1-2, pp. 87–95.

Droppo, I.G., G.G. Leppard, D.T. Flannigan & S.N. Liss (1997), The freshwater floc: a functional relationship of water and organic and inorganic floc constituents affecting suspended sediment properties. Water, Air and Soil Pollution 99/1-4, pp. 43–54.

Droppo, I.G., D.E. Walling & E.D. Ongley (1998), Suspended sediment structure: implications for sediment and contaminant transport modelling. IAHS Publication 249, pp. 437–444.

Droppo, I.G., D.E. Walling & E.D. Ongley (2000), The influence of floc size, density and porosity on sediment and contaminant transport. IAHS Publication 263, pp. 141–147.

Eisma, D. (1993), Suspended matter in the aquatic environment. Berlin: Springer.

Eisma, D., T. Schuhmacher, H. Boekel, J. van Heerwaarden, H. Franken, M. Laan, M. Vaars, F. Eijgenraam & J. Kalf (1990), A camera and image analysis system for in-situ observation of flocs in natural waters. Netherlands Journal of Sea Research 27, pp. 43–56.

Eisma, D., A.J. Bale, M.P. Dearnaley, M.J. Fennessy, W. van Leussen, M-A Moldiney, A. Pfeiffer & J.T. Wells (1996), Intercomparison of in situ suspended matter (floc) size measurements. Journal of Sea Research 36/1-2, pp. 3–14.

Gibbs, R.J., M.D. Matthews & D.A. Link (1971), The relationship between sphere size and settling velocity. Journal of Sedimentary Petrology 41/1, pp. 7–18.

Hardy, R.J., P.D. Bates & M.G. Anderson (2000), Modelling suspended sediment deposition on a fluvial floodplain using a two-dimensional dynamic finite element model. Journal of Hydrology 229/3-4, pp. 202–218.

Hill, P.S., J.P. Syvitski, E.A. Cowan & R.D. Powell (1998), In situ observations of floc settling velocities in Glacier Bay, Alaska. Marine Geology 145/1-4, pp. 85–94.

James, C.S. (1985), Sediment transfer to overbank sections. Journal of Hydraulic Research 23/5, pp. 435–452.

Lambert, C.P. & D.E. Walling (1987), Floodplain sedimentation: a preliminary investigation of contemporary deposition within the lower reaches of the River Culm, Devon, U.K. Geografiska Annaler 69A/3-4, pp. 393–404.

Li, D.-H. & J. Ganczarczyk (1987), Stroboscopic determination of settling velocity, size and porosity of activated sludge flocs. Water Research 21, pp. 257–262.

Middelkoop H & N.E.M. Asselman (1998), Spatial variability of floodplain sedimentation at the event scale in the Rhine-Meuse delta, The Netherlands. Earth Surface Processes and Landforms 23/6, pp. 561–573.

Middelkoop, H. & M. van der Perk 1998. Modelling spatial patterns of overbank sedimentation on embanked floodplains. Geografiska Annaler 80A/2, pp. 95–109.

Mie, G. (1908), Beiträge zur Optik trüber Medien, speziell kolloidaler Metallösungen. Annale der Physik 25, pp. 377–452.

Mikkelsen, O.A. (2002), Examples of spatial and temporal variations of some fine-grained suspended particle characteristics in two Danish coastal water bodies. Oceanologica Acta 25/1, pp. 39–49.

Mikkelsen, O.A. & M. Pejrup (2001), The use of a LISST-100 laser particle sizer for in-situ estimates of floc size, density and settling velocity. Geo-Marine Letters 20/4, pp. 187–195.

Millward, G.E., T.K. Sands & C.F. Jago (1999), Particulate metals and their settling velocities in the Humber Estuary, uk. Marine Chemistry 68/1-2, pp. 145–168.

Nicholas, A.P. & D.E. Walling (1996), The significance of particle aggregation in the overbank deposition of suspended sediment on river floodplains. Journal of Hydrology 186/1-4, pp. 275–293.

Nicholas, A.P. & D.E. Walling (1997), Modelling flood hydraulics and overbank deposition on river floodplains. Earth Surface Processes and Landforms 22/1, pp. 59–77.

Owen, M.W. (1971), The effect of turbulence on the settling velocities of silt flocs. Proceedings 14th IAHR Congress 4, pp. D4-1-DA-5.

Phillips, J.M. & D.E. Walling (1999), The particle size characteristics of fine-grained channel deposits in the River Exe Basin, Devon, U.K. Hydrological Processes 13/1, pp. 1–19.

Slattery, M.C. & T.P. Burt (1995), Size characteristics of sediment eroded from agricultural soil: dispersed versus non-dispersed, ultimate versus effective. In: E.J. Hickin, ed., River geomorphology. Chichester, U.K.: John Wiley, pp. 1–17.

Slattery, M.C. & T.P. Burt (1997), Particle size characteristics of suspended sediment in hillslope runoff and stream flow. Earth Surface Processes and Landforms 22/8, pp. 705–719.

Sternberg, R.W., I. Berhane & A.S. Ogston (1999), Measurement of size and settling velocity of suspended aggregates on the northern California continental shelf. Marine Geology 154/1-4, pp. 43–53.

Thonon I & M. van der Perk (2003), Measuring suspended sediment characteristics using a LISST-ST in an embanked flood plain of the River Rhine. IAHS Publication 283, pp. 37–44.

Van der Lee, W.T.B. (2000), The settling of mud floc in the Dollard estuary, The Netherlands. Utrecht: Koninklijk Nederlands Aardrijkskundig Genootschap/Faculteit Geowetenschappen, Universiteit Utrecht (Netherlands Geographical Studies 274).

Van Kessel, T. (2003), Analysis of LISST-ST-data. Delft, The Netherlands: WL|Delft Hydraulics (Report Z3671).

Van Leussen, W. & J.M. Cornelisse (1993), The determination of the size and settling velocities of estuarine flocs by an underwater video system. Netherlands Journal of Sea Research 31, pp. 321–341.

Van Wijngaarden, M. (1997), Sedimentatie en erosie van zwevend stof in nevengeulen. Lelystad, The Netherlands: RIZA, Rijkswaterstaat (RIZA rapport 97.078).

Van Wijngaarden, M. (1999), A two-dimensional model for suspended sediment transport in the southern branch of the Rhine-Meuse estuary, The Netherlands. Earth Surface Processes and Landforms 24/13, pp. 1173–1188.

Van Wijngaarden, M. & J.R. Roberti (2002), In situ measurements of settling velocity and particle size distribution with the LISST-ST. In: J.C. Winterwerp & C. Kranenburg, eds., Fine sediment dynamics in the marine environment. Amsterdam: Elsevier, pp. 295–311.

Walling, D.E. & J.C. Woodward (1993), Use of a field-based water elutriation system for monitoring the in situ particle size characteristics of fluvial suspended sediment. Water Research 27, pp. 1413–1421.

Walling, D.E. & J.C. Woodward (2000), Effective particle size characteristics of fluvial suspended sediment transported by lowland British rivers. IAHS Publication 263, pp. 129–139.

Wyżga, B. (1999), Estimating mean flow velocity in channel and floodplain areas and its use for explaining the pattern of overbank deposition and floodplain retention. Geomorphology 28/3-4, pp. 281–297.

5 Modelling floodplain sedimentation using particle tracking

Accepted in revised form as: Thonon, I., K. de Jong, M. van der Perk & H. Middelkoop, Modelling floodplain sedimentation using particle tracking. Hydrological Processes.

"*The deposition of silt and clay is (…) not sufficiently understood for deterministic modelling.*" (Brookes 1996).

"*There have been few studies that attempt to model the spatial variability of floodplain soil pollution.*" (Stewart *et al*. 1998).

"*Relatively few attempts have been made to model flow and sediment transport processes in topographically complex floodplain environments.*" (Nicholas & McLelland 1999).

Abstract

Both climate change and river rehabilitation projects induce changes in floodplain sedimentation. Notably along the lower Rhine River, the pattern and quantities of sediment deposition are subject to change. To assess the magnitude of these changes, we developed the MoCSED model, a floodplain sedimentation model within a geographical information system (GIS) for the lower Rhine River. We based MoCSED on the 'Method of Characteristics' (MoC), a particle tracking method that minimises numerical dispersion. We implemented the MoCSED model in the *PCRaster Dynamic Modelling Language*. The model input comprises of initial suspended sediment concentrations, water levels, flow velocities, longitudinal and transverse dispersivities. We used a combination of the Krone and Chen concepts to calculate the subsequent sedimentation (SED routine). We compared the model results with observed amounts of deposited sediment on the Bemmel floodplain along the Dutch Waal River during the 2003 inundation. This comparison showed that MoCSED was able to simulate the pattern of sediment deposition. In addition, the model proved to be an improvement in comparison to a conventional raster-based floodplain sedimentation model for the lower Rhine River. MoCSED confirms another model for the lower Rhine River by predicting the same average yearly sedimentation of 1.7 kg m^{-2} y^{-1}. In future, MoCSED may serve well to study the impact of a changing discharge regime due to climate change and floodplain rehabilitation plans on deposition of (contaminated) sediments.

Keywords

Suspended sediment; floodplain; River Rhine; sedimentation modelling; numerical dispersion; Method of Characteristics; particle tracking.

5.1 Introduction

Floodplains sequester large amounts of sediments and associated pollutants (e.g., Walling *et al.* 1998; Owens *et al.* 1999). Consequently, floodplain sedimentation may account for a considerable part of the sediment budget of river systems (Walling 1999). For instance, Walling *et al.* (1986), Lambert & Walling (1987) and Sweet *et al.* (2003) report conveyance losses up to 60 % for a small river (the River Culm, with a catchment area of 276 km^2). For large river systems such as the Amazon River, Mertes (1994) reports losses of 46 to 64 %. The Upper Mississippi River deposited during the 1993 summer flood an estimated 22 to 36 % of the suspended sediment load on its floodplains (Gomez *et al.* 1997). Middelkoop & Asselman (1998) calculated a 19 % conveyance loss for the Rhine River in The Netherlands during the 1993 winter flood.

Floodplain topography and flow patterns are the key controlling parameters for both the conveyance loss and sedimentation patterns (Walling *et al.* 1999). Both parameters are subject to change on the lower Rhine River floodplains. To minimise flood risk, the Dutch government recently proposed floodplain rehabilitation measures, such as lowering or removal of minor embankments, lowering of floodplains and construction of secondary channels (Silva *et al.* 2001; RIZA 2003). In combination with climate change, which causes larger winter discharges in the Rhine River (Shabalova *et al.* 2003), floodplain rehabilitation will likely cause more and longer floodplain inundations and changes in flow patterns. This, in turn, may lead to increased inputs of sediment and associated contaminants on the floodplains along the Rhine River (Asselman 1999a; Middelkoop *et al.* 2002) and changes in sedimentation patterns. To study the present and future amounts and patterns of sediment and contaminant deposition, a detailed floodplain sedimentation model is needed.

In the past decade, several authors have developed one- and two-dimensional models to simulate patterns of sediment deposition on floodplains. Some of these models are based on a finite-element approach (e.g., Stewart *et al.* 1998; Hardy *et al.* 2000), other models on a finite-difference approach (e.g., Nicholas & Walling 1997, 1998; Middelkoop & Van der Perk 1998). Finite-element models have the advantage of employing a mesh that can be optimised for local situations (e.g., a finer mesh in environments with higher suspended sediment concentration gradients) to minimise numerical errors. However, these models have the disadvantage that their output cannot be imported directly into a raster GIS for further processing, which is relatively easy using finite-difference or raster-based models. Furthermore, raster-based models suffer from numerical dispersion, which is an unwanted artefact of the numerical modelling technique and should be avoided.

In the present study we develop a raster-based floodplain sedimentation model for the lower Rhine River. We propose the 'Method of Characteristics' or MoC (Garder *et al.* 1964; Konikow

& Bredehoeft 1978) as a particle tracking method that minimises numerical dispersion within this model. Although Stewart *et al.* (1998) successfully applied MoC in finite-element modelling, it has not previously been integrated in a raster-based model. First, we adapted MoC to compute suspended sediment transport in surface water. Then we included it in a raster-based floodplain sedimentation model: MoCSED. To facilitate post-processing of the results and embedding of the model in other environmental models, we implemented MoCSED in the generic *PCRaster Dynamic Modelling Language* (Wesseling *et al.* 1996; http://pcraster.geo.uu.nl/). PCRaster is a geographical information system for numerical modelling of environmental processes.

This paper describes MoCSED and its application. We applied the model to the 2003 inundation of the Bemmel floodplain along the Waal River, a distributary of the lower River Rhine, and compared the model output with observed sedimentation patterns. Finally, we compared the results from MoCSED with the results from two other floodplain sedimentation models for the lower Rhine River.

5.2 Model concept

The MoCSED model simulates two-dimensional suspended sediment transport and deposition in river channels and submerged floodplain areas using a 2D water flow velocity field. This flow field in orthogonal x and y directions is the key model input and is calculated using an external hydraulic model. The sediment transport equation has been modified from the MoC model by Konikow & Bredehoeft (1978), which simulates two-dimensional solute transport and dispersion in groundwater. The MoC model solves the transport equation taking flowing reference particles as a basis instead of grid nodes. Garder *et al.* (1964) called the flow lines along which the reference particles move "characteristic curves", hence the name 'Method of Characteristics'.

The general equation for sediment transport and deposition is:

$$\frac{\partial C}{\partial t} = E_{xx}\frac{\partial^2 C}{\partial x^2} + E_{yy}\frac{\partial^2 C}{\partial y^2} + (E_{xy} + E_{yx})\frac{\partial^2 C}{\partial x \partial y} - u_x\frac{\partial C}{\partial x} - u_y\frac{\partial C}{\partial y} - k_s \cdot C \qquad (5.1)$$

with C = suspended sediment concentration (SSC) [g m^{-3}], t = time [s], x_i and y_j = Cartesian coordinates [m], h = water depth [m], E = hydrodynamic dispersion coefficient [m^2 s^{-1}], u_x and u_y = flow velocity in x and y direction [m s^{-1}] and k_s = first-order sedimentation rate constant [s^{-1}]. The first term on the right-hand side is the dispersion term, the second and third terms are the advection terms, and the fourth term is the sedimentation term. Note that Eq. 5.1 does not consider erosion.

If advective transport dominates sediment transport, it is possible to define concentration changes for *flowing reference particles* that pass *fixed grid nodes* (i.e., dC/dt), rather than the conventional way of defining concentration changes for *fixed reference grid nodes* passed by *flowing particles* ($\partial C/\partial t$). The changes in concentration for flowing reference particles (dC/dt) is defined as follows:

$$\frac{dC}{dt} = \frac{\partial C}{\partial x} + \frac{\partial C}{\partial y}\frac{dx}{dt} + \frac{\partial C}{\partial y}\frac{dy}{dt}. \tag{5.2}$$

Note that dx/dt and dy/dt and substituting Eq. 5.1 in Eq. 5.2 makes it possible to reduce Eq. 5.1 to the following form:

$$\frac{\partial C}{\partial t} = E_{xx}\frac{\partial^2 C}{\partial x^2} + E_{yy}\frac{\partial^2 C}{\partial y^2} + E_{xy}\frac{\partial^2 C}{\partial x \partial y} - k_s \cdot C \tag{5.3}$$

Note also that the two advective terms of Eq. 5.1 have been eliminated in Eq. 5.3. The hydrodynamic dispersion coefficient E is described by two equations:

$$E_L = \varepsilon_L \cdot \overline{uv} \text{ and } E_T = \varepsilon_T \cdot \overline{uv} \tag{5.4, 5.5}$$

with E_L = longitudinal dispersion coefficient [$m^2\ s^{-1}$], ε_L = longitudinal dispersivity [m], $\overline{uv}$ = absolute flow velocity [$m\ s^{-1}$], E_T = transverse dispersion coefficient [$m^2\ s^{-1}$], ε_T = transverse dispersivity [$m\ s^{-1}$].

Numerical formulation of Eq. 5.3 yields:

$$\Delta C = \Delta C_t - \Delta C_s = \Delta C_t - DF \cdot C \tag{5.6}$$

with ΔC = change in SSC [$mg\ l^{-1}$], ΔC_t = change in SSC due to transport, mixing and diffusion [$mg\ l^{-1}$], ΔC_s = change in SSC due to sediment deposition [$mg\ l^{-1}$], Δt = model time step [s], DF = deposition factor [–]. Note that in Eq. 5.4, the first-order sediment rate constant k_s has been replaced by a dimensionless deposition factor DF with a domain of between 0 and 1. We derived DF using a concept developed by Chen (1975) in combination with the Krone (1962) concept. Van Rijn (1993), Narinesingh (1995), Asselman (1999c) and Asselman & Van Wijngaarden (2002)

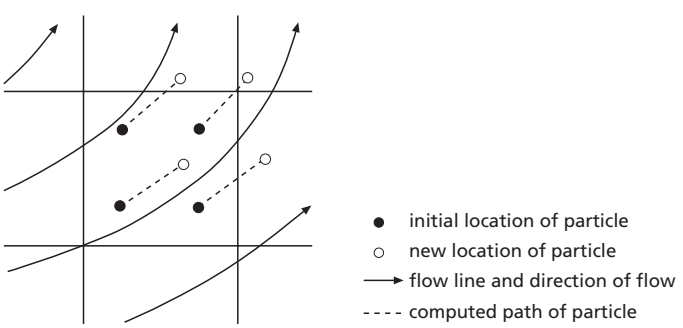

Figure 5.1 The location of the particles in the raster cells and subsequent displacement by the model. The flow lines are the 'characteristic curves'. Adapted from: Konikow & Bredehoeft (1978).

previously used the Chen concept to calculate sedimentation. The Krone concept is widely used in models like Delft3D (WL|Delft Hydraulics) and Mike21 (Danish Hydraulics) and by Middelkoop & Van der Perk (1998), Stewart *et al.* (1998), Van Wijngaarden (1999), Hardy *et al.* (2000) and Sweet *et al.* (2003).

The deposition factor is defined as (Chen 1975):

$$DF = 1 - e^{-(\alpha \cdot w_s/h)\Delta t} \tag{5.7}$$

with DF = deposition fraction [–], and w_s = settling velocity [m s^{-1}] and α = the 'Krone factor' in Eq. 5.8 & 5.9 [–]. The 'Krone factor' is defined as (Krone 1962):

$$\alpha = 1 - (\tau / \tau_{cr}) \qquad \text{for } \tau < \tau_{cr}\,, \tag{5.8}$$

$$\alpha = 0 \qquad \text{for } \tau \geq \tau_{cr} \tag{5.9}$$

with τ = shear stress [Pa] and τ_{cr} = critical shear stress for sediment deposition [Pa]. Eqs. 5.8 & 5.9 state that sedimentation only takes place for shear stresses lower than the critical shear stress for sediment deposition. Otherwise the sediment will remain in suspension. We calculated τ with:

$$\tau = \rho \cdot g \frac{\overline{uv}^2}{Cz^2} \tag{5.10}$$

with ρ = density of water [kg m^{-3}], g = gravity acceleration [m s^{-2}], Cz = Chézy coefficient [m$^{0.5}$ s^{-1}].

When the model has reached a steady-state solution for the SSC field, the sedimentation for one event is calculated using:

$$D = \sum_{i=1}^{m} (w_{s,i} \cdot \alpha_i \cdot C_i) \cdot T \tag{5.11}$$

with D = amount of deposition [kg m^{-2}] and T = total inundation time [s]. The index i denotes a grain size class. Each grain size class has its own w_s and hence specific C. Note that $w_{s,i}$ can also be an effective settling velocity $w_{s,e}$ that represents a range of grain sizes. In that case, τ_{cr} in Eqs. 5.8 & 5.9 is also an effective critical shear stress $\tau_{cr,e}$. In case the event consists of several discharge classes, adding D for every discharge class gives the total amount of deposition the events under consideration.

5.3 Model setup

5.3.1 Calculation procedure

The initial step in the calculation procedure of the SSC (C) involves placing four, five or nine particles in each cell of a grid (Fig. 5.1). All particles in the same grid cell have the same initial C. The calculation of the new C starts for a number of time steps. If necessary, the model subdivides this time step into smaller ones (Δt) to ensure that particles cannot move more than one cell length per time step. The model bases this division on four stability criteria, including the dispersivity values, water depth and flux, and flow velocities in x- and y-direction. When the model has run for a sufficient number of time steps, it will reach a steady-state equilibrium for SSC. This steady-state SSC is used to calculate the amount of sediment deposited (see Eq. 5.11).

The first action during a time step is the displacement of all particles according to flow velocity and direction in the cells (i.e., the curved lines in Fig. 5.1). The distance moved is at most one grid cell and the *particles*' SSC does not change in this action. Instead, the model calculates a temporal average concentration C^* for each *grid node* given the new spatial arrangement of particles. C^* is used as basis for the two following calculations.

Second, the change in concentration due to transport, mixing and diffusion (ΔC_t) is calculated at the *grid node*. If ΔC_t is positive, its value is simply added to C. However, if ΔC_t is negative, C is lowered with the fraction $\Delta C_t / C^*$. If ΔC_t is negative and larger than C^*, C will become zero.

Third, MoCSED lowers the concentration due to sedimentation. For each *particle*, C decreases according to $\Delta C_s = DF \cdot C^*$ (see also Eq. 5.6). After change of C for each *particle* due to transport, mixing, diffusion (ΔC_t) and sedimentation (ΔC_s), the resulting concentration is the new concentration for the next time step. At the end of each time increment MoCSED can write PCRaster maps with the average concentration and the number of reference particles per cell.

5.3.2 Implementation in PCRaster

The MoCSED model script in *PCRaster Dynamic Modelling Language* consists of two modules: the internal SED module and the links to the external MoC module. The MoC module – written in C^{++} – is linked to PCRaster by means of two links and commands in the PCRaster script. The links show where the dynamic link libraries of MoC are located and initiate MoC. MoC externally calculates the change in SSC for every reference particle due to transport and deposition. The internal SED module specifies the amount of this deposition by calculating DF and transferring this to MoC. In its calculation MoC uses and returns all data in raster format, while preserving the location and concentration of the reference particles. In this way MoCSED preserves both the flexibility of MoC and the functionality of PCRaster.

5.3.3 Boundary conditions

MoCSED works with two types of model boundaries: flux boundaries and no-flow boundaries. Flux boundaries are defined at the upstream and downstream boundaries of the model area, with a sediment flux being either constant or transient. The user has to provide an input map with positive sediment fluxes across the upstream model boundary cells and negative sediment fluxes across the downstream boundary cells. Explicit definition of no-flow boundaries (for example,

at the locations of embankments or around higher terrain in the floodplains that remains dry during high discharges) is not needed. MoCSED recognises missing values in the flow velocity maps as grid cells in which no flow occurs.

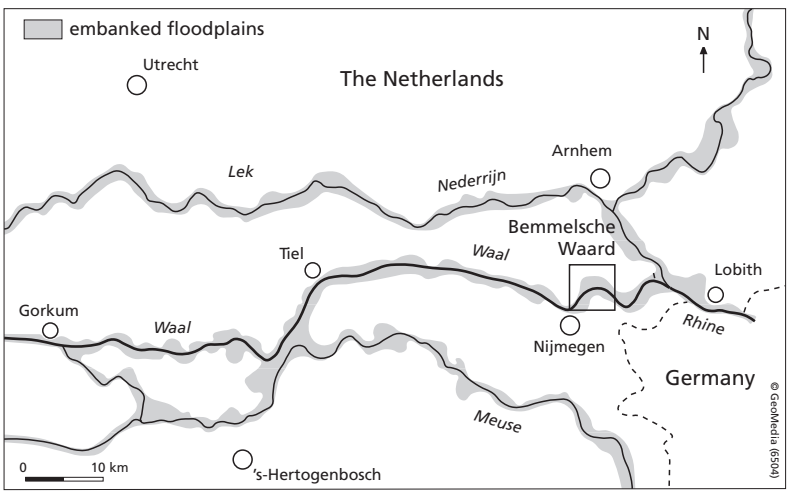

Figure 5.2 Location of the Bemmel floodplain along the Waal River.

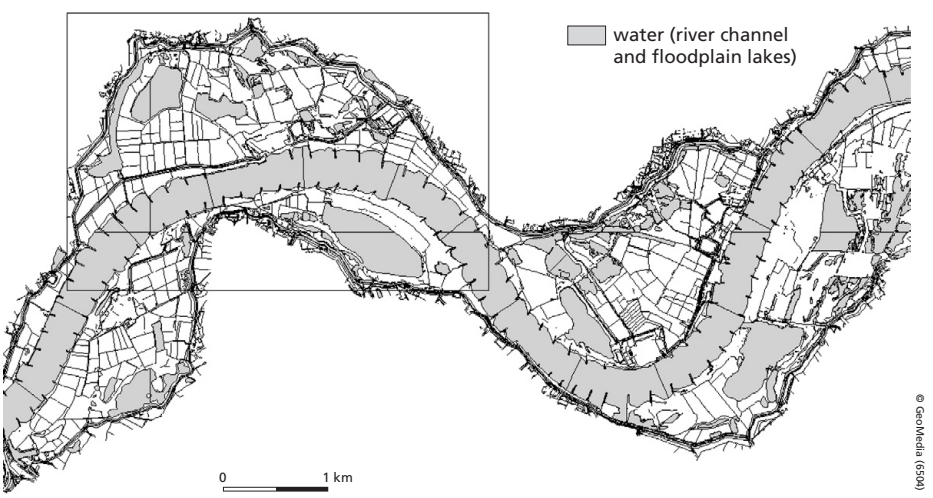

Figure 5.3 The total model area. The Bemmel floodplain (Fig. 5.4) is located within the box.

5.4 Model application

5.4.1 Model area

We applied MoCSED to the Bemmel floodplain in the east of The Netherlands (Figs. 5.2 & 5.3) for its inundation at the beginning of 2003 (Fig. 5.5). The Bemmel floodplain is located along an outer bend of the Waal River (Figs. 5.3 & 5.4), which is a distributary of the lower River Rhine. Two-third of the River Rhine discharge enters the Waal River. Between 1901 and 2004, the Waal River inundated the Bemmel floodplain 72 times. Inundation occurs when the discharge at the Dutch-German border exceeds approximately 6500 $m^3 s^{-1}$.

5.4.2 Data collection

During the last weeks of 2002 and the first weeks of 2003, the River Rhine experienced a period of high discharges. Discharge reached its peak of 9372 $m^3 s^{-1}$ at 6 January 2003 (Fig. 5.5). We obtained SSC and discharge data for the Dutch-German border from V&W (2005). We classified the discharges in the following classes: 3750–4250, 4250–4750, 4750–5250, 5250–5750, 5750–6500, 6500–7500, 7500–8500 and 8500–9500 $m^3 s^{-1}$. We also calculated the average SSC per class during the event (Fig. 5.5). We checked these values in the Waal River channel near the Bemmel floodplain. Following the method in Thonon & Van der Perk (2003) the values for the Waal River were checked against water samples in the river channel (Fig. 5.4) on the day of peak discharge. These samples delivered SSCs of 138.5 and 146 mg l^{-1}.

In advance of the inundation of the Bemmel floodplain, we placed 53 sediment traps in seven transects (Fig. 5.4). Lambert & Walling (1987) and Middelkoop & Asselman (1998) used similar traps. Of these 53 traps, seven were located in arable fields. These traps were discarded, since they also contained locally remobilized soil material. We subsequently used kriging to interpolate the sedimentation amounts for the Bemmel floodplain from the remaining 46 traps (Fig. 5.6a).

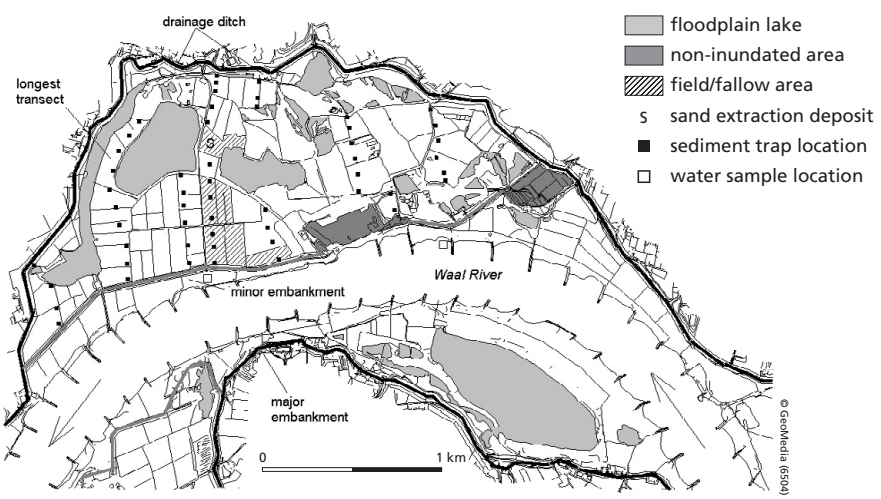

Figure 5.4 The Bemmel floodplain with the locations of the sediment traps (with traps on fields included).

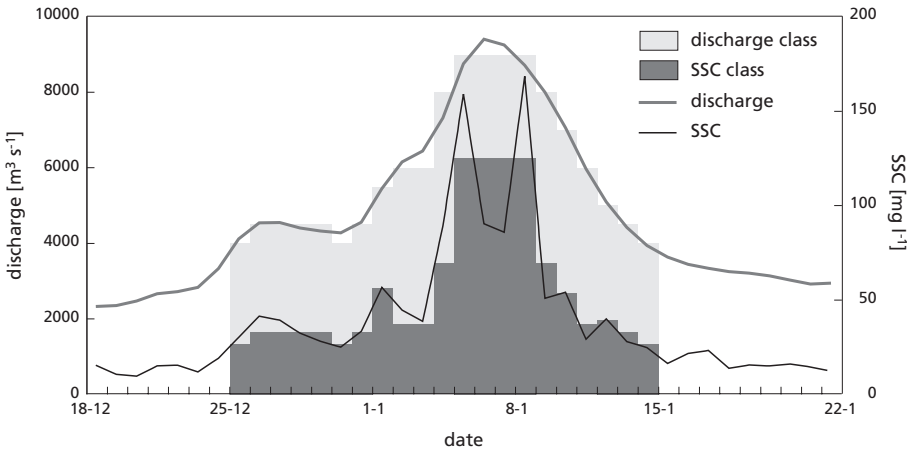

Figure 5.5 The discharge peak in the Rhine River at the Dutch-German border for the period between 18 December 2002 and 23 January 2003. We only modelled sedimentation for discharge classes of 4000 to 9000 $m^3 s^{-1}$. The SSC values were derived from V&W (2005).

When the water level drops below the level of the minor embankment, the minor embankment traps the inundation water. This turns the floodplain into a settling basin in which all suspended sediment can settle. To see how much sedimentation this accounted for, we multiplied the SSC value for the day on which the water level dropped below the minor embankment with the water depth of the floodplain. This gives the amount of sedimentation because of the 'settling basin effect'. We added this to the amount of sedimentation calculated by MoCSED.

5.4.3 Model input data

The total model area for which we performed calculations measured 10 by 5 km (Fig. 5.3) and had a cell size of 50 m. The Bemmel floodplain, approximately 3 by 2 km (Fig. 5.4), was located 8 km from the upstream boundary of the model area to allow the model to reach equilibrium before the floodplain. We obtained the input data for the model in the following ways:

- Flow velocities in x and y-direction, u and v [m s^{-1}]: we derived u and v from WAQUA (MX.Systems 2003). WAQUA is a stand-alone hydraulic model that is used by the Dutch governmental Institute for Inland Water Management and Waste Water Treatment (RIZA). It works with a curved grid that is more or less parallel to the river channel. In this grid it solves the Saint-Venant equations and calculates flow velocities and water levels. Its boundary conditions are discharges (upstream) and water levels (downstream). We interpolated the flow velocities as calculated using the WAQUA grid to the orthogonal grid used in the MoCSED model.
- Water depth, h [m]: for each discharge, we calculated the water depth by subtracting the ground level used in the WAQUA calculations from the water level that WAQUA generated.

- Transverse dispersivity, ε_T [m s^{-1}]: we used an equation proposed by Holley & Abrahams (1973):

$$\varepsilon_T = c \cdot h \tag{5.12}$$

with ε_T = transverse dispersivity [m] and c = an empirical constant [–]. Holley & Abrahams (1973) found an approximate value of 0.03 for c for the Waal River. We assumed this value to be valid for both the river channel and its floodplains.
- Longitudinal dispersivity, ε_L [m]: we used an equation by Fischer *et al.* (1985):

$$\varepsilon_L = 0.011 \frac{\overline{uv} \cdot b^2}{h \cdot u^*} \tag{5.13}$$

with ε_L = longitudinal dispersivity [m], 0.011 = an empirical constant, b = cell width and u^* = shear velocity [m s^{-1}].
- Suspended sediment concentration, C [mg l^{-1}]: we used a standard value of 100 mg l^{-1} to run MoCSED for every discharge class. Next, we scaled the model-derived SSC field to the measured SSC by applying

$$C = C_{model} \cdot (C_{meas} / C') \tag{5.14}$$

where C = SSC used in Eq. 5.11 [mg l^{-1}], C_{model} = SSC calculated by MoCSED [mg l^{-1}], C_{meas} = measured SSC (Fig. 5.5), C' = standard SSC, in this case 100 [mg l^{-1}].
- Settling velocity, w_s [m s^{-1}]: Thonon *et al.* (2005) measured settling velocities in a Waal River floodplain for two inundations in 2002. From their data we derived an effective settling velocity $w_{s,e}$ of 6.7 10^{-5} m s^{-1} for a floc range from 2.5 to 500 μm. This is close to the value of 7.0 10^{-5} m s^{-1} used in floodplain sedimentation models by Middelkoop & Van der Perk (1998), Asselman (1999b) and Asselman & Van Wijngaarden (2002).
- Flow shear stress, τ [Pa]: we used Eq. 5.10 with ρ = 1000 kg m^{-3}, g = 9.81 m s^{-2} and derived $\overline{uv}$ and Cz values from WAQUA. The Cz values were spatially distributed and generally varied between 5 and 65 $m^{0.5}$ s^{-1}.
- Critical shear stress for deposition, τ_{cr} [Pa]: when calibrating their sedimentation models for Dutch floodplains, Middelkoop & Van der Perk (1998), Asselman (1999b) and Asselman & Van Wijngaarden (2002) independently obtained the same value of 2.0 Pa. Because of this consistency, and because of close agreement between their calibrated and the measured $w_{s,e}$ in Thonon *et al.* (2005), we adopted their τ_{cr}.

5.4.4 Model calculation

We used 40,000 time steps of 10 seconds each to allow the model to reach a steady-state SSC field. After scaling with Eq. 5.14, we used the SSC field and Eq. 5.11 to calculate the deposition. We repeated this procedure for each discharge class. Adding the deposition maps for all discharge classes to the map with the 'settling basin' deposition delivered the final deposition map for the 2003 inundation event. We also obtained average annual sedimentation amounts using the average annual durations for each discharge class (T in Eq. 5.11). In this exercise, we

used sediment rating curves by Asselman (2000) for the Dutch-German border to determine C_{meas} in Eq. 5.14.

5.5 Model results and comparison with field data

For the last 1000 time steps of each model run, C_{model} varied on average 0.22 to 0.46 % per cell for all discharge classes. Therefore, we assumed the model to have reached a steady-state equilibrium for all discharge classes. The average mass balance error had an average absolute value of 2.68 %.

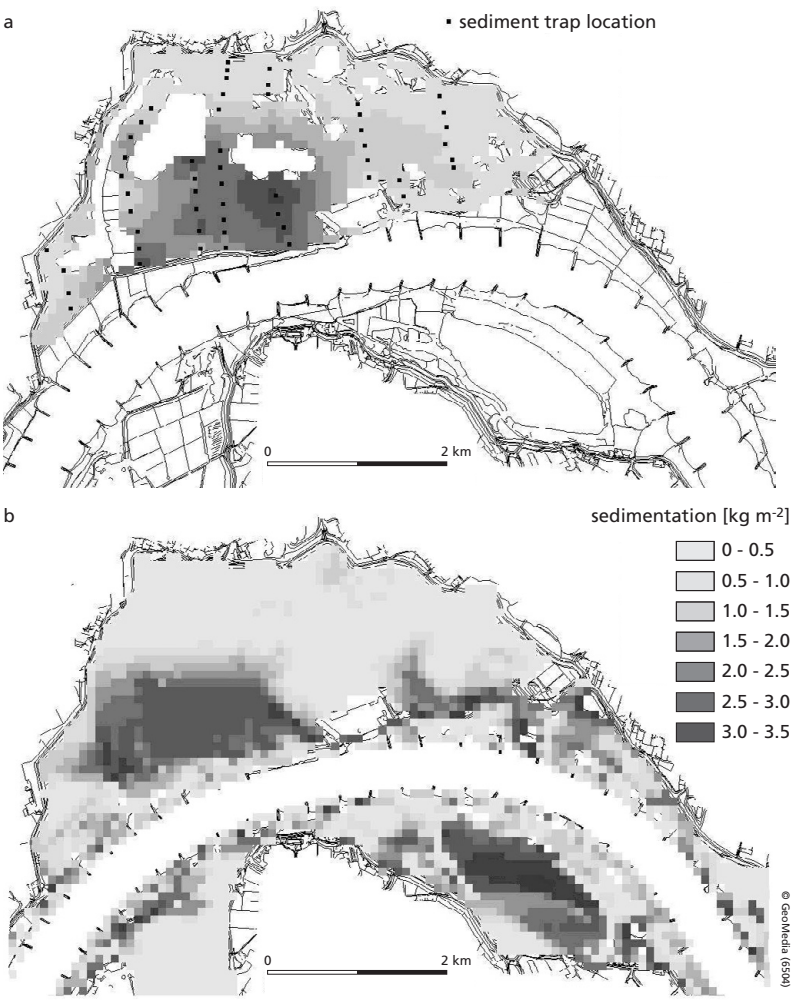

Figure 5.6 Amount of sediment deposition according to measurements (a) and MoCSED (b) for 2003 inundation event.

In this case a negative mass balance error means that sedimentation or outflow of sediment is slightly overestimated.

The final sediment deposition map (Fig. 5.6b) depicts a sedimentation pattern that is similar to the measured pattern (Fig. 5.6a). Most deposition occurs close to the minor embankment, in the downstream part of the floodplain. In the distal part, at the far downstream and upstream part, less deposition was measured and modelled. MoCSED predicted an average amount of 1.40 kg m^{-2} for the floodplain, while the sediment traps trapped 1.53 kg m^{-2} on average. The correlation coefficient for the measured and modelled data at the locations of the sediment traps is .72 (r^2 = .52), while the Nash-Sutcliffe efficiency coefficient *E* is 0.51 (Nash & Sutcliffe 1970). All three parameters are statistically significant (p = .000, n = 46).

For the longest transect of sediment traps (Fig. 5.4) we compared the modelled and measured sedimentation quantities (Fig 5.6). In the central part of the transect, the model overestimates sedimentation, while it underestimates at the distal parts of the floodplain. Still, the model follows the same trend as the measured data.

5.6 Discussion

5.6.1 Model performance

Comparison with field data shows that MoCSED performs reasonably well, despite not being calibrated nor optimized for the floodplain under study. MoCSED is able to simulate the general trend of the sedimentation. Its average amount of sedimentation approaches the measured amount, although it slightly underestimates the amount of deposition. There are four main reasons for this underestimation.

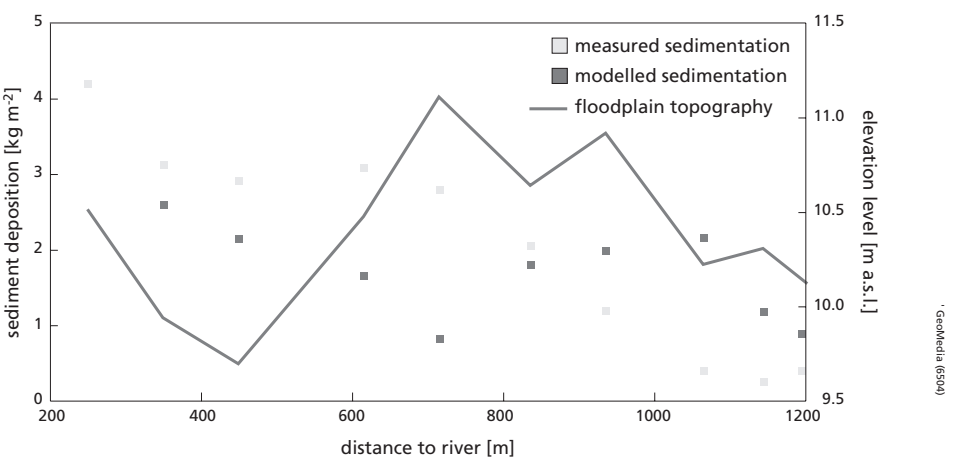

Figure 5.7 Measured and modelled amounts of sediment deposition on the second transect from the east (see Fig. 5.4).

First, the peak discharge on 6 and 7 January was approximately 9300 $m^3 s^{-1}$, which is 300 $m^3 s^{-1}$ more than the largest discharge for which we calculated sediment transport and deposition (Fig. 5.5). It is likely that during the higher peak discharge more sediment was conveyed to the distal parts of the floodplain than the model calculated. This problem could have been overcome by calculating sediment deposition during a higher discharge, for example 9500 $m^3 s^{-1}$.

Second, the SSC values we retrieved from V&W (2005) and used as model input for the validation event are probably too low. V&W (2005) gives a value of only 89.8 mg l^{-1} at 6 January the Dutch-German border. This yielded an average value for the 9000 $m^3 s^{-1}$ class of 125.4 mg l^{-1} (Fig. 5.5). However, at 6 January we measured in the river channel close to the Bemmel floodplain (indicated in Fig. 5.4) higher values of 138.5 and 146 mg l^{-1}. Using a lower SSC as input in the model leads to underestimation of the sedimentation amounts.

Third, MoCSED does not account for water flow after the flood event. After the flood event, the level of the inundation water drops. The remaining water flows to the low-lying distal parts of the floodplain, where the ground level is lower (Fig. 5.7) and a drainage ditch is located (Fig. 5.4). Part of the sediment carried by the water settles here instead of at its original location. This effect on the deposition pattern is not considered by the model.

Fourth, the centre of the floodplain contains fallow fields (the dashed areas in Fig. 5.4), which may have acted as local sediment source. Middelkoop & Asselman (1998) observed this in another floodplain along the Waal River for the 1993 inundation. At the beginning of the inundation stage, fast-flowing water may have eroded some of the uncovered soil from the fields. Some of the eroded soil may have been deposited close to the source, some may be transported to the back of the floodplain. MoCSED does not account for this local erosion and redistribution of sediment.

5.6.2 Comparison with other models

There are two other models with which the results of MoCSED can be compared. First, there is the 2D SEDIFLUX model by Middelkoop & Van der Perk (1998) who also applied their model to the Bemmel floodplain. Second, Asselman & Van Wijngaarden (2002) constructed the Silt-1D model for the whole lower River Rhine. We used the average annual sediment deposition to compare MoCSED with these other two models.

Table 5.1 Average annual sedimentation amounts for MoCSED and two other models [kg $m^{-2} y^{-1}$].

Location	MoCSED	SEDIFLUX	Silt-1D
Downstream part	1.2	2.3	
Close to major embankment	0.25	0.6	
In front of minor embankment	2.2	>4	
Total embanked floodplain	0.5	1.0	
Total model area	1.5		1.7

In the case of the Bemmel floodplain, the SEDIFLUX model predicts twice as much sedimentation as the MoCSED model (Table 5.1). The SEDIFLUX model indeed calculates overestimated values for most of the floodplain, especially for the distal and upstream parts (Middelkoop & Van der Perk 1998). MoCSED, however, shows an underestimation for these areas. This may be caused by too little dispersion. The empirical nature of the equations for dispersivity (Eqs. 5.12 & 5.13) may be responsible for this. Still, the model fit of MoCSED is better than that of SEDIFLUX, for which Middelkoop & Van der Perk (1998) obtained a r^2 of only .40.

The Silt-1D model predicts a slightly larger average yearly sedimentation for the whole lower River Rhine than MoCSED for the model area (Table 5.1). However, Asselman & Van Wijngaarden (2002) applied the Silt-1D model with different discharge and SSC classes *for 1901–1989*. If the frequencies of occurrence for 1901–1989 instead of 1901–2004 in combination with our discharge classes are used in MoCSED, MoCSED returns the same value as Silt-1D: 1.7 kg m^{-2} y^{-1}. However, if the discharge frequencies *for 1901–2004* in combination with the Silt-1D discharge classes are used in MoCSED, a value of 1.85 kg m^{-2} y^{-1} results. This shows MoCSED is sensitive for the frequency distribution of the discharges. Asselman & Van Wijngaarden (2002) noted the same for the Silt-1D model.

5.7 Conclusions and perspectives

The model performs reasonably well, taking into account we neither calibrated the model nor optimized it for the model area. With MoCSED it is possible to calculate sedimentation amounts and patterns for individual discharge classes, events or average years. These calculations are carried out within the raster-GIS PCRaster. This has two main advantages: it preserves the flexibility and functionality of a raster-GIS and it minimises numerical dispersion, which is normally one of the drawbacks of raster models.

The modelled average of 1.40 kg m^{-2} is somewhat lower than the measured average of 1.53 kg m^{-2} for the 2003 inundation of the Bemmel floodplain. We explain this underestimation by pointing at errors in the input data and local sediment sources that the model did not take into account. Notably uncertainties in the classification of discharge classes and suspended sediment concentrations may lead to errors. Despite these sources of errors, MoCSED performs better than a previous raster-based model for the River Rhine (SEDIFLUX). MoCSED model results, however, are similar to the Silt-1D model that was also developed for the lower River Rhine floodplains. Both models predict an average yearly sedimentation amount of 1.7 kg m^{-2} y^{-1}.

In future, MoCSED may serve several purposes. First, the calculation of the impact of the river rehabilitation plans (Silva *et al.* 2001; RIZA 2003) on the deposition of contaminated sediments on the Dutch floodplains. Second, the simulation of the impact of a changing discharge regime on the pattern and amount of sediment deposition. A similar study could be done to assess the effect of changes in upstream land use on sediment transfer and deposition on downstream floodplains. Third, the MoC routine could be used in other models within PCRaster or similar raster environments to minimise numerical dispersion.

Acknowledgements

We are greatly indebted to Ton Visser (RIZA-WST, Dordrecht), Gertjan Zwolsman (now KIWA, Nieuwegein) and Claus van den Brink (RIZA-WSR, Arnhem) for providing the flow velocities and water levels. Menno Straatsma took the water samples in the river channel. Boris Nolte helped to collect the sediment traps and Koos Jan Niesink retrieved the sediment from the traps. Roel van Elsas (Vrije Universiteit Amsterdam) helped to weigh the retrieved sediment. Job Spijker helped out with the cluster of personal computers that carried out the calculations. For more information about PCRaster, MoC and MoCSED, visit the website at http://pcraster.geo.uu.nl/projects/moc.

References

Asselman, N.E.M. (1999a), The use of floodplain sedimentation measurements to evaluate the effects of river restoration works. Geological Society Special Publication 163, pp. 111–122.

Asselman, N.E.M. (1999b), Effective discharge for overbank sedimentation on an embanked floodplain along the River Waal, The Netherlands. Special Publication of the International Association of Sedimentologists 28, pp. 61–69.

Asselman, N.E.M. (1999c), Slibmodellering in RvR. Delft, The Netherlands: WL|Delft Hydraulics (WL report R3337).

Asselman, N.E.M. (2000), Fitting and interpretation of sediment rating curves. Journal of Hydrology 234/3-4, pp. 228–248.

Asselman, N.E.M. & M. van Wijngaarden (2002), Development and application of a 1D floodplain sedimentation model for the River Rhine in The Netherlands. Journal of Hydrology 268/1-4, pp. 127–142.

Brookes, A. (1996), Floodplain restoration and rehabilitation. In: M.G. Anderson, D.E. Walling & P.D. Bates, eds., Floodplain processes. Chichester, U.K.: John Wiley, pp. 553–576.

Chen, C-N. (1975), Design of sediment retention basins. In: National symposium on urban hydrology and sediment control. Lexington, Kentucky, USA, pp. 285–298.

Fischer, H.B., E.J. List, R.C.Y. Koh, J. Imberger & N.H. Brooks (1985), Mixing in inland and coastal waters. Orlando, USA: Academic Press.

Garder, A.O., D.W. Peaceman & A.L. Pozzi Jr (1964), Numerical calculation of multidimensional miscible displacement by the method of characteristics. Society of Petroleum Engineers Journal 4/1, pp. 26–36.

Gomez, B., D. Phillips, F.J. Magilligan & L.A. James (1997), Floodplain sedimentation and sensitivity: summer 1993 flood, Upper Mississippi Valley. Earth Surface Processes and Landforms 22/10, pp. 923–936.

Hardy, R.J., P.D. Bates & M.G. Anderson (2000), Modelling suspended sediment deposition on a fluvial floodplain using a two-dimensional dynamic finite element model. Journal of Hydrology 229/3-4, pp. 202–218.

Holley, E.R. & G. Abraham (1973), Field tests on transverse mixing in rivers. Journal of the Hydraulic Division ASCE 99/HY12, pp. 2313–2331.

Konikow, L.F. & J.D. Bredehoeft (1978), Computer model of two-dimensional solute transport and dispersion in ground water. Alexandria, Virginia, USA: United States Geological Survey (Techniques of water-resources investigations of the United States Geological Survey, Book 7).

Krone, R.B. (1962), Flume studies of the transport of sediment in estuarial shoaling processes. Berkeley, USA: Hydraulic Engineering and Sanitary Engineering Research Laboratory, University of California.

Lambert, C.P. & D.E. Walling (1987), Floodplain sedimentation: a preliminary investigation of contemporary deposition within the lower reaches of the River Culm, Devon, U.K. Geografiska Annaler 69A/3-4, pp. 393–404.

Mertes, L.A.K. (1994), Rates of flood-plain sedimentation on the central Amazon River. Geology 22, pp. 171–174.

Middelkoop, H. & N.E.M. Asselman (1998), Spatial variability of floodplain sedimentation at the event scale in the Rhine-Meuse delta, The Netherlands. Earth Surface Processes and Landforms 23/6, pp. 561–573.

Middelkoop, H., I. Thonon & M. van der Perk (2002), Effective discharge for heavy metal deposition on the lower River Rhine flood plains. IAHS Publication 276, pp. 151–159.

Middelkoop, H. & M. van der Perk (1998), Modelling spatial patterns of overbank sedimentation on embanked floodplains. Geografiska Annaler 80A/2, pp. 95–109.

MX.Systems (2003), User's Guide WAQUA. Rijswijk/The Hague, The Netherlands: MX.Systems/Ministerie van Verkeer & Waterstaat (SIMONA-report 92-10).

Narinesingh, P. (1995), Nature restoration and floodplain sedimentation. Delft, The Netherlands: IHE (MSc Thesis H.H. 218).

Nash, J.E. & J.V. Sutcliffe (1970), River flow forecasting through conceptual models; Part I, A discussion of principles. Journal of Hydrology 10/3, pp. 282–290.

Nicholas, A.P. & D.E. Walling (1997), Modelling flood hydraulics and overbank deposition on river floodplains. Earth Surface Processes and Landforms 22/1, pp. 59–77.

Nicholas, A.P. & D.E. Walling (1998), Numerical modelling of floodplain hydraulics and suspended sediment transport and deposition. Hydrological Processes 12/8, pp. 1339–1355.

Nicholas, A.P. & S.J. McLelland (1999), Hydrodynamics of a floodplain recirculation zone investigated by field monitoring and numerical simulation. Geological Society Special Publication 163, pp. 15–26.

Owens, P.N., D.E. Walling & G.J.L. Leeks (1999), Deposition and storage of fine-grained sediment within the main channel system of the River Tweed, Scotland. Earth Surface Processes and Landforms 24/12, pp. 1061–1076.

RIZA (2003), Boven-Rijn Waal maatregelenboek – een overzicht van mogelijke rivierverruimende maatregelen in het stroomgebied. Lelystad, The Netherlands: RIZA (RIZA-report 2003.022).

Shabalova, M.V., W.P.A. van Deursen & T.A. Buishand (2003), Assessing future discharge of the river Rhine using regional climate model integrations and a hydrological model. Climate Research 23/3, pp. 233–246.

Silva, W., F. Klijn & J.P.M. Dijkman (2001), Room for the Rhine branches in The Netherlands – what the research has taught us. Arnhem/Delft, The Netherlands: RIZA/WL|Delft Hydraulics (RIZA-report 2001.031).

Stewart, M.D., P.D. Bates, D.A. Price & T.P. Burt (1998), Modelling the spatial variability in floodplain soil contamination during flood events to improve chemical mass balance estimates. Hydrological Processes 12/8, pp. 1233–1255.

Sweet, R.J., A.P. Nicholas, D.E. Walling & X. Fang (2003), Morphological controls on medium-term sedimentation rates on British lowland river floodplains. Hydrobiologia 494/1-3, pp. 177–183.

Thonon, I., J.R. Roberti, H. Middelkoop, M. van der Perk & P.A. Burrough (2005), *In situ* measurements of sediment settling characteristics in floodplains using a LISST-ST. Earth Surface Processes and Landforms 30/10, pp. 1327–1343.

Thonon, I. & M. van der Perk (2003), Measuring suspended sediment characteristics using a LISST-ST in an embanked flood plain of the River Rhine. IAHS Publication 283, pp. 37–44.

Van Rijn, L.C. (1993), Principles of sediment transport in rivers, estuaries and coastal seas. Amsterdam: Aqua Publications.

V&W, (2005), Waterbase; http://www.waterbase.nl. The Hague: Ministerie van Verkeer & Waterstaat.

Van Wijngaarden, M. (1999), A two-dimensional model for suspended sediment transport in the southern branch of the Rhine-Meuse estuary, The Netherlands. Earth Surface Processes and Landforms 24/13, pp. 1173–1188.

Walling, D.E. (1999), Linking land use, erosion and sediment yields in river basins. Hydrobiologia 410, pp. 223–240.

Walling, D.E., S.B. Bradley & C.P. Lambert (1986), Conveyance losses of suspended sediment within a flood plain system. IAHS Publication 159, pp. 119–131.

Walling, D.E., P.N. Owens & G.J.L. Leeks (1998), The role of channel and floodplain storage in the suspended sediment budget of the River Ouse, Yorkshire, U.K. Geomorphology 22/3–4, pp. 225–242.

Walling, D.E., P.N. Owens & G.J.L. Leeks (1999), Rates of contemporary overbank sedimentation and sediment storage on the floodplains of the main channel systems of the Yorkshire Ouse and River Tweed, U.K. Hydrological Processes 13/7, pp. 993–1009.

Wesseling, C.G., D. Karsenberg, W.P.A. van Deursen & P.A. Burrough (1996), Integrating dynamic environmental models in GIS: the development of a dynamic modelling language. Transactions in GIS 1/1, pp. 40–48.

6 The impact of river rehabilitation, climate and land-use change on the deposition of sediment and heavy metals on floodplains

Submitted as: Thonon, I., H. Middelkoop & M. van der Perk, The impact of river rehabilitation, climate and land-use change on the deposition of sediment and heavy metals on floodplains. River Research and Applications.

Abstract

Climate change, upstream land-use change and change in floodplain topography may all alter the functioning of floodplains as sediment and contaminant sinks. Both climate change and floodplain rehabilitation may increase the inundation frequency of floodplains, thereby increasing the possible deposition of contaminated sediments. However, upstream land abandonment probably leads to a decrease in input of sediments and associated heavy metals to rivers, reducing sediment loads and potential floodplain deposition rates. We studied the impact of these contrasting changes on the deposition of sediment and heavy metals on the lower River Rhine floodplains and assessed their relative importance.

We calculated the deposition of sediment and heavy metals for the current situation and four scenarios for two floodplain along the lower River Rhine: two scenarios with increased inundation frequencies (with and without decreased sediment loads), one scenario with rehabilitation projects and one scenario with both upstream and local changes.

Currently, approximately 1.5 kg m^{-2} y^{-1} of sediment and 0.5 g m^{-2} y^{-1} Zn, 0.085 g m^{-2} y^{-1} Pb, 0.08 g m^{-2} y^{-1} Cu and 1.5 10^{-3} g m^{-2} y^{-1} Cd are deposited on the lower River Rhine floodplains. These amounts may increase more than five times after embankment removal. Where floodplain rehabilitation leads to lower water levels, deposition could decline drastically, whereas the combination of climate and land-use change will often lead to only little change. Yet, the impact of lower sediment loads is remarkably larger in areas with natural sediment sinks such as frequently-flooded areas and floodplain lakes. The impact of increased inundation frequencies is most noticeable in less flooded areas. The impact of floodplain rehabilitation equals or exceeds that from climate and land-use change. At the level of the river branch, rehabilitation will lead to a spatial shift of sinks for sediments and contaminants.

Keywords

Floodplain, River Rhine, sedimentation, heavy metals, modelling, climate change, river rehabilitation.

6.1 Introduction

Floodplains serve as a link between the adjacent terrestrial and aquatic ecosystems (Brunet *et al.* 1994), regulate water levels by temporarily storing water during discharge peaks, sequester sediments (e.g., Walling *et al.* 1998a), and associated contaminants such as heavy metals (Middelkoop 2000), nutrients (Walling *et al.* 2003) and organic micro pollutants (Japenga & Salomons 1993). With respect to the last function, conveyance losses of contaminated sediments can be considerable. For instance, Walling *et al.* (2003) reported conveyance losses of up to 48.6 % for Pb for the Swale river in North-West England. Marron (1992) reported metal conveyance losses of 29 to 44 % for the Belle Fourche River in South Dakota, USA. Middelkoop (2000) calculated a loss of 17–25 % for Cd, Cu, Pb and Zn for the 1993 flood of the Waal River in The Netherlands.

Several factors influence the floodplain sequestration function. In general, larger upstream inputs of sediments (Asselman *et al.* 2003) and heavy metals (Foster & Charlesworth 1996; Hudson-Edwards *et al.* 1998, 1999; Middelkoop 2002), higher inundation frequencies (Hren *et al.* 2001; Middelkoop *et al.* 2002), lower flow velocities (Lecce 1997; Thonon *et al.* 2005) and longer inundation durations (Moody & Troutman 2000; Lecce & Pavlowsky 2001) lead to more deposition of sediments and associated heavy metals. Upstream land use and emissions govern the input of sediments and heavy metals, while climate and floodplain topography govern inundation frequencies. Floodplain topography also controls flow patterns and inundation duration. Yet, land-use change, environmental regulation, climate change and floodplain rehabilitation projects may change the above factors and hence influence the sequestration function of floodplains:

- Land-use change may consist of either increased pressure on land due to more grazing or deforestation, or decreased pressure due to land abandonment or reforestation. In the first case, this leads to enhanced erosion and higher sediment loads (e.g., Longfield & Macklin 1999), while the second case most probably results in less erosion and lower sediment loads (e.g., Keesstra *et al.* 2005).
- Environmental regulations, including the European Urban Wastewater Treatment Directive (EEC 1991) or Water Framework Directive (EC 2000), have often resulted in lower upstream inputs of heavy metals over the past two decades (Foster & Charlesworth 1996). However, in general, inputs have remained stable since the 1990s (e.g., CIW 2000).
- Houghton *et al.* (2001) predicted that climate change will probably cause a global increase in precipitation and frequency of extreme precipitation events. This increase may often take place during the winter season (Shabalova *et al.* 2003). Together with enhanced snowmelt in spring due to higher temperatures, this may result in an increased frequency of peak flows

(Knox 1993) and hence more frequent inundations of lowland river floodplains (Middelkoop *et al*. 2001).

- Floodplain rehabilitation may include lowering of floodplains by excavation, the construction of secondary channels and the removal of obstacles and minor embankments. These measures may lead to more flow over floodplains during peak discharges, longer inundations and different flow patterns (e.g., Narinesingh *et al.* 2000).

The evidence for both climate change and floodplain rehabilitation suggests more frequent and longer inundations of floodplains. This may result in increased conveyance losses of sediment (Asselman 1999a). Moreover, sediment carried at lower discharges contains more heavy metals than at higher discharges (Salomons & Förstner 1984). When floodplain inundation occurs at earlier flood stages, this may lead to enhanced deposition of sediment-associated heavy metals. However, land abandonment in upstream areas may lead to lower sediment loads and hence less sediment and heavy-metal deposition on floodplains. But until now, the individual and combined impacts of these local and upstream changes on sediment and heavy-metal deposition have not been thoroughly assessed.

In this paper we investigate the combined impact of a change in river discharges and upstream land use, the implementation of environmental policy and landscaping measures on the deposition of sediment and associated Zn, Pb, Cu and Cd on lower River Rhine floodplains. This is one of the major areas where both local topographical changes and upstream changes interact.

For this purpose we

- quantify the impact on sediment and heavy-metal deposition of both the upstream (climate change, land-use change, environmental policy) and local (floodplain rehabilitation) changes;
- assess changes in sedimentation and contamination patterns in floodplains because of the local and upstream changes.

First, we defined scenarios for the upstream changes for the year 2050. Second, we chose two floodplains along the lower River Rhine where the national government will implement different rehabilitation plans (RIZA 2003). Next, we calculated sediment and heavy-metal deposition for every scenario and floodplain using a 2D floodplain sedimentation model and compared the model results.

6.2 Study area

We selected two floodplains along the Waal River for our study: the Afferdensche & Deestsche Waarden (ADW) floodplain in the Middle Waal River reach (MWR reach) and Bemmelsche Waard (BW) floodplain in the Upper Waal River reach (UWR reach) (Fig. 6.1). The MWR reach measures 4 by 11.6 km, the UWR reach 5 by 9.9 km. The Waal River is the largest River Rhine branch in The Netherlands: two thirds of the discharge of the lower River Rhine enters the Waal River. At the Dutch-German border, the River Rhine has an average discharge of about 2250 $m^3 s^{-1}$ and a catchment area of 165,000 km^2 (Asselman *et al*. 2003).

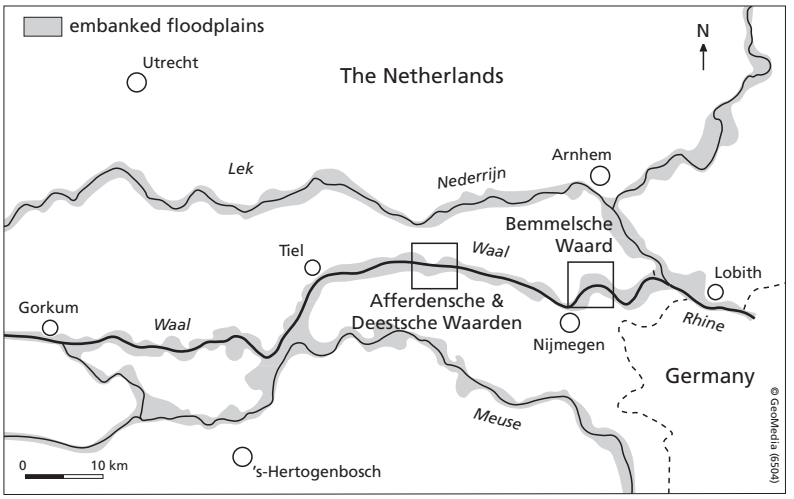

Figure 6.1 Location of the study areas.

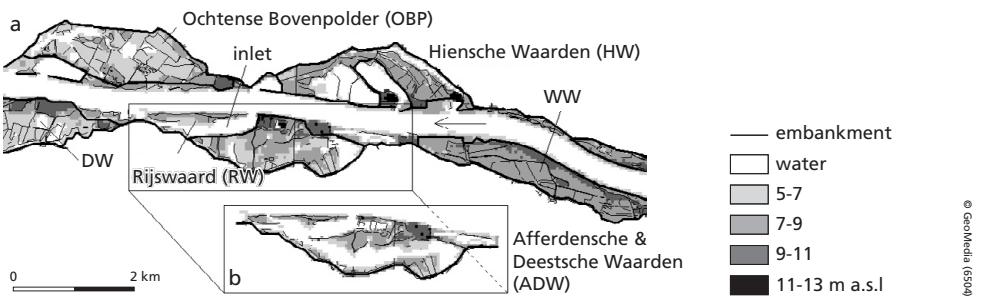

Figure 6.2 Present (a) and future (b) lay-out of the ADW floodplain and the Middle Waal River reach (MWR reach). The Rijswaard is an unembanked part of the ADW floodplain. DW = Drutensche Waarden; WW = Winssensche Waarden.

Table 6.1 Characteristics of floodplains in the MWR reach. Q_{ind} = discharge at which a floodplain is inundated in $m^3 s^{-1}$ before and after rehabilitation.

Floodplain	Embanked?	Measures	Q_{ind} before	Q_{ind} after
ADW	Yes	Secondary channel	6300	4000
RW	No	Secondary channel	3500	3500
DW	Yes	None	5500	6000
WW	Yes	None	7000	7500
HW	Yes	Lowering minor embankment	6300	5000
OBP	Yes	Lowering minor embankment	7000	6500

Table 6.1 gives the characteristics of all the floodplains in the UWR reach. The ADW floodplain section (Fig. 6.2) consists of an embanked and unembanked part. The embanked part has an inlet in the northeast. The unembanked part, the Rijswaard (RW) floodplain is located northwest of the inlet (Fig. 6.2a). Rehabilitation plans in the ADW floodplain encompass the creation of a secondary channel and the removal of higher areas (Fig. 6.2b; RIZA 2003). This will cause the ADW floodplain to be (partly) inundated at discharges of approximately 4000 $m^3 s^{-1}$ instead of 6300 $m^3 s^{-1}$ as in the current situation (Table 6.1).

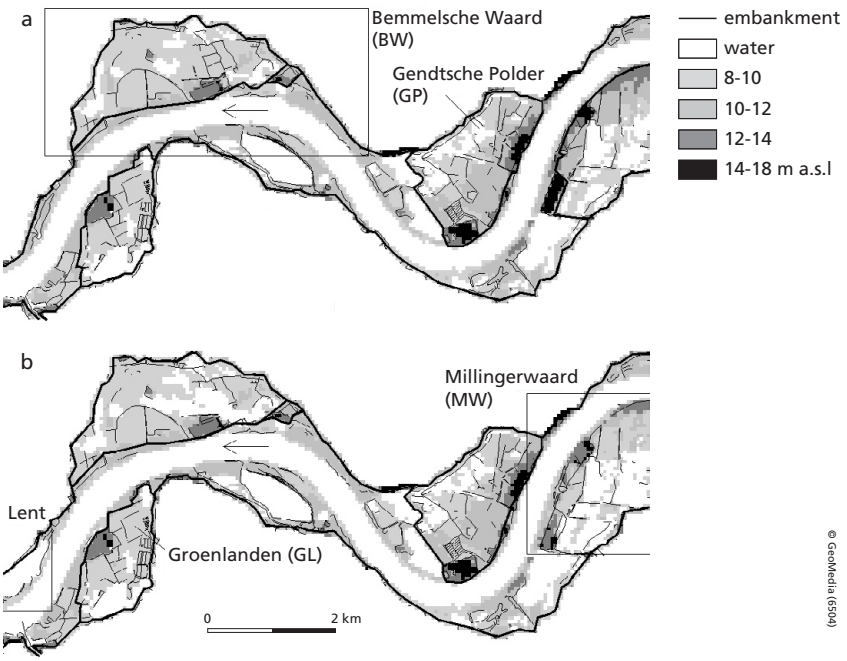

Figure 6.3 Present (a) and future (b) lay-out of the bw floodplain and the Upper Waal River reach (UWR reach).

Table 6.2 Characteristics of floodplains in the UWR reach. Q_{ind} = discharge at which a floodplain is inundated in $m^3 s^{-1}$ before and after rehabilitation measures taken.

Floodplain	Embanked?	Measures	Q_{ind} before	Q_{ind} after
BW	Yes	Floodplain lake	6500	7200
MW	Yes	Removing minor dyke and terrain	5500	4500
Lent	–	Dyke reallocation	–	5000
GP	Yes	None	7200	6500
GL	Yes	None	7500	8000
Lakes	No	None	5000	5000

Table 6.2 gives the characteristics of all floodplains in the UWR reach. The Bemmel floodplain (northern part of box in Fig. 6.3a) has a higher minor embankment than the ADW floodplain. Consequently, the floodplain is inundated at discharges exceeding 6500 $m^3 s^{-1}$. The unembanked part is located between the river channel and the minor embankment. Rehabilitation consists of the construction of a large floodplain lake by excavating the area between two existing smaller lakes (Fig. 6.3b; RIZA 2003). Other rehabilitation plans in the model area include the reallocation of the major embankment at Lent (Fig. 6.3b) and the excavation of large parts of the MW floodplain in combination with the removal of its minor embankments (Fig. 6.3b). Because these measures result in an increased transport capacity of the river reach, a certain discharge after rehabilitation causes a lower water level than before. Consequently, the floodplains in the UWR reach will only become inundated at higher discharges (Table 6.2). Since the BW floodplain's minor embankment will hardly change, the floodplain will only become inundated at discharges exceeding 7200 $m^3 s^{-1}$.

6.3 Scenario setup

We developed five different scenarios for which we calculated the sediment and heavy-metal deposition on the ADW and BW floodplains:

1. The current situation;
2. The situation with only *c*limate *c*hange in 2050: the 'CC' scenario;
3. The situation with *c*limate and *l*and-use *c*hange in 2050: the 'CLC' scenario, reflecting changes in upstream inputs of water and sediment;
4. The situation with *f*loodplain *r*ehabilitation: the 'FR' scenario, reflecting topographical changes;
5. The situation with climate change, land-use change and floodplain rehabilitation in 2050: the 'CLC+FR' scenario.

We expressed the influence of climate change in a new discharge regime for 2050. We assessed the influence of land-use change by calculating new sediment loads for 2050. Heavy-metal loads were assumed to remain equal to the current loads. These three parameters served as input for the floodplain sedimentation model.

6.3.1 Discharge regime

The discharge regime of a river may change under the influence of climate change and land-use change. Since Pfister *et al.* (2004) concluded that land-use change hardly affects peak discharges in the Rhine River, we only estimated the influence of climate change. We calculated the influence of climate change using the UKHI upper estimate for 2050 (Hulme *et al.* 1994). Middelkoop & Kwadijk (2001) and Middelkoop *et al.* (2001) used this estimate in earlier climate change impact studies for the River Rhine. This estimate, based on a temperature increase of 2 °C, is still within the range given by the IPCC (Houghton *et al.* 2001) and follows the same trend as the more recent HadRM2 estimates for the Rhine basin (Shabalova *et al.* 2003). Use of the UKHI projections ensures consistency with estimates of future changes in sediment load, which were based on the same estimate (Asselman *et al.* 2003).

Table 6.3 UKHI upper estimates for climate change in different regions of the Rhine basin (Asselman *et al.* 2003).

Region	Winter T [°C]	Summer T [°C]	Winter P [%]	Summer P [%]
Alps	+2.3	+2.0	+8.6	−5.1
Central	+2.4	+1.9	+12.6	−1.9
South	+2.2	+1.7	+16.9	+5.6

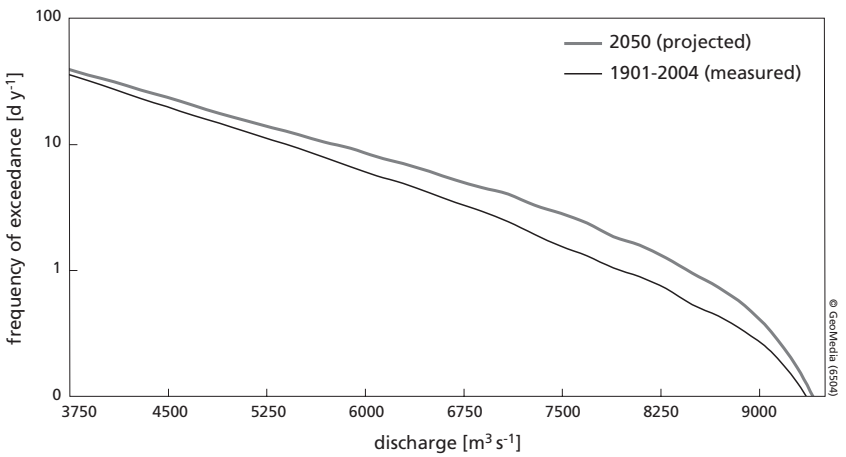

Figure 6.4 Exceedance frequencies for the higher domain of the reference and projected discharges for the Rhine River at the Dutch-German border.

According to the UKHI-2050 projections, both summer and winter temperatures will increase in the Rhine basin area. In summer, precipitation drops in the Alps and the central part of the basin, whereas it increases during winter and also during summer in the northern part (Table 6.3).

Van Deursen (2002) used the RhineFlow-3 model to calculate the impact of climate change on the discharge regime. RhineFlow is a water balance model for the Rhine basin that works within a Geographical Information System (Van Deursen & Kwadijk 1993; Kwadijk & Rotmans 1995). The model calculates 10-day average discharges for the Rhine River at the Dutch-German border on a 1 × 1 km resolution. Van Deursen (2002) calculated the new frequency distribution for 2050 as follows:

1. He calculated the average 10-day temperature and precipitation in the reference period 1961–1995.
2. He superimposed the temperature and precipitation changes according to the projections for 2050 on the reference averages. This gave 36 projected 10-day averages for temperature and precipitation.
3. He used the reference and projected temperature and precipitation in RhineFlow-3 calculations. This yielded 36 10-day average discharges for both the reference and projected

data. Then he divided the projected discharge for each 10-day period by the reference discharge for the same 10-day period to give 36 multiplication factors.

4. We linearly interpolated these 36 multiplication factors to 365.25 daily factors per year. We multiplied these by the daily discharges for the River Rhine for 1901–2004. This yielded projected daily discharges for 104 years.
5. From the 104 years of original and projected daily discharges, we calculated two frequency distributions (Fig. 6.4, Table 6.5). The projected average discharge in 2050 is 2228 $m^3\ s^{-1}$, which is 4 $m^3\ s^{-1}$ less than the average discharge of 2232 $m^3\ s^{-1}$ for 1901–2004.

6.3.2 Sediment loads

In the River Rhine, an increase in discharge (Q) leads to an increase in suspended sediment concentration (SSC) and sediment load. A sediment-rating curve describes this relationship. Asselman (2000) gives the sediment-rating curve for the present relation between discharge and SSC for the Dutch-German border as:

$$C = 29.3 + 1.96 \cdot 10^6 \cdot Q^{1.93}\ (n = 6148, r^2 = .44) \tag{6.1}$$

with C = SSC [mg l^{-1}], Q = discharge [$m^3\ s^{-1}$].

Using the current frequency distribution of discharges and sediment rating curve of Eq. 6.1, we calculated a yearly sediment load (Q_s) of 2.87 10^9 kg in the Rhine River. Asselman *et al.* (2003) projected land abandonment to cause no net change in erosion rates in the Rhine basin in 2050. However, since climate change will increase erosivity of rain showers, they predicted 12 % more erosion. Due to low sediment delivery, sediment loads will probably be still 13 % lower at the Dutch-German border. Together with the change in the frequency distribution of discharges (Fig. 6.4), this decrease in sediment load changes the relationship between discharges and SSC. It was therefore necessary to calculate a projected sediment rating curve for 2050. For this purpose we adapted an iterative procedure from Asselman (1999b):

$$Q_{s,2050} = \left[\sum_{i=1}^{n} Q_{i,2050} \cdot C_{i,2050} \cdot f_{i,2050} \right] \cdot 86.4 \tag{6.2}$$

with

$$C_{i,2050} = (29.3x) + 1.9 \cdot 10^6\ Q_{i,2050}^{1.93y} \tag{6.3}$$

with $Q_{s,2050}$ = total projected yearly sediment load in 2050 = 2.50 10^9 kg, $Q_{i,2050}$ = discharge class [$m^3\ s^{-1}$], $C_{i,2050}$ = SSC class [mg l^{-1}], $f_{i,2050}$ = frequency of occurrence [d y^{-1}], x and y are iteration factors and n = number of discharge classes.

The combination of a decrease in sediment load and a changed discharge regime yielded x = 0.87 and y = 0.98. This gave a new sediment rating curve for 2050:

$$C_{2050} = 25.5 + 1.96 \cdot 10^6\ Q_{2050}^{1.89}\ . \tag{6.4}$$

6.3.3 Heavy-metal loads

Analogous to the relationship between discharges and SSC, there is also a relationship between discharge and sediment-associated heavy-metal concentrations: 'metal rating curves' (Foster & Charlesworth 1996). Metal concentrations in suspended sediment have a negative relation with the *ultimate* (i.e., dispersed) grain size of the sediment to which the metals are bound (Förstner & Wittmann 1983). Since deposition patterns also have a relationship with ultimate grain size (cf. Walling *et al.* 1998b), this may influence the modelling of metal deposition patterns. Thonon *et al.* (2005), however, showed that sediment mainly settles on floodplains in the form of flocs. In these flocs all ultimate grain sizes are present, causing flocs to have one general metal concentration, which can be represented by one general metal rating curve.

We established the present metal rating curves using data for the period 1995–2003 from V&W (2005) (Fig. 6.5). We obtained the following metal rating curves using ordinary least squares curve fitting (all relations are statistically significant with p = .000):

$$[Zn] = 262 + (354029 / Q),\ n = 233,\ r^2 = .43 \text{ (Fig. 6.6)}; \tag{6.5}$$

$$[Pb] = 37.6 + (108022 / Q),\ n = 233,\ r^2 = .54; \tag{6.6}$$

$$[Cu] = 43.6 + (52583 / Q),\ n = 233,\ r^2 = .43; \tag{6.7}$$

$$[Cd] = 0.57 + (2040 / Q),\ n = 223,\ r^2 = .27 \tag{6.8}$$

Because of environmental policy, future heavy-metal loads could be lower than the current loads, which could lead to different metal rating curves. However, environmental laws such as the European Urban Wastewater Treatment Directive (EEC 1991; EC 1998) and the Water Framework Directive (EC 2000) are mainly targeted at point sources. Since point sources

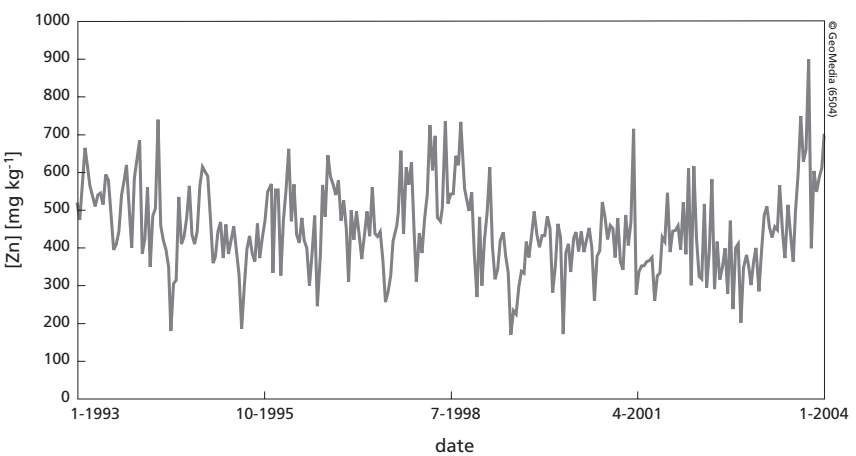

Figure 6.5 Zn concentration in suspended matter in the lower River Rhine at Dutch-German border for the period 1993–2003.

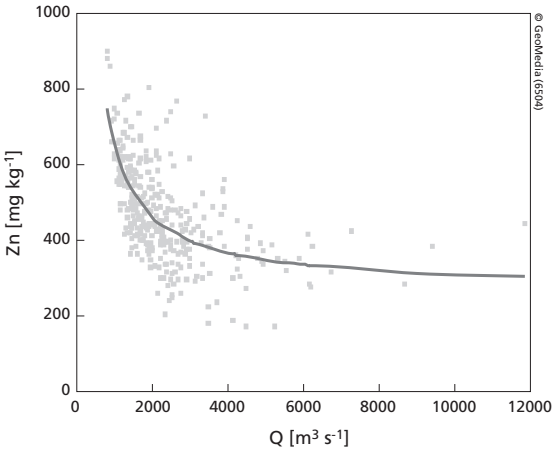

Figure 6.6 Relation between discharge and sediment-bound Zn concentration in the River Rhine at the Dutch-German border for 1995–2003.

only contribute less than 30 % of the heavy-metal loads in the River Rhine, Vink & Behrendt (2002) argued that environmental policy may have only little impact on total heavy-metal loads. In addition, point sources only make an important contribution to heavy-metal loads at low discharges. During higher discharges, when deposition of sediment-associated heavy metals takes place, a decreased importance of point sources is expected to have little effect. We therefore only derived the current metal rating curves and assumed them also to be valid for the projected situation of 2050.

6.3.4 Deposition of heavy metals and sediment

We calculated the pattern and amount of deposition of heavy metals and sediment using the MoCSED floodplain sedimentation model (Thonon *et al.* 2004; *accepted*). MoCSED calculates 2D patterns of sediment transport and deposition within the raster GIS PCRaster (Wesseling *et al.* 1996) using flow patterns from the hydrodynamic model WAQUA (MX.Systems 2003) as input. The area in Fig. 6.2 and 6.3 covers the area that we used in MoCSED. We performed calculations using eight discharge classes (Table 6.4) and a resolution of 50 m × 50 m.

First, the model calculates the sediment transport pattern using a standard SSC of 100 mg l^{-1} for one discharge class. We calculated sediment deposition during transport using the Chen (1975) and Krone (1962) concept:

$$C_t = C_{t-1} \cdot (1 - e^{-(\alpha \cdot w_{s,e}/h)\Delta t}), \text{ with } \alpha = 1 - (\tau / \tau_{cr}) \text{ for } \tau < \tau_{cr} \qquad (6.9, 6.10)$$

with C_t = the new SSC after each time step, C_{t-1} = the SSC in the preceding time step, $w_{s,e}$ = effective settling velocity [m s^{-1}], Δt = time step [s], h = water depth [m], τ = flow shear stress [Pa] and τ_{cr} = critical shear stress for sediment deposition [Pa].

Table 6.4 MoCSED discharge classes with the average yearly frequency of occurrence for the present and 2050 scenario and the change in between.

Discharge class [$m^3 s^{-1}$]	Class range [$m^3 s^{-1}$]	Frequency [$d y^{-1}$]	Freq. 2050 [$d y^{-1}$]	Change [%]
4000	3750–4250	10.8	10.3	–5
4500	4250–4750	6.9	7.9	+15
5000	4750–5250	4.7	5.0	+6
5500	5250–5750	3.5	3.5	+2
6000	5750–6500	3.2	3.8	+20
7000	6500–7500	2.2	2.9	+30
8000	7500–8500	0.9	1.8	+94
9000	8500–9500	0.5	0.8	+71
Total	All classes	32.7	36.0	+10

We derived a value for $w_{s,e}$ of 6.7 10^{-5} m s^{-1} from settling velocity data for the ADW floodplain in Thonon *et al.* (2005). When calibrating their models using a similar $w_{s,e}$ (7.0 10^{-5} m s^{-1}), Middelkoop & Van der Perk (1998), Asselman (1999c) and Asselman & Van Wijngaarden (2002) independently derived a value of 2.0 Pa for τ_{cr}. Because of this consistency, and because of close agreement between their calibrated and the measured $w_{s,e}$ in Thonon *et al.* (2005), we adopted their τ_{cr}.

After MoCSED had arrived at a steady-state SSC field, we scaled this field to the SSC of the sediment rating curves in Eq. 6.1 or 6.4. Next, we applied the steady-state SSC field in the calculation of sediment and heavy-metal deposition:

$$D = \left[\sum_{i=1}^{8} w_{s,e} \cdot (C_i \cdot \alpha_i \cdot T_i)\right] + (f_{pond} \cdot h_{pond} \cdot 10^{-3}) \tag{6.11}$$

with D = yearly sediment deposition rate [kg m^{-2} y^{-1}], T_i = average yearly duration of a discharge class [s y^{-1}], f_{pond} = flooding frequency of floodplain [y^{-1}], h_{pond} = water level at flooding of floodplain [m], C_{pond} = SSC at flood stage [mg l^{-1}], i denotes discharge class.

The first part at the right-hand side in Eq. 6.11 represents settling of sediment from flowing water. The second part represents settling from ponding. This is the amount of sediment that settles because water is trapped behind a minor embankment. T_i and f_{pond} follow from the frequency distribution of discharges (Table 6.4; Fig. 6.4). To derive the amount of heavy-metal deposition we multiplied for each discharge class the sediment deposition by the metal concentration according to the metal rating curves (Eqs. 6.5–6.8). The yearly metal deposition rate was the sum of the deposition for the eight discharge classes.

6.4 Results and discussion

6.4.1 Sediment and metal deposition amounts

The current average yearly sediment deposition rate for the UWR reach is 1.4 kg m^{-2}, while it amounts 1.6 kg m^{-2} for the MWR reach (Table 6.5; Figs. 6.9 & 6.10). These values agree well

Table 6.5 The present sediment deposition rates [kg m^{-2} y^{-1}] and the rates under the different scenarios with changes in parentheses [%].

Reach	Area	Current	Scenarios			
			CC	CLC	FR	CLC+FR
MWR	Model area	1.59	1.97 (+24)	1.50 (–3)	1.97 (+24)	1.90 (+20)
	ADW	0.34	0.48 (+41)	0.37 (+9)	2.18 (+541)	2.16 (+535)
	RW floodpl.	1.97	2.31 (+17)	1.81 (–8)	2.47 (+25)	2.26 (+15)
UWR	Model area	1.43	1.47 (+3)	1.15 (–20)	1.30 (–9)	1.23 (–14)
	BW	0.49	0.49 (0)	0.37 (–25)	0.20 (–59)	0.22 (–55)
	Unemb. part	2.16	2.19 (+1)	1.73 (–20)	1.59 (–26)	1.45 (–33)

Table 6.6 Heavy-metal deposition rates [mg m^{-2} y^{-1}] and changes in parentheses [%] with respect to the current situation for the MWR reach.

Metal	Area	Current	Scenarios			
			CC	CLC	FR	CLC+FR
Zn	Model area	519	635 (+22)	497 (–4)	642 (+19)	615 (+19)
	Floodplain	105	149 (+42)	113 (+8)	704 (+560)	693 (+560)
	Unemb. part	643	751 (+17)	590 (–8)	817 (+27)	744 (+27)
Pb	Model area	91	110 (+22)	86 (–5)	112 (+24)	107 (+18)
	Floodplain	18	25 (+41)	19 (+8)	122 (+590)	120 (+576)
	Unemb. part	113	131 (+16)	103 (–9)	145 (+28)	131 (+16)
Cu	Model area	85	104 (+23)	81 (–4)	105 (+24)	100 (+19)
	Floodplain	17	24 (+42)	19 (+11)	115 (+568)	113 (+558)
	Unemb. part	105	122 (+17)	96 (–8)	133 (+27)	121 (+16)
Cd	Model area	1.5	1.8 (+21)	1.4 (–5)	1.9 (+24)	1.8 (+18)
	Floodplain	0.3	0.4 (+43)	0.3 (+7)	2.0 (+598)	2.0 (+582)
	Unemb. part	1.9	2.2 (+16)	1.7 (–9)	2.4 (+29)	2.2 (+17)

with the rate of 1.7 kg m^{-2} y^{-1} that Asselman & Van Wijngaarden (2002) calculated for the total lower Rhine River. Most deposition occurs on the unembanked parts (approximately 2 kg m^{-2} y^{-1}, Table 6.5). Current amounts of metal deposition differ little between the two model areas (Tables 6.6 & 6.7). Average metal deposition rates are approximately 0.5 g m^{-2} y^{-1} Zn, 0.09 g m^{-2} y^{-1} Pb, 0.08 g m^{-2} y^{-1} Cu and 1.5 10^{-3} g m^{-2} y^{-1} Cd. The metal deposition closely follows the sediment deposition. Figs. 6.9 & 6.10 show this for sediment deposition and Zn, the most abundant metal in the sediment (Tables 6.6 & 6.7). In addition, Zn follows the same trend as the other metals (Tables 6.6 & 6.7). This is because metal concentrations differ little over the range of discharges we studied (Fig. 6.6; Table 6.4) and their rating curves are similar (Eqs. 6.5–6.8). We therefore focus the discussion of the amounts and patterns on sediment deposition and the discussion of metal deposition on Zn.

A first striking difference between the two studied reaches is the different impact the CC and CLC scenarios have (Figs. 6.7 & 6.8). The CC scenario hardly changes the deposition

Table 6.7 Heavy-metal deposition rates [mg m^{-2} y^{-1}] and changes in parentheses [%] with respect to the current situation for the UWR reach.

Metal	Area	Current	Scenarios			
			CC	CLC	FR	CLC+FR
Zn	Model area	469	486 (+3)	373 (–20)	423 (–10)	398 (–15)
	Floodplain	152	151 (–1)	114 (–25)	62 (–59)	67 (–56)
	Unemb. part	708	715 (+1)	563 (–21)	518 (–27)	471 (–34)
Pb	Model area	82	85 (+3)	65 (–21)	74 (–10)	69 (–16)
	Floodplain	26	25 (–1)	19 (–25)	10 (–60)	11 (–57)
	Unemb. part	124	125 (+1)	98 (–21)	91 (–27)	82 (–34)
Cu	Model area	76	79 (+4)	61 (–20)	69 (–10)	65 (–15)
	Floodplain	25	25 (0)	19 (–25)	10 (–59)	11 (–56)
	Unemb. part	115	117 (+1)	92 (–21)	84 (–27)	77 (–33)
Cd	Model area	1.4	1.4 (+2)	1.1 (–21)	1.2 (–10)	1.1 (–16)
	Floodplain	0.4	0.4 (–2)	0.3 (–26)	0.2 (–60)	0.2 (–57)
	Unemb. part	2.0	2.1 (+1)	1.6 (–21)	1.5 (–27)	1.4 (–34)

rates for the UWR reach (Table 6.7), whereas in the MWR reach it probably leads to 21–24 % more sediment and metal deposition (Tables 6.5 & 6.6). The reverse is true for the CLC scenario, yielding only a small decline for the MWR reach and even a small increase for the ADW floodplain, yet one fifth less deposition in the UWR reach. It seems that the increase in inundation frequency under the CLC scenario is more important for the ADW floodplain than the decrease in SSC, while the reverse is true for the total MWR reach and the UWR reach, including the BW floodplain. We may explain these contrasting results for the CC and CLC scenario with the different impacts of an increase in inundation frequencies. This increase is largest for the highest discharges (Table 6.4). On lower floodplains, these highest discharges are often combined with higher flow velocities, when trapping efficiencies are less and less or no sedimentation occurs. Since lower floodplains are more abundant in the UWR reach than in MWR reach (Tables 6.1 & 6.2), the impact of increased inundation frequencies is less in the UWR reach. This shows that local floodplain topography determines the extent of the impact of climate change on sediment and metal deposition.

A second considerable difference is the impact of the FR and CLC+FR scenarios on the two river reaches (cf. Figs. 6.9 & 6.10). Deposition is projected to increase with 24 % to 2.0 kg m^{-2} y^{-1} in the MWR reach, while it will probably decline to 1.3 kg m^{-2} y^{-1} in the UWR reach due to lower water levels. The increase in the MWR reach mainly takes place in the ADW floodplain, where the construction of the side channel may lead to almost six times more sediment and metal deposition (Tables 6.5 & 6.6). Apparently the side channel increases sediment influx but does not lead to a proportional increase in flow velocities. Still, the lowering of the minor embankments along the HW and OBP floodplains may also contribute to enhanced deposition. In the UWR reach, however, the deposition may decrease with 9 % and even with 60 % in the BW floodplain to only 0.2 kg m^{-2} y^{-1}, despite the construction of the floodplain lake. This relatively small decrease in the UWR reach is probably due to other rehabilitation measures in the MW floodplain and near Lent (Fig. 6.3b). These measures will probably increase sediment deposition,

limiting the reducing effect of lower water levels on the sedimentation rates in the rest of the UWR reach. This shows that in the assessment of the impact of floodplain rehabilitation on sediment and metal deposition in one floodplain, the impact on other surrounding floodplains cannot be neglected.

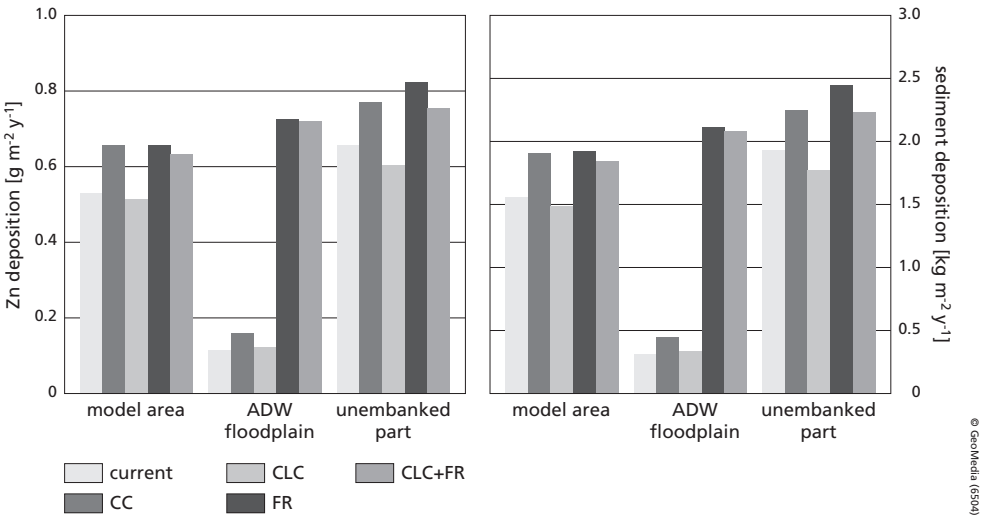

Figure 6.7 The sediment and Zn deposition rates for the MWR reach, ADW floodplain and unembanked part (RW floodplain) for the current situation and four scenarios.

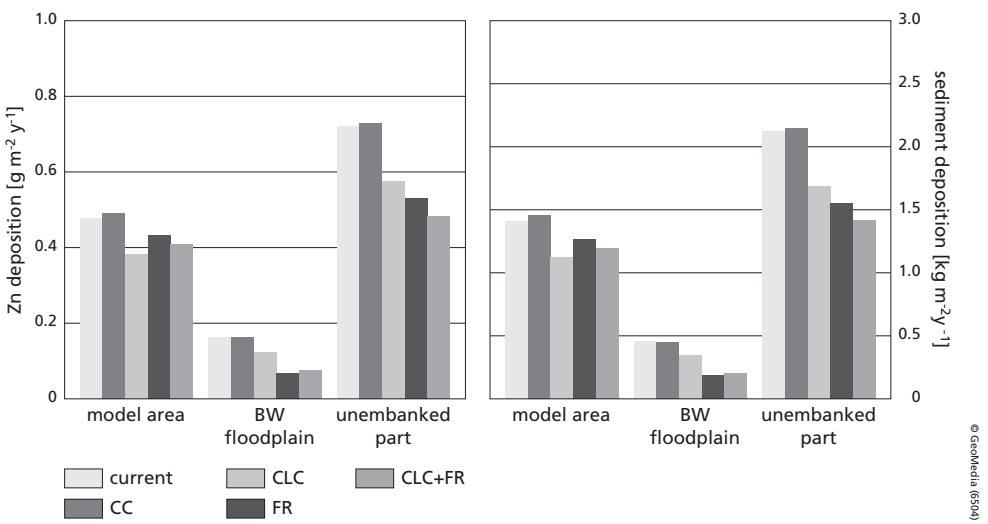

Figure 6.8 The sediment and Zn deposition rates for the UWR reach, the BW floodplain and its unembanked part for the current situation and four scenarios.

6.4.2 Patterns of sediment and metal deposition

The current sediment deposition rate for the ADW floodplain (0.3 kg m^{-2} y^{-1}) is lower than for the BW floodplain: 0.5 kg m^{-2} y^{-1}. This is because only little sediment is conveyed over the ADW floodplain during an inundation (Thonon *et al.* 2004), yielding only considerable sediment deposition in the north-western part and in the north-eastern floodplain lake (Fig. 6.9a). The BW floodplain is however located in the outer bend of the Waal River in the direction of

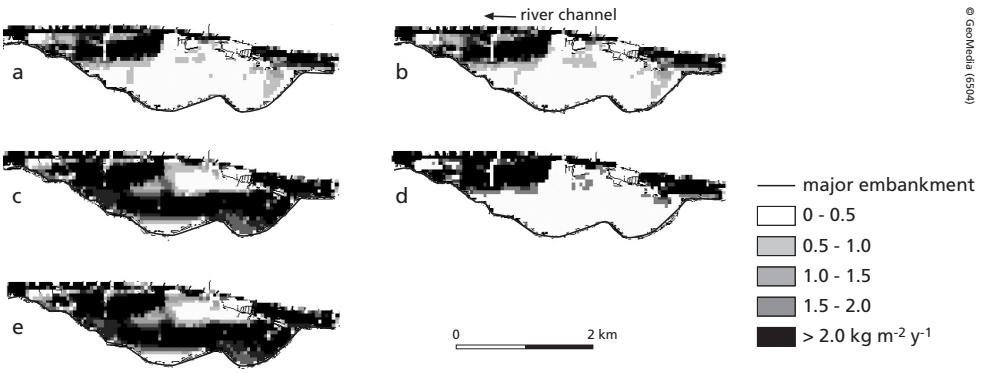

Figure 6.9 The yearly sedimentation amount for the ADW floodplain for the current situation (a), CLC scenario (b), FR scenario (c), CC scenario (d) and CLC+FR scenario (e).

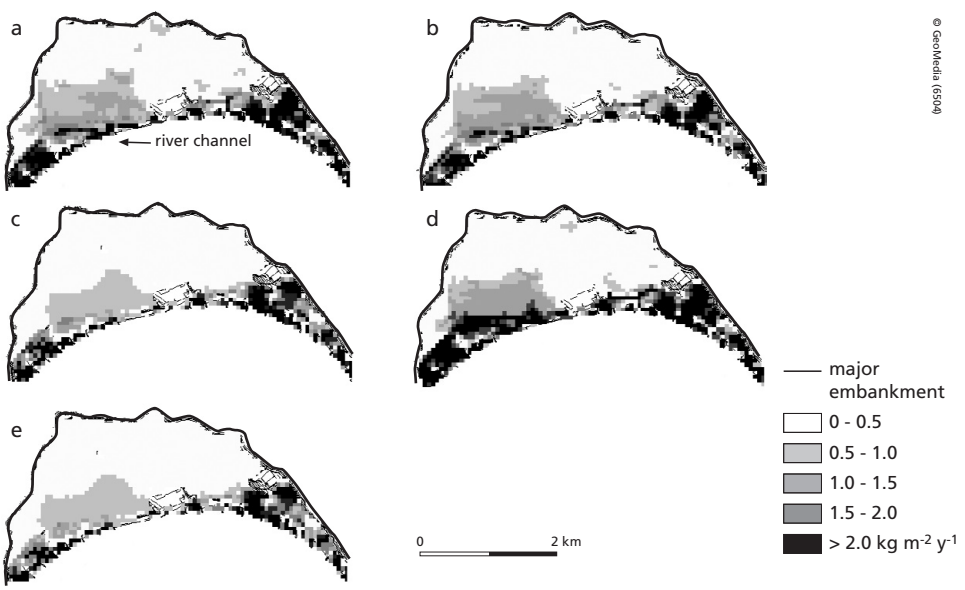

Figure 6.10 The yearly sedimentation amount for the BW floodplain for the current situation (a), CLC scenario (b), FR scenario (c), CC scenario (d) and CLC+FR scenario (e).

water flow (Fig. 6.3). This means that during inundations more sediment is conveyed over this floodplain, which notably leads to sediment deposition in the downstream part (Fig. 6.10a).

The impact of the FR scenario on the deposition patterns in the ADW and BW floodplains is clearly larger than of the CC scenario (Figs. 6.9 & 6.10). Under the CC and CLC scenario the patterns in the ADW and BW floodplain hardly change (Figs. 6.9b & d, 6.10b & d). Yet, under the FR and CLC+FR scenarios the effect of the secondary channel is clearly visible in the ADW floodplain (Figs. 6.9c & e). Since the secondary channel will convey most of the extra sediment influx over the floodplain, the increased sedimentation occurs mostly along that channel. In the BW floodplain, the deposition zone will become considerably smaller under the FR and CLC+FR scenarios (Fig. 6.10c & e). This is a direct effect of lower water levels in combination with the unchanged height of the minor embankment, which probably leads to less sediment conveyance to the downstream part of the BW floodplain.

6.4.3 Effective discharge for metal deposition

The discharge that contributes most to metal deposition is the effective discharge for metal deposition (Middelkoop *et al.* 2002). In the current situation and under the CC scenario, only the three upper discharge classes yield Zn deposition in the ADW floodplain (Fig. 6.11), yielding 9000 $m^3 s^{-1}$ as the effective discharge. The FR scenario introduces a more even distribution of Zn deposition rates (Fig. 6.11), yielding 7000 $m^3 s^{-1}$ as effective discharge. For the unembanked RW floodplain, currently having an effective discharge of 5500 $m^3 s^{-1}$, 4000 $m^3 s^{-1}$ would become the effective discharge under the FR scenario. Climate change thus hardly affects or even tends to increase the major contribution of higher discharges, whereas floodplain rehabilitation probably leads to a shift to lower effective discharges in the MWR reach.

Fig. 6.12 shows that the contribution every discharge class makes to the annual Zn deposition hardly changes for the UWR reach. Currently, 8000 $m^3 s^{-1}$ is the effective discharge for the BW

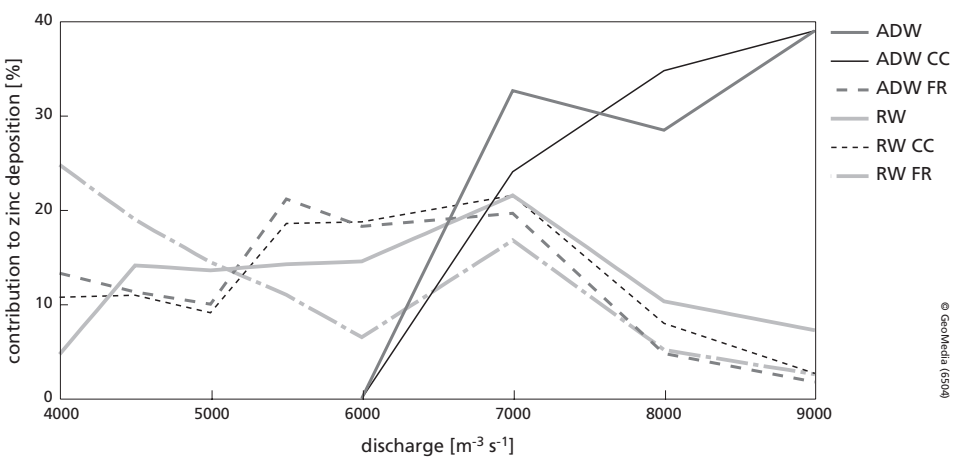

Figure 6.11 Proportion of Zn deposition per discharge class for the ADW and RW floodplains for the current situation, CC and FR scenario.

floodplain and this does not change under the CC scenario. Under the FR scenario, however, the 8000 $m^3 s^{-1}$ class even increases in importance and contributes almost 70 % of the metal deposition. For the unembanked part, the current effective discharge is 5000 $m^3 s^{-1}$. This increases to 6000 $m^3 s^{-1}$ under the FR scenario, whereas the higher discharges will only slightly increase their contribution under the CC scenario. This increase contrasts with the decrease in effective discharge for the ADW floodplain. It shows that both floodplains not only have contrasting changes in sediment and metal deposition due to floodplain rehabilitation, but also in the way the discharges contribute to this deposition.

6.5 Conclusions

6.5.1 The impact of climate and land-use change

According to our model results, current annual sedimentation rates on the lower River Rhine floodplains are 1.4 to 1.6 kg m^{-2}, while annual Zn deposition rates are about 0.5 g m^{-2}. Increased inundation frequencies due to climate change probably lead to more sediment and metal deposition in river reaches where minor embankments protect floodplains from inundations during moderate peak discharges. In reaches with more natural sinks such as lakes and low-lying floodplains, higher flow velocities may result in lower trapping efficiencies and hence no change in sediment deposition. In combination with lower sediment loads due to upstream land abandonment, deposition will nevertheless probably decrease, which confirms Asselman *et al.* (2003).

Both deposition patterns and the effective discharge for metal deposition hardly change due to climate and land-use change. In the embanked parts, conveyance of river water over the minor embankments will still govern the sedimentation pattern. However, sediment conveyance mainly takes place during high discharges and their share in total deposition will rise. In addition, the

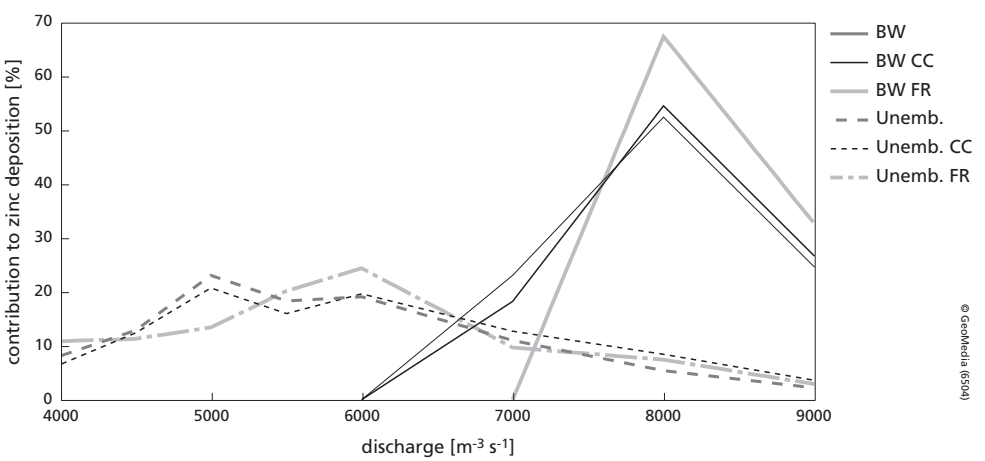

Figure 6.12 Proportion of Zn deposition per discharge class for the BW floodplain and its unembanked part for the current situation, CC/CLC and FR scenario.

unembanked parts and floodplain lakes will still receive most sediment and heavy metals. Areas with more of these natural 'sediment traps' will experience a larger impact of climate and land-use change. This shows that floodplain topography determines part of the sensitivity of river reaches for climate and land-use change.

6.5.2 The impact of floodplain rehabilitation

The impact of floodplain rehabilitation seems to depend on the scale (floodplain or river reach) and local topography. In a river reach where many floodplains are protected by minor embankments, lowering or removal of these embankments may have the same impact as climate change. However, at the level of an individual floodplain, the impact of floodplain rehabilitation by far exceeds that from climate and land-use change. This impact may be an increase due to more sediment influx or a decrease in deposition due to lower water levels. The measures that reduce these water levels are nevertheless mainly taken in other areas. Moreover, although they may enhance local deposition (e.g., in the case of floodplain lowering or embankment removal), they may lower deposition rates elsewhere because of reduced water levels. This shows that when assessing the impact of floodplain rehabilitation on deposition, changes in a wider area have to be taken into account.

Currently, higher discharges contribute most to the deposition of metals and sediment in embanked floodplains. Floodplain rehabilitation leads to a shift in the contribution of discharges and in sedimentation patterns. In case of embankment removal, lower discharges will become more important and the effective discharge for deposition will decrease. If the embankment does not change, lower water levels due to rehabilitation measures will lead to decreased inundation frequencies. Therefore, only higher discharges will inundate the floodplain and become more important for deposition. Because the impact of rehabilitation measures may vary considerably between floodplains, this could also lead to a shift in deposition pattern on the level of the river branch. Former important sinks for sediment and metals may become marginal, whereas other areas may increase in importance. This stresses the need for an integral assessment of the impacts of climate, land-use and topographical changes on floodplain deposition at the scale of the entire river branch.

Acknowledgements

We are greatly indebted to Ton Visser (RIZA-WST, Dordrecht) and Claus van den Brink (RIZA-WSR, Arnhem) for providing the WAQUA calculations. We also thank Kor de Jong for programming MoCSED and Job Spijker (now RIVM, Bilthoven) for helping out with the cluster of personal computers that carried out the MoCSED calculations.

References

Asselman, N.E.M. (1999a), The use of floodplain sedimentation measurements to evaluate the effects of river restoration works. Geological Society Special Publication 163, pp. 111–122.

Asselman, N.E.M. (1999b), The impacts of changes in climate and land use on transport and deposition of fine suspended sediment in the river Rhine. Utrecht: Universiteit Utrecht (Report of the NRP project 952210).

Asselman, N.E.M. (1999c), Effective discharge for overbank sedimentation on an embanked floodplain along the River Waal, The Netherlands. Special Publication of the International Association of Sedimentologists 28, pp. 61–69.

Asselman, N.E.M. (2000), Fitting and interpretation of sediment rating curves. Journal of Hydrology 234/3-4, pp. 228–248.

Asselman, N.E.M., H. Middelkoop & P.M. van Dijk (2003), The impact of changes in climate and land use on soil erosion, transport and deposition of suspended sediment in the River Rhine. Hydrological Processes 17/16, pp. 3225–3244.

Asselman, N.E.M. & M. van Wijngaarden (2002), Development and application of a 1D floodplain sedimentation model for the River Rhine in The Netherlands. Journal of Hydrology 268/1-4, pp. 127–142.

Brunet, R.C., G. Pinay, F. Gazelle & L. Roques (1994), Role of the floodplain and riparian zone in suspended matter and nitrogen retention in the Adour River, South-West France. Regulated Rivers: Research & Management 9, pp. 55–63.

Chen, C.-N. (1975), Design of sediment retention basins. In: National symposium on urban hydrology and sediment control. Lexington, Kentucky, USA, pp. 285–298.

CIW (2000), Water in beeld 2000 – Voortgangsrapportage over het waterbeheer in Nederland. The Hague: Commissie Integraal Waterbeheer, Ministerie van Verkeer & Waterstaat.

EC (1998), Commission Directive 98/15/EC of 27 February 1998 amending Council Directive 91/271/EEC with respect to certain requirements established in Annex I thereof (Text with EEA relevance). Official Journal L 067, pp. 29–30.

EC (2000), Directive 2000/60/EC of the European Parliament and of the Council of 23 October 2000, establishing a framework for Community action in the field of water policy. Official Journal L 327, pp. 1–72.

EEC (1991), Council Directive 91/271/EEC of 21 May 1991 concerning urban waste-water treatment. Official Journal L 135, pp. 40–52.

Foster, I.D.L. & S.M. Charlesworth. Heavy metals in the hydrological cycle: trends and explanation. Hydrological Processes 10, pp. 227–261.

Houghton, J.T., Y. Ding, D.J. Griggs, M. Noguer, P.J. van der Linden, X. Dai, K. Maskell & C.A. Johnson CA., eds. (2001), Climate change 2001: the scientific basis – Contribution of Working Group I to the Third assessment report of the Intergovernmental Panel on Climate Change. Cambridge, U.K.: Cambridge University Press.

Hren, M.T., C.P. Chamberlain & F.J. Magilligan (2001), A combined flood surface and geochemical analysis of metal fluxes in a historically mined region: a case study from the New World Mining District, Montana. Environmental Geology 40/11-12, pp. 1334–1346.

Hudson-Edwards, K.A., M.G. Macklin, C.D. Curtis & D.J. Vaughan (1998), Chemical remobilization of contaminant metals within floodplain sediments in an incising river system: implications for dating and chemostratigraphy. Earth Surface Processes and Landforms 23/8, pp. 671–684.

Hudson-Edwards, K.A., M.G. Macklin & M.P. Taylor (1999), 2000 years of sediment-borne heavy metal storage in the Yorkshire Ouse basin, NE England, U.K. Hydrological Processes 13/7, pp. 1087–1102.

Hulme, M., D. Conway, O. Brown & E. Barrow (1994), A 1961-90 baseline climatology and future climate change scenarios for Great Britain and Europe, part III: climate change scenarios for Great Britain and Europe. Norwich, U.K.: Climate Research Unit.

Japenga, J. & W. Salomons (1993), Dyke-protected floodplains: a possible chemical time bomb? Land Degradation & Rehabilitation 4/4, pp. 373–380.

Keesstra, S.D., J. van Huissteden, J. Vandenberghe, O. van Dam, J. de Gier & I.D. Pleizier (2005), Evolution of the morphology of the river Dragonja (SW Slovenia) due to land-use changes. Geomorphology 69/1-4, pp. 191–207.

Knox, J.C. (1993), Large increases in flood magnitude in response to modest changes in climate. Nature 361, pp. 430–432.

Krone, R.B. (1962), Flume studies of the transport of sediment in estuarial shoaling processes. Berkeley, USA: Hydraulic Engineering and Sanitary Engineering Research Laboratory, University of California.

Kwadijk, J. & J. Rotmans (1995), The impact of climate change on the river Rhine: a scenario study. Climatic Change 30, pp. 397–426.

Lecce, S.A. (1997), Spatial patterns of historical overbank sedimentation and floodplain evolution, Blue River, Wisconsin. Geomorphology 18/3-4, pp. 265–277.

Lecce, S.A. & R.T. Pavlowsky (2001), Use of mining-contaminated sediment tracers to investigate the timing and rates of historical flood plain sedimentation. Geomorphology 38/1-2, pp. 85–108.

Longfield, S.A. & M.G. Macklin (1999), The influence of recent environmental change on flooding and sediment fluxes in the Yorkshire Ouse basin. Hydrological Processes 13/7, pp. 1051–1066.

Marron, D.C. (1992), Floodplain storage of mine tailings in the Belle Fourche river system: a sediment budget approach. Earth Surface Processes and Landforms 17, pp. 675–685.

Middelkoop, H. (2000), Heavy-metal pollution of the river Rhine and Meuse floodplains in the Netherlands. Netherlands Journal of Geosciences 79/4, pp. 411–428.

Middelkoop, H. (2002), Reconstructing floodplain sedimentation rates from heavy metal profiles by inverse modelling. Hydrological Processes 16/1, pp. 47–64.

Middelkoop, H., K. Daamen, D. Gellens, W. Grabs, J.C.J. Kwadijk, H. Lang, B.W.A.H. Parmet, B. Schädler, J. Schulla & K. Wilke (2001), Impact of climate change on hydrological regimes and water resources management in the Rhine Basin. Climate Change 49/1-2, pp. 105–128.

Middelkoop, H. & J.C.J. Kwadijk (2001), Towards integrated assessment of the implications of global change for water management – The Rhine experience. Physics and Chemistry of the Earth (B) 26/7-8, pp. 553–560.

Middelkoop, H., I. Thonon & M. van der Perk (2002), Effective discharge for heavy metal deposition on the lower River Rhine flood plains. IAHS Publication 276, pp. 151–159.

Middelkoop, H. & M. van der Perk (1998), Modelling spatial patterns of overbank sedimentation on embanked floodplains. Geografiska Annaler 80A/2, pp. 95–109.

Moody, J.A. & B.M. Troutman (2000), Quantitative model of the growth of floodplains by vertical accretion. Earth Surface Processes and Landforms 25/2, pp. 115–133.

MX.Systems (2003), User's Guide WAQUA. Rijswijk/The Hague, The Netherlands: MX.Systems/Ministerie van Verkeer & Waterstaat (SIMONA-report 92-10).

Narinesingh, P., G.J. Klaassen & D. Ludikhuize (2000), Floodplain sedimentation along extended river reaches. Journal of Hydraulic Research 37, pp. 827–845.

Pfister, L., J. Kwadijk, A. Musy, A. Bronstert & L. Hoffmann (2004), Climate change, land use change and runoff prediction in the Rhine-Meuse basins. River Research and Applications 20/3, pp. 229–241.

RIZA (2003), Boven-Rijn Waal maatregelenboek – een overzicht van mogelijke rivierverruimende maatregelen in het stroomgebied. Lelystad, The Netherlands: RIZA (RIZA-report 2003.022).

Salomons, W. & U. Förstner (1984), Metals in the hydrocycle. Berlin: Springer.

Shabalova, M.V., W.P.A. van Deursen & T.A. Buishand (2003), Assessing future discharge of the river Rhine using regional climate model integrations and a hydrological model. Climate Research 23/3, pp. 233–246.

Silva, W., F. Klijn & J.P.M. Dijkman (2001), Room for the Rhine branches in The Netherlands – what the research has taught us. Arnhem/Delft, The Netherlands: RIZA/WL|Delft Hydraulics (RIZA-report 2001.031).

Thonon, I., K. de Jong, M. van der Perk & H. Middelkoop (2004), A particle tracking method to simulate sediment transfer over flood plains. IAHS Publication 288, pp. 404–409.

Thonon, I., K. de Jong, M. van der Perk & H. Middelkoop (*accepted*), Modelling floodplain sedimentation using particle tracking. Hydrological Processes.

Thonon, I., J.R. Roberti, H. Middelkoop, M. van der Perk & P.A. Burrough (2005), *In situ* measurements of sediment settling characteristics in floodplains using a LISST-ST. Earth Surface Processes and Landforms 30/10, pp. 1327–1343.

V&W (2005), WaterBase; http://www.waterbase.nl. The Hague: Ministerie van Verkeer & Waterstaat.

Van Deursen, W. (2002), Klimaatveranderingen in de stroomgebieden van Rijn en Maas – Modelstudies met Rhineflow-3 en Meuseflow-2. Rotterdam: Carthago Consultancy.

Van Deursen, W.P.A. & J.C.J. Kwadijk (1993), RHINEFLOW: an integrated GIS water balance model for the river Rhine. IAHS Publication 211, pp. 507–518.

Vink R. & H. Behrendt (2002), Heavy metal transport in large river systems: heavy metal emissions and loads in the Rhine and Elbe river basins. Hydrological Processes 16/16, pp. 3227–3244.

Walling, D.E., P.N. Owens & G.J.L. Leeks (1998a), The role of channel and floodplain storage in the suspended sediment budget of the River Ouse, Yorkshire, U.K. Geomorphology 22/3-4, pp. 225–242.

Walling, D.E., P.N. Owens & G.J.L. Leeks (1998b), Erratum to "The characteristics of overbank deposits associated with a major flood event in the catchment of the River Ouse, Yorkshire, U.K.". Catena 32/3-4, pp. 309–331.

Walling, D.E., P.N. Owens, J. Carter, G.J.L. Leeks, S. Lewis, A.A. Meharg & J. Wright (2003), Storage of sediment-associated nutrients and contaminants in river channel and floodplain systems. Applied Geochemistry 18/2, pp. 195–220.

Wesseling, C.G., D. Karsenberg, W.P.A. van Deursen & P.A. Burrough (1996), Integrating dynamic environmental models in GIS: the development of a dynamic modelling language. Transactions in GIS 1/1, pp. 40–48.

7 Synthesis

7.1 Introduction

The general aim of the research was to predict changes in patterns and quantities of deposition when environmental variables such as climate, land use and floodplain topography change. The research aimed to answer the following questions:

1. What are the *current spatial patterns* in amounts and characteristics of sediment and associated heavy metal deposition on floodplains of large lowland river branches?
2. What is the *relative importance* of the key factors controlling the deposition of sediments and heavy metals on floodplains along large lowland rivers and how do these factors interact?
3. How do *future changes* in climate, land use, heavy-metal emissions and floodplain topography interact and affect patterns and amounts of sediment and metal deposition on lowland river floodplains?

The main achievements of the study are:

- An overview of factors and processes in the river basin that control the deposition of sediment and associated heavy metals on floodplains of large lowland rivers.
- An assessment of the current patterns, amounts and characteristics of overbank deposition along the lower River Rhine branches.
- *In situ* measurements of settling flocs in inundated floodplains.
- A floodplain deposition model in a raster-GIS environment that uses particle tracking (the Method of Characteristics) to minimise numerical dispersion.
- Quantitative estimates of the patterns and amounts of deposition of sediment and associated heavy metals on lower River Rhine floodplains that may result from future changes in climate, upstream land use and floodplain topography.

The next three sections discuss, integrate, and compare these outcomes to answer the above research questions. The first section discusses the current deposition rates and the conveyance losses per river branch and the spatial patterns in deposition characteristics (i.e., grain size, heavy metal concentrations). The second section discusses the factors that govern these rates, losses and patterns. The third section gives estimates for changes in the patterns and conveyance losses due to changes in the governing factors. This is followed by a discussion of the likelihood for remobilisation of the stored heavy metals in the lower River Rhine. Where possible, the sections give recommendations for further research or to policy.

7.2 Current sediment and heavy-metal deposition patterns and amounts

7.2.1 Current deposition rates and conveyance losses

According to empirical measurements (Chapter 3) the sediment deposition is on average 1.0 kg m^{-2} on the IJssel River floodplains, and 1.5 kg m^{-2} on the Waal River floodplains *during the studied events*. For comparison, however, it is necessary to calculate annual average deposition *rates* [kg m^{-2} y^{-1}]. These rates are obtained by multiplying the amount of sediment and heavy-metal deposition per event (in kg m^{-2} or mg m^{-2}) by the inundation frequency of the floodplain (in y^{-1}). For the IJssel River, the values for the Ravenswaarden (IJ-RaW) floodplain are considered representative (Chapter 3), whereas for the Waal River the area-weighted values for all floodplains were used. Although the method provides rough estimates, it enables to compare the deposition rates of sediment and associated heavy metals for the IJssel and Waal River floodplains. In addition, it enables comparison of modelled (Chapter 6) and measured (Chapter 3) deposition rates for the Waal River. Furthermore, multiplying the floodplain area (105 km^2 along the IJssel and 87 km^2 along the Waal River; Wolters *et al.* 2001) by the overbank deposition rates (in kg m^{-2} y^{-1}) and dividing this number by the total annual sediment and metal transport at the Dutch-German border (in kg y^{-1}) gives the sediment and metal budgets for the two river branches.

Table 7.1 presents the sediment and metal deposition rates on the Waal and IJssel River floodplains. Heavy-metal deposition rates are highly correlated with sediment deposition rates. Sediment deposition rates explain more than 90 % of the variance in metal deposition rates.

Although the sediment deposition amounts per inundation event are lower for IJssel River floodplains than for the Waal River floodplains (Chapter 3), this situation reverses for the deposition rates. This is due to the higher inundation frequencies of the IJssel River floodplains. The deposition rates for the IJssel River floodplains (2.3 kg m^{-2} y^{-1}) are about 1.5 times higher than the Waal River floodplains (1.6 kg m^{-2} y^{-1}). Taken together, this results in an average annual

Table 7.1 Sediment, Zn, Pb and Cu deposition rates on the Waal and IJssel River floodplains calculated with sediment trap data (Chapter 3). See Table 3.1 for floodplain codes.

Floodplain code	Inund. freq. [y^{-1}]	Sed. dep [kg m^{-2} y^{-1}]	Zn dep. [mg m^{-2} y^{-1}]	Pb dep. [mg m^{-2} y^{-1}]	Cu load [mg m^{-2} y^{-1}]
W-BW	0.7	1.08	298	91	55
W-ADW	0.75	1.25	452	126	74
W-RWd	3	3.11	876	225	156
W-RWw	1.5	2.16	582	162	89
Waal		1.56	457	129	75
IJ-ReW [b]	3	4.51	1194	312	186
IJ-RaW [a]	3	2.29	729	201	132
IJ-VW [b]	3	1.31	420	111	54
IJssel [a]		2.29	729	201	132
Total		1.96	569	155	93

a. IJ-RaW floodplain is representative for the IJssel River floodplains. b. Probably overestimated rates.

Table 7.2 Sediment and metal conveyance losses [%] with respect to the annual sediment and metal transport in two river branches (Waal and IJssel River) and the total annual sediment and metal amount entering The Netherlands (lower River Rhine).

River	Sediment		Zn		Pb		Cu	
	Branch	Total	Branch	Total	Branch	Total	Branch	Total
Waal	7	5	5	3	7	5	5	4
IJssel	76	8	60	7	82	9	67	8
Lower Rhine		13		10		14		12

deposition of 2.0 kg m^{-2} of sediment and 0.5 g m^{-2} of zinc, 0.2 g m^{-2} of copper and 0.1 g m^{-2} of lead on the floodplains of the two river branches (Table 7.1).

Because of the larger floodplain area of the IJssel River and its higher overbank deposition rates, the IJssel River floodplains trap 6 to 8 % of all sediments and associated metals that enter The Netherlands via the River Rhine, whereas the Waal River floodplains only trap 3–5 % (Table 7.2). However, the IJssel River transports only 11 % of all sediment and associated metals that enter the lower River Rhine, whereas the Waal River transports 67 % of this amount. Of its own load, the IJssel River deposits over 60 % of the sediment-associated Cu and Zn and more than 80 % of the sediment and associated Pb on its floodplains (Table 7.2). The Waal River, on the contrary, deposits only 5–7 % of its load on its floodplains. The floodplains along the two river branches together account for 10 to 14 % of all sediment and heavy-metal deposition along the lower River Rhine.

These empirical figures confirm the estimates from previous model studies. Narinesingh *et al.* (2000) calculated an 80 % conveyance loss for grains of 32 μm for the IJssel River. Their grain size is similar to the median floc size for the IJssel River floodplains (25 μm, Chapter 4). Asselman & Van Wijngaarden (2002) calculated sediment budgets using suspended sediment data and a large-scale floodplain sedimentation model. They found sediment conveyance losses of 50 to 80 % for discharges above 4000 m^3 s^{-1} for the IJssel River. In addition, they obtained an average deposition rate of 1.7 kg m^{-2} y^{-1} and a loss of 13 % for the total lower River Rhine (including the Nederrijn/Lek River branch). Using the same model as Asselman & Van Wijngaarden (2002), Van der Lee *et al.* (2004) calculated a conveyance loss for sediment-associated phosphorus of 18 % for the IJssel River, 5 % for the Waal River and 7 % for the total lower River Rhine area. This shows that, although the discharge of sediment and heavy metals through the IJssel River is far less than through the Waal River, its floodplains clearly play a more important role in the sediment and heavy metal budget of the total lower River Rhine.

7.2.2 Current deposition patterns

At the scale of the individual floodplain section, the empirical and model results of Chapters 3 to 6 confirm a number of spatial trends mentioned in Chapter 2:

1. The amount of sediment deposition [kg m^{-2}] increases with:
   a. increasing inundation frequency;

b. increasing sediment supply (SSC);
c. increasing water depth;
d. decreasing distance to the river channel;
e. decreasing flow velocity or shear stress;

2. The median grain size decreases and the organic matter and clay content increase with decreasing floodplain elevation or increasing water depth.

3. The heavy-metal concentration in floodplain deposition increases with:
   a. increasing organic matter content;
   b. increasing clay content.

However, in three instances the empirical and modelling results do not confirm the general trends from the literature review in Chapter 2. Firstly, observations do not support the view that sediment deposition decreases with decreasing valley width, or, as in the case of the lower River Rhine, floodplain width. The embanked Waal River floodplains are narrower than the IJssel River floodplains, which results in higher water levels during inundations. Despite the higher water levels, flow velocities in the Waal River floodplains are low due to the insulating effect of the minor embankments. This leads to more efficient trapping of sediment and hence more deposition per event in the Waal River floodplains than in the broader IJssel River floodplains (Chapters 3 & 4). The reasoning of Lecce (1997), Wyżga (1999) and Thoms *et al.* (2000) that narrower valley floors lead to increased shear stresses and hence less potential for sediment deposition is thus only valid for floodplains without minor embankments.

Secondly, the observations do not confirm that sediment deposition decreases with increasing distance from the river. Preferential flow towards the distal parts of the floodplains (e.g., via sluices or drainage ditches), erosion of arable fields by inflowing inundation water and subsequent deposition in distal areas, and secondary channels acting as sediment source may weaken, disturb or even reverse this trend (Chapters 3, 5 & 6).

Thirdly, the results do not confirm the increasing trend in clay, organic matter and heavy metal content with distance from the river. The sharp rise in relative amounts of clay, organic matter and heavy metals near the river is primarily due to the decline of sand deposition. At distances of more than 100 to 500 meter from the river channel, clay, organic matter and heavy metal content exhibit a weak or no trend with distance to the river (Chapter 3). Walling *et al.* (2003) found similar results for small U.K. rivers.

7.3 Key factors controlling sediment and metal deposition

There are three groups of key factors that control overbank deposition of sediment and associated heavy metals on *individual lowland river floodplains* in a large, moderately-polluted river basin. These groups of factors are, in order of decreasing importance, the floodplain topography, overbank flow and suspended sediment. Within each group, the factors are arranged according

to decreasing importance (denoted by a 'larger than' sign) or following a causal relationship (indicated by an arrow):

1. topography: presence of minor embankments/natural levees > elevation (differences) > floodplain width/sinuosity of the river channel;
2. overbank flow: inundation frequency > flow velocity, discharge > inundation duration, water depth > flood magnitude;
3. suspended sediment: concentration > composition/mineralogy → effective grain size → settling velocity, ultimate grain size, heavy metal concentration.

The ranking of the groups follows a causal hierarchy: floodplain topography influences overbank flow patterns and suspended sediment characteristics. Particularly floodplain topography and overbank flow patterns are intertwined and therefore they are discussed in one section. Overbank flow subsequently influences the suspended sediment characteristics. The ranking also follows a scalar hierarchy (Fig. 7.1): factors controlling deposition close to the individual floodplain section are more important than those exerting their influence more upstream.

7.3.1 Floodplain topography and overbank flow

The most important topographical characteristic, the presence of a minor embankment or natural levee, exerts a major influence on the amount of sediment influx and hence deposition amounts per floodplain. Firstly, because minor embankments lower the inundation frequency, deposition rates are lower behind them. Secondly, Chapters 3 & 6 show that with pronounced natural or

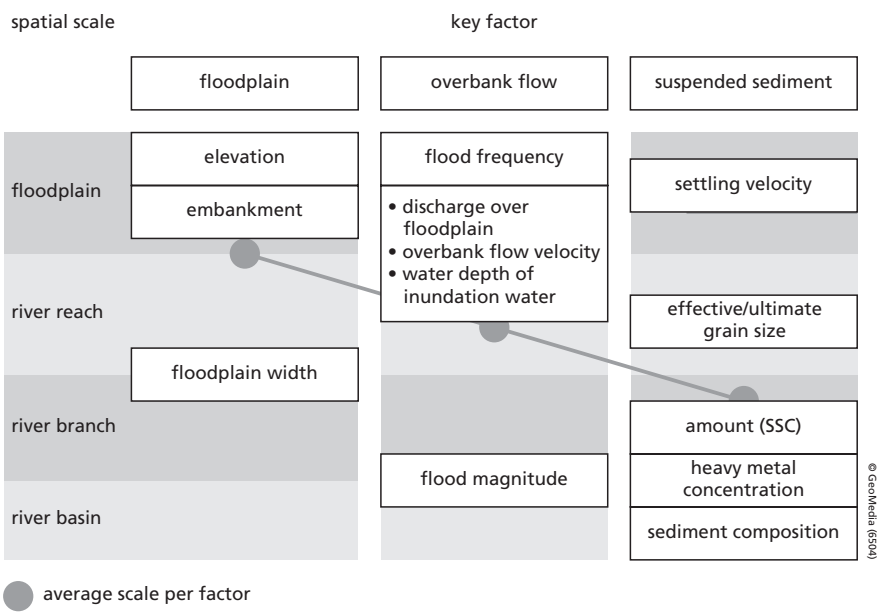

Figure 7.1 The approximate scale at which a factor determining sediment and metal deposition on individual floodplain sections is constituted.

artificial levees far less sediment enters the floodplain. Consequently, less sedimentation can potentially take place during an event than without those features. Thirdly, as noted in Section 7.2, minor embankments reduce flow velocities and thereby enhance sediment deposition. Fourthly, the ponding behind a minor embankment causes 0.1 to 0.2 kg m^{-2} extra sediment deposition per inundation event (Chapter 5).

Minor embankments may also induce increased shear stress by causing supercritical flow over their brink, which we observed during inundations. This enhanced shear may result in floc breakup. Hence, minor embankments could be the reason for the 2.5 times smaller flocs in the Afferdensche & Deestsche Waarden floodplain (W-ADW, with minor embankment) in comparison to the flocs in the Spankerensche Waard (IJ-SW, without minor embankment). Because smaller flocs are more widely dispersed, it may be one of the reasons for the rather homogeneous deposition amounts behind minor embankments (Chapter 3). Still, this explanation is tentative and requires more study.

Floodplain elevation is the topographical factor that predominantly determines overbank flow patterns and hence deposition patterns at the floodplain scale (Fig. 7.1). Floodplain lakes and other enclosed depressions receive more and finer sediment than higher areas, because ponding of water leads to deposition of the smallest flocs that do not settle in flowing water (Chapters 3 & 4). These fine flocs contain smaller grains and, accordingly, more heavy metals. This leads to higher heavy metal concentrations in sediment deposited in depressions. In the study area, ridges receive sediment containing only 3 mg Cd per kg and 25 mg Cu per kg, whereas swales receive sediment with significantly higher concentrations of almost 5 mg Cd kg^{-1} and 45 mg Cu kg^{-1} (Uijtdewilligen 2004). Deposition of sediment with higher metal concentrations may also take place in secondary channels, since these already conduct water at low discharges, when heavy metal concentrations in sediment are higher (Chapter 6).

The third topographical factor is floodplain width, which exerts its influence mainly at the scale of the river reach to branch (Fig. 7.1). In addition to the effects mentioned in Section 7.2.2, a larger floodplain width also means that distances to the river channel (the sediment source) are longer, causing less sediment to reach the distal parts of the floodplains (Chapters 3 & 5). The settling of flocs before reaching the distal parts also results in little deposition in remote areas, which is often not more than 0.2–0.5 kg m^{-2} y^{-1} (Chapters 3 to 6).

7.3.2 Suspended sediment

Suspended sediment concentrations (SSCs) vary within and between floods (Chapter 3) and generally increase with flood magnitude (Chapter 2). In addition to hysteresis during a single flood, exhaustion of sediment between successive floods plays an important role, leading to less sediment transport during the second flood. Chapters 3 & 4 illustrate this, showing that five times lower SSCs during a second inundation shortly after a first inundation led to five times lower sedimentation amounts in the W-ADW floodplain.

The suspended sediment composition (i.e., clay mineralogy and organic matter content) and metal concentrations are mainly determined at the river basin scale (Chapter 2, Fig. 7.1). Temporal variation in suspended sediment composition and heavy metal concentrations at

higher discharges (> 4000 m^3 s^{-1}) is generally low. As a result, variation in overbank sediment composition and heavy metal concentrations between individual floodplain sections inundated during the same event is small (Chapters 3 & 6).

Sediment composition influences the constituency of flocs and thereby the effective grain size and settling velocities (Chapter 4). Furthermore, characteristics such as clay mineralogy and organic matter content also determine the heavy metal concentration since they influence the number of binding sites on the sediment (Chapters 2 & 3). Because the floc composition encompasses a wide range of ultimate grain sizes (Chapter 4; Nicholas & Walling 1996) and different kinds of organic matter (Droppo 2001), heavy metals are not associated with a certain settling fraction (Millward *et al.* 1999). This permits modelling of sediment and heavy metal deposition using one effective floc size (Chapter 5). *In situ* measurements showed that this effective floc size has a settling velocity of 6.7 10^{-5} m s^{-1} (Chapter 4).

7.4 Sensitivity of sediment and metal deposition to changes in climate, land use and topography

Climate and upstream land-use change and changes in floodplain topography affect the key factors identified in Section 7.3. Their effects on floodplain deposition were explored in a scenario study in Chapter 6.

Fig. 7.2 gives estimated deposition rates based on the weighted average deposition rates for the Upper and Middle Waal River reaches (Chapter 6). Fig. 7.2 gives the average modelled sediment and zinc deposition rates for the Waal River branch. Currently, 1.5 kg m^{-2} y^{-1} of sediment and

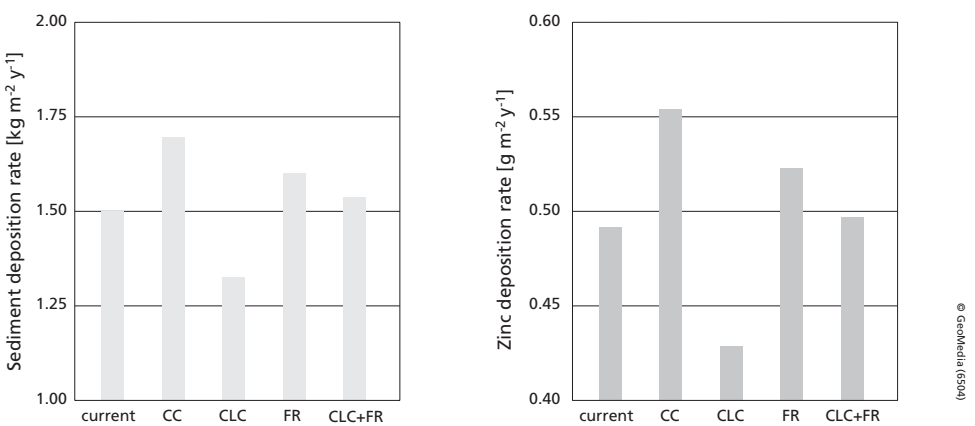

Figure 7.2 The current and future sediment and zinc deposition rates on the Waal River floodplains according to the different scenarios with reference year 2050. CC = climate change, CLC = climate and land-use change, FR = floodplain rehabilitation. See Chapter 6 for explanation of the scenarios.

almost 0.5 g m^{-2} y^{-1} of zinc are deposited, which is almost similar to the empirical figures of Section 7.2.1.

Climate change results in an increase in deposition rates. Under the applied scenario, this increase is approximately 13 %. Land-use change in the River Rhine basin and the resulting lower sediment yields appear to drastically decrease sediment and metal deposition. A scenario including climate and land-use change resulted in a decline of deposition rates by 12 %.

Floodplain topography will change due to floodplain rehabilitation measures. Changes may include removal of minor embankments, construction of secondary channels and lowering of floodplain levels. Floodplain rehabilitation measures increase the deposition rates with only 6 % for the entire Waal River branch under the scenario applied. Nevertheless, floodplain rehabilitation may lead to substantial changes in individual floodplains (Chapter 6). For instance, construction of secondary channels leads to approximately five to six times higher deposition rates. When a minor embankment is removed, the enhanced yearly influx of suspended sediment may cause a three- to fivefold increase of sediment and metal deposition rates. Where the rehabilitation measures result in lower water levels during floods, lower inundation frequencies may lead to a decline in deposition rates by more than 50 %.

Fig. 7.3 depicts the conveyance losses and their projected future changes for the Waal River branch. The Waal River floodplains currently trap about 7 % of the sediment and around 5 % of the heavy metals that yearly enter the Waal River. These values are very similar to the empirical values in Table 7.1. Because of low metal concentrations and high suspended sediment concentrations during high-magnitude discharges, inundated floodplains trap relatively less heavy metals than sediment.

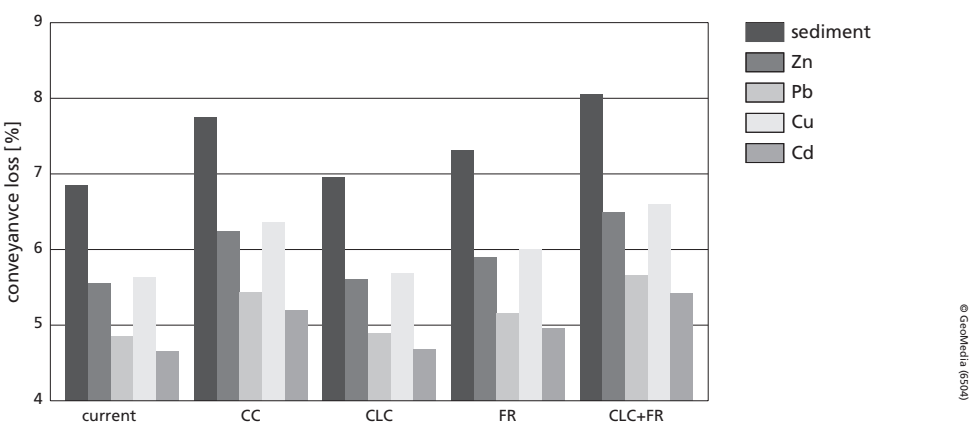

Figure 7.3 Conveyance losses for sediment, zinc, lead, copper and cadmium for the current situation in the Waal River branch and for different scenarios with reference year 2050. See caption of Fig. 7.2 for the scenario names.

The projected future conveyance losses increase according to all four scenarios (Fig. 7.3), although the increase due to the combination of climate and land-use change is negligible. These changes apparently cancel out each other's impact at the scale of the river branch. The estimated increases under the climate change scenario (13 %) and floodplain rehabilitation scenario (7 %) are similar. The largest increase takes place under the scenario that combines all local and upstream changes: 18 %. Under this scenario, the sediment conveyance loss increases to almost 8 % and the metal conveyance losses to about 6 %. It appears that not only the local and upstream changes cancel out each other at the reach scale (Chapter 6), but that changes in different Waal River reaches also cancel out each other at the river branch scale. The budget calculations indicate that the combination of future changes appear to have at most a moderate influence on the sediment and heavy metal budget of the total Waal River branch, but the deposition patterns within the river branch may manifest more pronounced changes.

In the calculation of the conveyance losses for the total river branch the exhaustion of the suspended matter due to sedimentation along the river branch is neglected. In the Waal River the conveyance loss is small, hence the error by neglecting the exhaustion is also small. By contrast, for a river branch such as the IJssel River this exhaustion is very important, as Chapter 3 and Asselman & Van Wijngaarden (2002) have shown. Model calculations for the *total* lower River Rhine should therefore give a more accurate sediment and metal budget. Furthermore, such a model exercise would give a better insight in the consequences of climate, land-use and topographical change on the deposition patterns of sediment and heavy metals *at the delta scale*. Taking the IJssel River into account in this exercise seems indispensable.

7.5 Remobilisation of heavy metals in the lower River Rhine

Many authors have pointed out that remobilisation of floodplain storages of sediment-attached heavy metals forms a potential source for downstream contamination of river floodplains (Leenaers & Schouten 1989; Bradley & Cox 1990; Leenaers 1991; Walling *et al*. 1996, 1998; Ciszewski 2001; Dennis *et al*. 2003). Remobilisation often proceeds through bank erosion during floods (Lecce & Pavlowsky 1997; Dennis *et al*. 2003), meander migration (Leenaers & Schouten 1989) or resuspension of freshly deposited sediments (Schouten *et al*. 2000). In the lower River Rhine, however, these mechanisms for remobilizing contaminated sediments hardly occur.

Firstly, bank erosion is prevented by bank protection. The river branches of the lower River Rhine have all been trained (Chapter 3). Groynes keep the river channel of the three branches in place since 1850 (Hesselink *et al*. 2003), while in 1965–1975 the IJssel River banks have also been reinforced with riprap (Ten Brinke 2004). Furthermore, floodplain soils are very cohesive and hence resistant to erosion or re-suspension. In case soil erosion still occurs, e.g., on fallow arable fields, the eroded soil is mainly deposited within the same floodplain section and does not leave the floodplain (Chapter 5).

Secondly, the erosivity of overbank flows is generally insufficient to cause widespread soil erosion of floodplain soils. Lecce & Pavlowsky (1997) stated that stream power in downstream reaches of rivers is often too low to erode major amounts of bank sediments. Flow shear stress calculations

confirm this for the lower River Rhine floodplains (Chapter 5). Moreover, they show that the shear stress of most overbank flows remains well below the critical threshold for deposition. Since the critical threshold for deposition is by definition even lower than the critical threshold for erosion, erosion of floodplain soils by flowing water is very unlikely. Thus, it is unlikely that physical processes in the lower River Rhine floodplains cause remobilisation of sediment-associated heavy metals. Rehabilitation measures, on the contrary, often involve excavation of floodplain soil and hence remobilisation of heavy metals. Most remobilisation can therefore be expected to result from human action instead.

References

Asselman, N.E.M. & M. van Wijngaarden (2002), Development and application of a 1D floodplain sedimentation model for the River Rhine in The Netherlands. Journal of Hydrology 268, pp. 127–142.

Bradley, S.B. & J.J. Cox (1990), The significance of the floodplain to the cycling of metals in the River Derwent catchment, U.K. The Science of the Total Environment 97-98, pp. 441–454.

Ciszewski, D. (2001), Flood-related changes in heavy metal concentrations within sediments of the Biała Przemsza River. Geomorphology 40/3-4, pp. 205–218.

Dennis, I.A., M.G. Macklin, T.J. Coulthard & P.A. Brewer (2003), The impact of the October-November 2000 floods on contaminant metal dispersal in the River Swale catchment, North Yorkshire, U.K. Hydrological Processes 17/8, pp. 1641–1657.

Droppo, I.G. (2001), Rethinking what constitutes suspended sediment. Hydrological Processes 15, pp. 1551–1564.

Hesselink, A.W., H.J.T. Weerts & H.J.A. Berendsen (2003), Alluvial architecture of the human-influenced river Rhine, The Netherlands. Sedimentary Geology 161/3-4, pp. 229–248.

Leenaers, H. (1991), Deposition and storage of solid-bound heavy metals in the floodplains of the River Geul (The Netherlands). Environmental Monitoring and Assessment 18/3, pp. 79–103.

Leenaers, H. & C.J. Schouten (1989), Soil erosion and floodplain soil pollution: related problems in the geographical context of a river basin. IAHS Publication 184, pp. 75–83.

Lecce, S.A. (1997), Spatial patterns of historical overbank sedimentation and floodplain evolution, Blue River, Wisconsin. Geomorphology 18, pp. 265–277.

Lecce, S.A. & R.T. Pavlowsky (1997), Storage of mining-related zinc in floodplain sediments, Blue River, Wisconsin. Physical Geography 18/5, pp. 424–439.

Millward, G.E., T.K. Sands & C.F. Jago (1999), Particulate metals and their settling velocities in the Humber Estuary, U.K. Marine Chemistry 68, pp. 145–168.

Narinesingh, P., G.J. Klaassen & D. Ludikhuize (2000), Floodplain sedimentation along extended river reaches. Journal of Hydraulic Research 37, pp. 827–845.

Nicholas A.P. & D.E. Walling (1996), The significance of particle aggregation in the overbank deposition of suspended sediment on river floodplains. Journal of Hydrology 186, pp. 275–293.

Ten Brinke, W. (2004), De beteugelde rivier – Bovenrijn, Waal, Pannerdensch Kanaal, Nederrijn-Lek en IJssel in vorm. Diemen, The Netherlands: Veen Magazines.

Thoms, M.C., C.R. Parker & M. Simons (2000), The dispersal and storage of trace metals in the Hawkesbury River valley. In: S. Brizga, & B. Finlayson, eds., River management: The Australasian experience. Chichester, U.K.: John Wiley, pp. 197–219.

Uijtdewilligen, A.M. (2004), Zware metalen in uiterwaarden – Een ruimtelijke koppeling tussen sedimentatie en de opname door vegetatie. MSc Thesis, Utrecht: Milieu-natuurwetenschappen, Faculteit Geowetenschappen, Universiteit Utrecht.

Van der Lee, G.E.M., H. Olde Venterink & N.E.M. Asselman (2004), Nutrient retention in floodplains of the Rhine distributaries in The Netherlands. River Research and Applications 20/3, pp. 315–325.

Walling, D.E., He, Q. & A.P. Nicholas (1996), Floodplains as suspended sediment sinks. In: M.G. Anderson, D.E. Walling & P.D. Bates, eds., Floodplain processes. Chichester, U.K.: John Wiley, pp. 399–439.

Walling, D.E., P.N. Owens & G.J.L. Leeks (1998), The role of channel and floodplain storage in the suspended sediment budget of the River Ouse, Yorkshire, U.K. Geomorphology 22, pp. 225–242.

Walling, D.E., P.N. Owens, J. Carter, G.J.L. Leeks, S. Lewis, A.A. Meharg & J. Wright (2003), Storage of sediment-associated nutrients and contaminants in river channel and floodplain systems. Applied Geochemistry 18/2, pp. 195–220.

Wolters, H.A., M. Platteeuw & M.M. Schoor, eds. (2001), Richtlijnen voor inrichting en beheer van uiterwaarden – ecologie en veiligheid gecombineerd. Lelystad, The Netherlands: RIZA (RIZA rapport 2001.059).

Wyżga, B. (1999), Estimating mean flow velocity in channel and floodplain areas and its use for explaining the pattern of overbank deposition and floodplain retention. Geomorphology 28, pp. 218–297.

Samenvatting

Afzetting van slib en daaraan gebonden zware metalen op uiterwaarden

Inleiding

Overstromingsvlakten of uiterwaarden van rivieren zijn niet alleen waardevolle gebieden voor de natuur, maar zijn ook voor de mens van grote betekenis. Al sinds de oudste geschiedenis worden de vlakke gebieden langs rivieren bewoond. De rivier levert drinkwater en daarnaast irrigatiewater voor de landbouw. Rivieren zijn belangrijke verbindingsassen tussen steden, het achterland en de kust. Bovendien zijn de bodems langs de rivier vruchtbaar. Door afzetting van verontreinigd slib, zijn veel uiterwaardbodems verontreinigd geraakt, onder ander met zware metalen. Hierdoor kunnen de functies van de uiterwaarden worden verstoord. Daarom is het nodig meer te weten te komen over hoe de rivier slibgebonden zware metalen meevoert en waar ze uiteindelijk terecht komen.

Hoewel het belang van uiterwaarden voor de natuur en de maatschappij groot is, is er in het verleden weinig onderzoek naar de afzetting van slib op uiterwaarden gedaan. De aandacht richtte zich vooral op processen in het rivierbed. Pas de afgelopen decennia is het onderzoek naar sedimentatie van slib op uiterwaarden op gang gekomen. Na een pioniersfase richtte het onderzoek zich meer op de hoeveelheden slibafzetting, de ruimtelijke variatie erin en de factoren die het proces van afzetting bepalen. De kenmerken van het slib (vooral korrelgrootte), de valsnelheid en de verontreinigingsgraad ontvangen momenteel veel aandacht in de wetenschappelijke literatuur omdat deze gegevens nodig zijn in de calibratie van modellen. Verder richt een deel van het onderzoek zich op de toekomstige veranderingen van slibafzetting op uiterwaarden door klimaatverandering. Naast het klimaat zullen er echter meer factoren veranderen die van invloed zijn op de afzetting van slib en zware metalen op uiterwaarden, bijvoorbeeld als gevolg van ecologisch en morfologisch herstel van uiterwaarden en veranderingen in emissies van zware metalen. Tot nu toe zijn de effecten van al deze veranderingen nog niet integraal bestudeerd.

Dit proefschrift behandelt de volgende onderzoeksvragen en concentreert zich daarbij op het stroomgebied van de Rijn en zijn Nederlandse uiterwaarden:

1. Wat zijn de huidige afzettingspatronen en kenmerken van slib en slibgebonden zware metalen in uiterwaarden van laaglandrivieren?
2. Wat is het relatieve belang van de belangrijkste factoren die de patronen en kenmerken van slibafzetting bepalen en hoe is de interactie daartussen?

3. Wat zijn de interacties tussen veranderingen in klimaat, bovenstrooms landgebruik, de emissies van zware metalen en de inrichting van uiterwaarden en hoe veranderen deze factoren de afzetting van slib en de daaraan gebonden zware metalen?

De keten van factoren en processen die de afzetting van slib en daaraan gebonden zware metalen op uiterwaarden bepaalt

Hoofdstuk 2 van dit proefschrift behandelt aan de hand van literatuur de keten van factoren en processen die bepaalt hoeveel en waar slib en daaraan gebonden zware metalen op de uiterwaarden wordt afgezet. De keten begint bovenin het stroomgebied bij bodemerosie, die voor de productie van sediment zorgt. Niet alle bodemdeeltjes die door bodemerosie losgemaakt worden bereiken de rivier. In het Rijnstroomgebied bereikt slechts 27 % van de geërodeerde bodemdeeltjes Lobith, wat overeenkomt met 72 ton km^{-1} per jaar of $3.1\ 10^6$ ton per jaar. De tweede groep van processen (uitspoeling, afspoeling en puntlozingen) zorgt voor de toevoer van zware metalen naar de rivier. Ongeveer driekwart van de zware metalen is van diffuse bronnen afkomstig, zoals de landbouw, atmosferische depositie en bodemerosie. Tegenwoordig zijn de afvoer van regenwater uit stedelijke gebieden en rioolwaterzuiveringsinstallaties verantwoordelijk voor ongeveer 40 % van de input van zware metalen in rivieren. In het rivierwater verdelen de zware metalen zich over de water- en sedimentfase, waarbij de laatste veruit het belangrijkste is met een aandeel van 40 % voor koper tot 90 % voor zink. In de sedimentfase hechten zware metalen zich vooral aan kleideeltjes en organische stof, vanwege hun grote bindingscapaciteit.

Door de tijd doen zich op meerdere tijdschalen grote veranderingen in de metaalconcentraties van het slib voor:

- Op de lange termijn is het vooral sinds de Industriële Revolutie dat de metaalconcentraties zijn verhoogd. In de Rijn bereikten de concentraties rond 1930 een piek. Na een tijdelijke afname ten tijde van de Tweede Wereldoorlog bereikten de concentraties een tweede piek in de jaren zeventig van de vorige eeuw. De daarna in werking getreden wetgeving in de jaren '70 en '80 zorgde voor een daling in de emissies. De huidige concentraties rond de 500 mg kg^{-1} Zn, 90 mg kg^{-1} Pb, 80 mg kg^{-1} Cu en 1.5 mg kg^{-1} Cd liggen echter nog steeds aanzienlijk boven de natuurlijke achtergrondconcentraties.
- Door het jaar heen kunnen in de metaalconcentraties verschillen optreden door variaties in bovenstroomse factoren zoals neerslag, landbewerking en industriële activiteiten. Een voorbeeld hiervan is het eerste hoogwater van het hoogwaterseizoen (november-mei), wanneer hogere metaalconcentraties voorkomen dan tijdens eventuele latere hoogwaters.
- Op de tijdschaal tussen en tijdens hoogwaters geldt over het algemeen dat metaalconcentraties in het rivierslib afnemen als de afvoer toeneemt. Tijdens een hoogwater treedt er hysterese op, waardoor in de Rijn de hoogste metaalconcentraties gemiddeld drie dagen voor de afvoerpiek optreden.

In het benedenstroomse gebied wordt een deel van het slib en de slibgebonden zware metalen op de uiterwaarden afgezet. Daarbij gelden een aantal vuistregels. De belangrijkste zijn dat a) de hoeveelheid slib afneemt met de afstand tot de rivier en een toenemende hoogteligging,

b) de metaalconcentraties vooral afnemen met een lagere overstromingsfrequentie en c) de metaalconcentraties ook afnemen met lagere klei en organische stofgehalten in het slib. Omdat deze vuistregels niet voldoende zijn om afzettingspatronen te verklaren, zijn modellen nodig om de afzetting van slib te simuleren. Na afzetting volgt een herverdeling van het slib door het bodemprofiel door bioturbatie. De zware metalen verspreiden zich ook door uitspoeling en opname door planten en dieren.

Verschillende factoren in de procesketen zullen in de komende jaren gaan veranderen. Als gevolg van klimaatverandering zullen piekafvoeren in de Rijn waarschijnlijk toenemen, zodat uiterwaarden vaker en langer overstromen. Aanscherping van wetgeving (zoals de Europese Kaderrichtlijn Water) richten zich op het verder terugdringen van emissies van zware metalen. Doordat de Europese Unie zijn landbouwsubsidies verlaagt wordt het areaal landbouwgrond steeds kleiner, waardoor bodemerosie steeds minder zal voorkomen. Tot slot zal het herinrichten van uiterwaarden de omstandigheden voor slibafzetting veranderen en daarnaast mogelijk tot meer uitspoeling van zware metalen leiden. Het vaststellen van het gecombineerde effect van deze veranderingen op het afzetten van slib en zware metalen blijft dan ook een uitdaging voor onderzoekers en een noodzaak voor beleidsmakers.

De invloed van uiterwaardmorfologie en aanpassingen van het rivierbed op afzettingspatronen van slib en zware metalen

Sedimentatie van slib op uiterwaarden is een belangrijk onderdeel van de sedimentbalans van veel grote rivieren. De hoeveelheden, kenmerken en patronen van afzetting worden op het niveau van de riviertak bepaald door factoren zoals sinuositeit en de breedte van het winterbed. Op de schaal van de uiterwaard spelen vooral de lokale morfologie en stromingspatronen een rol. Menselijke invloed verandert de factoren op beide schalen. Hoe die invloed vervolgens doorwerkt op de afzetting van slib en zware metalen is echter nog maar weinig onderzocht.

Ik onderzocht de verschillen in sedimentatie van slib en zware metalen langs twee takken van de Benedenrijn: de Waal en de IJssel. De mens heeft de uiterwaarden langs de Waal (gemiddelde afvoer: 1500 m^3 s^{-1}) sterk beïnvloed. Zomerdijken beschermen de uiterwaarden tegen overstromingen door lage hoogwaters en het lokale reliëf is vaak afwezig door egalisatie. De brede uiterwaarden van de IJssel (gemiddelde afvoer: 250 m^3 s^{-1}) hebben daarentegen hun klassieke kronkelwaardreliëf en natuurlijke oeverwallen behouden.

De slibafzetting langs beide riviertakken kenmerkt zich door een aantal ruimtelijke trends: met een toenemende afstand tot de sedimentbron neemt de hoeveelheid afzetting van slib af. Klei, organische stof en zware metalengehalte nemen toe met afnemende hoogteligging. Metaalgehalten nemen toe met klei- en organisch stofgehalte in het slib. Deze trends zijn echter aanzienlijk minder uitgesproken in de Waal- dan de IJsseluiterwaarden. Daarnaast duiden lokale afwijkingen van deze 'vuistregels' op de invloed van ruimtelijke verschillen in stroming tijdens een hoogwater. Dit laat zien dat in sommige gevallen een modelaanpak nodig is. Verder zet de Waal duidelijk meer (1.5 kg m^{-2}) en fijner slib (mediane korrelgrootte: 7 μm) per overstroming op haar uiterwaarden af dan de IJssel (1.0 kg m^{-2} en >10 μm). Dit komt omdat de invangcapaciteit

van een Waaluiterwaarden door de zomerkades hoger is dan van een IJsseluiterwaard. Op het niveau van de riviertak blijkt echter dat de IJsseluiterwaarden vanwege hun uitgestrektheid een groter deel van het slibtransport invangen dan de gezamenlijke Waaluiterwaarden, waar over maar een klein deel van het slibtransport plaatsvindt. Daardoor treedt in de IJssel een significant grotere daling in slibgehalte in stroomafwaartse richting op. Dit laat zien dat bij het verklaren van sediment- en zware metalenbalansen naar zowel het uiterwaardniveau als het riviertakniveau gekeken moet worden.

In situ metingen van slib in uiterwaarden met een LISST-ST

Vanwege een gebrek aan empirische gegevens over valsnelheden en korrelgrootteverdelingen van het sediment in het rivierwater in uiterwaarden gebruiken veel sedimentatiemodellen gecalibreerde in plaats van gemeten waarden. Omdat de kenmerken van al afgezet slib anders zijn dan die van slib in suspensie (vlokken), is het niet mogelijk om op basis van afgezet slib de waarden te bepalen. Daarom is het nodig om *in situ* slibconcentraties, valsnelheden, vlokgroottes en sedimentatiefluxen te bepalen. Voor deze metingen heb ik de LISST-ST gebruikt. De LISST-ST is een valbuis en korrelgroottemeter in één apparaat.

Tijdens overstromingen in 2002 (twee keer) en 2004 heb ik de LISST-ST in twee uiterwaarden in Nederland opgesteld: in een uiterwaard zonder zomerdijk langs de IJssel en een uiterwaard mét zomerdijk langs de Waal. De metingen laten zien dat de slibconcentraties in het overstromingswater die in de rivier volgen. Een groot deel van het gesuspendeerde slib bestaat uit kleine vlokken, maar de grote vlokken domineren de potentiële sedimentatie. De *in situ* vlokgroottes waren aanmerkelijk groter in de IJssel- dan in de Waaluiterwaard (mediaan: 25 tegenover 9 μm) hoewel de grootte van de primaire sedimentdeeltjes ongeveer gelijk was (5 μm). De *in situ* vlokken waren dan ook gemiddeld twee tot vijf keer zo groot als de primaire slibdeeltjes.

De *in situ* vlokgrootte heeft een sterk positief verband met de valsnelheid hoewel deze voor de grotere vlokken wel flink uiteenloopt. In de sedimentatieflux, en dus ook in sedimentatiemodellen, kunnen vlokken tot 20 μm verwaarloosd worden. In die modellen kan beter de hier gevonden relatie tussen vlokgrootte en valsnelheid gebruikt worden, aangezien de wet van Stokes alleen maar geldt voor primaire bodemdeeltjes.

Het modelleren van afzetting van slib met particle tracking

Zowel klimaatverandering als herinrichting van uiterwaarden leidt tot veranderingen in afzetting van slib op uiterwaarden. Om de omvang van deze veranderingen in sedimentatie vast te stellen is het MoCSED sedimentatiemodel voor uiterwaarden ontwikkeld. Dit model werkt binnen een Geografisch Informatie-Systeem (GIS) en is toegespitst op de Benedenrijn. Ik heb het model gebaseerd op de 'Methode van Karakteristieken' (MoC), een methode die numerieke dispersie minimaliseert. Het MoCSED model is geïmplementeerd in de *PCRaster Dynamic Modelling Language*. Het model gebruikt invoergegevens zoals slibconcentratie, waterdiepte,

stroomsnelheden en longitudinale en transversale dispersiecoëfficiënten en berekent daarmee de slibconcentraties en vervolgens de sedimentatie.

Ik heb de modeluitkomsten vergeleken met gemeten sedimentatiepatronen in de Bemmelsche Waard voor de overstroming van januari 2003. Deze vergelijking laat zien dat MoCSED in staat is de sedimentatiepatronen te simuleren. Verschillen tussen waarnemingen (gemiddelde sedimentatie 1.5 kg per m^2) en modeluitkomsten (1.4 kg per m^2) zijn vooral te wijten aan fouten in de metingen en lokale, moeilijk te modelleren omstandigheden. Daarnaast is het model een verbetering ten opzichte van een conventioneel rastermodel voor hetzelfde gebied en bevestigt het een ander model voor de gehele Benedenrijn, dat met iets andere afvoerfrequenties een gemiddelde hoeveelheid sedimentatie van 1.7 kg per m^2 per jaar voorspelt. In de toekomst kan MoCSED gebruikt worden om de invloed van de veranderingen in klimaat en uiterwaardinrichting op de afzetting van slib te onderzoeken.

De invloed van herinrichting, klimaat- en landgebruiksverandering op de afzetting van slib en zware metalen op uiterwaarden

Klimaatverandering en herinrichting van uiterwaarden volgens Ruimte voor de Rivier kunnen beide leiden tot meer overstromingen en zo tot toename in de hoeveelheid sedimentatie in uiterwaarden. Toekomstige landgebruiksveranderingen zullen waarschijnlijk leiden tot een verminderde aanvoer van slib en zware metalen, en zo in potentie voor een lagere sedimentatie zorgen. Ik heb het gecombineerde effect van deze drie veranderingen op de afzetting van slib en zware metalen onderzocht op uiterwaarden van de Benedenrijn.

Ik heb de hoeveelheid afzetting van slib en zware metalen in de huidige situatie en volgens vier scenarios berekend voor de Afferdensche & Deestsche Waarden bij Druten en de Bemmelsche Waard bij Bemmel: twee scenarios met meer overstromingen (één met en één zonder verminderde aanvoer van slib), één scenario met daarin de herinrichtingsplannen van Ruimte voor de Rivier verwerkt en één scenario met alle veranderingen.

Op dit moment wordt 1.5 kg m^{-2} j^{-1} sediment en 0.5 g m^{-2} j^{-1} Zn, 0.085 g m^{-2} j^{-1} Pb, 0.08 g m^{-2} j^{-1} Cu en 1.5 10^{-3} g m^{-2} j^{-1} Cd op de Waaluiterwaarden afgezet, wat empirische resultaten uit hoofdstuk 7 bevestigen. Deze hoeveelheden kunnen zes keer zo groot worden na het verwijderen van zomerkades of het aanleggen van een nevengeul. Stroomafwaarts leiden deze maatregelen tot lagere waterstanden en daarmee tot minder afzetting van slib en zware metalen. De effecten van klimaat- en landgebruiksveranderingen heffen elkaar veelal op en hebben gezamenlijk weinig invloed op slibafzetting. In het geval er veel natuurlijke slibvangen zoals lage, onbedijkte uiterwaarden en meren aanwezig zijn, heeft de lagere bovenstroomse aanvoer van slib naar het modelgebied ook een afname in de sedimentatie van rond de 20 % tot gevolg. De verhoogde overstromingsfrequenties hebben vooral een verhoging van de sedimentatie in weinig overstroomde gebieden tot gevolg, tot gemiddeld 25 %. Op het schaalniveau van de riviertak zal het gecombineerde effect van de drie veranderingen ertoe leiden dat locaties met veel en weinig sedimentatie op een andere plek komen te liggen.

Synthese

Volgens de empirische resultaten is de jaarlijkse sedimentatie op een gemiddelde IJsseluiterwaard (2.3 kg m^{-2} j^{-1}) hoger dan op een doorsnee Waaluiterwaard (1.5 kg m^{-2} j^{-1}). Dit komt door de hogere overstromingsfrequenties van de onbedijkte IJsseluiterwaarden en de lage hoeveelheid slib die over de bedijkte Waaluiterwaarden meegevoerd wordt. Van de variatie in de hoeveelheid afzetting van zware metalen kan 90 % verklaard worden door de hoeveelheid slibsedimentatie. Omgerekend naar het percentage slib en zware metalen dat op de uiterwaarden achterblijft is het contrast tussen de twee riviertakken nog sterker. Van alle slib en daaraan gebonden zware metalen dat Nederland via de Rijn binnenkomt vangen de IJsseluiterwaarden 6 tot 8 % in. Van het slib en daaraan gebonden zware metalen dat de IJssel zelf binnenkomt blijft 60 tot 80 % achter op de uiterwaarden. Voor de Waal liggen deze percentages een stuk lager: 3 tot 5 % van de totale slib- en zware metalenvracht in de Rijn blijft achter op de Waaluiterwaarden, wat gelijk staat aan 5 tot 7 % van de vracht in de Waaltak zelf. Dit komt omdat de invangcapaciteit en de overstromingsfrequentie van de IJsseluiterwaarden een stuk hoger ligt terwijl het slib- en metalentransport door de IJssel een stuk lager is, zodat per saldo een groter gedeelte op de uiterwaarden achterblijft.

Wat betreft de afzettingspatronen van slib en zware metalen bevestigt het onderzoek een groot aantal vuistregels uit hoofdstuk 2. In drie gevallen zijn de resultaten echter tegenstrijdig met eerder onderzoek. Ten eerste is het voor de Nederlandse rivieren vanwege de zomerkades niet zo dat een smaller winterbed door hogere stroomsnelheden en schuifspanningen tot minder sedimentatie leidt. Ten tweede blijkt het niet altijd zo te zijn dat de hoeveelheid afzetting van slib afneemt met de afstand tot de rivier door hoogteverschillen en lokale stromingen. Ten derde bevestigt het onderzoek niet dat het zware metalengehalte toeneemt met de afstand tot de rivier.

Er zijn drie sleutelfactoren die een rol spelen in slibafzetting op uiterwaarden, waarbij de lokaal bepaalde factoren belangrijker zijn voor afzettingspatronen dan de bovenstrooms bepaalde:

1. De meest bepalende factor is de topografie van de uiterwaarden: de aan- of afwezigheid van zomerkades, hoogteverschillen binnen de uiterwaaard en de breedte van het winterbed. Deze factor beïnvloedt ook de twee andere factoren:
2. Stromingscondities: overstromingsfrequentie, stroomsnelheden en de overstromingsduur.
3. De kenmerken van het meegevoerde slib: concentratie, samenstelling, vlokgrootte en primaire korrelgrootte, valsnelheid en zware metalengehalte.

Als de modelberekeningen van hoofdstuk 6 worden gemiddeld, blijkt dat in scenario met klimaatverandering 13 % meer sedimentatie per jaar op de Waaluiterwaarden optreedt. Dit slaat om in een daling van 12 % als de landgebruiksveranderingen in het scenario worden meegenomen. De herinrichting van de uiterwaarden leidt tot gemiddeld 6 % meer sedimentatie. Als alle veranderingen gecombineerd worden blijken hun effecten tegen elkaar weg te vallen. Het beeld verandert als we bekijken welk percentage slib en zware metalen op de uiterwaarden achterblijft. Dat blijkt juist het meeste te stijgen (+ 18 %) onder het 'alles-in-één'-scenario, terwijl het scenario met klimaat- en landgebruiksverandering nauwelijks effect sorteert. In onderzoek naar de effecten van omgevingsveranderingen op slibsedimentatie is het dan ook nodig om zowel

de sedimentatie per jaar als het percentage transportverliezen te bekijken. Remobilisatie van de met het slib afgezette zware metalen komt waarschijnlijk eerder voor rekening van de mens dan voor de natuur, aangezien de mens bij herinrichting de uiterwaarden vaak sterk vergraaft.

Curriculum vitae

Ivo Thonon was born on July 27th, 1978 in Dommelen in the municipality of Valkenswaard, Noord-Brabant. From 1990 till 1996, he attended the grammar school *Scholengemeenschap Were Di* in Valkenswaard, which he represented in the Dutch Geography Olympiad finals in 1995. He was one of the winners of the Universiteit van Amsterdam's Geography Prize in 1996. In September of that year, he started studying Physical Geography at Universiteit Utrecht, specialising in Soil & Water Systems and following all subjects in Hydrology as well. In his spare time he was goalkeeper of both the indoor soccer team *De Driftkikkers* and the hockey team *HOD Heren 7*. In the summer of 1999, he did his graduation fieldwork in Austria. His MSc thesis was entitled 'The effect of skiing on soil, hydrology and erosion hazard in the ski area of Sölden, Tyrol, Austria'. In 2000, he participated in the UNESCO program 'Capacity Building for Natural Disaster Reduction' (CBNDR) in Central America. Upon his return, he did an internship in Spain at the Soil Science Department of the Universidade da Coruña. There he worked with the LISEM soil erosion model, learned Spanish and gave courses in that language on erosion modelling and geostatistics.

He graduated (*cum laude*) in February 2001. After a week of holidays, he started his PhD study on what was originally called 'The fate of sediment-associated pollutants in the Rhine-Meuse delta'. He carried out this study within the multidisciplinary 'Networks in the Delta' programme of the Faculty of Geosciences, Universiteit Utrecht. Besides studying polluted mud, he was member of the PhD committees of the Physical Geography Research Institute (PGRI), the Netherlands Centre for River Studies (NCR) and the Centre for Geo-ecological research (ICG). In 2001 and 2002, he returned to the Universidade da Coruña for two short stays. In addition, he continued to participate in the CBNDR program and went to El Salvador and Guatemala in 2002 and 2003. Other journeys were to international conferences in Strasbourg (2001), Oslo (2002), Alice Springs (2002), Ghent (2003), Turin (2004) and Moscow (2004). He also attended around ten national symposia. In the field of education, he assisted in the courses 'Morphodynamics of the Earth Surface' and 'The Earth's System'. He was also a mentor during two excursions to the Belgian Ardennes and supervised one MSc and two BSc theses. In his spare time, he was active in politics (secretary-general of D66 Utrecht and trainer for the *Jonge Democraten*), played badminton, swam once a week and read books in Dutch, German, Spanish and French. After finishing his PhD research and a short project on change detection (*Mutatis Mutandis*), he went to Canada for a year.

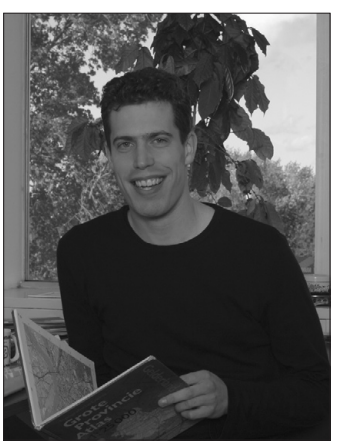

Publications

International scientific journal articles (peer reviewed)

Thonon, I., J.R. Roberti, H. Middelkoop, M. van der Perk & P.A. Burrough (2005), *In situ* measurements of sediment settling characteristics in floodplains using a LISST-ST; Earth Surface Processes and Landforms 30/10, pp. 1327–1343.

Thonon, I., K. de Jong, M. van der Perk & H. Middelkoop (*accepted*), Modelling floodplain sedimentation using particle tracking. Hydrological Processes.

Wijnhoven, S., **I. Thonon**, G. van der Velde, R.S.E.W. Leuven, M.I. Zorn, H.J.P. Eijsackers & A.J.M. Smits (*submitted*): The impact of bioturbation by small mammals on heavy metal redistribution in floodplains. Water, Air and Soil Pollution.

Thonon, I., H. Middelkoop & M. van der Perk (*submitted*), The impact of river rehabilitation, climate and land-use change on the deposition of sediment and heavy metals on floodplains. River Research and Applications.

Thonon, I., H. Middelkoop & M. van der Perk (*submitted*), The influence of floodplain morphology and river works on spatial patterns of overbank sediment and heavy-metal deposition. Netherlands Journal of Geosciences.

Reviewed conference series and other academic publications

Thonon, I. & M. Cacheiro Pose (2001), Geostatistical interpolation of topographical field data in order to obtain a dem of a small forest catchment in Northwest Spain. Cadernos Laboratorio Xeolóxico de Laxe 26, pp. 179–190.

Middelkoop, H., **I. Thonon** & M. van der Perk (2002), Effective discharge for heavy metal deposition on the lower River Rhine flood plains. IAHS Publication 276, pp. 151–159.

Barillas Cruz, M., C. van Westen, E. Orozco, **I. Thonon**, E. Lira, G. Peters Guarín & P. Tax (2003), Zonificación de amenazas naturales en la cuenca del río Samalá y análisis de vulnerabilidad y riesgo en la población de San Sebastián Retalhuleu, Guatemala; GEOS 23/1, pp. 17–24.

Thonon, I. & M. van der Perk (2003), Measuring suspended sediment characteristics using a LISST-ST in an embanked flood plain of the River Rhine; IAHS Publication 283, pp. 37–44.

Thonon, I., K. de Jong, M. van der Perk & H. Middelkoop (2004), A particle tracking method to simulate sediment transfer over flood plains; IAHS Publication 288, pp. 404–409.

Thonon, I., H. Middelkoop & M. van der Perk (*submitted*), The impact of changes in climate, upstream land use and flood plain topography on overbank deposition. IAHS Publication.

Conference proceedings

Paz González, A., **I. Thonon**, F.C. Bertolani, Mª M. Taboada Castro, E. Vidal Vázquez & J. Dafonte Dafonte (2001): Variabilidad espacial de la infiltración en una ladera determinada con permeámetro de Guelph e infiltrómetro de tensión. In: J.J. López Rodríguez & M. Quemada Saéz-Badillos, eds., Temas de investigación en zona no saturada. Navarra, Spain: Universidad Pública de Navarra, pp. 51–60.

Thonon, I., H. Middelkoop & M. van der Perk (2001), Processes determining sediment-associated heavy metal pollution on the lowland river floodplains of the Dutch Rhine-Meuse delta. In: E. Stouthamer & A.G. van

Os, eds., NCR-Days 2001. Delft, The Netherlands: Netherlands Centre of River Studies, pp. 26–27 (NCR Publication 7-2001).

Thonon, I. & A. Paz González (2003), The evolution of the saturated hydraulic conductivity in a small agricultural catchment in NW-Spain during the wet season. In: D. Gabriels & W. Cornelis, eds., Proceedings Symposium 25 Years of assessment of erosion; Ghent, Belgium: Vakgroep Bodembeheer en Bodemhygiëne, Universiteit Gent, pp. 195–200.

Van der Perk, M., S. Borghuis, D. Mourad & **I. Thonon** (2003), Fluxes and retention of nutrients and contaminants in river basins. In: R.S.E.W. Leuven, A.G. van Os & P.H. Nienhuis, eds., Proceedings NCR-days 2002: Current themes in Dutch river research; Delft, The Netherlands: Netherlands Centre for River Studies, pp. 138–140 (NCR-publication 20-2003).

Thonon, I. (2003): The effect of river rehabilitation projects on the sediment-associated heavy metal pollution of the Dutch floodplains. In: R.S.E.W. Leuven, A.G. van Os & P.H. Nienhuis, eds., Proceedings NCR-days 2002: Current themes in Dutch river research; Delft, The Netherlands: Netherlands Centre for River Studies, pp. 142–143 (NCR-publication 20-2003).

De Nooij, R.J.W., M.G. Kleinhans, R.S.E.W. Leuven, B.C. Van Prooijen, M. Straatsma, **I. Thonon,** & A.J. Wesselink (2003), New educational activities of the NCR. In: R.S.E.W. Leuven, A.G. van Os & P.H. Nienhuis, eds., Proceedings NCR-days 2002: Current themes in Dutch river research; Delft, The Netherlands: Netherlands Centre for River Studies, pp. 174–175 (NCR-publication 20-2003).

Thonon, I., A.M. Uijtdewilligen & A. Barendregt (2004), Spatial patterns of cadmium deposition and its uptake by vegetation in Dutch floodplains. In: Proceedings of the first Soil & Water Symposium. Gouda, The Netherlands: SKB, pp. 10–11.

Thonon, I. & A. Paz (2004), A geostatistically interpolated Digital Elevation Model of Galicia (Northwest Spain). In: X. Sanchez-Vila, J. Carrera & J.J. Gómez-Hernández, eds., geoENV IV – Geostatistics for Environmental Applications. Dordrecht, The Netherlands: Kluwer Academic, pp. 532–533 (Quantitative Geology and Geostatistics 13).

Thonon, I., K. de Jong, M. van der Perk & H. Middelkoop (2004), Modelling sediment dispersion over floodplains using a particle tracking method. In: N. Douben & A.G. van Os, eds., NCR-days 2003: Dealing with floods within constraints. Delft, The Netherlands: Netherlands Centre for River Studies, pp. 96–97 (NCR-publication 24-2004).

Thonon, I., M. van der Perk, H. Middelkoop & K. de Jong (2005), How does a secondary channel affect deposition of contaminated sediments on floodplains? The Afferdensche and Deestsche Waarden as a case study. In: Proceedings of the second Soil & Water Symposium. Gouda, The Netherlands: SKB, pp. 36–37.

Thonon, I. H. Middelkoop & M. van der Perk (*accepted*), The impact of 'Room for the River', climate and land-use change on deposition of sediment and heavy metals on Dutch floodplains. In: H. Hooghart & A.G. van Os, eds., NCR-days 2005. Delft, The Netherlands: Netherlands Centre for River Studies (NCR-publication).

Professional publications

Thonon, I. (2002), The fate of sediment-associated heavy-metal pollution in the Dutch Rhine-Meuse Delta. SSEO Newsletter 3, pp. 14–17.

Thonon, I. & A. Wielinga (2003), Het herverontreinigingsniveau voor zware metalen in de Beleidsnotitie Actief Bodembeheer Rijntakken. Bodem 13/5, pp. 186–188.

Thonon, I. (2003): Het modelleren van zwevend stoftransport over uiterwaarden. Landschap 20/5, pp. 55–59.

Scientific report

Middelkoop, H., M. van der Perk & **I. Thonon** (2003), Herverontreiniging van uiterwaarden langs de Rijntakken met sediment-gebonden zware metalen. Utrecht: Departement Fysische Geografie, Faculteit Ruimtelijke Wetenschappen, Universiteit Utrecht (ICG Rapport 03/3).